



HAL
open science

The Renal Cysts and Diabetes syndrome: from transcriptional profiling and functional analysis of a novel mouse model to biomarkers evaluation in human patients

Pierbruno Ricci

► **To cite this version:**

Pierbruno Ricci. The Renal Cysts and Diabetes syndrome: from transcriptional profiling and functional analysis of a novel mouse model to biomarkers evaluation in human patients. *Development Biology*. Sorbonne Université, 2018. English. NNT : 2018SORUS111 . tel-02344993v2

HAL Id: tel-02344993

<https://theses.hal.science/tel-02344993v2>

Submitted on 29 Nov 2019

HAL is a multi-disciplinary open access archive for the deposit and dissemination of scientific research documents, whether they are published or not. The documents may come from teaching and research institutions in France or abroad, or from public or private research centers.

L'archive ouverte pluridisciplinaire **HAL**, est destinée au dépôt et à la diffusion de documents scientifiques de niveau recherche, publiés ou non, émanant des établissements d'enseignement et de recherche français ou étrangers, des laboratoires publics ou privés.

Sorbonne Université

Ecole doctorale Complexité du Vivant

Laboratoire de Biologie du Développement

**The Renal Cysts and Diabetes syndrome:
from transcriptional profiling and functional analysis of a novel
mouse model to biomarkers evaluation in human patients**

Présenté par

Pierbruno Ricci

Thèse de doctorat de Biologie du Développement

Dirigée par **Silvia Cereghini** and **Muriel Umbhauer**

Présentée et soutenue publiquement le 24 septembre 2018

Devant un jury composé de:

Dr. Muriel UMBHAUER

Directrice de Thèse

Dr. Silvia CEREGHINI

Co-directrice de Thèse

Dr. Pierre RONCO

Examineur, Président du jury

Dr. Christine PERRET

Rapporteur

Dr. Adrian WOOLF

Rapporteur

Dr. Petra ZÜRBIG

Examineur

Ringraziamenti



Non è facile sintetizzare la gratitudine, specialmente se data dalla somma di tre anni di vita, ma ci proverò lo stesso.

Il mio più sincero ringraziamento va innanzitutto ai membri della commissione che hanno accettato senza esitazioni di valutare questa tesi di dottorato: Pierre Ronco, Christine Perret, Adrian Woolf e Petra Zürbig. Voi mi avete dedicato il vostro tempo, la vostra attenzione e avete contribuito a rendere concreto questo progetto lavorativo e di vita. GRAZIE.

Un ringraziamento particolare va a Silvia Cereghini, mia supervisor e co-direttrice di tesi dal primo giorno. Con te ho capito realmente cosa significa “amore per la ricerca”. Mi hai accompagnato in questi tre anni con grande umanità e sapienza, chiedendomi tanto ma anche lasciandomi i miei spazi. Il mio pragmatismo e la mia ambizione si sono perfettamente fusi con la tua laboriosità e il tuo rigore. Tornassi indietro, ti sceglierei ancora senza esitazioni come tutor.

Un grazie sincero anche a Muriel Umbhauer, mia direttrice di tesi e co-supervisor. Nonostante le occasioni di confronto siano state più rare rispetto che con Silvia, ho sempre apprezzato i tuoi consigli e la tua competente capacità critica. So che mi hai seguito con gli occhi da lontano a ogni step, avvicinandoti solo quando necessario. Per questo e per la gentilezza sempre dimostrata ti ringrazio.

Un grazie speciale va gridato a tutti i pilastri dell’equipe Signalling and Morphogenesis dell’IBPS: Thierry Darribere, Valerie Bello-Delavaissiere e Isabelle Gervi che mi hanno sempre supportato con simpatia; Jean-François Riou, Ronan Le Bouffant, Isabelle Buisson, Alexis Eschstruth e Mélanie Paces-Fessy, che mi hanno aiutato infinite volte con gli esperimenti e mi hanno sempre dimostrato il loro bene. Anche grazie ai vostri sorrisi e consigli non ho mai perso la motivazione e l’energia. Grazie a Laura Goea e Jennifer Durant-Vesga, con cui ho instaurato un bellissimo rapporto di amicizia. I nostri discorsi hanno dato brio alle dure giornate in laboratorio, “Keep strong” ragazze, un brillante futuro vi attende.

Grazie ai miei amici di TP Maxime Chaulet, Marie-Thérèse Daher, Gabrielle Devienne e Claire Nguyen. Siete mitici! Il nostro progetto di didattica che abbiamo realizzato da zero mi ha riempito di orgoglio, mi ha fatto conoscere la bellezza dell’insegnamento e la felicità che ci può essere dietro un semplice basilico. Vi aspetto presto davanti a una pizza margherita.

Grazie anche a tutti gli amici e conoscenti dei piani cinque, sei e sette del palazzo C, a partire dai giovani di belle speranze tra cui Camille, Mafalda, Antoine, Abraham, Ludovic, Saurabh, Alice fino a passare per i ricercatori, i principal investigators e i segretari/gestionali come Marie, Sylvie, Clémence, Raphaëlle, Hari, Isabelle, Viviane, Sophie e tanti altri. Una chiacchierata o un sorriso con voi per i corridoi mi hanno sempre messo di buon umore. Vi ricorderò tutti con grande affetto.

Non posso dimenticare di ringraziare il mio grande amico Pedro Magalhães, co-autore di uno dei miei articoli e confidente personale. Lavorare con te è stato fantastico, anzi, “WUNDERBAR!”. Sei il mio collega ideale e spero che in futuro le nostre vite lavorative

s'incontreranno di nuovo. "Testa!" my friend. E non tornare indietro neanche per prendere la rincorsa.

Grazie anche al mio amico Girisaran Gangatharan, ci siamo conosciuti quasi alla fine del mio percorso di dottorato ma i nostri pranzi e le nostre chiacchierate sulla vita e sul mondo lavorativo hanno avuto un grande effetto sulla mia immaginazione. Sogna sempre in grande.

Inoltre, grazie di cuore ai membri della mia famiglia francese preferita: Sidonie, Fabrice e Malo. La vostra genuinità e complicità mi arricchiscono a ogni incontro; siete un esempio.

E ora, passiamo ai ringraziamenti sul fronte bellico italiano. Vivere in terra straniera non è mai stato facile per nessuno. Ma voi tutti siete stati il ponte emotivo che mi ha tenuto coi piedi per terra, motivandomi e incoraggiandomi costantemente. Siete voi, famigliari e amici, la mia vera forza. Anche il 24 settembre so che guardandomi intorno incrocerò molti vostri sguardi e spero che voi incrociando il mio penserete "Non lo sta facendo da solo, lo stiamo facendo insieme".

Grazie ai miei amici inossidabili: Luigi, Ilaria, Giovanna, Eleonora, Matteo, Pamela, Martin, Federica, Oscar, Valentina, Marica, Annalisa, Antonio, Loris, Stefano, Pierluigi, Valentina D, Simone R, Serena, Rocco C, Letizia, Giulia, Giorgio, Marco, Carlo, Michela, Simone D, Rocco F, Valentina P, Giovanni, Francesca, Marzia, Giuseppe, Paolo e tutti gli altri! I giochi, le confidenze e le risate non basteranno mai tra di noi. Siete forti, siete belli, siete partecipi, in alto i calici, questa festa è anche per voi.

Grazie a tutti i miei famigliari, gli zii straordinari, i cugini amorevoli, i nonni imbattibili. Siete le radici del mio essere e per voi sarà sempre il mio primo pensiero.

Grazie a Mauro, che sotto uno sguardo umile nasconde una grande saggezza. Hai una bella anima e so di poter imparare sempre da te. "Lean on me, brother".

Grazie a Giampaolo, ciò che ci unisce è tanto più forte quanto invisibile agli occhi. Continua a segnare e fare magie coi numeri per me, e io continuerò a stupirti.

Grazie a Maria Irene, mia preferita. In te giacciono la purezza di una bambina e la fame di una leonessa. Ti stimo ancor prima di volerti bene, illumina il paesaggio come sai fare solo tu.

Grazie a papà Francesco, da cui ho ereditato la bontà e il desiderio del quasi impossibile. Da grande voglio diventare come te.

Grazie a mamma Marisa da cui ho ereditato pazienza e tenacia. Se esistessero i supereroi tu saresti il loro capo.

Grazie a Giulia, Daniel, Patrizia e Luciano. Siete la mia seconda famiglia e una mia certezza primaria. La vita ha ancora così tanto da mostrarci, e so che lo scopriremo insieme.

Grazie a Mariagrazia, mia sposa, mia metà più emozionante e temeraria. Ogni mio successo è per te, ogni gesto è per noi. Mi hai seguito in questa folle vita lontano da casa e ti sarò sempre grato per questo. Tra tutte le luci sei la più intensa e durevole. Abbiamo fatto vedere al mondo cosa possono fare due ragazzi che si amano, e siamo ancora in cammino.

I nomi elencati qui sopra rappresentano davvero ciò che s'intende all'estero per grande Famiglia Italiana. Ci saremo sempre gli uni per gli altri, è questo ciò che conta.

Infine voglio ringraziare il Consorzio RENALTRACT e l'Unione Europea. Senza di voi nulla di tutto questo sarebbe stato possibile.

GRAZIE A TUTTI VOI!

Remerciements



Il n'est pas facile de résumer la gratitude, surtout si elle est donnée par la somme de trois années de vie, mais je vais quand même essayer.

Mes plus sincères remerciements vont tout d'abord aux membres du jury qui ont accepté sans hésiter d'évaluer cette thèse de doctorat: Pierre Ronco, Christine Perret, Adrian Woolf et Petra Zürbig. Vous m'avez donné votre temps, votre attention et vous avez contribué à concrétiser ce projet de travail et de vie. MERCI.

Un merci spécial à Silvia Cereghini, mon superviseur et co-directrice de thèse dès le premier jour. Avec toi j'ai vraiment compris ce que signifie "l'amour de la recherche". Tu m'a accompagné pendant trois ans avec beaucoup d'humanité et de sagesse, en me demandant beaucoup mais en me laissant aussi mon espace. Mon pragmatisme et mon ambition se sont parfaitement harmonisés avec ton application au travail et ta rigueur. Si je pouvais y retourner, je te choiserais sans hésiter comme tuteur.

Merci également à Muriel Umbhauer, directrice de thèse et co-superviseur. Bien que les possibilités d'échanger des idées aient été plus rares qu'avec Silvia, j'ai toujours apprécié tes conseils et tes compétences critiques. Je sais que tu m'as suivi des yeux de loin à chaque pas, ne m'approchant que lorsque c'était nécessaire. Pour cela et pour la gentillesse toujours montrée je te remercie.

Un merci tout particulier à tous les piliers de l'équipe Signalisation et Morphogenèse d'IBPS: Thierry Darribere, Valérie Bello-Delavaissiere et Isabelle Gervi qui m'ont toujours soutenu avec sympathie; Jean-François Riou, Ronan Le Bouffant, Isabelle Buisson, Alexis Eschstruth et Mélanie Paces-Fessy, qui m'ont aidé d'innombrables fois avec les expériences et m'ont toujours montré leur amitié. Grâce à vos sourires et à vos conseils, je n'ai jamais perdu de motivation et d'énergie. Merci à Laura Goea et Jennifer Durant-Vesga, avec qui j'ai établi une formidable amitié. Nos discours nous ont donné vivacité aux journées difficiles en laboratoire. «Keep strong», vous avez un avenir prometteur.

Merci à mes amis du TP Maxime Chautet, Marie-Thérèse Daher, Gabrielle Devienne et Claire Nguyen. Vous êtes légendaires! Notre projet pédagogique que nous avons développé à partir de zéro m'a rempli de fierté, m'a fait connaître la beauté de l'enseignement et le bonheur qui peut exister derrière un simple basilic. Je vous attends bientôt devant une pizza margherita.

Merci également à tous les amis et connaissances des étages cinq, six et sept du bâtiment C, surtout aux jeunes pleins d'espoirs comme Camille, Mafalda, Antoine, Abraham, Ludovic, Saurabh, et Alice ; merci aux chercheurs, aux PI et aux secrétaires / gestionnaires tels que Marie, Sylvie, Clémence, Raphaëlle, Hari, Isabelle, Viviane, Sophie et bien d'autres. Une conversation ou un sourire avec vous dans les couloirs m'a toujours mis de bonne humeur. Je me souviendrai de vous tous avec beaucoup d'affection.

Je ne peux pas oublier de remercier mon grand ami Pedro Magalhães, co-auteur d'un de mes articles et confident personnel. Travailler avec toi a été fantastique, en effet, "WUNDERBAR!". Tu es mon collègue idéal et j'espère que nos vies professionnelles se rencontreront à l'avenir. « Testa ! » mon ami.

Merci aussi à mon ami Girisaran Gangatharan, nous nous sommes rencontrés presque à la fin de mon parcours doctoral mais nos déjeuners et nos discussions sur la vie et le monde du travail ont eu un grand impact sur mon imagination. Ose rêver grand !

Aussi, merci aux membres de ma famille française préférée: Sidonie, Fabrice et Malo. Votre authenticité et votre complicité m'enrichissent à chaque réunion; vous êtes un exemple.

Et maintenant, passons aux remerciements sur le front italien.

Vivre dans un pays étranger n'a jamais été facile pour personne. Mais vous avez tous été le pont émotionnel qui m'a gardé sur terre, me motivant et m'encourageant constamment. Vous êtes ma famille et mes amis, ma vraie force. Aussi, le 24 septembre, je sais que quand j'irai regarder autour de moi, je rencontrerai beaucoup de vos regards et j'espère qu'en croisant mon esprit, vous penserez "Il ne le fait pas seul, nous le faisons ensemble".

Merci à mes amis inoxydables: Luigi, Ilaria, Giovanna, Eleonora, Matteo, Pamela, Martin, Federica, Oscar, Valentina, Marica, Annalisa, Antonio, Loris, Stefano, Pierluigi, Valentina D, Simone R, Serena, Rocco C, Letizia, Giulia, Giorgio, Marco, Carlo, Michela, Simone D, Rocco F, Valentina P, Giovanni, Francesca, Marzia, Giuseppe, Paolo et tous les autres! Les jeux, les confidences et les rires ne suffiront jamais entre nous. Vous êtes fort, vous êtes beaux, vous participez. Levez vos verres, cette fête est aussi pour vous.

Merci à tous mes proches, mes oncles et tantes extraordinaires, mes cousins affectueux, mes grands-parents imbattables. Vous êtes les racines de mon être et ma première pensée sera pour vous.

Merci à Mauro qui, sous un regard humble il cache une grande sagesse. Tu as une belle âme et je sais que je peux toujours apprendre de toi. « Lean on me », mon frère.

Merci à Giampaolo, ce qui nous unit est aussi fort qu'invisible pour les yeux. Continue à marquer et à faire de la magie avec les chiffres pour moi, et je continuerai à t'étonner.

Merci à Maria Irene, ma préférée. En toi réside la pureté d'un enfant et la faim d'une lionne. Je te respecte avant même de t'aimer, éclaire le paysage comme tu peux le faire.

Merci à mon père Francesco, dont j'ai hérité la bonté et le désir du « presque impossible ». Quand je serai grand, je veux devenir comme toi.

Merci à maman Marisa, dont j'ai hérité de patience et de ténacité. Si les super-héros existaient, tu serais leur chef.

Merci à Giulia, Daniel, Patrizia et Luciano. Vous êtes ma deuxième famille et ma certitude primaire. La vie a encore beaucoup à nous montrer, et je sais que nous allons la découvrir ensemble.

Merci à Mariagrazia, mon épouse, ma moitié plus douce et audacieuse. Chaque succès est pour toi, chaque geste est pour nous. Tu m'as suivi dans cette folle vie loin de chez nous et j'en serai toujours reconnaissant. Parmi toutes les lumières, tu es la plus intense et durable. Nous avons montré au monde ce qu'ils pouvaient faire deux jeunes qui s'aiment, et nous sommes encore sur le chemin.

Les noms mentionnés ci-dessus représentent vraiment ce que l'on entend à l'étranger pour grande famille italienne. Nous serons toujours là l'un pour l'autre, c'est ce qui compte.

Enfin, je tiens à remercier le consortium RENALTRACT et l'Union européenne. Sans vous, rien de tout cela n'aurait été possible.

MERCI À TOUS!

Aknowledgments

It is not easy to summarize gratitude, especially if given by the sum of three years of life, but I will try anyway.

My sincerest thanks go first of all to the members of the jury who accepted without hesitation to evaluate this doctoral thesis: Pierre Ronco, Christine Perret, Adrian Woolf and Petra Zürbig. You have given me your time, your attention and you have contributed to make this "work and life project" concrete. THANK YOU.

A special thanks goes to Silvia Cereghini, my supervisor and co-director of thesis from day one. With you I really understood what "love for research" means. You have accompanied me in these three years with great humanity and wisdom, asking me a lot but also giving me my space. My pragmatism and my ambition have blended perfectly with your diligence and your rigor. If I could go back, I would still choose you as a tutor without hesitation.

Sincere thanks also to Muriel Umbhauer, my thesis director and co-supervisor. Although the opportunities for exchange of ideas were more rare than with Silvia, I have always appreciated your advice and your competent critical skills. I know you followed me with your eyes from a distance at every step, approaching only when necessary. For this and for the kindness always shown thank you.

Another special thanks goes to all the pillars of the IBPS Signalling and Morphogenesis team: Thierry Darribere, Valerie Bello-Delavaissiere and Isabelle Gervi who have always supported me with sympathy; Jean-François Riou, Ronan Le Bouffant, Isabelle Buisson, Alexis Eschstruth and Mélanie Paces-Fessy, who have helped me countless times with the experiments and have always shown me their good. Thanks to your smiles and advice I never lost motivation and energy. Thanks to Laura Goea and Jennifer Durant-Vesga, with whom I established a brilliant friendship. Our speeches gave me liveliness during difficult days in the laboratory. Keep strong, you have a promising future.

Thanks to my TP friends Maxime Chaulet, Marie-Thérèse Daher, Gabrielle Devienne and Claire Nguyen. You are legendary! Our didactic project that we have created from scratch has filled me with pride, has made me know the beauty of teaching and the happiness that there can be behind a simple basil. I'll be waiting for you in front of a pizza Margherita.

Thank you also to all friends and acquaintances on floors five, six and seven of the C building, especially to young hopefuls like Camille, Mafalda, Antoine, Abraham, Ludovic, Saurabh, and Alice; thanks to the researchers, PIs and secretaries/managers such as Marie, Clémence, Raphaëlle, Hari, Isabelle, Viviane, Sophie and many others. A conversation or a smile with you in the corridors always put me in a good mood. I will remember all of you with great affection.

I can not forget to thank my great friend Pedro Magalhães, co-author of one of my articles and personal confidant. Working with you was fantastic, even better, "WUNDERBAR!". You are my ideal colleague and I hope that in the future our working lives will meet again. "Testa!" my friend. And do not go back even to get a running start.

Thanks also to my friend Girisaran Gangatharan, we met almost at the end of my doctoral path but our lunches and our talks about life and the working world had a great effect on my imagination. Keep dreaming big.

Also, thank you very much to the members of my favorite French family: Sidonie, Fabrice and Malo. Your genuineness and complicity enrich me at every meeting; you are an example.

And now, let's move on acknowledgments on the Italian front.

Living in a foreign land has never been easy for anyone. But you all have been the emotional bridge that has kept me down to earth, motivating me and encouraging me constantly. You are my family and friends, my true strength. On September the 24th I know that when I will look around I will meet many of your eyes and I hope that by crossing mine you will think "He is not doing it alone, we are doing it together".

Thanks to my stainless friends: Luigi, Ilaria, Giovanna, Eleonora, Matteo, Pamela, Martin, Federica, Oscar, Valentina, Marica, Annalisa, Antonio, Loris, Stefano, Pierluigi, Valentina D, Simone R, Serena, Rocco C, Letizia, Giulia, Giorgio, Marco, Carlo, Michela, Simone D, Rocco F, Valentina P, Giovanni, Francesca, Marzia, Giuseppe, Paolo and all the others! Games, confidences and laughters will never be enough between us. You are strong, you are beautiful, you participate. Raise your glasses, this feast is also for you.

Thanks to all my relatives, extraordinary uncles, loving cousins, unbeatable grandparents. You are the roots of my being and my first thought will always be for you.

Thanks to Mauro, who under a humble gaze hides a great wisdom. You have a beautiful soul and I know I can always learn from you. "Lean on me, brother".

Thanks to Giampaolo, what unites us is as strong as it is invisible to the eyes. Keep scoring and making magic with numbers for me, and I will continue to amaze you.

Thanks to Maria Irene, my favorite. In you lies the purity of a child and the hunger of a lioness. I respect you even before loving you, keep illuminating the landscape as you can.

Thanks to my father Francesco, from whom I inherited the goodness and the desire of the "almost impossible". When I grow up I want to become like you.

Thanks to my mother Marisa, from whom I inherited patience and tenacity. If the superheroes exist you would be their leader.

Thanks to Giulia, Daniel, Patrizia and Luciano. You are my second family but my primary certainty. Life still has so much to show us, and I know we'll find out together.

Thanks to Mariagrazia, my bride, my half more sweet and daring. Every success is for you, every gesture is for us. You followed me in this crazy life away from home and I will always be grateful for it. Among all the lights you are the most intense and durable. We showed to the world what two young people who love each other can do, and we are still on the way.

The names listed above really represent what is meant abroad for "Big Italian Family". We will always be there for each other, this is what matters.

Finally I want to thank the RENALTRACT Consortium and the European Union. Without you, none of this would have been possible.

THANK YOU ALL!

SUMMARY

Heterozygous mutations in the gene encoding the transcription factor *HNF1B* are the cause of a complex multisystem syndrome known as Renal Cysts And Diabetes (RCAD). A novel mouse model, previously generated by introducing a human splicing mutation, was shown to reproduce several features of the human disease, including bilateral cystic embryonic kidneys, delayed proximal tubule differentiation, genital tract abnormalities and postnatal pancreas dysfunction. To further understand how miRNAs, mRNAs and the HNF1B transcriptional factor are integrated into gene regulatory networks underlying the disease phenotype, we performed high-throughput mRNA and microRNA sequencing at different developmental stages (E14.5, E15.5, E17.5). We showed that the most down-regulated genes are expressed in proximal tubules and to a lesser extent in the loop of Henle and collecting ducts and are involved in transport, lipid and organic acid metabolic processes. Consistent with the disease phenotype of our model de-regulated genes are related to abnormal renal/urinary system physiology and kidney diseases.

microRNAs sequencing showed that, depending of the stage, 11 to 25 microRNAs were significantly de-regulated. The higher number of differentially expressed miRNAs was observed at E15.5 and the majority was down-regulated. Moreover, different microRNAs were predicted to be involved in kidney development and maintenance. Taking advantage of a HNF1B ChIP sequencing data generated from E14.5 kidneys we selected two microRNAs (mir-802 and 192), which were down-regulated at all the three developmental stages analyzed, mir-194-2 down-regulated at E15.5 and at E17.5 and mir-30a down-regulated only at E15.5. Luciferase assays in HEK-293 cells showed that HNF1B was able to specifically transactivate in a dose response mode these microRNAs through the binding to consensus binding sites in their regulatory promoter/enhancer upstream sequences. We subsequently showed using vectors luciferase containing the 3'UTR of *Hnf1b* and miRNA MIMICS, that mir-802, mir-194-2 and mir-192 were able to inhibit luciferase activity. These results together show that HNF1B and mir-802, mir-194-2 and mir-192 are linked by an autoregulatory-loop. Moreover, HNF1B is able to transactivate mir-30a gene through a far upstream enhancer element.

In parallel, proteomic analysis on urines of RCAD adult mice carried out by capillary electrophoresis coupled to mass spectrometry (CE-MS) uncovered 40 differentially excreted peptides including an increase of collagen fragments and a strong decrease of EGF and uromodulin fragments. Because of such characterized signature of the urinary proteome of the RCAD mice, we decided to investigate the urinary proteome of a pediatric cohort of RCAD patients searching for a similar urinary proteome signature. Analysis of urine samples from 22 RCAD patients and 22 healthy controls led to the identification of 146 peptides differentially excreted and associated with RCAD including a similarity regarding collagen and uromodulin fragments with the RCAD mouse model. Combining the peptides into a mathematical model we used independent cohorts of patients exhibiting different renal diseases to validate the prediction of the RCAD syndrome. Our classifier efficiently predicted RCAD syndrome with 91.7% sensitivity and 91.1% specificity on a wide population of control patients (including patients with unrelated cystic diseases and nephrotic syndromes).

In conclusion, the combined analysis of a unique RCAD mouse model and urinary proteomic approaches allowing the identification of a unique urinary proteomic signature of RCAD children, our work deepens different aspects of this complex and heterogeneous syndrome and provides new insights on the molecular basis underlying this disease.

TABLE OF CONTENTS

INTRODUCTION

CHAPTER 1. Hepatocyte Nuclear Factor 1B

- 1.1 The HNF1B transcriptional factor: genomic organization and functional domains
- 1.2 HNF1B expression pattern during mouse development
- 1.3 HNF1B during mouse development
 - 1.3.1 Early post-implantation stages
 - 1.3.2 Role of HNF1B during organogenesis
 - 1.3.2.1 Pancreas
 - 1.3.2.2 Liver
 - 1.3.2.3 Intestine
 - 1.3.3 HNF1B during kidney development
 - 1.3.3.1 Overview of kidney development and function
 - 1.3.3.2 HNF1B requirement for ureteric bud branching morphogenesis and nephrogenesis induction
 - 1.3.3.3 HNF1B and patterning of early nephron structures
 - 1.3.3.4 Collecting duct morphogenesis and cystic medullar tubules 1.4
- HNF1B regulatory network and gene targets
 - 1.5 HNF1B transcriptional homologs, cofactors and coactivators
 - 1.6 Regulation of HNF1B
 - 1.7 The conservation of HNF1B in other species

CHAPTER 2. Renal Cysts and Diabetes syndrome

- 2.1 HNF1B expression in human
- 2.2 Overview of the RCAD syndrome
- 2.3 HNF1B mutations and genetic analysis
- 2.4 RCAD clinical features
 - 2.4.1 Renal abnormalities
 - 2.4.2 Renal physiological imbalances
 - 2.4.3 Diabetes
 - 2.4.4 Pancreas morphological abnormalities and exocrine dysfunctions
 - 2.4.5 Liver dysfunctions
 - 2.4.6 Genital tract abnormalities
 - 2.4.7 Other clinical features
- 2.5 RCAD diagnosis and treatment
- 2.6 Molecular mechanisms underlying the RCAD disease

CHAPTER 3. microRNAs and renal diseases

- 3.1 Overview of microRNAs
- 3.2 microRNAs biogenesis
- 3.3 microRNAs mechanisms of action
- 3.4 microRNAs in renal development and diseases
- 3.5 HNF1B and microRNAs

CHAPTER 4. The urinary proteome as research tool

- 4.1 The urinary proteome
- 4.2 Analytic approaches
- 4.3 CE-MS workflow

RESULTS

TOPIC I. The RCAD mouse model

- I.1. Context of the study
- I.2. Results and discussion
- I.3. Conclusions

SCIENTIFIC ARTICLE 1

TOPIC II. Analysis of HNF1B regulating microRNAs in the renal pathogenesis of a mouse model of the RCAD syndrome

- II.1. Introduction
- II.2. Summary of results
- II.3. Discussion and conclusions

PROGRESS SCIENTIFIC REPORT (ongoing)

TOPIC III. Urinary proteome signature of Renal Cysts and Diabetes syndrome in children

- III.1. Context of the study
- III.2. Results and discussion
- III.3. Conclusions

SCIENTIFIC ARTICLE 2

CONCLUSIONS AND DISCUSSION

BIBLIOGRAPHY

“*Now is the time to understand more, so that we may fear less*” stated Maria Skłodowska-Curie more than 80 years ago. This quote can be attributed to any phenomenon that scare us and we do not fully comprehend; nowadays among the most imperative mysteries to disclose there is the understanding of diseases.

The etiologies of diseases are often complex and unclear, but almost all have a genetic component. This thesis work was aimed to bring novel knowledge on a rare disease named Renal Cysts and Diabetes syndrome (RCAD), which is caused by mutations of a single gene. Heterozygous mutations in the gene Hepatocyte Nuclear Factor-1-Beta (*HNF1B*) are responsible for the broad spectrum of symptoms that characterize the disease. Consistent with HNF1B role during development of different organs, RCAD clinical features are extremely heterogeneous and associates with morphological or functional anomalies of the kidneys, pancreas, liver and genital tract. This autosomal dominant disorder is not yet been comprehensively understood as shown by a lack of unequivocal prevalence or diagnostic tools and the difficulty in establishing its pathophysiological basis.

We studied this disease in two closely related mammals, the mouse and the human.

Regarding the murine approach a first mouse model that reproduces different phenotype of the RCAD disease was created in the laboratory. Using this model, we investigated transcriptional profiling, renal anomalies, and kidney functionalities at different time either during development or post-natal, uncovering significant data on the disease origination. Moreover, we reveal in this mouse model a tight regulation between HNF1B and three microRNAs.

Regarding the human approach, within a collaborative project involving three European centers, we characterized the first urinary proteome of children affected by RCAD syndrome, providing new insights on the main elements that differentiate this disease from other renal disorders.

This thesis manuscript consist in six main parts:

1. **Hepatocyte Nuclear Factor 1B**: structure, expression pattern, role during development, transcriptional network and regulation
2. **Renal Cysts and Diabetes syndrome**: clinical features and molecular basis
3. **microRNAs**: microRNAs biogenesis and function, microRNAs studies in kidneys and regulation with HNF1B
4. **Urinary proteome**: urinary proteome scientific significance and analytic approaches
5. **Results**:
 - a. Topic I (the RCAD mouse model manuscript);
 - b. Topic II (HNF1B and microRNAs in RCAD mouse model analysis);
 - c. Topic III (the urinary proteome of RCAD children)
6. **Conclusions and discussion**

INTRODUCTION

CHAPTER 1. Hepatocyte Nuclear Factor 1B

1.1 The HNF1B transcriptional factor: genomic organization and functional domains

Hepatocyte nuclear factor-1-beta (HNF1B), also known as LF-B3, HNF-1- β , vHNF1, and TCF2 (Transcription Factor 2), belong to a class of POU-like homeodomain of transcription factors, composed by two genes: HNF1A and HNF1B. HNF1B is located on Chr 17q12 in humans (position 17: 37,686,432-37,745,247; Ensembl); Chr11 in mice (11: 83,850,063-83,905,819).

The *Hnf1b* mRNA is approximately 2.8 kb split into 9 exons (**Figure 1**). Alternative splicing generates two main isoforms, named *Hnf1b-A* and *Hnf1b-B*, which are expressed at the same level in different tissues. Studies on human cells and mouse showed that *Hnf1b-A* transcript has an additional exon of 78 bp inserted between exon two and exon three generating 26 amino acids more at the end of the POU_S domain (Rey-Campos J et al., 1991) and is the predominant form both in embryonic and adult tissues compared with *Hnf1b-B* (Cereghini S et al., 1992). They display distinct activation potential depending on the context of the promoter and appear to complement each other during development (Haumaitre C et al., 2003). A third isoform named *Hnf1b-C* was identified in human liver; it is shorter than the transcript *-A* and *-B*, and generated by the use of alternative polyadenylation site (Bach I et al., 1993). In vitro analyzes have shown that this isoform act as a dominant negative, repressing the expression of certain targets (Bach I et al., 1993). Comparative expression analysis in rat, mouse and human tissues showed controversial results concerning the relative expression levels of the three isoforms in different species (Cereghini S et al., 1992; Harries L et al., 2009; Haumaitre C et al., 2006). The amino acid sequences of the different HNF1B isoforms are highlighted in **Figure 2**.

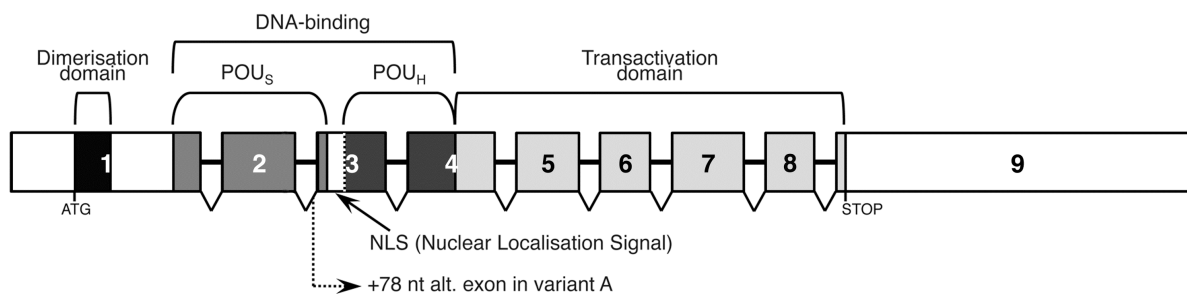


Figure 1. Genomic organization of the Hnf1b locus illustrating the 9 coding exons and main functional domains (N-terminal Dimerization, the POU-specific (POU_S) and POU-homeodomain (POU_H) and the C-terminal transactivation domains). Exons, but not introns, are depicted in nucleotides scale size.

HNF1B-A	MVSKLTSLQQ	ELLSALLSSG	VTKEVLVQAL	EELLPSPNFG	VKLETPLPLSP
HNF1B-B	MVSKLTSLQQ	ELLSALLSSG	VTKEVLVQAL	EELLPSPNFG	VKLETPLPLSP
HNF1B-C	MVSKLTSLQQ	ELLSALLSSG	VTKEVLVQAL	EELLPSPNFG	VKLETPLPLSP
HNF1B-A	GSGAEPDTKP	VFHTLTNGHA	KGRLSGDEGS	EDGDDYDTPP	ILKELQALNT
HNF1B-B	GSGAEPDTKP	VFHTLTNGHA	KGRLSGDEGS	EDGDDYDTPP	ILKELQALNT
HNF1B-C	GSGAEPDTKP	VFHTLTNGHA	KGRLSGDEGS	EDGDDYDTPP	ILKELQALNT
HNF1B-A	EEAAEQRAEV	DRMLSEDPWR	AAKMIKGYMQ	QHNIPQREVV	DVTGLNQSHL
HNF1B-B	EEAAEQRAEV	DRMLSEDPWR	AAKMIKGYMQ	QHNIPQREVV	DVTGLNQSHL
HNF1B-C	EEAAEQRAEV	DRMLSEDPWR	AAKMIKGYMQ	QHNIPQREVV	DVTGLNQSHL
HNF1B-A	SQHLNKGTPM	KTQKRAALYT	WYVRKQREIL	RQFNQTVQSS	GNMTDKSSQD
HNF1B-B	SQHLNKGTPM	KTQKRAALYT	WYVRKQREIL	RQF.....
HNF1B-C	SQHLNKGTPM	KTQKRAALYT	WYVRKQREIL	RQF.....
HNF1B-A	QLLFLFPEFS	QQSHGPGQSD	DACSEPTNKK	MRRNRFKWGP	ASQQILYQAY
HNF1B-BS	QQSHGPGQSD	DACSEPTNKK	MRRNRFKWGP	ASQQILYQAY
HNF1B-CS	QQSHGPGQSD	DACSEPTNKK	MRRNRFKWGP	ASQQILYQAY
HNF1B-A	DRQKNPSKEE	REALVEECNR	AECLQRGVSP	SKAHGLGSNL	VTEVRVYNWF
HNF1B-B	DRQKNPSKEE	REALVEECNR	AECLQRGVSP	SKAHGLGSNL	VTEVRVYNWF
HNF1B-C	DRQKNPSKEE	REALVEECNR	AECLQRGVSP	SKAHGLGSNL	VTEVRVYNWF
HNF1B-A	ANRRKEEAFR	QKLAMDAYS	NQTHSLNPLL	SHGSPHHQPS	SSPPNKLSGV
HNF1B-B	ANRRKEEAFR	QKLAMDAYS	NQTHSLNPLL	SHGSPHHQPS	SSPPNKLSGV
HNF1B-C	ANRRKEEAFR	QKLAMDAYS	NQTHSLNPLL	SHGSPHHQPS	SSPPNKLSGV
HNF1B-A	RYSQQGNEI	TSSSTISHHG	NSAMVTSQSV	LQQVSPASLD	PGHNLLSPDG
HNF1B-B	RYSQQGNEI	TSSSTISHHG	NSAMVTSQSV	LQQVSPASLD	PGHNLLSPDG
HNF1B-C	RYSQQGNEI	TSSSTISHHG	NSAMVTSQSV	LQQVSPASLD	PGHNLLSPDG
HNF1B-A	KMISVSGGGL	PPVSTLTNIH	SLSHHNPQQS	QNLIMTPLSG	VMAIAQSLNT
HNF1B-B	KMISVSGGGL	PPVSTLTNIH	SLSHHNPQQS	QNLIMTPLSG	VMAIAQSLNT
HNF1B-C	KMISVSGGGL	PPVSTLTNIH	SLSHHNPQQS	QNLIMTPLSG	VMAIAQSSST
HNF1B-A	SQAQSVPVIN	SVAGSLAALQ	PVQFSQQLHS	PHQQPLMQQS	PGSHMAQQPF
HNF1B-B	SQAQSVPVIN	SVAGSLAALQ	PVQFSQQLHS	PHQQPLMQQS	PGSHMAQQPF
HNF1B-C	SLVMPHTHLL	RAQQQGPCFP	HHHPLGSCHG	KAQ.....
HNF1B-A	MAAVTQLQNS	HMYAHKQEP	QYSHTSRFPS	AMVVTDTSSI	STLTNMSSSK
HNF1B-B	MAAVTQLQNS	HMYAHKQEP	QYSHTSRFPS	AMVVTDTSSI	STLTNMSSSK
HNF1B-C
HNF1B-A	QCPLQAW				
HNF1B-B	QCPLQAW				
HNF1B-C				

Figure 2. NCBI protein blast of HNF1B isoforms highlighting conservation in amino acid sequences

The transcription factor HNF1B was identified after HNF1A in hepatic cells where it binds to the same promoter sequences of Hnf1A (Baumhueter S et al., 1988; Cereghini S et al., 1988; Cereghini S et al., 1990). Subsequently, it has been confirmed that these two transcription factors were encoded by two different genes (Bach I et al., 1991; Rey-Campos J et al., 1991; De Simone V et al., 1991).

HNF1B-A/B/C isoforms encode respectively 557-, 531-, and 457- proteins; the isoform A is the longest, has a molecular weight of 61,324 Da and showed a stronger transactivation activity than HNF1B-B (Ringeisen F 1993 et al., 1993). With the exception of the isoform C which corresponds to a truncated protein, the isoforms A and B present three distinct functional domains: an N-terminus dimerization domain, a conserved DNA binding domain, and a C-terminus transactivation domain (**Figure 3**).

- The dimerization domain of HNF1B is a structure composed by 32 amino acids forming four α -helices (Pastore A et al., 1992; Rose RB et al., 2000 bis; Narayana N et al., 2001) and through binding this domain HNF1B can act as a homodimer or as a heterodimer with HNF1A to regulate gene expression (Chouard T et al., 1990; Rey-Campos J 1991; Frain M et al., 1989; Nicosia A et al., 1990). This domain presents 72% of homology between the two transcription factors. When dimerization domain is mutated, less ability to form dimers and less affinity for the DNA binding site were described (Chouard T et al., 1990; Tomei L et al., 1992).
- The DNA binding domain is divided into a Pit-1/Oct-1/Unc-86 specific domain (POU_S) and a POU homeodomain (POU_H). POU_S confers to the protein its DNA binding specificity (Tomei L et al., 1992). It is atypical as it is composed of at least one α -helice more than the canonical POU_S domains; HNF1A possess five α -helices and HNF1B six α -helices (**Figure 4 A**). Crystallography analyses suggest that the supplementary N-terminal α -helix could lead to a decrease in DNA binding (Chi YI et al., 2002; Lu P et al., 2007). POU_H forms three α -helices, the last of which is involved in the interaction with the nucleobases at the level of the major groove of DNA (Ceska TA et al., 1993; Leiting B et al., 1993; Schott O et al., 1997). Unlike the other characteristic POU domains, the fifth helix of the POU_S domain, the region between the two POU domains and the second helix of the POU_H domain are longer. These characteristics would lead to an increase in the interaction between the POU_S and POU_H domains and a greater rigidity in the DNA interaction. Between the POU_S and POU_H domains (amino acids 186-229) there is the nuclear localization signal (NLS) ₂₂₉KKMRRNRFK₂₃₇ (Wu G et al., 2004). HNF1B recognizes the consensus sequence

5'-GTTAATNATTAAC-3' (**Figure 4 B**) and binds to the promoters of target genes and activate transcription, even though transcriptional repression has been demonstrated (Ferrè S et al., 2013). HNF1A, sharing 91% of identity in this domain, recognize the same consensus sequence (Mendel DB et al., 1991 bis; Tomei L et al., 1992). The isoforms HNF1B-A and HNF1B-B exhibited equivalent DNA binding affinities for their specific target sites (Haumaitre C et al., 2003).

- The C-terminal transactivation domain shares only 47% of homology with HNF1A and was reported to interact with the co-regulators HDAC-1 and PCAF (Barbacci E et al., 2004; Hiesberger T et al., 2005). It contains a glutamine-serine-proline (QSP)-rich domain, highly conserved in HNF1 factors, named DAIII (Activation Domain III) (Sourdive DJ et al., 1993°) whose deletion abolishes transactivation (Barbacci E et al., 2004). Overexpression experiments in different cell types using the promoters of various target genes demonstrated that HNF1A and HNF1B display similar transactivation activity. Yet HNF1A is in general a more potent transactivator than HNF1B (Bach I and Yaniv M, 1993; Rey-Campos J 1991). Interestingly, HNF1B was also shown repress the transcription of the *Socs3* gene (Ma Z et al., 2007), thus showing that in some rare cases can function as a repressor.

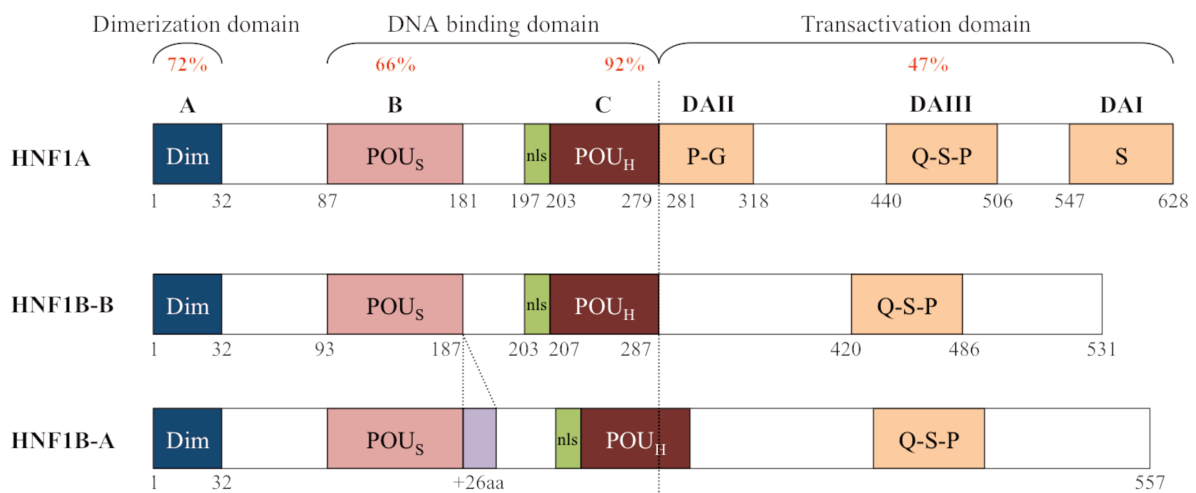


Figure 3. HNF1A and HNF1B transcription factors share different levels of conservation depending on the domain. Structure of HNF1A, HNF1B-A and HNF1B-B proteins. N-terminal domain of DNA binding and subdomains A: dimerization, B: POU_S, (specific), C: POU_H (homeodomain), C-terminal domain of transactivation and subdomains DAI, DAII, DAIII (Domain of Activation) rich in proline-glycine (PG), glutamine-serine-proline (QSP), serine (S). nls: nuclear localization signal.

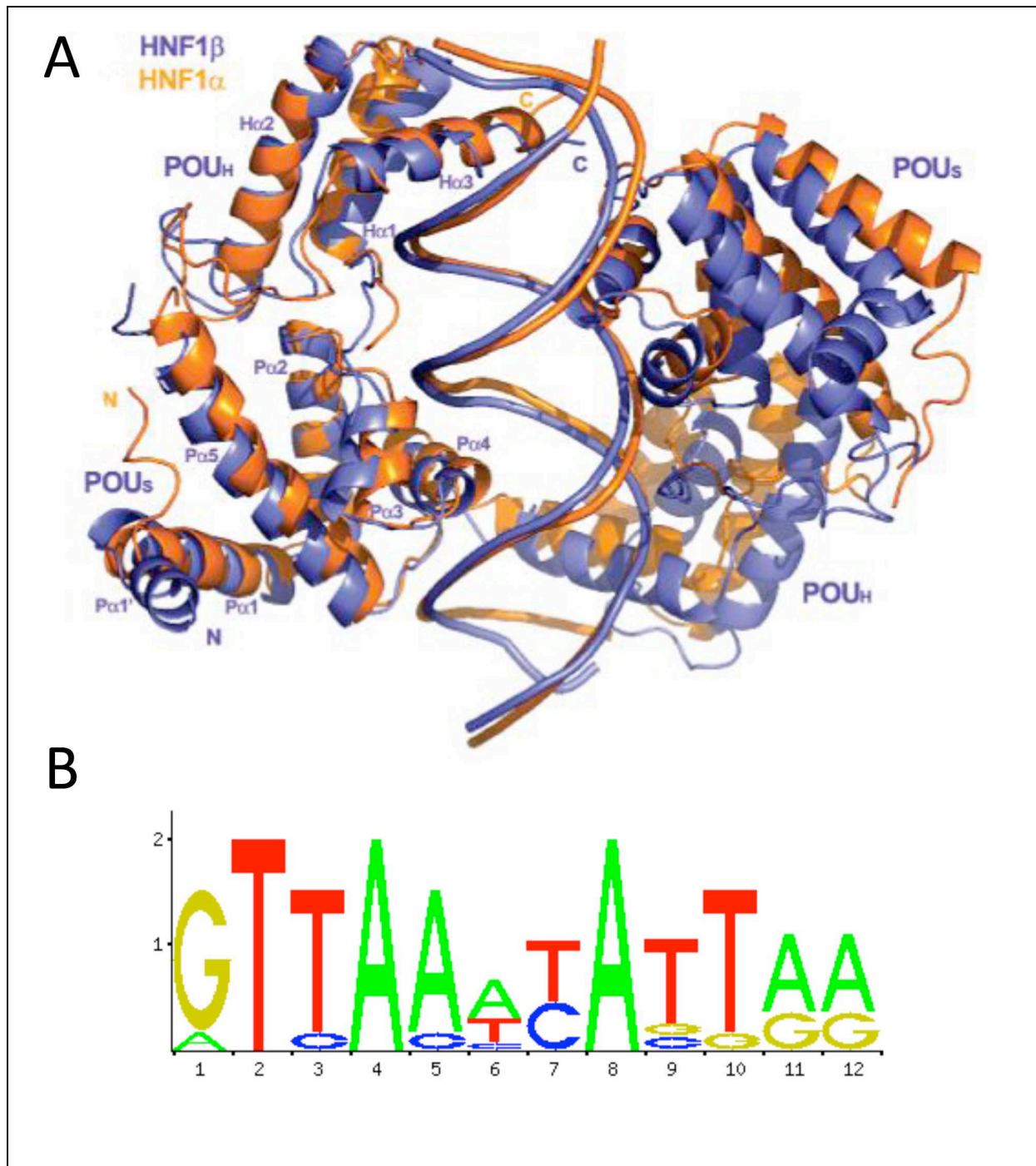


Figure 4. **A.** Crystallographic structure in ribbon comparison between HNF1A and HNF1B binding a DNA double helix (source RCSB protein data bank). **B.** HNF1B binding motif to DNA from JASPAR (source <http://jaspar.binf.ku.dk/> Khan A et al., 2018) (Adapted from Lu P et al., 2007).

1.2 HNF1B expression pattern during mouse development

Mouse genetic studies by replacing the first exon of *Hnf1b* with *lacZ* reporter gene reproduced the endogenous expression profile of the gene and allowed a detailed analysis at cellular level in heterozygous mutant embryos (Barbacci E et al., 1999; Coffinier C et al., 1999b). *Hnf1b* is initially expressed in the primitive endoderm, the precursor of both visceral and parietal endoderm (Barbacci E et al., 1999). From E5.5, β -gal staining, encoded by *lacZ* cassette, is observed in the extra-embryonic endoderm; at E6.5 is highly expressed in the proximal visceral endoderm (ve) (embryonic) and in the parietal endoderm (pe), (Barbacci E et al., 1999) and subsequently in the yolk sac (Cereghini S et al., 1992). (**Figure 5**).

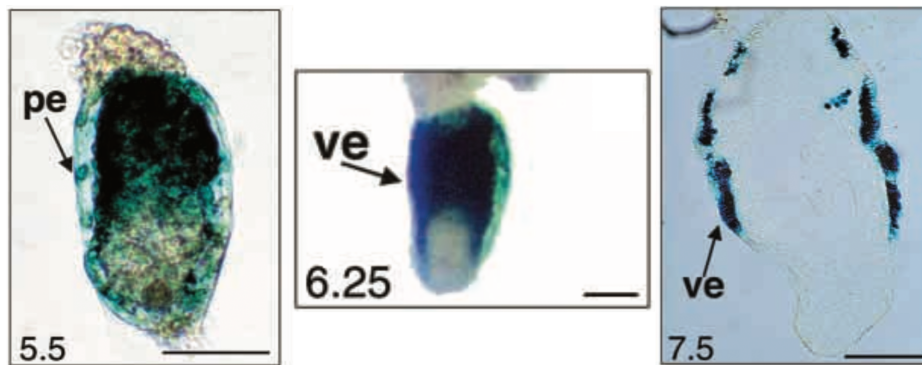


Figure 5. Analysis of the β -galactosidase expression pattern in *Hnf1b* heterozygous mouse embryos. β -gal express in parietal endoderm (pe), and visceral endoderm (ve) surrounding the primitive ectoderm. Scale bar (1-2-3): 100 μ m. (Adapted from Barbacci et al., 1999)

Up to the early stages of gastrulation, expression is confined to the extraembryonic lineage. From E8.5, the β -galactosidase activity is detected for the first time in the embryo at the level of the anterior endoderm, in the liver primordium and transiently in the neural tube (nt) (**Figure 6**). At E9.5, the expression in the neural tube (nt) extends from the otic vesicle (ov). Neural crest cells, spinal ganglia, and lungs also express *Hnf1b* (Barbacci E et al., 1999). By E9.5, *Hnf1b* expression is detected in the polar epithelial cells of the primitive intestine (g) and its derivatives (stomach, liver, pancreas), as well as in the mesonephros (m) and then in the entire urogenital system (Barbacci E et al., 1999; Cereghini S et al., 1992; Coffinier C et al., 1999b; Ott MO et al., 1991; Reber M and Cereghini S, 2001).

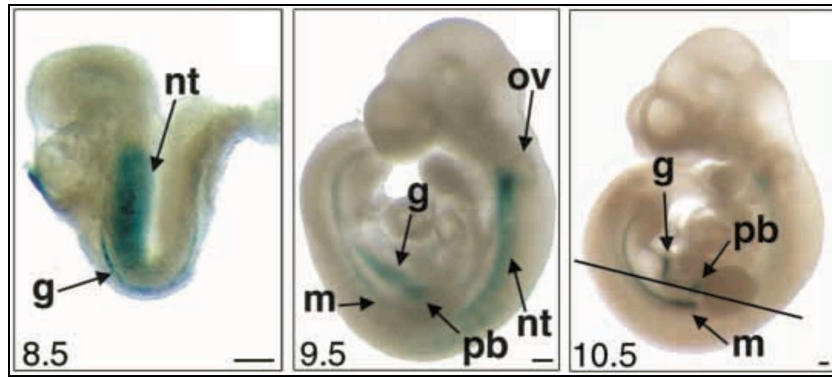


Figure 6. Analysis of the β -galactosidase expression pattern in *Hnf1b* heterozygous mouse embryos. Expression in the gut epithelium (g), neural tube (nt), mesonephric duct (m), pancreatic bud (pb), otic vesicle (ov). Scale bar (1-2-3): 200 μ m. (Adapted from Barbacci E et al., 1999)

During kidney development, its expression is detected in the mesonephric tubules, the entire Wolffian duct (WD) from E9.0 and at E10.5 at the level of the emerging ureteric bud (UB) (**Figure 7**). Its expression is maintained in the epithelium of the UB during its arborization. Then, *Hnf1b* is found throughout the nephrogenesis in the distal part of the renal vesicles (RV), and comma-shaped and S-shaped bodies in a proximal-distal pattern at E13.5. At E16.5, the expression pattern is similar to the adult (Cereghini S et al., 1992) with both proximal and distal tubules staining positive (Barbacci E et al., 1999, De Simone V et al., 1991, Ott MO et al., 1991).

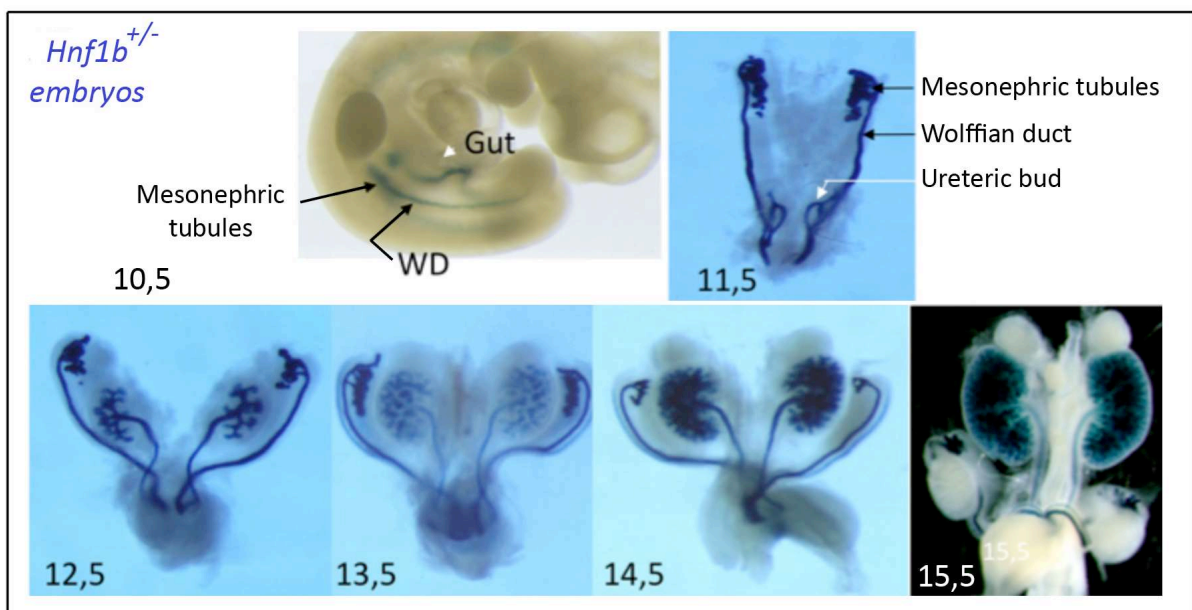
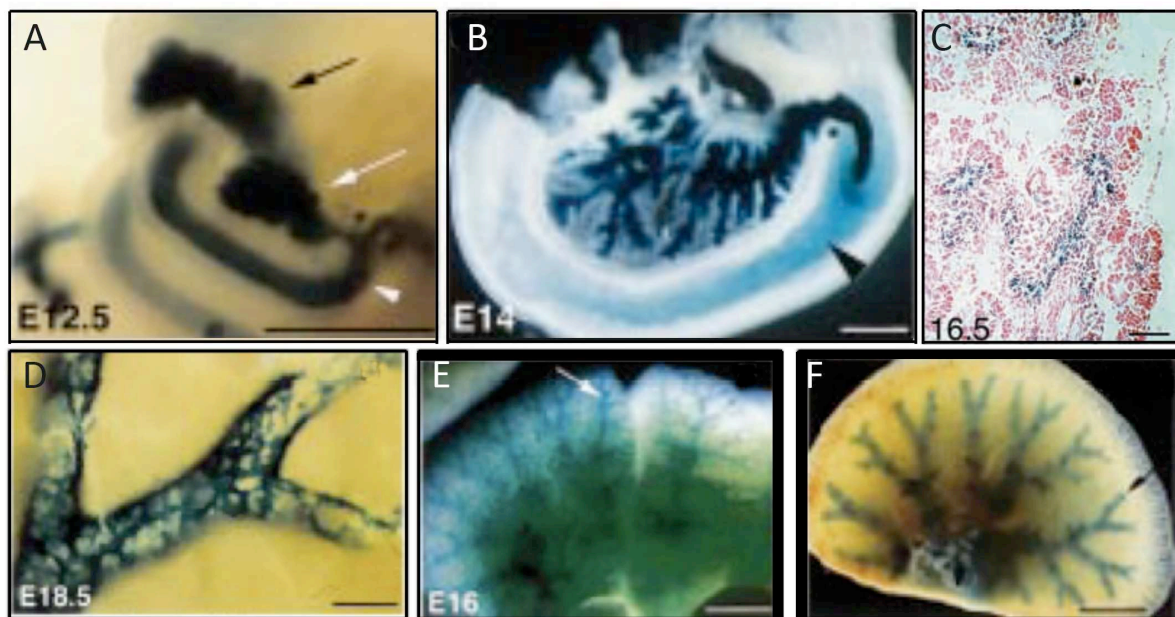


Figure 7. Analysis of the β -galactosidase expression pattern in *Hnf1b* heterozygous mouse embryos and microdissected urogenital tract at the indicated developmental stage showing mesonephric tubules, Wolffian ducts (WD), and ureteric bud (Adapted from Lokmane L et al., 2010).

Hnf1b is expressed in the endoderm of the primitive gut and the multipotent pancreatic precursors of the pancreatic bud. From E14.5 until birth, its expression is restricted in the pancreatic duct network (Haumaitre C et al., 2005; Maestro MA et al., 2003; De Vas MG et al., 2015) (**Figure 8 A, B, C**).

Hnf1b is also expressed during the development of the gallbladder, bile ducts and lungs. A subpopulation of hepatocytes, the periportal hepatocytes, located at the periphery of the hepatic lobules, also expresses *Hnf1b* at the end of embryogenesis and in adults (Coffinier C et al., 2002). Finally, as early as E16.5, the bronchi and bronchioles of the lungs express *Hnf1b* (Coffinier C et al., 1999b) (**Figure 8 D, E, F**). In adult mice, *Hnf1b* is strongly expressed in the polarized epithelial tubes of the kidney (all segments of the nephron and in renal collecting ducts), and at lower levels in the lungs, gonads, biliary and pancreatic ducts, stomach and intestine epithelia (Cereghini S et al., 1992; Lazzaro D et al., 1992; De Simone V et al., 1991; Rey-Campos J et al., 1991;).



(**Figure 8**) Analysis of the β -galactosidase expression pattern in developing pancreas and other endoderm derived organs in *Hnf1b*^{lac/+} heterozygous mouse embryos. **A**. Pancreas buds at E12.5: black arrow, dorsal pancreatic bud; white arrow, ventral pancreatic bud; arrowhead, duodenum. **B**. Dissected pancreas at E14: arrowhead, duodenum. Note the restriction of the staining to the ductular part of the pancreas. **C**. Sagittal section of the pancreas; **D**. Biliary duct network surrounding a vessel in a E18.5 liver; **E**. *Hnf1b* expression in the lung: arrows, bronchiole; **F**. Adult polmonary lobe: arrows, bronchiole. Scale bar (A-B): 100 μ m; (C): 200 μ m; (D-E): 1 mm; (F) 400 μ m. (Adapted from Coffinier C et al., 1999b and Barbacci et al., 1999)

1.3 HNF1B during mouse development

1.3.1 Early post-implantation stages

In normal embryos, *Hnf1b* is initially expressed in extraembryonic tissues, and subsequently in the primitive endoderm (the precursor of both visceral and parietal endoderm) (Barbacci E et al., 1999).

Constitutive inactivation of *Hnf1b* causes a severe disorganization of all embryonic and extraembryonic tissues, leading to embryonic lethality around E6.5 (Barbacci et al., 1999; Coffinier et al., 1999a). This early lethality is due to the absence of the visceral endoderm, an extraembryonic tissue essential for the nutrition and the hemopoietic function of the embryo. Chimera tetraploid morulae aggregation strategy, obtained by fusing blastomers at the 2cells stage, has been used to overcome the early lethality linked to its germline inactivation and further examine the role of Hnf1b during early organogenesis. This technique consists in the aggregation of *Hnf1b*-deficient embryonic stem (ES) cells with wild-type tetraploid embryos, which contribute exclusively to the formation of extraembryonic tissues, while the ES Hnf1^{-/-} will contribute to the embryo (epiblast). These studies confirmed that the early lethality is due to the absence of visceral endoderm formation and highlight the crucial role of Hnf1b in the establishment of this tissue and its importance for proper growth and differentiation of pregastrulating embryos (Barbacci et al., 1999).

1.3.2 Role of HNF1B during organogenesis

1.3.2.1 Pancreas

Hnf1b deficient embryos rescued by tetraploid aggregation show an absence of ventral pancreas and a significant reduction of the dorsal pancreas, which degenerates causing pancreatic agenesis at E13.5 (Haumaitre et al., 2005). At E11.5 the residual dorsal pancreatic bud of the mutant embryos expresses *Pdx1*, a very early pancreatic marker (Offield MF et al., 1996), and *Hlxb9*, which is a transcription factor involved in the dorsal pancreas specification (Harrison KA et al., 1999; Li H et al., 1999). On the other hand, the transcription factor *Ptfla*, which is involved in the pancreatic fate acquisition, is not detected (Lokmane L et al., 2008). These results show that Hnf1b is necessary for the specification of the ventral pancreas and the differentiation and proliferation of the dorsal pancreas. The conditional inactivation of *Hnf1b* in pancreatic progenitors with the Pdx1-Cre line highlighted the major role of this transcription factor in the morphogenesis of the pancreas. These mutants show significant

pancreatic hypoplasia associated with a decrease in the number of acinar cells, the formation of cysts at the level of the ducts and a defect in morphogenesis and generation of endocrine progenitors via the direct regulation of Ngn3. Interestingly ductal cells exhibit aberrant polarity and decreased expression of several cystic disease genes, including the known HNF1B targets *Pkhd1*, *Kif12*, *Bicc1* as well as the novel identified *Hnf1b* targets, *Cys1* and *Glis3* (De Vas et al., 2015). Conditional inactivation of *Hnf1b* in the β -pancreatic cells uncovered a later role of *Hnf1b* in glycolytic signaling using cells (Wang L et al., 2004). These mice present a normal level of insulin and glucose but their insulin secretion after glucose injection is impaired. The analysis of different markers revealed a deregulation of transcription factors involved in the differentiation of β -pancreatic cells including *Pdx1* and *Hnf4 α* .

1.3.2.2 Liver

Hnf1b is expressed very early in the liver primordium, in the hepatoblast and subsequently is restricted to the bile ducts. Rescued embryos by tetraploid aggregation show a lack of hepatic bud formation associated with the deregulation of the expression of genes encoding hepatic key transcription factors such as *Hnf4 α* , *Prox1*, *Foxa1*, *Foxa2* and *Foxa3*, thus revealing a critical role at the earliest steps of liver induction: the acquisition of endoderm competence and the hepatic specification (Lokmane L et al., 2008). Interestingly analysis of liver induction in zebrafish indicated a conserved role of HNF1B in vertebrates (Lokmane L et al., 2008) (see also chapter 1.7).

Conditional invalidation of *Hnf1b* in hepatocytes and the biliary system by using an *Alfp-Cre* mouse strain (Kellendonk et al., 2000) leads to a severe defect in intrahepatic biliary ducts development and metabolic abnormalities at E15-E18. Mutant mice also suffer from severe jaundice and hepatic metabolic effects (Coffinier C et al., 2002; Kellendonk C et al., 2000). A recent study has shown that in the absence of *Hnf1b* or *Hnf6*, the polarity of the bile duct cells is defective and is accompanied by a decrease in the expression of the cystic gene associated with the eyelash: *Cystin1* (*Cys1*) (Raynaud et al. al., 2011). These studies highlight the role of HNF1B in liver morphogenesis, lipid metabolism by hepatocytes and in the maintenance of the polarity of the bile duct epithelium.

1.3.2.3 Intestine

In mice, the specific inhibition of *Hnf1b* in the adult intestine lead to a lack of differentiation of the epithelial cells of the intestine followed by early lethality. This study demonstrates a

redundant role of Hnf1b and Hnf1a for the regulation of cell fate and function of the intestinal epithelium (D'Angelo et al., 2010). The combination of germline inactivation of Hnf1a associated to a intestinal specific inactivation of Hnf1b, leads to an impaired terminal differentiation of the secretory and absorptive lineage, due to a defective Notch signaling (D'Angelo et al. 2010). Moreover, studies on embryos rescued by tetraploid aggregation show a defect in the regionalization of the primary intestine in these mutants since they present an ectopic expression of *Sonic hedgehog (Shh)* associated with the absence of *Indian hedgehog (Ihh)* and *Pancreatic and duodenal homeobox 1 (Pdx1)* in the posterior stomach and the duodenum (Haumaitre et al., 2005; Lokmane L et al., 2008). .

1.3.3 HNF1B during kidney development

1.3.3.1 Overview of kidney development and function

Despite the crucial role of *Hnf1b* in mouse endoderm derived organs (pancreas, liver, intestine), its major site of expression is the kidney both during development and in adults. Consistently with the mouse studies described in the next chapter, the most common pathological features related to *HNF1B* heterozygous mutations in humans affect the kidneys. Since the thesis studies were focused essentially on the role of HNF1B in kidney development and disease, the development of this organ will be described more in-depth.

Kidney development in mice begins at embryonic day E10.5 and depends on an appropriate interaction between the ureteric bud (UB), which originally derives from the mesonephric duct (also called Wolffian duct, WD) and the adjacent metanephric mesenchyme (MM). The population of metanephric mesenchyme cells capping each branch encompass two lineage compartments: (A) nephron progenitors that produce all cell types of the nephron (from proximal podocytes to distal connecting segments) (Kobayashi A et al., 2008; Boyle S et al., 2008), and (B) interstitial progenitors that give rise to all interstitial cell types, mesangial cells within the glomerulus, vascular associated pericytes, and interstitial fibroblasts (Humphreys BD et al., 2010; Little MH et al., 2007). On the other hand, ureteric bud cells give rise to collecting ducts and the number of ureteric branches determines nephron number (Schedl A 2007).

A process of reciprocal signaling between the MM and the UB is the basis for renal development. UB undergoes branching morphogenesis to give rise to the renal collecting system composed of the ureter, renal pelvis and collecting duct. In parallel, groups of MM cells proximal to the ureteric bud tips, are induced to form the pretubular aggregates, which start epithelial transitions to form renal vesicles (RV) (McMahon AP et al., 2016). RV differentiates into the comma-shaped and then S-shaped bodies. S-shaped bodies finally elongate and differentiate into the various segments of the nephron (Dressler GR et al., 2004; Dressler GR et al., 2009; Kato N et al., 2009 bis) (**Figure 9**). As a consequence of this continuous process, primitive nephrons are found in regions close to the outer cortex, whereas more mature structures reside next to the medulla (Schedl A 2007). At the first postnatal week, nephrogenesis ceases and the number of mature nephrons present in each kidney is definitive. At this point, the mouse kidney (the mammalian kidney in general) looks like a complex organ comprising over 25 distinct cell types organized in tissues that accomplish a

large amount of tasks including blood filtration, regulation of blood pressure and pH, re-absorption of water and compounds required by the body.

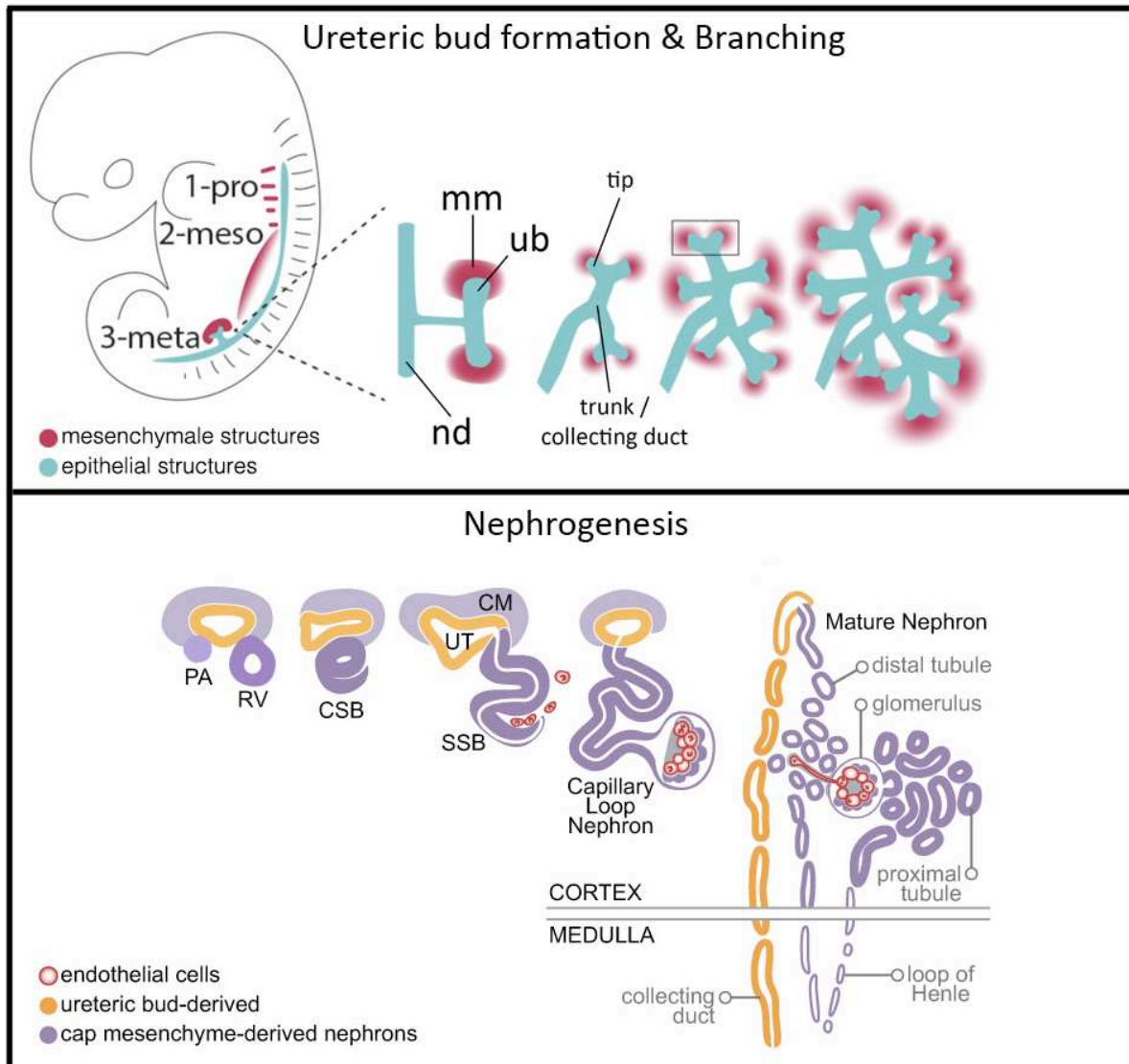


Figure 9. Ureteric bud formation, brunching and nephrogenesis. **Above:** renal morphogenesis in mouse; in red the mesenchymal structures, blue corresponds to epithelial structures. **Below:** Nephron formation in the kidney is simultaneous with ureteric tree branching. Schematic representation of the major stages of kidney development in mice. All nephrons in the kidney develop from cap mesenchyme (CM) cells (purple). To develop into a nephron, CM cells form a pretubular aggregate (PA), with each aggregate developing in a specific region of the kidney, underneath the tips (UT) of the growing ureteric tree. Subsequently, these mesenchymal aggregates differentiate into nephrons by undergoing a mesenchyme to epithelial transition (MET). The formed renal vesicles (RV) develop into comma-shaped bodies (CSB), S-shaped bodies (SSB) and capillary loop stage nephrons, which finally differentiate into mature nephrons. Each mature nephron is comprised of a glomerulus connected via distinct tubules to the collecting ducts, which drain into the pelvis of the kidney. The pelvis is connected to the bladder via the ureters. The collecting ducts develop from the ureteric tree epithelium (orange). ub, ureteric bud; mm, metanephric mesenchyme; nd, nephric duct; pa, pretubular aggregate; rv, renal vesicle;

csb, comma shaped bodies; ssb, S-shaped bodies; cm, cap mesenchyme; ut, ureteric tip (adapted from Little M 2010; Rumballe B et al., 2010; Desgrange A et al., 2017).

The mature nephron is the structural and functional unit of the kidney and it is segmented in different portion:

- **Glomerulus:** composed of an intricate arrangement of endothelial, mesangial and podocyte cells; it is responsible for the filtration of blood (**Figure 10**). The glomerulus is composed of a complex net of anastomosed capillaries surrounded by podocytes. The blood is filtered through a filtration barrier made by three layers: a fenestrated endothelial layer, a basal membrane and the filtration slits created by podocytes. This barrier is highly selective and allows only low molecular weight molecules to pass (small proteins or ions) meanwhile cells and high molecular weight proteins are normally retained in the circulation.

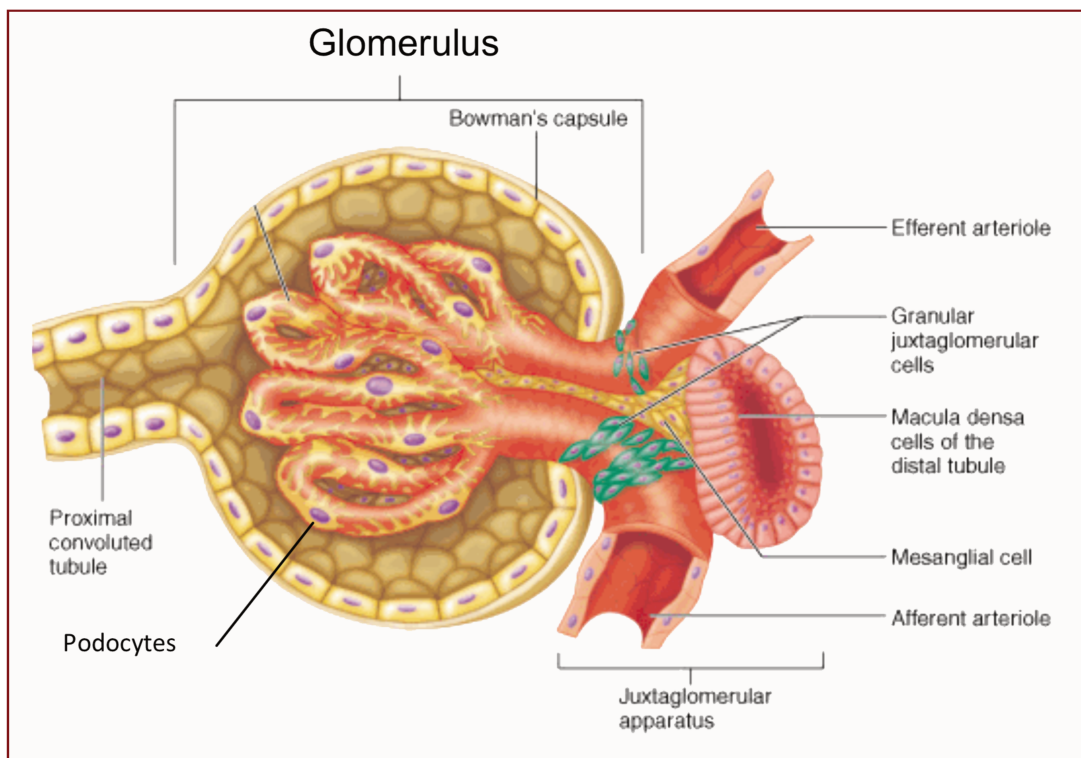


Figure 10. The Bowman capsule surrounds the glomerular tuft delimiting the urinary space. The macula densa cells are located between the afferent and efferent arterioles, associated to juxtaglomerular cells (adapted from Human Anatomy and Physiology, 5th Edition)

- **Proximal tubule (PT):** a segment located between the glomerulus and the loop of Henle. It is characterized by a brush-border that consists of densely packed microvilli that increase the surface area to reabsorb small molecules from the filtrate to the interstitium. It is responsible for passive and active resorption of solutes from the pre-urine.

- **Loop of Henle:** intermediate portion of the nephron between the proximal and the distal tubule. This tubular segment enters the medulla of the kidney and returns back to the cortex where it contacts its own glomerulus. Two functionally distinct limbs form the Henle's loop segment: the thin descending (TDL) limb and the thick ascending (TAL) limb of Henle. It is responsible for the resorption of water and ions from the pre-urine.

- **Distal convolute tubule (DCT):** a segment located after the Loop of Henle and connected to the collecting ducts. It continues to reabsorb useful solutes from the filtrate to the peritubular capillaries, actively pumping small molecules out of the tubule lumen into the interstitial space. It regulates the pH and salt concentration of calcium, potassium and sodium.

- **Collecting Duct (CD):** structure formed in the renal cortex by the connection of several nephrons. Collecting ducts enter in the cortex, penetrate the outer and the inner medulla where they successively fuse together to bring the urine produced by the nephrons into the ureter and finally in the bladder.

The four vital functions performed by kidneys thanks to its different structures are:

- (1) filtration of the blood and reabsorption of water, glucose, and amino acids from the filtrate;
- (2) excretion of wastes such as urea and ammonium;
- (3) regulation of the balance of electrolytes and acid base;
- (4) production of hormones, including calcitriol, erythropoietin, and the enzyme rennin, which modulates blood pressure.

A comprehensive picture of a mouse kidney and its structures is depicted in **Figure 11**.

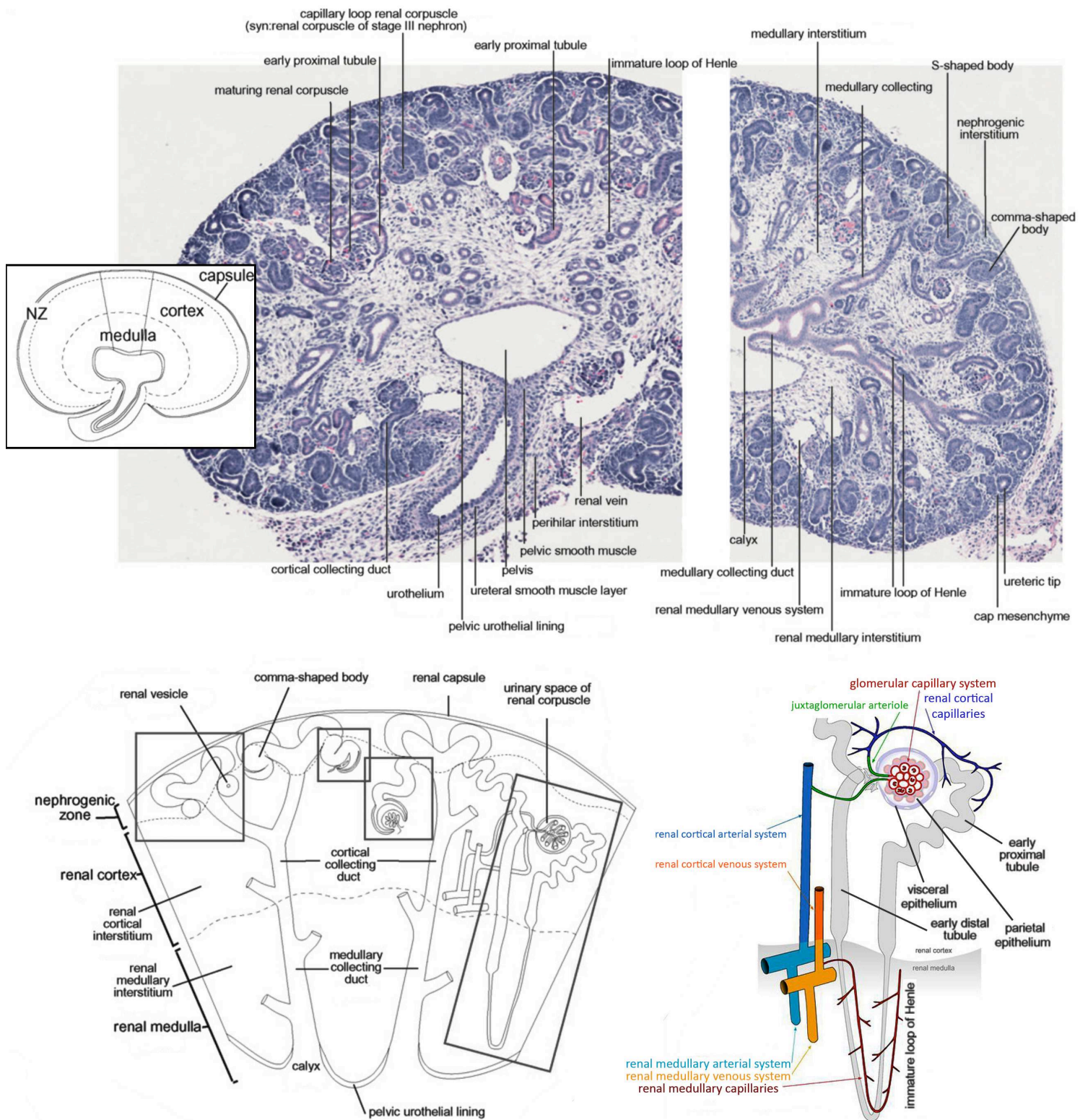


Figure 11. Diagram and histological sections of the complete murine metanephros at E15. The histology sections (haematoxylin and eosin) show sagittal sections through the metanephros and ureter (left) and just beyond the midline of the metanephros (right). Below (left): diagrammatic representation of a wedge of the E15 metanephros, from renal capsule to pelvis next to a maturing nephron structure. Below (right): nephron structure and vascularization (Adapted from gudmap.org and *Little MH et al., 2007*)

Macroanatomic features are conserved in the human and mouse, although with distinct organization, temporal/spatial dynamics and differences in associated gene expression (Lindström NO et al., 2018). 3D architecture and composition of human and mouse nephrogenic niches follow a similar developmental progression in their reduction of progenitor cells but proceed at different time-scales (Lindström NO et al., 2018). In the end, the human kidney generates approximately 1,000,000 nephrons (Bertram JF et al., 2011) whereas mouse around 16,000 (Short KM et al., 2014).

Interestingly and unlike the mouse, the human kidney is made up of multiple lobes (Oliver J 1968) and in human is possible to observe the formation of rosette-like clusters of ureteric tips, where nephrogenic niches face outwards away from the center (Lindström NO et al., 2018). Another major difference is related to the anchor genes that identify discrete structures in kidney; only three of 26 anchor genes conserved what appeared to be a “mouselike” expression pattern in the human kidney (Little MH et al., 2014).

1.3.3.2 HNF1B requirement for ureteric bud branching morphogenesis and nephrogenesis induction

Hnf1b transcripts and protein are detected in the WD epithelium and cranial mesonephric tubules at E9.5; at E10.5 *Hnf1b* is expressed in the epithelium of the emerging UB and UB branches and nascent nephrons (renal vesicles, Comma- and S- shaped bodies) (**Figure 12**). However, *Hnf1b* is not expressed in the MM. From E17.5 to the adult it is expressed in all tubular epithelial cells of the nephrons (but not in the glomeruli) and the collecting duct system.

Consistent with the early expression pattern, constitutive inactivation of *Hnf1b* in the epiblast leads to severe defects in UB branching and WD and Mullerian duct differentiation, in addition, the MM covering the extremities of the UB is unable to condense, to achieve the mesenchymal-epithelial transition (MET) and thus to initiate nephrogenesis. Transcriptional and ChIP-PCR studies suggest that HNF1B exert these functions, at least in part via the direct control of key regulators, including *Pax2*, *Lhx1* and *Wnt9*. In particular, acting directly upstream of *Wnt9b* control non-cell-autonomous Wnt-signaling and the initiation of nephrogenesis (Lokmane L et al., 2010) (**Figure 13**).

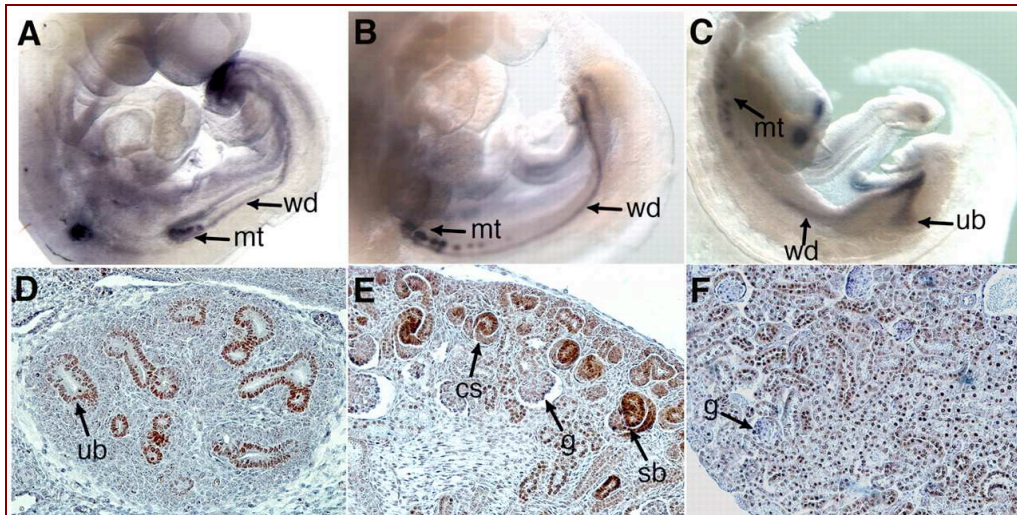


Figure 12. Expression pattern of *Hnf1b* during kidney development. Whole-mount in situ hybridization of *Hnf1b* in WT embryos at E9.5 (A), E10.5 (B) and E11.5 (C). Immunostaining of HNF1B on sagittal sections of the kidney at E13 (D), E17.5 (E) and in the adult (F). g, glomeruli; cs, comma-shaped bodies; mt, mesonephric tubules; sb, S-shaped bodies; ub, ureteric bud; wd, Wolffian duct (Adapted from Lokmane L et al., 2010).

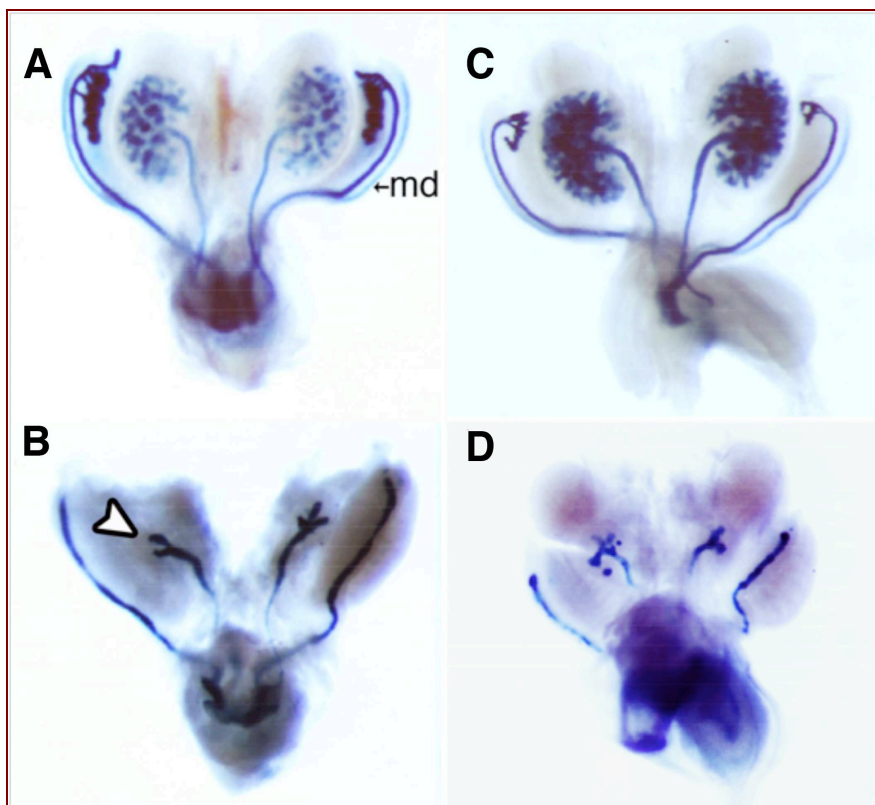


Figure 13. X-gal staining of WT *Hnf1b*^{lacZ} (A,C) and *Hnf1b*^{-/-} (B,D) urogenital tracts dissected at E13.5 (A, B) and E14.5 (C, D). At E14.5 homozygous mutants exhibited arrested UB branching, severe hypoplastic kidneys and hypertrophic adrenal glands. Note interrupted WTs and absence of mesonephric tubules. The white arrowhead in B shows the strong reduction in UB branching in mutants relative to heterozygous (A) (Adapted from Lokmane L et al., 2010)

1.3.3.3 HNF1B and patterning of early nephron structures

Inactivation of *Hnf1b* in pretubular aggregates using the *Wnt4-Cre* leads to rudimentary nephrons composed of a glomerulus connected to the collecting duct by a short tubule with distal like features. Major defects are at the S-shaped bodies, which exhibit defective morphology, associated with the downregulation of the Notch signalling components *Dll1*, *Lfng*, *Jag1* as well as the transcription factors *Irx1* and *Irx2* and *Hnf4 α* . Moreover, HNF1B was found recruited to the regulatory sequences of most of these genes (Heliot C et al., 2013). Interestingly, *Hnf1b* inactivation in early nephron progenitors (Cap mesenchyme) using the *Six2-cre* leads to similar defects in nephron segmentation and is also associated with the downregulation of *Irx1*, *Dll1*, *Osr2*, *Pou3f3* (Massa F et al., 2013). These studies show that *Hnf1b* is required for the acquisition of a proximo-intermediate segment fate in vertebrates and uncovers an unappreciated function of a novel SSB sub-compartment in global nephron segmentation and further differentiation (**Figure 14**). This role in nephron segmentation is conserved in Zebrafish (Naylor RW 2013) and in *Xenopus* embryos (Heliot C et al., 2013).

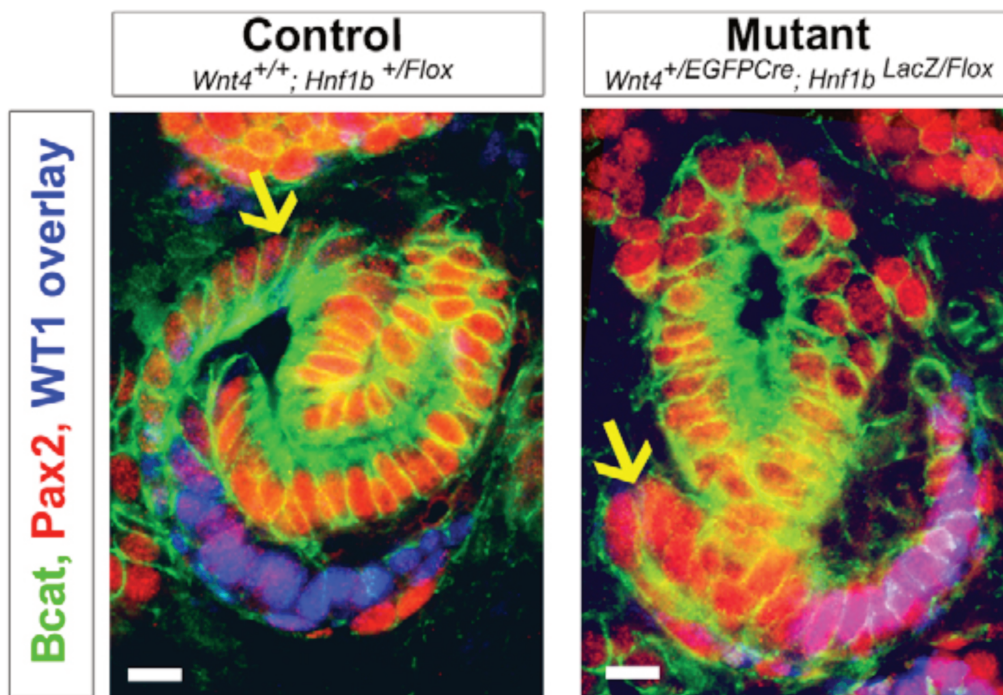


Figure 14. Abnormal morphology and regionalization of *Hnf1b* mutant S-shaped bodies (SSBs). Mutant SSBs exhibit abnormal morphology and regionalization. Immunostaining and ISH analyses on mouse E16.5 kidneys. Proximal tubule precursors are PAX2^{low} in controls but remain PAX2^{high} in mutants (yellow arrows) and co-express with WT1 (blue) (Adapted from Heliot C et al., 2013).

1.3.3.4 Collecting duct morphogenesis and cystic medullar tubules

Specific *Hnf1b* kidney inactivation was obtained using a *Ksp-cadherin-Cre* mouse line at a later time point when tubules have already formed but are still elongating (Gresh L et al., 2004). Adult transgenic mice from this line expressed Cre recombinase in medullar collecting ducts and thick ascending limbs of Henle's loops (Shao X et al., 2002). These mutants present a polycystic kidney phenotype associated with death by postnatal day 28 (Gresh L et al., 2004) (**Figure 15**). The involvement of HNF1B in the differentiation of tubular cells and cyst formation was also demonstrated using a transgenic mouse line expressing a dominant negative form of HNF1B under control of the Ksp-Cadherin promoter. (Hiesberger T et al., 2005). *Hnf1b* inactivation in medullar renal tubules is associated with the downregulation of genes involved in cystogenesis, including *Pkd2*, *Pkhd1*, *Nphp1*, *Tg737/polaris (Ift88)* and *Umod* (Gresh L et al., 2004), thus potentially linking the HNF1B transcriptional regulatory cascade to ciliogenesis.

By performing inducible inactivation of *Hnf1b* at different postnatal stages, *Verdeguer et al.* showed that inactivation just until P10, at a time when proliferative morphogenetic elongation is ongoing, cause cystic tubular dilations, (Verdeguer F et al., 2009). They propose a time window of action for HNF1B for the maintenance of renal tubule morphology. Moreover, they studied the role of the transcription factor after P10 forcing *Hnf1b* deficient quiescent cells to proliferate following induced lesions; in this conditions, cysts appeared showing a potential role of Hnf1b in cell proliferation for tissue reparation. This has been related to the role proposed for HNF1B as a “bookmarking factor” thus remaining attached to chromatin during mitosis and then reopening the chromatin of its target genes immediately after completion of cell division and activating transcription (Verdeguer F et al., 2009). It should be noted that similar findings were observed with other cystic disease genes as *Pkd1* (Piontek K et al., 2007). Although the molecular mechanism remains poorly understood, it appears in this case not to be related to cellular proliferation. Recently, *Desgrange A et al.* found the requirement of *Hnf1b* for the formation of a specialized UB tip domain through conditionally inactivation in the UB and collecting duct system. Using the *HoxB7-Cre* line allowing the conditional inactivation of *Hnf1b* in the entire WD and UB derivatives, they observed that HNF1B is required in cellular organization and epithelial polarity during UB branching and collecting duct (CD) morphogenesis. Molecular analysis reveals downregulation of Gdnf-Ret pathway components and suggests that HNF1B acts both upstream and downstream of Ret signaling by directly regulating the Ret-co-receptor *Gfra1* and the Ret direct target *Etv5*.

At later stages, *Hnf1b* deletion leads to massively mispatterned ureteric tree network, defective collecting duct maturation and disrupted tissue architecture, leading to cystogenesis and perinatal death. Late-stage embryos or P0 mutants exhibit severe urogenital abnormalities reminiscent of CAKUT (Desgrange A et al., 2017).

Expression of dominant-negative mutant HNF1B or kidney-specific knock-out of *Hnf1b* in mice reduces the levels of *Pkhd1* mRNA transcripts in the kidney via direct downregulation of *Pkhd1* promoter activity in renal collecting ducts (CDs) (Hiesberger T et al., 2004; Hiesberger T et al., 2005; Williams SS et al., 2014).

Aboudehen et al. showed that mice where *Hnf1b* was specifically deleted in renal collecting ducts at rather later stages using the *Pkhd1*/Cre reporter, survived long term and developed slowly progressive cystic kidney disease, renal fibrosis, and hydronephrosis. Moreover, they observed that treatment of HNF1B mutant mIMCD3 cells with hypertonic NaCl inhibited the induction of osmoregulated genes, including *Nr1h4*, which encodes the transcription factor FXR that is required for maximal urinary concentration (Aboudehen K et al., 2017). *Aboudehen K et al.*, further confirmed by chromatin immunoprecipitation and sequencing experiments that HNF1B binds to the *Nr1h4* promoter, suggesting an additional role of HNF1B in osmoregulation.

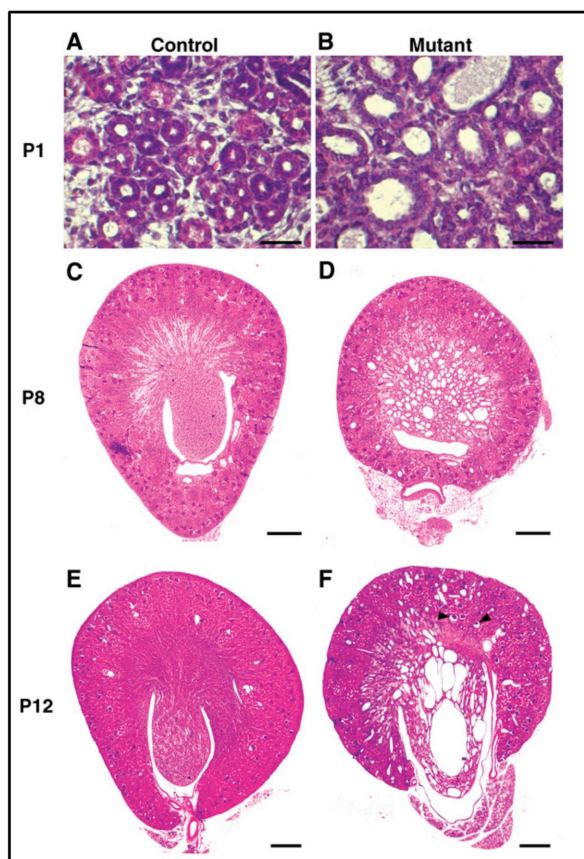


Figure 15. Inactivation of HNF1B in kidney cells leads to polycystic kidney disease. Kidney sections from control and mutant mice at P1 (A, B), P8 (C, D) and P12 (E, F) stained with hematoxylin–eosin. At P1 tubular dilations were visible in the medullary region of mutants, with an increased number of nuclei per tubule section compared to controls (B versus A). In mutants, the medulla was completely disrupted by large cysts by P8 (D). The size of cysts increased with age (F). A few glomerular cysts were observed in the deep cortex (F, black arrowheads). Scale bars: A, B: 100 mm, C–F: 400 mm (Adapted from Gresh L et al., 2004).

1.4 HNF1B regulatory network and gene targets

As mentioned in the precedent chapter several studies have been carried out to define the complex regulatory network of HNF1B involved in early UB branching, nephron segmentation, tubular epithelial morphogenesis, ion transport, and intrarenal metabolism. These studies were primarily performed in constitutive or conditional inactivation mouse models as well as in renal cellular systems combining with transcriptional profiling, in vitro assays and HNF1B ChIP assays.

Key HNF1B target genes involved in early branching morphogenesis and induction of nephrogenesis were identified by constitutive inactivation of *Hnf1b* in the epiblast and include *Pax2*, *Lim1*, and *Wnt9b* (Lokmane L et al., 2010). Further studies, showed that HNF1B directly controls the Ret-coreceptors *Gfra1*, and *Etv5* during the early steps of UB branching (Desgrange A et al., 2017).

During the differentiation of nascent nephrons from the Renal Vesicle stage, HNF1B was shown to control the Notch signaling components, *Dll1*, *Jag1*, *Lfng* and the transcription factors *Irx1-2*, *Pou3f3*, and *Hnf4a* thus contributing to the establishment of the regulatory network involved in the acquisition of proximo-medial fates during early nephron segmentation (Heliot C et al., 2013; Massa F et al., 2013) (**Figure 16**).

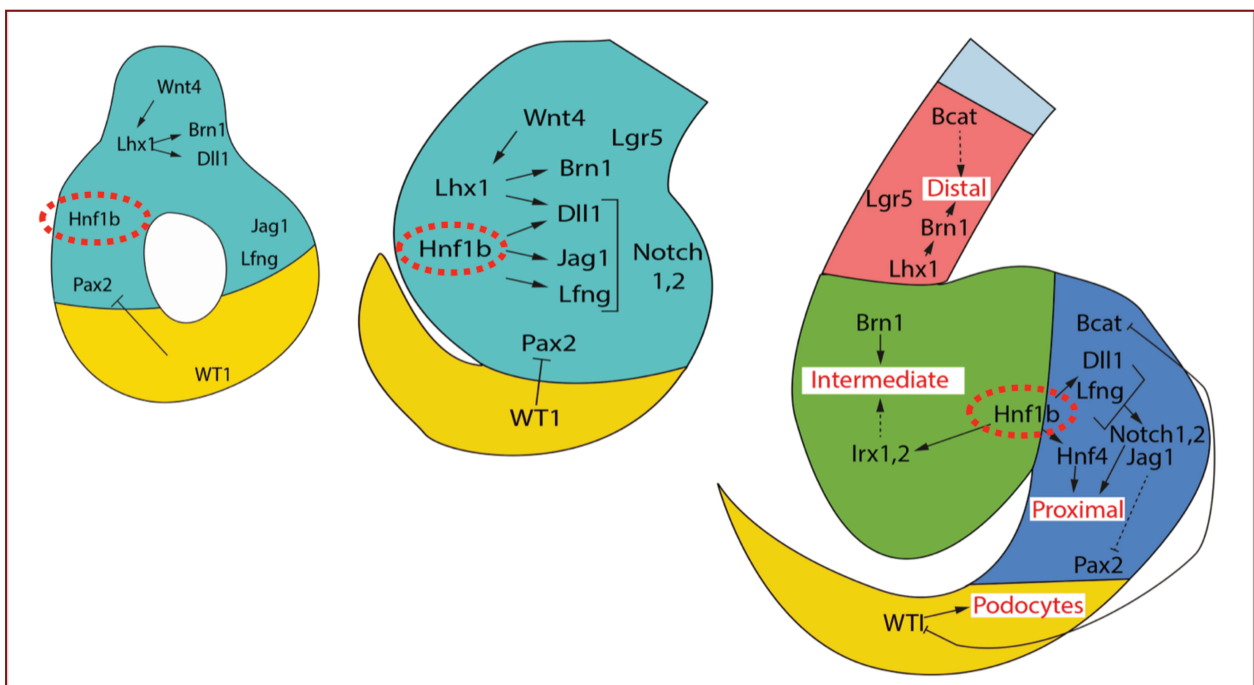


Figure 16. Proposed role of HNF1B in the nephron patterning regulatory circuit. Schematic representation of early nephron structures. First picture renal vesicle, RV; second picture comma shaped body (CSB); third picture S-shaped bodies divided in distal, intermediate and proximal SSB segments (Adapted from Desgrange A and Cereghini S, 2015).

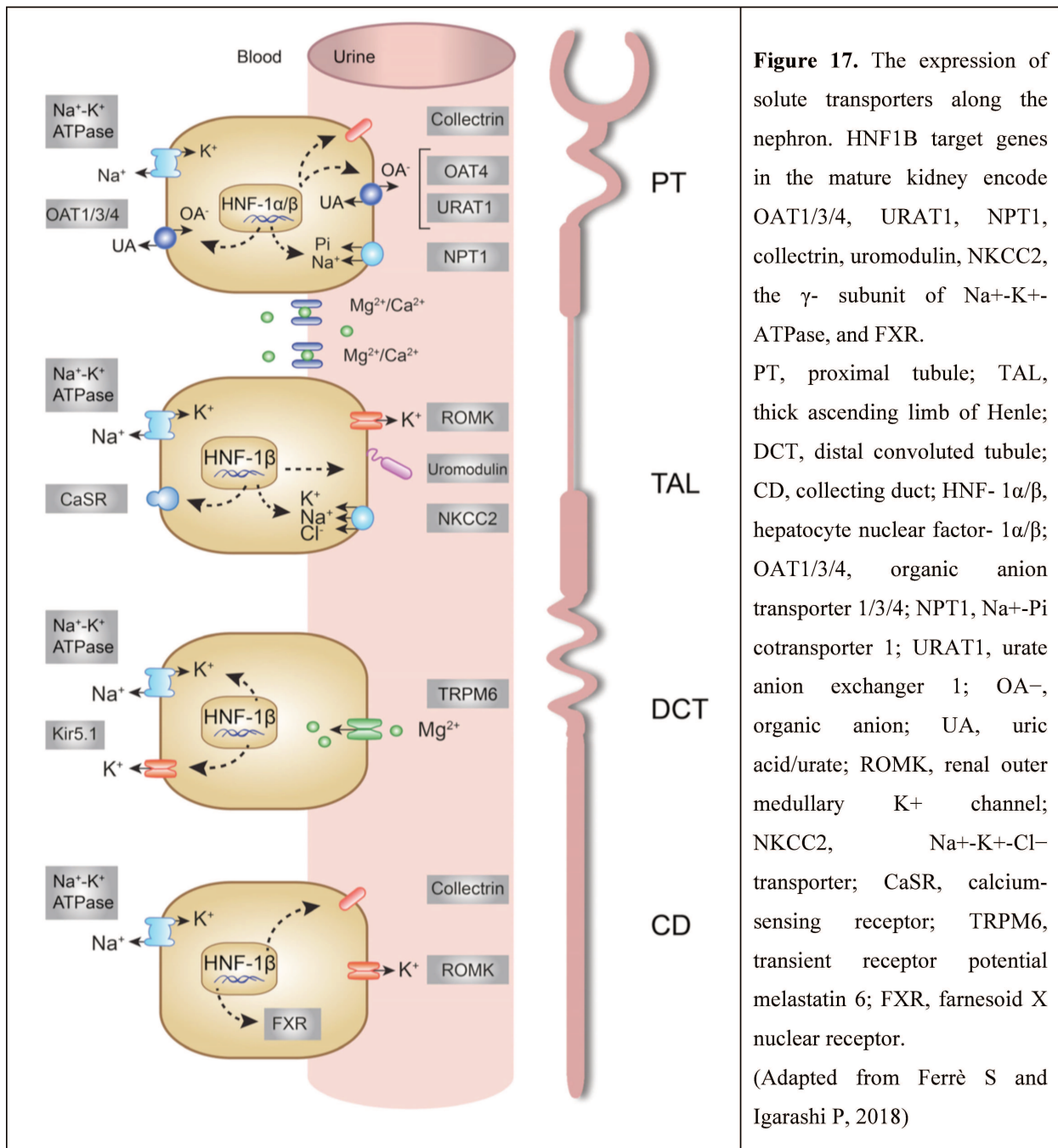
Notably, a direct transcriptional regulatory cascade has also linked HNF1B with several cystic disease genes; studies in postnatal cystic kidneys, upon *Hnf1b* inactivation in medullar renal tubules, reported reduced expression of genes including *Umod*, *Pkhd1*, *Pkd2*, *Nphp1* and *Tg377/Polaris (Ift88)* (Gresh L et al., 2004). Further *in vivo* ChIP experiments in adult kidneys confirmed that HNF1B is recruited on the regulatory regions of these genes.

In addition to control nephron patterning and renal tubular morphogenesis, HNF1B regulates different genes associated with ion transport as *FXYD2*, *KCNJ10*, and *UMOD*. Whereas a deregulation of *FXYD2*, encoding for the γ subunit of Na^+/K^+ -ATPase, is associated with hypomagnesemia in human patients (Adalat S et al., 2009; Ferrè S et al., 2011), impairment of *KCNJ10* function, that encodes for the K^+ channel Kir5.1, cause a salt-wasting syndrome characterized by hypomagnesemia and hypokalemia (Kompatscher A et al., 2017; Simon DB et al., 1996). HNF1B can directly regulate the transcription of *UMOD*, which is involved in K^+ handling (Gresh L et al., 2004). Moreover, the calcium-sensing receptor *CaSR* present in the TAL and contributing potentially to hypocalciuria in some RCAD patients (Kompatscher A et al., 2018) and the osmosensitive gene *FXR*, which is related to polyuria (Aboudehen K et al., 2017) were recently found as novel targets of HNF1B. Moreover, HNF1B directly regulates the proximal tubule urate transporter I (*URATI/SLC22A12*), which has been related hyperuricemia (Kikuchi R et al., 2007) and the trans-membrane transporter *TMEM27* gene, encoding collectrin, and whose disruption in mice result in a severe defect in renal amino acid uptake (Zhang Y et al., 2007; Desgrange A et al., 2017) (**Figure 17**).

The epithelial cell differentiation and the cell polarity are other domains handled by HNF1B as it has been shown to regulate *Crb3* (encoding crumbs homolog-3), *Bicc1* (encoding bicaudal C homolog 1) *AP-2 β* (*Tcfap2b*) (Verdeguer F et al., 2010), *Atp6v1b1*, *Slc26a4*, *Pdzk1*, *Aqp5*, *Hpn* and *Tmem27* (Desgrange A et al., 2017).

Recent findings correlated HNF1B with the intrarenal cholesterol metabolism as well as mitochondrial respiration of proximal tubule renal cells. Kidney-specific inactivation of HNF1B or the expression of dominant negative mutant HNF1B decreased the expression of genes that are essential for cholesterol synthesis, including sterol regulatory element binding factor 2 (*Srebf2*) and HMG-CoA reductase (*Hmgcr*) (Aboudehen K et al., 2015) (**Figure 18**).

Another intrarenal metabolic control by HNF1B is accomplished through the mitochondrial respiration in renal cells: in vitro experiments have shown that HNF1B regulates *PPARGC1A* and mitochondrial respiration, whereas ablation of *Hnf1b* in proximal tubule cells leads to a shift from oxidative phosphorylation to glycolysis (Casemayou A et al., 2017) (**Figure 19**).



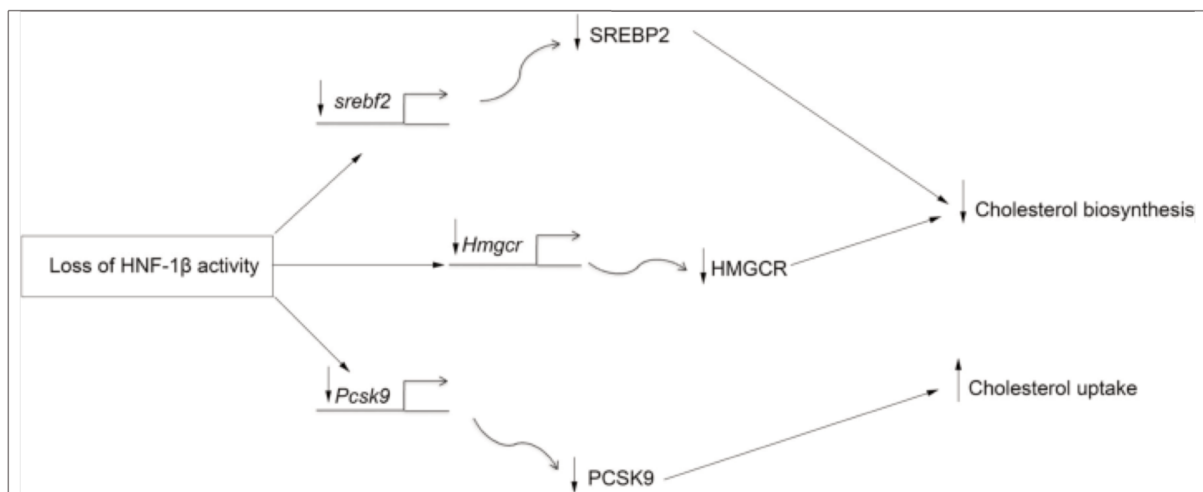


Figure 18. Multilevel regulation of renal cholesterol metabolism by HNF1B. Loss of HNF1B inhibits the transcription of genes involved in cholesterol synthesis either directly (*Hmgcr*) or indirectly through inhibition of *Srebf2*. In addition, loss of HNF1B inhibits the transcription of *Pcsk9*, which may increase cholesterol uptake (Adapted from Aboudehen K et al., 2015).

Function	BRANCHING	CYSTIC DISEASE GENES	NEPHROGENESIS	TRANSPORT
Target genes	Pax2 Lim1 Wnt9b Gfra1 Etv5	Pkhd1 Pkd2 Umod Nphp1 Tg377/Polaris (Ift88)	Dll1 Jag1 Lfng Pou3f3 Irx1/2 Hnf4a	Fxyd2 Kcnj10 Umod CaSR Tmem27/Osteopontin Nr1h4/Fxr Slc5a1/Slgt1 Slc5a2/Slgt2 Slc17a1/Npt1 Slc17a3/Npt2 Slc22a12/Urat1 Slc22a6/Oat1 Slc22a7/Oat3 Slc22a11/Oat4 Lrp2/Megalin Cubn/Cubilin
Function	EPITHELIAL POLARITY, DIFFERENTIATION AND PROLIFERATION	CHOLESTEROL METABOLISM	MITOCHONDRIAL RESPIRATION	OTHERS
Target genes	Crb3 Bicc1 Tcfab2b Atp6v1b1 Slc26a4 Pdzk1 Aqp5 Hpn Tmem27	Srebf2 Hmgcr	Ppargc1a	Kif12 Socs3 Cdh16 Ace2 Opn/Osteopontin Dpp4 Cd24

Figure 19. Major target genes of HNF1B in kidney. Genes directly controlled by HNF1B discovered in mouse or in cell lines divided for principal functions.

1.5 HNF1B transcriptional homologs, cofactors and coactivators

HNF1B functions as a homodimer or heterodimer with the structurally related protein **HNF1A** (Frain M et al., 1989; Chouard T et al., 1990), with which it shares more than 50% of the amino acid sequence (Cereghini S et al., 1996) (**Figure 20**). The two heterologous proteins appeared presumably by duplication of a common ancestral gene as they map to parts of the genome known to have duplicated in early vertebrate evolution, namely 12q24.31 (HNF1A, near LHX5 and on the same arm as the HOXC cluster) and 17q12 (HNF1B between LHX1 and the HOXB cluster). HNF1A, also known as HNF1 or TCF1, is encoded by a gene of 10 exons whose locus in the chromosomes 12 and 5 in human and mouse respectively (Holland PW et al., 2007). Overexpression experiments in different cell types showed that HNF1A and HNF1B can regulate gene transcription via binding the same consensus sequence (Liu H et al., 2010). However, it seems that HNF1B has lower transcriptional activation efficiency than HNF1A (Bach I et al., 1993; Rey-Campos J et al., 1991). *Mendel DB et al.* demonstrated that the 12kDa cofactor **DCoH** (Dimerisation Cofactor of HNF1, also known as pterin-4 alpha-carbinolamine dehydratase, **PCDB1**) interact with HNF1A-HNF1B dimers forming a tetrameric structure that stabilize the complex (Mendel DB et al., 1991 bis; Rose RB et al., 2000). PCDB1 is also important for renal Mg²⁺ imbalances as it regulates the HNF1B-mediated FXYD2 transcription, influencing active renal Mg²⁺ reabsorption in the distal convolute tubule (Ferrè S et al., 2014).

An increase in the transcriptional activity of HNF1B has been described in the case of interactions in the C-terminal transactivation domain with histone acetyltransferases such as **CBP** [cyclic adenosine monophosphate (cAMP)-responsive element binding protein (CREB) binding protein], and **P/CAF** [p300/CBP-associated factor], **SRC-1** and **RAC3** (Soutoglou E et al., 2000; Barbacci E et al., 2004). HNF1B is also able to interact *in vitro* and *in vivo* with **HDAC1** histone deacetylase (Barbacci E et al., 2004). **Zyxin** is another HNF1B cofactor, which form a transcriptional complex that include CBP, binding to the POU domain and the C-terminal transactivation domain of HNF1B (Choi YH et al., 2013).

A functional association of the N-terminal domain of HNF1B with two other regulatory proteins, **ZFP36L1** (predominant in the cytoplasm, activator) and **E4F1** transcription factor (predominant in the nucleus, inhibitory), has been shown. Their overexpression in *Xenopus* embryos leads to defects in pronephros formation suggesting their control of HNF1B during kidney development (Dudziak K et al., 2008).

HNF1B	1	MVSKLTSLQQELLSALLSSGVTKEVLVQALEELLSPNFGVKLETPLSPGSGAEPDTKP	60
		MVSKL+ LQ ELL+ALL SG++KE L+QAL E P P + + E PL G +	
HNF1A	1	MVSKLSQLQTELLAALLLESGLSKEALIQUALGE--PGP-YLLAGEG-PLDKGESCG-GGRG	55
HNF1B	61	VFHTLTNGHAKGRLSGDEGSDDGDDYDTPPILKELQALNTEAAEQRAEVDRLSEDPWR	120
		L NG + R S DE +DG+D+ TPPILKEL+ L+ EEAA Q+A V+ +L EDPWR	
HNF1A	56	ELAELPNGLGETRGESEDETDDDGEDF--TPPILKELENLSPEEAAHQKAVVETLLQEDPWR	114
HNF1B	121	AAKMIKGYMQQHNIHQREVVDVDTGLNQSHLSQHLNKGTPMKTQKRAALYTWYVRKQREIL	180
		AKM+K Y+QQHNIHQREVVD TGLNQSHLSQHLNKGTPMKTQKRAALYTWYVRKQRE+	
HNF1A	115	VAKMVKSYLQQHNIHQREVVDVDTGLNQSHLSQHLNKGTPMKTQKRAALYTWYVRKQREVA	174
HNF1B	181	RQFNQTVQSSGNMTDKSSQDQLLFLFPEFSQQSHGPGQSDDACSEPTNKKMRRNRFKWWP	240
		+QF Q G + ++ + D+L PT KK RRRNRFKWWP	
HNF1A	175	QQFTHAGQ--GGLIEEPTGDEL-----PT-KKRRNRFKWWP	208
HNF1B	241	ASQQILYQAYDRQKNPSKEEREALVEECNRAECLQRGVSPSKAHGLGNSLVTEVRVYNWF	300
		ASQQIL+QAY+RQKNPSKEERE LVEECNRAEC+QRGVSPS+A GLGNSLVTEVRVYNWF	
HNF1A	209	ASQQILFQAYERQKNPSKEERETLVEECNRAECIQRGVSPSQAQGLGNSLVTEVRVYNWF	268
HNF1B	301	ANRRKEEAFRQKLAMDAYS--SNQTHSLNPLLSHGSPHHQPSSSPPNKLSGVRYSQGN	358
		ANRRKEEAFR KLAMD YS L +H SP P + P+K+ GVMRY Q +	
HNF1A	269	ANRRKEEAFRHLAMDYSGPPPGPGPALPAHSSPGLPPPALSPEKVGVRYPGQPAT	328
HNF1B	359	EITSSSTISHHGNSAMVTSQSVLQQVSPASLDPGHLLSPDGKMISVSGGGLPPVSTLTN	418
		E ++ + +VT + L QVSP L+P H+LLS + K++S +GG LPPVSTLT	
HNF1A	329	E---TAEVPSSSGGPLVTVSTPLHQVSPGLEPSHLLSTEAKLVAAGGPLPPVSTLTA	385
HNF1B	419	IHSLSHHNP---QQSQNLIMTPLSGVMAIAQ-----SLNTSQAQS	455
		+HSL +P QQ QNLIM L GVM I L ++QAQS	
HNF1A	386	LHSLEQTSPLNQPNLIMASLPGVMTIGGEPASLGPTFTNTGASTLVIGLASTQAQS	445
HNF1B	456	VPVINSVAGSLAALQPVQFSQQLHSPHQPLMQQSPGSHMAQQPFMAAVTQLQNSH-MYA	514
		VPVINS+ SL LQPVQFSQ LH +QQPLM SH+ Q PFMA + QLQ+ H +Y+	
HNF1A	446	VPVINSMGSSLTTLQPVQFSQQLHPSYQQPLMPV-QSHVTQSPFMAATMAQLQSPHALYS	504
HNF1B	515	HKQEPPQYSHTSRFPSAMVVDTSSTLTMSSSKQ	551
		HK E QY+HT P M++TDT+++S L +++ +KQ	
HNF1A	505	HKPEVAQYTHTGLLPQTMLITDTTNSALASLTPKQ	541

Figure 20. NCBI protein blast of human HNF1A and HNF1B show 54% of amino acid identity (314 on 577)

1.6 Regulation of HNF1B

In order to better understand the regulation of *Hnf1b*, the promoter of this gene has been cloned and analyzed (Power SC and Cereghini S, 1996). This study reveals five sites of interaction between DNA and proteins at the first 260 base pairs upstream of the transcription initiation site involving at least three major families of transcription factors. Two of these sites are particularly important for the activity of the promoter. Gel delay and transient transfection experiments show that several members of the steroid hormone receptor family such as **HNF4 α** , **COUP-TF1/Ear3**, **COUPTFII/Arp1** as well as retinoic acid receptors **RXR** and **RAR** may play a role in the regulation of *Hnf1b* expression. In addition, a proximal Octamer protein binding site (OCT) is required for transactivation of *Hnf1b* by **COUP-TF1/Ear3** and **COUP-TFII/Arp1**. Several studies suggest that HNF1B is a mediator downstream of retinoic acid signaling. Indeed, *Hnf1b* is induced in the embryonic carcinoma cells F9 after treatment with retinoic acid. In addition, retinoic acid appears necessary for the induction of *Hnf1b* and *Hoxb1* for the establishment of the identity of the rhombomers and the r4/r5 border, but also during the development of the endocrine pancreas of the zebrafish (Hernandez RE et al., 2004; Sirbu IO et al., 2005; Song et al., 2007). A highly conserved 800-bp enhancer element located in the fourth intron of *Hnf1b* integrating direct inputs from the retinoic acid signaling cascade and MAF-related factors was identified (Pouilhe M et al., 2007).

The recruitment of HNF4 α on the *Hnf1b* promoter was confirmed by chromatin immunoprecipitation (ChIP) in human hepatocytes and pancreatic islets (Boj SF et al., 2001, Odom DT et al., 2004). However, it does not appear that this factor is essential to the expression of *Hnf1b*. It has been shown that **PDX1** is able to bind to the *Hnf1b* promoter in the embryonic pancreas and that mice deficient for Pdx1 show a decrease in *Hnf1b* suggesting that PDX1 participate in the transcriptional regulation of *Hnf1b* in pancreatic progenitors (Oliver-Krasinski JM et al., 2009). In addition, **HNF6** transactivates the *Hnf1b* promoter in vitro and also during the development of bile ducts and pancreatic ducts (Clotman F et al., 2002; Pierreux CE et al., 2006; Poll AV et al., 2006). Despite a number of studies, it remains to determine which regulatory elements are involved in the induction of *Hnf1b* expression during kidney and endoderm derived tissues during development as well as in adult tissues.

1.7 The conservation of HNF1B in other species

Formation of the basic nephron with its segments took place probably more than 360 million years ago in a common ancestor of mammals and amphibians (Schedl A 2007). Since then, many evolutionary events succeeded until the arrival of the transcription factor HNF1B. No orthologue of the HNF1 factors exists in the invertebrates (**Figure 21**). On the other hand, different studies on vertebrates such as *Danio rerio* (Gong HY et al., 2004; Song J et al., 2006), *Salmo salar* (Deryckere F et al., 1995), and *Xenopus laevis* (Bartkowski S et al., 1993; Zapp D et al., 1993; Demartis A et al., 1994; Heliot C et al., 2013) showed similarity with mice in the expression pattern and its corresponding role in their organogenesis.

In zebrafish, *hnf1b* expression pattern is remarkable relative to mice and begins early during embryogenesis between stage 256 and 1000 cells (Sun and Hopkins 2001). *Hnf1b* expression was shown in gut, liver, pancreas (Sun and Hopkins 2001; Gong HY et al., 2004; Lokmane L et al., 2008), hindbrain (Wiellette EL et al., 2003) and pronephric duct (Naylor RW et al., 2013). Tubular cysts have been observed in the pronephric tubules of *hnf1b*-mutated zebrafish (Sun and Hopkins 2001).

In *Xenopus* embryos, *hnf1b* start to be expressed in the pronephros, in liver and pancreas (Raciti D et al., 2008) and transgenic expression of HNF1B carrying human mutations in the DNA binding domain leads to pronephros abnormal development (Bohn S et al., 2003). *Wu et al.* showed that three domains must be present in the mutated protein to obtain a reduction in the pronephros; these include the dimerization domain, the 26 amino acid segment specific for splice variant A as well as the POU_H domain. (Wu G et al., 2004). Moreover, the role of *Hnf1b* in morphogenesis of all nephron segments was confirmed in *Xenopus* (Heliot C et al., 2013) as well in Zebrafishi (Naylor RW et al., 2012).

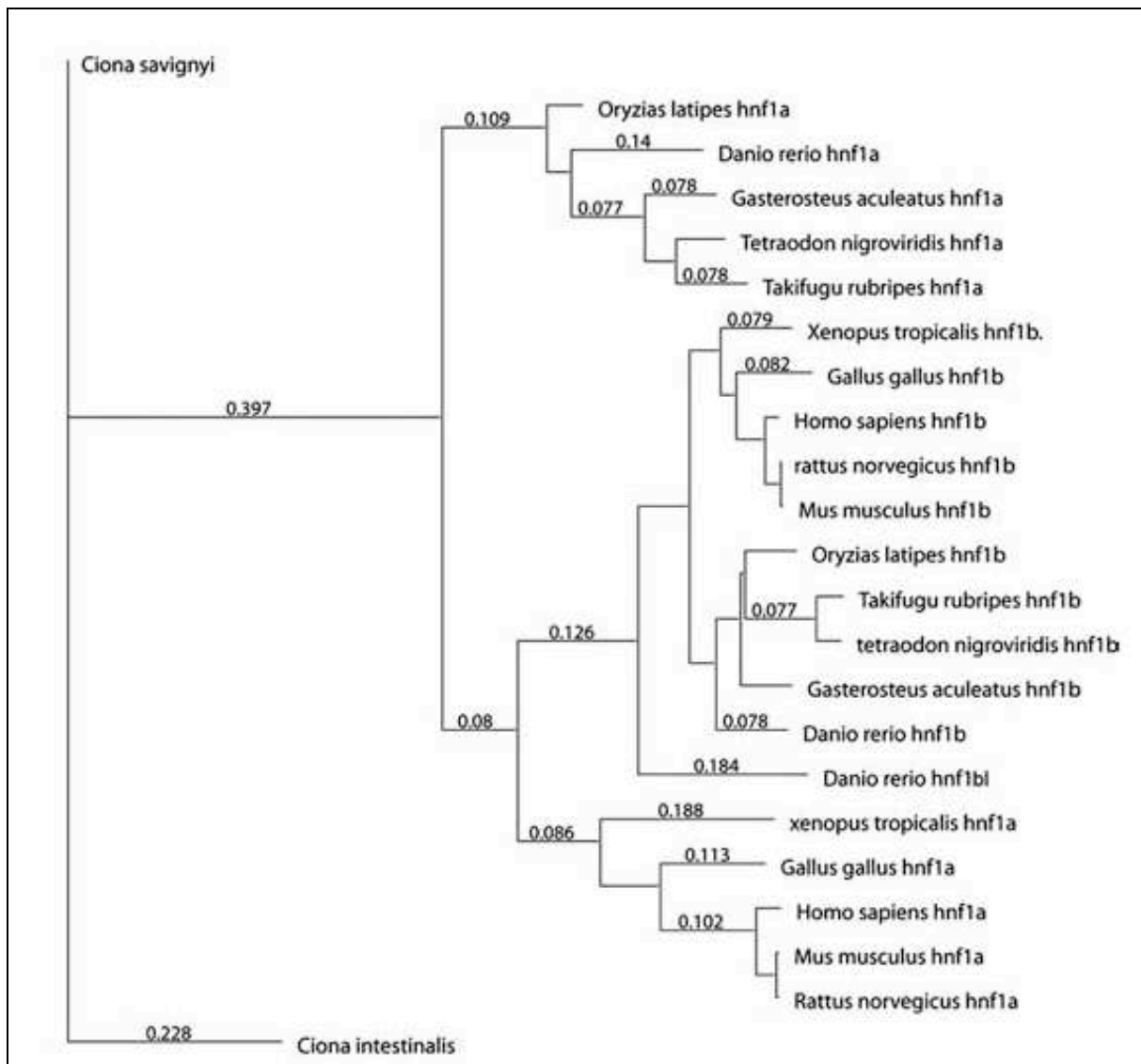


Figure 21. Comparative alignments of Hnf1b genomic sequences from different species reconstructs its phylogenetic history and show its conservation during evolution

CHAPTER 2. Renal Cysts and Diabetes syndrome

2.1 HNF1B expression in human

Not only the amino acid sequence of HNF1B is strongly conserved from mouse to human (96% conservation), but also its expression pattern, which is consistent with its epithelial differentiation role during early human organogenesis. Studies on human fetuses carrying *HNF1B* mutations revealed a fundamental function during kidney, urogenital tract and pancreas development (Haumaitre C et al., 2006; Kato N et al., 2009; Duval H et al., 2016; Haldorsen IS et al., 2008; Body-Bechou D et al., 2014). In situ hybridization (ISH) of a 56-day gestation human embryo, which corresponds to gestation day 15 (E15) in the mouse, revealed that *HNF1B* is highly expressed in the fetal metanephric kidney and in epithelium of the lung, pancreas, biliary duct, duodenum, stomach, and Müllerian duct with no expression in mesenchyme of the same organs (Haumaitre C et al., 2006). ISH of a human fetus at 91-days of gestation further highlighted *HNF1B* expression in medullar and cortical collecting ducts as well as primitive nephron tubules of the metanephric kidney (Kolatsi-Joannou M et al., 2001) (**Figure 22**). Immunohistochemistry analysis for HNF1B confirmed these findings (Kato N et al., 2009). At 25 weeks this expression profile is maintained.

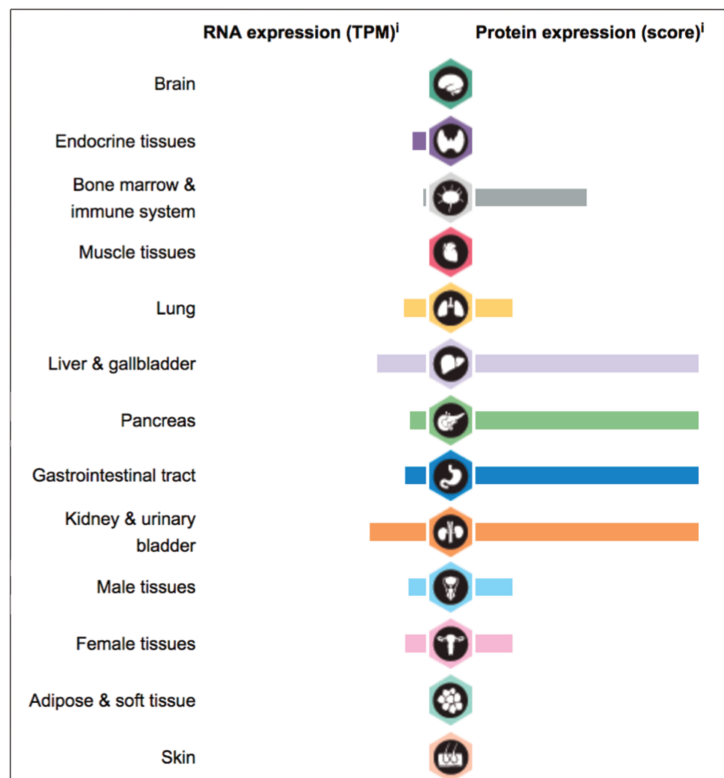


Figure 22. HNF1B RNA and protein expression. Graph representing HNF1B RNA and protein expression in human (source proteatlas.org)

2.2 Overview of the RCAD syndrome

Consistent with multiorgan expression pattern of HNF1B, heterozygous mutations of hepatocyte nuclear factor 1B gene (*HNF1B*), were reported associated with the Renal Cysts and Diabetes Syndrome (RCAD, OMIM #137920) (Bingham C et al., 2001), originally referred Maturity Onset Diabetes of the Young type 5 (MODY5) (Horikawa Y et al., 1997). The disease is inherited in an autosomal dominant fashion (Bingham C et al., 2004) and is characterized by a wide range of phenotypes encompassing multiple organs (reviewed by Chen YZ et al., 2010; Clissold RL et al., 2015). The most prominent clinical features in HNF1B-associated syndrome are developmental kidney disease and diabetes mellitus. Besides, other manifestations include genital tract malformations, pancreas and liver structural anomalies and dysfunctions, and electrolytes imbalances. *HNF1B* mutations are also associated with two autosomal dominant disorders: the Hypoplastic Glomerulocystic Kidney Disease (GCKD) and the Autosomal Dominant Tubulointerstitial Kidney Disease (ADTKD).

The phenotype of *HNF1B* mutant carriers is highly variable both within and between families and no correlation was observed between the type or position of a given mutation and the severity of the phenotype. These observations led to the hypothesis that non-allelic factors, as well as stochastic variation in temporal *HNF1B* gene expression and environmental factors, could bring the strong intrafamilial variability of RCAD patients (Edghill EL et al., 2006; Clissold RL et al., 2015). The origin of the pathology can, therefore, be associated with a reduction of the HNF1B activity with haploinsufficiency being the main disease mechanism. In the following part of the chapter, the various phenotypes observed in RCAD patients are described individually (**Figure 23**).

2.3 HNF1B mutations and genetic analysis

The first mutation in *HNF1B* (R177X) was identified in 1997 as a monogenic diabetic gene (Horikawa Y et al., 1997). Subsequently, more than 150 mutations have been described in *HNF1B* gene including gross deletions (34% - 56%), missense mutations (31% - 24%), frameshift deletions, insertions or exon duplication (15% - 9,7%), nonsense mutations (11% - 4,5%), and splice-site mutations (8% - 5,1%) (Alvelos MI et al., 2015; Dubois-Laforgue D et al., 2017) (*Figure HNF1B gene transcript with known mutations*). Analysis in large cohort of patients (Bellanné-Chantelot C et al., 2005; Chen YZ et al., 2010; Edghill EL et al., 2006) identified two hot spot of mutations in the dimerization and in the binding domain: the first in the exon 2 and the second in the exon 4. Importantly, about 30-50% of *HNF1B* mutations occur *de novo* explaining the absence of a family history in many patients (Heidet et al., 2010; Weber S et al., 2006). To date no association was demonstrated between the type or position of the mutation and particular clinical features.

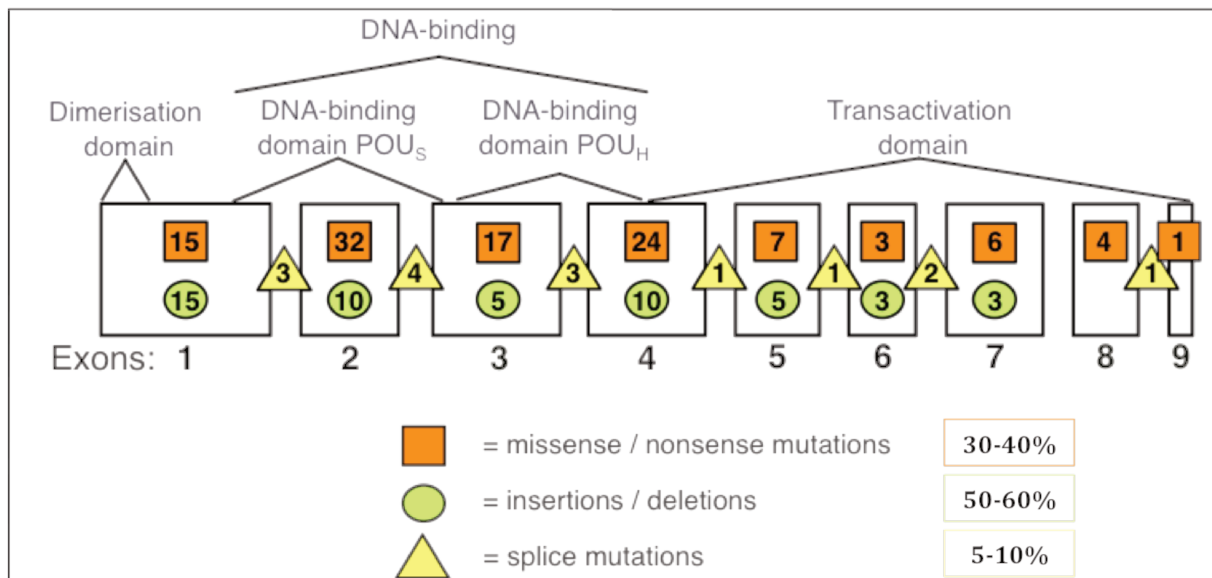


Figure 23. The mutations shown in the graph are registered in the Human Gene Mutation Database (Stenson PD et al., 2003, accessed on 20 February 2018); they are grouped by three mutation types within the nine exons and splice sites of the gene: missense/nonsense mutations, insertions/deletions, and splice mutations. The numbered white boxes correspond to the exons, and the different functional domains are shown above the gene transcript. The colored boxes correspond to the number of registered mutations up to date. The whole gene deletions are not depicted. Abbreviations: POU_S, POU specific; POU_H, POU homeodomain.

2.4 RCAD clinical features (Figure 25)

2.4.1 Renal abnormalities

HNF1B mutations are found in 20-30% of fetuses with renal abnormalities representing the most frequent prenatal cause of hyperechogenic kidneys (Bingham C et al., 2004; Decramer S et al., 2007) and represent the most frequent genetic cause of renal malformation during childhood (Heidet L et al., 2010; Ulinski T et al., 2006). *HNF1B*-related abnormalities have been recognized to cause congenital anomalies of the kidney and urinary tract (CAKUT) (Nakayama M et al., 2010; Madariaga L et al., 2013; Raaijmakers A et al., 2015), predominantly affecting bilateral renal malformations.

The most common kidney abnormality implicates the formation of cysts in the renal tubules, and the acronym RCAD (Renal Cysts And Diabetes) has been created to highlight this main feature together with diabetes. The cystic spectrum, observed in the majority of RCAD patients (62% Faguer S et al., 2011; ~75% Bingham C et al., 2002 and Dubois-Laforgue D et al., 2017; 83% Edghill EL et al., 2006), includes simple cysts, multicystic renal dysplasia, and glomerulocystic kidneys. The cysts may appear on a renal ultrasound (mostly in the renal cortex), they are usually small in size (Ulinski T et al., 2006) and were not reported to progressively increase in number over time (Faguer S et al., 2011).

In addition to cysts, other renal morphological anomalies have been reported as renal hypoplasia, renal agenesis, oligomeganephronia, solitary kidneys, horseshoe kidneys, and hydronephrosis (Ulinski T et al., 2006; Chen YZ et al., 2010; Clissold RL et al., 2015). Prenatal renal anomalies encompass renal failure, oligohydramnios and pulmonary hypoplasia (Madariaga L et al., 2013) and genetic variants in *HNF1B* are predicted to be the most common cause of isolated renal hypodysplasia in fetuses and children (Weber S et al., 2006; Thomas R et al., 2011). Renal interstitial fibrosis can be also present in RCAD patients and has been associated with a highly variable rate of decline of estimated glomerular filtration rate (eGFR) (Heidet L et al., 2010; Bellanné-Chantelot C et al., 2004; Edghill EL 2006). Kidney disease can get worse progressing from chronic kidney disease (CKD) to kidney failure, also called end-stage renal disease (ESRD) (Edghill EL et al., 2008) and between 13 and 20% of RCAD adult patients develop ESRD (Chen YZ et al., 2010; Faguer S et al., 2011; Dubois-Laforgue D et al., 2017). CKD has been reported in children (1-5%) (Verbitsky M et al., 2015; Thomas R et al., 2011) as well as in adults (15-40%) (Chen YZ et al., 2010; Dubois-Laforgue D et al., 2017; Musetti C et al., 2014).

2.4.2 Renal physiological imbalances

Physiological imbalances in plasma and urine include hypocalciuria, hypermagnesuria, hypomagnesemia (Adalat S et al., 2009; Heidet L et al., 2010; Faguer S et al., 2011; Verhave JC et al., 2015; van der Made CI et al., 2015), hyperuricemia (Bingham C et al., 2003; Dubois-Laforgue D et al., 2017) and hypokalemia (Faguer S et al., 2011). The prevalence of hypomagnesemia ranges drastically in different studies: 25% (Raaijmakers A et al., 2015), 44% (Adalat S et al., 2009), 45-60% (Faguer S et al., 2014), 72% (Ferrè S et al., 2013), 75% (Dubois-Laforgue D et al., 2017). Urinary magnesium wasting could be related to *HNF1B* transactivation role on *FXRD2* gene, which encodes the γ subunit of the $\text{Na}^+\text{-K}^+\text{-ATPase}$ involved in the reabsorption of Mg^{2+} in the distal convoluted tubule (Adalat S et al., 2009; Ferrè S et al., 2011). Potassium depletion may be related to magnesium depletion as a decrease in intracellular Mg^{2+} concentrations may lead to the release of inhibition of renal outer medullary potassium channel (ROMK) causing K^+ wasting (Yang L et al., 2010). Patients with *HNF1B* mutations display hyperuricemia and some present also early onset gout (Bingham C et al., 2003); also in these cases, the bibliography does not show the same values, attesting hyperuricemia between 11,6% and 63% (Chen YZ et al., 2010; Dubois-Laforgue D et al., 2017; Verhave JC et al., 2015; Bingham C et al., 2003). Gout is predicted between 20% and 27% (Verhave JC et al., 2015, Bingham C et al., 2003). It has been shown that a decrease in uric acid excretion was associated with mutations in the gene *UMOD*, encoding uromodulin (Bingham C et al., 2003; Heidet L et al., 2010); abnormal urate transport followed by elevated serum acid concentration, which leads to hyperuricemic nephropathy in some RCAD patients, could be related to *UMOD* gene misregulation since *Hnf1b*-conditional inactivation in mouse renal tubules results in reduced transcriptional activation of *Umod* (Gresh et al., 2004).

Proteinuria and microalbuminuria have also been reported in ~25% and ~30% of subjects of *HNF1B* mutant carriers respectively (Dubois-Laforgue D et al., 2017).

2.4.3 Diabetes

Mutations in *HNF1B* could lead to the monogenic form of diabetes called maturity-onset diabetes of the young type 5 (MODY5). However, *HNF1B* mutations account for only ~1-5% of MODYs (Beards F et al., 1998; Sadler TW et al., 1990; Edghill EL et al., 2013). Diabetes mellitus is the most frequent extra-renal feature present in *HNF1B*-associated patients and it is diagnosed at ~24 years old (Chen YZ et al., 2010). A diagnosis can be done sometimes also

during the neonatal period (Yorifuji T et al., 2004; Edghill EL et al., 2006 beta). Different studies evaluated the prevalence of diabetes in RCAD patients showing that it is still an ambiguous value among HNF1B-associated patients: 45% (Chen YZ et al., 2010), 48% (Faguer S et al., 2011), 56% (Bingham C et al., 2002), 60% (Edghill EL et al., 2008), 77% (Bellanné-Chantelot C et al., 2004), 82% (Dubois-Laforgue D et al., 2017).

The pathophysiology of diabetes in HNF1B mutations carriers is related to β -cell dysfunction and insulin resistance. The first results in reduced insulin secretion probably due to pancreatic hypoplasia and/or to a decrease in the number of β -cell available at birth (Haldorsen IS et al., 2008, El-Khairi R et al., 2016), the second is correlated with reduced insulin sensitivity to endogenous glucose production in RCAD patients (Pearson ER et al., 2004; Brackenridge A et al., 2006).

2.4.4 Pancreas morphological abnormalities and exocrine dysfunctions

Pancreas disorders could be divided into morphological abnormalities and exocrine dysfunctions. Pancreas structural abnormalities have been found in ~10% of RCAD patients (reviewed in Chen YZ et al., 2010; Dubois-Laforgue D et al., 2017) and encompass pancreatic hypoplasia (Haumaitre C et al., 2006; Haldorsen IS et al., 2008), atrophy, calcifications, pancreas divisum, ring pancreas, malrotation, intraductal papillary mucinous tumor and rarely cysts (Chen YZ et al., 2010). Pancreas exocrine dysfunctions are often subclinical as reduced Vitamin D and E concentration, or fecal elastase concentration (Bellanné-Chantelot C et al., 2004; Haldorsen IS et al., 2008).

2.4.5 Liver dysfunctions

Liver dysfunctions manifest as asymptomatic increase in levels of liver enzymes, such as alanine aminotransferase (ALT), aspartate aminotransferase (AST), alkaline phosphatase (ALP), leucine aminopeptidase (LAP), and γ -glutamyl transferase (GGT) in ~15% of RCAD patients (Chen YZ et al., 2010) but the percentage can increase drastically according to the different studies (71% Dubois-Laforgue D et al., 2017, 84% Bellanné-Chantelot C et al., 2004). On the other hand, liver structure anomalies as cholestasis (Beckers D et al., 2007), fibrosis, steatosis, and hepatomegaly account for less than ~5% (Chen YZ et al., 2010). Imaging evaluations highlighted abnormal biliary duct and biliary cysts in patients (32% Dubois-Laforgue D et al., 2017) and electron microscopy has shown a reduction of primary cilia on the epithelial cells of the bile duct (Roelandt P et al., 2012).

2.4.6 Genital tract abnormalities

Genital malformations are found in almost 14% of *HNF1B*-associated patients and are detected preferentially in females (~18%) than in males (~10%) (reviewed by Chen YZ et al., 2010). The prominent feature in female patients is uterus development abnormalities, which cover uterus agenesis, bicornuate uterus, and didelphic uterus (Avni FE et al., 2010; Chen YZ et al., 2010). In a cohort of females with congenital uterine abnormalities, *HNF1B* heterozygous mutations were detected in nine of 108 patients (8.3%) (Oram RA et al., 2010).

In male patients, genital tract abnormalities could be presented as cryptorchidism, testicular hypoplasia, vas deferens agenesis, epididymal cysts, enlarged seminal vesicles, hypospadias/phimosis, and asthenospermia (Bingham C et al., 2002; Bellanné-Chantelot C et al., 2004; Faguer S et al., 2011; Chen YZ et al., 2010).

HNF1B mutations could also lead to failure of the fusion of the Müllerian ducts producing rare congenital uterine and upper vaginal abnormalities or aplasia; this indicates *HNF1B* as a candidate gene for Mayer-Rokitansky-Küster syndrome (Bernardini L et al., 2009; Ledig S et al., 2010). Moreover, *HNF1B* mutations were found in two of 34 individuals (5,8%) with prune-belly syndrome, which is characterized by bilateral undescended testes, a triad of dilatation of the urinary tract and deficiency or absence of the abdominal wall musculature (Murray PJ et al., 2008; Haeri S 2010; Granberg CF 2011).

2.4.7 Other clinical features

Neurodevelopmental disorders have been associated with a 1.4 Mb deletion at chromosome 17q12, counting 15 genes including *HNF1B*. In a wide cohort of 15,749 patients with autism spectrum disorders or cognitive impairment, this deletion was found in 18 subjects (1.1%) (Moreno-De-Luca et al., 2010) suggesting that one or more of these genes in the deleted interval is dosage sensitive and essential for normal brain development and function. Findings suggested that prevalence of autistic spectrum disorders recorded in the general pediatric population (1:150-1:300) is lower than in cases of patients with whole gene deletions of *HNF1B* and cystic kidney disease (3:53). For this reason, nephrologists should be aware of this potential association and refer to psychiatric counseling in uncertain situations (Loirat C et al., 2010).

Different studies suggest that lack of *HNF1B* expression is related to chromophobe RCC (Rebouissou S et al., 2005; Lebrun G et al., 2005; Terasawa K et al., 2006; Wang CC et al., 2012). Moreover, overexpression of *HNF1B* has been found frequently in clear cell ovarian cancer (Tsuchiya A et al., 2003; Kato N et al., 2006; Kato N et al., 2007) and prostate

cancer (Berndt SI et al., 2011; Gudmundsson J et al., 2007). These observations suggest that HNF1B could act both as a tumor suppressor gene and as an oncogene, depending on the cellular context.

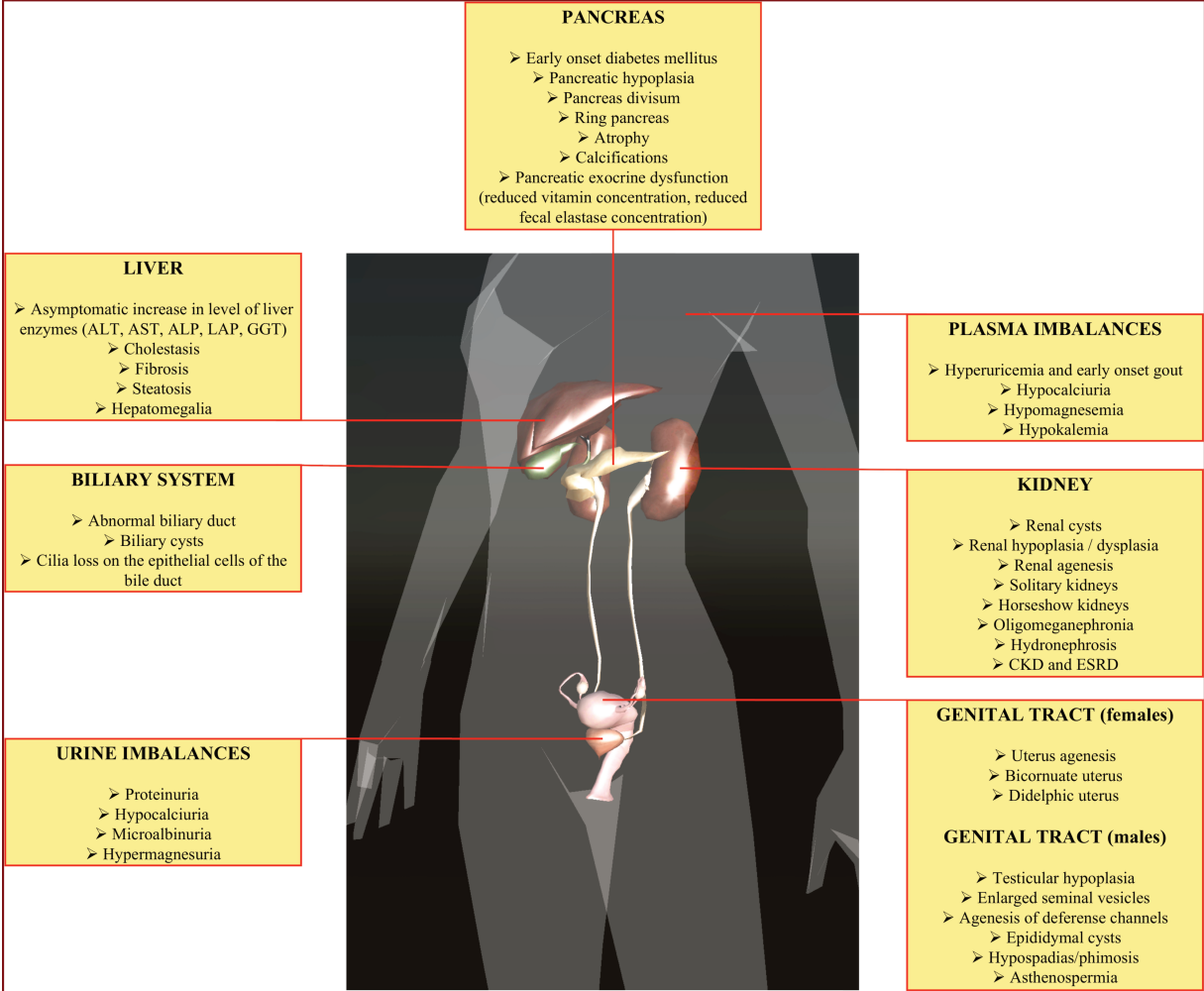


Figure 25. Schematic of renal and extra-renal phenotypes observed among patients with *HNF1B* heterozygous mutations (source: Organs 3D Anatomy APP)

2.5 RCAD diagnosis and treatment

There are presently no clear directives on which patients should be genetically tested to confirm the diagnosis. In general, nephrologists might request a genetic test to confirm *HNF1B* heterozygous mutations in patients referred with a suspected diagnosis of autosomal dominant polycystic kidney disease, medullary cystic kidney disease, diabetic nephropathy, or CKD of unknown cause (Clissold RL et al., 2014; Verhave JC et al., 2015). Other clinical features except for renal and glucose metabolic disorders as genital tract malformations, gout and elevated liver enzymes (Chen YZ et al., 2010), should provide extra clues to genetic testing analyses and early clinical intervention. Proteinuria is also a feature of RCAD syndrome as it has been found in almost one on three patients with *HNF1B*-associated disease (Dubois-Laforgue D et al., 2017). Importantly, mutations can occur spontaneously so family history may be absent. Because of this lack of familiarity in about 50% of patients and the intrafamilial variability, the prevalence of *HNF1B* gene mutations in the general population is unknown and it is probable that a large portion of RCAD patients was not recognized (Hattersley AT et al., 1998, Raaijmakers A et al., 2015).

Even if no casual therapy exists, an early diagnosis of RCAD syndrome is paramount for multiple reasons: to prevent unnecessary examination reducing costs to the healthcare system, to make (family) screening for diabetes, renal function decline, hypomagnesemia, to follow the degree of renal impairment and the presence of diabetes, to prevent diabetes complications and cardiovascular risk factors, to avoid the manifestation of gout adapting a diet and to prepare patients psychologically to potential limitation in their life (like a lack of a reproductive apparatus) (Verhave JC et al., 2015; Dubois-Laforgue D et al., 2017). *Faguer S et al.* have developed the most efficient tool to select patients for genetic analysis based on 17 clinical, imaging, and biological variables related to RCAD syndrome like renal hyperechogenicity, cystic kidney, MODY, pancreatic hypoplasia etc. (sensitivity 98,2%, specificity 41,1%) (Faguer S et al., 2014). The observations about the difficulty in recognizing the syndrome highlight the requirement for an improved method of patient selection for genetic testing. In fact, RCAD patients could be misdiagnosed with other diseases for similar features in common. First, the most frequently observed phenotype in fetuses with the *HNF1B*-gene mutation is isolated bilateral hyperechogenic kidneys of normal or slightly increased size (Ulinski et al., 2006; Decramer S et al., 2007); this phenotype is common with ARPKD, ADPKD, maternal induced diseases, infection, ischemia, metabolic diseases, dysplasia, and nephrotic syndromes. After birth, some patients with *HNF1B*

mutations would meet the diagnostic criteria for familial juvenile hyperuricemic nephropathy (Verhave JC et al., 2015) as different patients with *HNF1B* mutations present early-onset gout and kidney disease. The RCAD disease can mimic also polycystic kidney disease especially in the prenatal setting and early childhood (Bergmann C et al., 2014). *HNF1B* mutations could even mimic Gitelman syndrome because of the concomitant hypomagnesemia and hypocalciuria (Verhave JC et al., 2015). *Dubois-Laforgue D et al* hypothesized that some patients might be misdiagnosed as having type 1 diabetes at onset (Dubois-Laforgue D et al., 2017). RCAD patients with CKD in combination with renal cysts are easily falsely diagnosed as autosomal dominant polycystic kidney disease (ADPKD) or medullary cystic kidney disease (MCKD). *HNF1B*-associated disease in CKD patients with diabetes is frequently misdiagnosed as diabetic nephropathy, CKD with gout and/or hyperparathyroidism is easily misdiagnosed as complications secondary to CKD itself. In all the cases the presence of multiorgan symptoms should help in being alert for the RCAD syndrome.

Three main methods have been developed to analyze the *HNF1B* gene:

- 1) direct sequencing of proximal promoter and intron exon-junctions
- 2) QMPSF (Quantitative Multiplex PCR of Short Fragments)
- 3) MLPA (Multiplex Ligation-dependent Probe Amplification)

The first method is used to detect mutations primarily within the coding sequences as well as the splicing mutations, the two following methods are used to detect deletions or exonic duplications. As whole gene deletions are responsible for the most of cases (Decramer et al., 2007; Bellane-Chantelot et al., 2005; Alvelos et al., 2015; Dubois-Laforgue D et al., 2017) the search for a complete deletion by QMPSF is now the first molecular analysis followed by a direct sequencing in case of deletion absence.

The treatment is dependent on the degree of renal impairment and the presence of other features such as diabetes. Most of patients with *HNF1B*-associated diabetes mellitus need treatment with insulin as they respond poorly to sulphonylureas in contrast to *HNF1A*-associated diabetes (*MODY3*) (El-Khairi R et al., 2016). Renal transplantation should be considered for patients who require renal replacement therapy. (Pearson ER et al., 2004; Chen YZ et al., 2010).

2.6 Molecular mechanisms underlying the RCAD disease

The molecular mechanism by which heterozygous mutations in *HNF1B* produce the disease has been debated especially for the lacking of genotype-phenotype correlation even between members of the same family with identical mutations, suggesting haploinsufficiency as the underlying disease mechanism as mentioned in the chapter 2.3 (Clissold RL et al., 2014).

The production of dominant-negative mutant products has been proposed as a possible mechanism on the basis of in vitro functional analysis of several mutations either affecting DNA binding or within the C-terminal transactivation domain and preventing the recruitment of coactivators (Barbacci E et al., 2004; Igarashi P et al., 2005). An apparent gain-of-function mutation has been also reported (Wild W et al., 2000) leaving still open the molecular mechanisms by which *HNF1B* heterozygous mutations are responsible for the syndrome. It is worth noting that transgenic mouse overexpressing in the developing kidney a truncated version of *Hnf1b* functions in vivo as a dominant negative mutation (Igarashi P et al., 2005).

Yet, it is unknown whether the putative truncated mutant proteins encoded by the mutated *HNF1B* allele are produced in vivo or are unstable and degraded. Note also that not all intragenic mutations are predicted to function as dominant mutations and the potential dominant negative effect therefore does not explain the non-correlation between the type and position of the mutation and the phenotype

A recent study made by Dubois-Laforgue D et al. on 201 patients with *HNF1B* heterozygous mutations, showed marked differences in the phenotypes of the patients with *HNF1B* deletion compared with those with mutations (Dubois-Laforgue D et al., 2017): patients with the whole gene deletion were leaner than those with *HNF1B* point mutations and present a more severe diabetes phenotype. On the other hand, patients with *HNF1B* mutations had a poorer renal prognosis than those with a whole gene deletion (lower eGFR and higher frequency of CKD3-4 or ESRD), a more frequent need of renal transplantation, and a less frequent normal function at follow-up. The authors suggested that some intragenic *HNF1B* mutations might exert a dominant negative effect that results in a more severe phenotype, which as mentioned above still do not explain the non correlation genotype-phenotype. Alternatively,, the cause of this difference could be the lost of the protective effect from genes in the 17q12 deletion and the lost of other genes *predisposing to renal disease*. In fact, deletions in the 17q12 can encompass 15 genes (*AATF*, *ACACA*, *C17orf78*, *DDX52*, *DHRS11*, *DUSP14*, *GGNBP2*, *HNF1B*, *LHX1*, *MRM1*, *MYO19*, *PIGW*, *SYNRG*, *TADA2A*, and *ZNHIT3*). Interestingly no genotype/phenotype correlations in the two groups were

observed for kidney morphology, pancreas morphology and exocrine function, plasma C-peptide concentrations, liver tests, and genital tract abnormalities. Similar results concerning renal impairment were observed in patients with HNF1B deletions or mutations, but in smaller cohorts of patients. Other two publications from 2010 and 2016 (Heidet et al., 2010; Clissold RL et al., 2016) showed similar results concerning renal impairment in patients with *HNF1B* deletions or mutations, but in smaller cohorts of patients.

There are several additional potential mechanisms by which heterozygous mutations in HNF1B lead to variable pathogenic phenotypes, including:

- Single nucleotide polymorphisms (SNPs) in non-coding regions may affect the stability of HNF1B mRNA and/or HNF1B gene expression;
- Additional mutations in other genes that share the same biological pathways as HNF1B may either compensate or worsen HNF1B haploinsufficiency;
- Gene modifiers that either aggravate or increase the severity of phenotype as it has been identified for several diseases (Cutting GR 2010);
- Additionally, proteins interacting with HNF1B as cofactors or coactivators may present own variations depending on the patients; so, lack of interaction between mutated HNF1B and its partners may contribute to the misregulation of HNF1B functionality (Barbacci E et al., 2004; Hiesberger T et al., 2005; Soutoglou E et al., 2000) as observed for PCBD1 mutations (Ferrè S et al., 2014). Finally and related to this, the dysregulation of micro RNAs (miRNAs) targeting HNF1B or controlled by HNF1B, may also be involved in the disease phenotype.

Until now, the lack of mouse models that reproduce the RCAD syndrome at the heterozygous state has been a major limitation. Similarly, heterozygous mutations in HNF1A, HNF4A, and GATA6 lead to diabetes in humans, but have no effect in mice. It is known that diseases prompted by haploinsufficiency are more common in humans than in mice but molecular studies are still necessary to uncover the reasons. This variation in phenotype may exist because of species-specific differences in the dosage of the transcription factor that is needed for full function (El-Khairi R et al., 2016). Alternatively as in the case of *Hnfl* mutant mouse models, the mutations introduced do not replicate the human mutations and this could be another major lack in reproducing molecular events leading to a disease state.

The laboratory has generated a mouse model of RCAD syndrome introducing a human splicing mutation in *Hnflb* gene. Our phenotypic analysis of this model show that the heterozygous mutants for the splicing mutation exhibit several features of the human RCAD pathology. Although not replicating entirely the RCAD disease to our knowledge this mouse

line represent the first *Hnf1b* model that manifest a RCAD like phenotype at the heterozygous state, thus allowing to examine the consequences of the *Hnf1b* mutation in the context of the whole organism. In the Results section (Topic 1), a manuscript will be presented describing the development and the features of this model in detail with a major interest on the renal abnormalities, the main feature of the RCAD syndrome.

Furthermore, recent studies have demonstrated that HNF1B is recruited on the regulatory sequences of the miR-200 gene and directly controls the transcription of the miR-200b~429 cluster via a long non-coding RNA (Hajarnis SS et al., 2015). At the same time *Hnf1b* was reported to be controlled by several microRNAs (Kornfeld JW et al., 2013; Patel V et al., 2013). Taking in consideration this new tight molecular control, which may shed more light on HNF1B gene network and regulation, we decided to search for miRNAs potentially regulated by this transcription factor as well as microRNAs targeting HNF1B. This study will be described in detail in a separate section of Results (Topic 2).

CHAPTER 3. microRNAs and renal diseases

3.1 Overview of microRNAs

A microRNA is a small non-coding RNA molecule of ~22 nucleotides that negatively regulates gene expression at post-transcriptional level of numerous organisms including fungi, algae, plants, insects and animals (Bartel DP 2004; Griffiths-Jones S et al., 2008). The first microRNA (abbreviated miRNA), lin-4, was discovered in 1993 in *Caenorhabditis elegans* (Lee RC et al., 1993) but only in the early 2000s miRNAs were recognized as a real class of biological regulators able to silence gene products (Reinhart BJ et al., 2000; Pasquinelli AE et al., 2000; Lagos-Quintana M et al., 2001). Since then, hundreds of miRNAs were characterized and together with siRNAs (small inhibitory RNAs) and piRNAs (PIWI interacting RNAs) they constitute the small noncoding RNA world (Ghildiyal M and Zamore PD 2009). miRNAs induce gene silencing via base pairing to complementary sequences present on target molecules (mRNA or lncRNA) (Ameres SL and Zamore PD 2013). Considering that a single microRNA may regulate more than a hundred mRNAs (Rajewsky N 2006; Bartel DP 2009) and that microRNAs appear to target about 60% of all mammal genes (Friedman RC et al., 2009), the size of this regulation appear extremely elaborated. Recent analysis indicates the number of functional microRNAs in human at around 600 (Fromm B et al., 2015). Most of miRNAs are located within the cell, but some miRNAs (commonly known as circulating miRNAs), have been found in extracellular environment, including various biological fluids and cell culture media (Weber JA et al., 2010; Boeckel JN et al., 2014), thus potentially serving as powerful tools for diagnosis and treatment (Kaucsár T et al., 2010).

3.2 microRNA biogenesis

miRNAs are the final product of a multi-step biogenesis process (Bartel DP 2009) and their biogenesis may be resumed in four steps:

- i. transcription;
- ii. nuclear processing;
- iii. nuclear exportation;
- iv. cytoplasmic processing

i. Transcription.

miRNAs can be classified into four groups according to their genomic location: they are encoded either from non-coding or coding transcription units, and in both cases they can be intronic or exonic (Kim VN et al., 2009) (**Figure 26**).

Interestingly, about the 30% of mammalian miRNAs are clustered and transcribed into a single pri-miRNA (primary transcript of the polycistronic miRNA) (Lee Y et al., 2004).

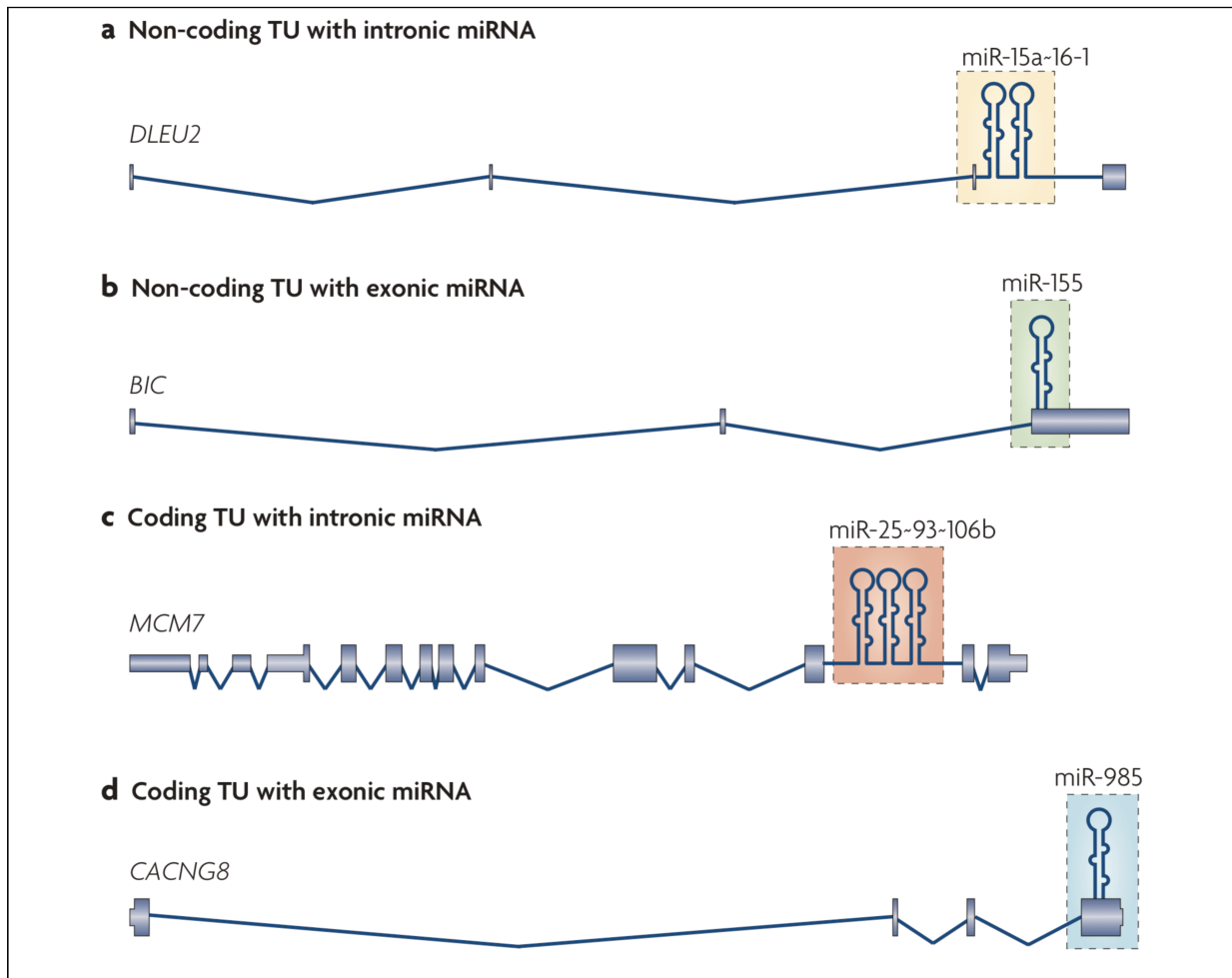


Figure 26. Genomic localization of miRNAs. MicroRNAs can be classified into four groups according to their genomic location: a) intronic miRNAs in the non-coding transcripts (40%); b) exonic miRNAs in non-coding transcripts (10%); c) intronic miRNAs in protein-coding transcripts (40%); d) exonic miRNAs in protein non coding transcripts (10%). TU, transcript unit (source: Kim VN et al., 2009)

The first transcription product made usually by RNA polymerase II (Lee Y et al., 2004) is called primary miRNA (pri-miRNA), which is between 500 and 3000 nt long and presents a 5' cap and a polyadenylated 3' tail (Cai X et al., 2004). The partial internal complementarity

within pri-miRNAs leads to the formation of stem-loop structures. A single pri-miRNA may contain more miRNA precursors clustered together.

ii. Nuclear processing.

The nuclear protein DiGeorge Syndrome Critical Region 8 (DGCR8), which associated with the enzyme Drosha forming the Microprocessor Complex (**Figure 27**), recognizes this double strand hairpin structure. Drosha is a RNase III dsRNA endonuclease that catalyze the cropping of the stem-loop structure producing the precursor miRNA (pre-miRNA), a short hairpin RNA of ~70 bp (Ha M and Kim VN 2014). Pre-miRNAs that are spliced directly out of introns, bypassing the Microprocessor complex, are known as mirtrons.

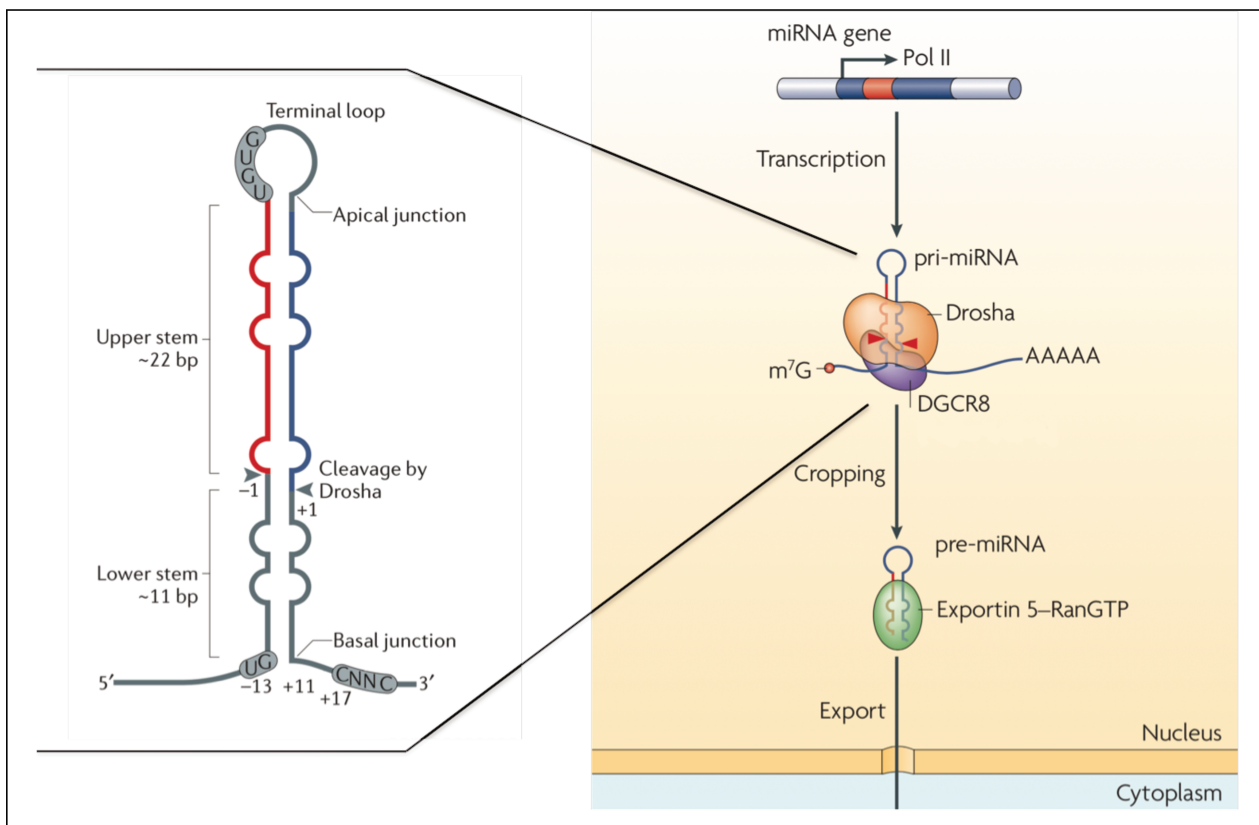


Figure 27. Nuclear processing. Following the transcription by RNA polymerase II (Pol II), primary transcripts (pri-miRNAs) are cropped by the Drosha–DGCR8 complex (also known as the Microprocessor complex) that recognizes the stem of ~ 35 bp in length of the pri-miRNA, together with its single-stranded RNA tails and its terminal loop. In fact, the Microprocessor complex measures ~11 bp from the basal junction and ~22 bp from the apical junction, and Drosha cleaves the pri-miRNA at this position. The pre-miRNAs originated has a short stem plus a ~2-nt 3' overhang, which is recognized by the nuclear export factor exportin 5 (EXP5) (adapted from Kim VN et al., 2009 and Ha M and Kim VN 2014). Left: pri-miRNA structure. Right: nuclear processing.

iii. Nuclear exportation;

The pre-miRNAs hairpins generated in the nucleus are actively exported into the cytoplasm by the nucleocytoplasmic shuttle Exportin-5 (XPO5) that is also responsible for the transport of other proteins from the nucleus to the cytoplasm through the nuclear pore complex (Yi R et al., 2003; Bohnsack MT et al., 2004) (**Figure 28**). Exportin-5-mediated transport to the cytoplasm requires energy that is obtained using GTP bounding to the Ran protein (Murchison EP and Hannon GJ 2004; Zeng Y and Cullen BR 2004). Pre-miRNA-exportin-Ran-GTP complex formation protects the pre-miRNA from nuclease degradation.

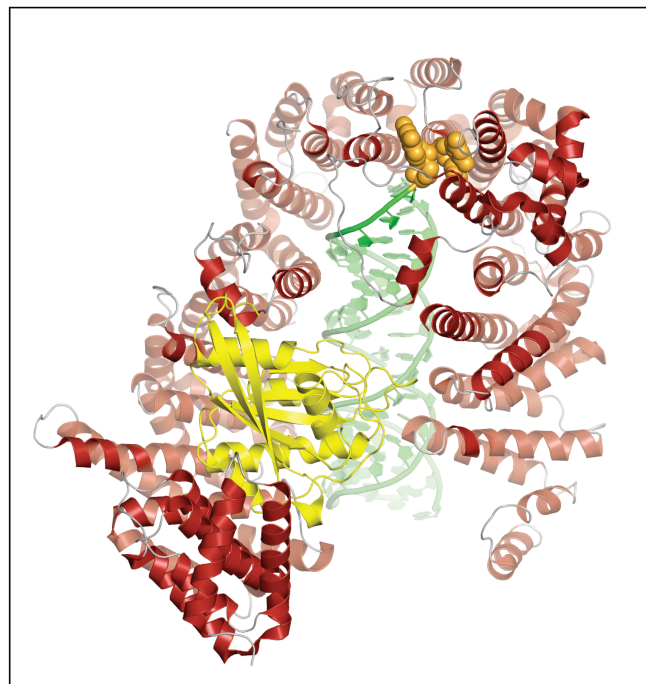


Figure 28. Nuclear exportation. The human exportin-5 (red) in complex with a pre-microRNA (green), showing two-nucleotide overhang recognition element (orange). In yellow Ran-GTP.

iv. Cytoplasmic processing

Pre-miRNAs are further processed by the RNase III endonuclease called Dicer (Hutvagner G et al., 2001). This enzyme interacts with pre-miRNA hairpin structure cleaving at the base of unpaired loop, forming an imperfect miRNA/miRNA* duplex of approximately 22 nucleotides in lengths (Lund E and Dahlberg JE 2006). Just one strand of the miRNA duplex, usually selected on the basis of thermodynamic stability and the first nucleotide (Schwarz DS et al., 2003; Frank F et al., 2010), is used as a miRNA guide strand; the other strand is called passenger strand (or miRNA*) and it is generally degraded. Subsequently, the guide mature microRNA is incorporated in the AGO2 protein that is the catalytic center of the RNA-

induced silencing complex (RISC) (Meister G et al., 2004). Mature microRNA then direct RISCs to target mRNAs, which are recognized through sequence complementarity to nucleotides at position 2-8 of the miRNA (called seed region) (**Figure 29**). This short recognizing region is usually located in the 3'UTR of the target transcripts and it is sufficient for the recruitment of the silencing complex (Lewis BP et al., 2005; Mazière P and Enright AJ, 2007).

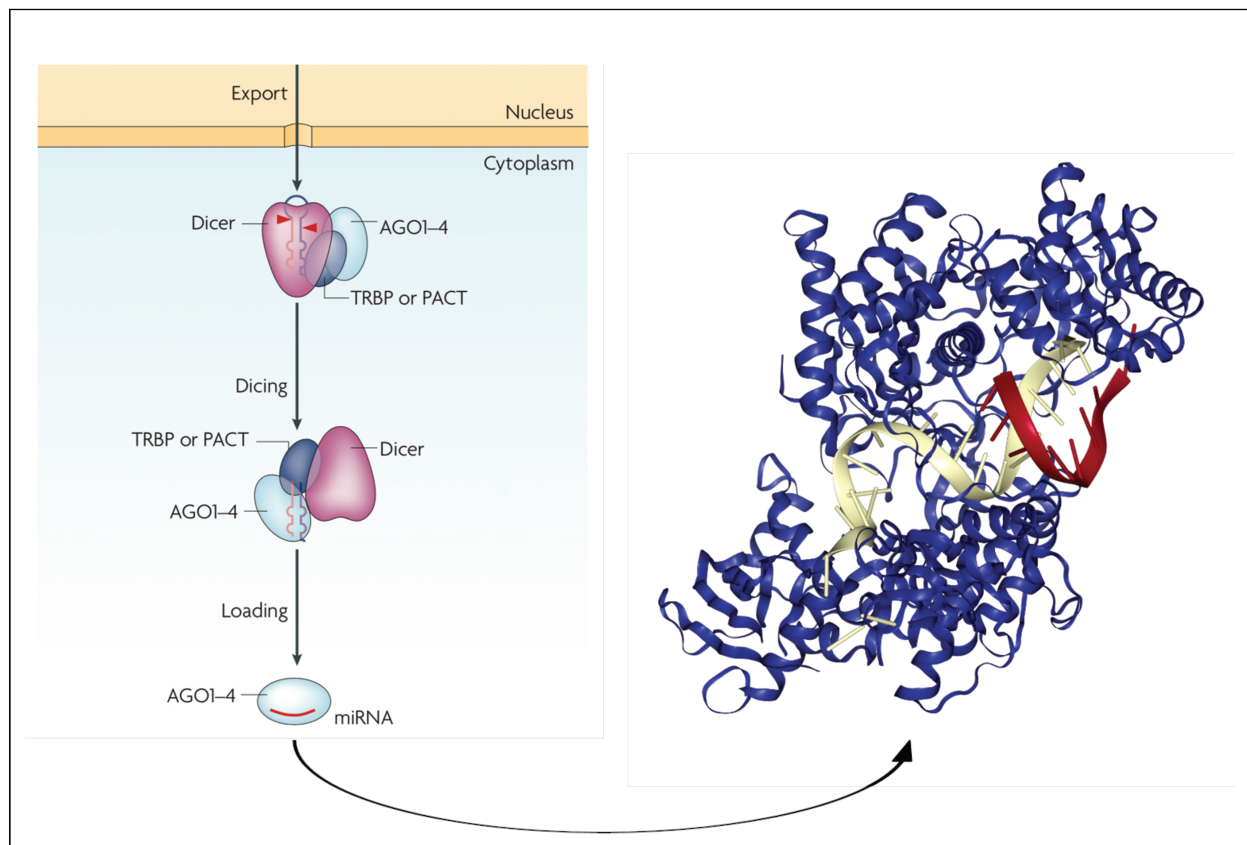


Figure 29. Cytoplasmic process. After exportation from the nucleus, pre-miRNA are processed by the cytoplasmic RNase III Dicer, which catalyses the second dicing step to produce miRNA duplexes. Dicer, TRBP or PACT, and Argonaute (AGO)1–4 mediate the processing of pre-miRNA and the assembly of the RISC (RNA-induced silencing complex) in humans. Left: cytoplasmic process. Right: crystal structures of human Argonaute-2 (Ago2) bound to a guide microRNA with target RNA representing miRNA recognition sites; in red the mature microRNA, in white a short mRNA target, in blue Ago2 protein (adapted from Ha M and Kim VN 2014 and Schirle NT et al., 2014).

3.3 microRNA mechanisms of action

The magnitude of microRNAs silencing is quite modest (Guo et al., 2010) but the synergic action of several microRNAs within the same transcript can amplify the process. This regulation appears elaborate also considering that mammalian cells often express 100–200 different species of miRNAs (Kuchen S et al., 2010), with a total amount of $1-2 \times 10^5$ copies of mature miRNAs in a cell (Calabrese JM et al., 2007; Janas MM and Novina CD, 2012). Depending on miRNAs, target genes, and cellular contexts, the outcome of miRNA target / mRNA interactions could be predominantly translation repression or mRNA degradation, or a mixture of both (Jin HY and Xiao C, 2015). Jin HY et al., (Jin HY and Xiao C, 2015) reviewed in more than 100 mouse studies that the action of microRNAs consist at 48% in translation repression, 29% in mRNA degradation, and 23% in both. It has also been reported rare cases of activation (Li LC et al., 2006). However, it is still unclear what determines the dominant mode of miRNA mechanism of action and how microRNAs actually act to induce this degradation or repression. Three main mechanisms have been postulated:

- (1) **translation repression:** microRNAs may have a role in blocking translational initiation, in poly(A) tail shortening or in the recruitment of protein cofactors that can interfere with translation;
- (2) **mRNA turnover:** microRNAs may directly target mRNA for decay through promoting deadenylation of the polyadenylated 3'-end or decapping at 5'-end;
- (3) **endonucleolytic cleavage:** microRNAs may direct cleavage (slicing) of mRNA targets in two pieces recruiting other proteins (**Figure 30**).

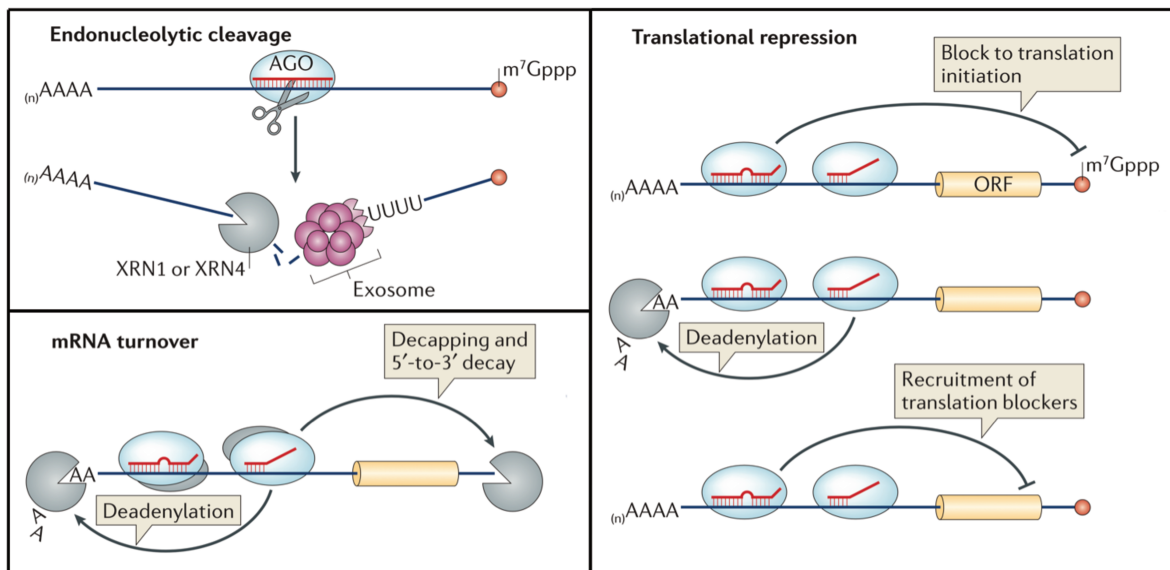


Figure 30. Proposed mechanisms of microRNA action (Adapted from Ameres et al., 2013)

3.4 microRNAs in renal development and diseases

miRNAs are essential for virtually all aspects of mammalian biology, including development of key organs such as the brain, the heart, and the kidney. This is demonstrated by the incompatibility with life in mouse models where factors involved in the maturation and functionality of microRNA are knocked-out (Wang Y et al., 2007; Bernstein E et al., 2003; Morita S et al., 2007). The striking conservation of microRNAs during evolution is frequently associated with the conservation of their gene targets, which further denotes additional evidences about their biological importance (Friedman RC et al., 2009).

This chapter is mainly constructed to highlight the role of microRNAs in the kidney, as we performed almost all our analysis in renal tissues or renal cells. microRNAs act at different levels in this organ: (i) during development, (ii) for maintenance of renal functions, and (iii) for the progression of kidney diseases.

(i) Starting from nephrogenesis to renal senescence, different studies demonstrated the role of microRNAs in kidney development. Conditionally ablating the function of Dicer using Six2Cre in cells of the nephron lineage promoted apoptosis, induced premature interruption of nephrogenesis, and disrupted branching morphogenesis (Nagalakshmi VK et al., 2010). Moreover, HoxB7Cre-mediated removal of Dicer from the ureteric bud and collecting system led to hydronephrosis and hydroureter, whereas some mutants with milder phenotypes retained most of the renal parenchyma but developed cysts in the collecting ducts (Nagalakshmi VK et al., 2010). This phenotype was accompanied by disrupted ciliogenesis within the ureteric bud epithelium and the development of renal cysts (Nagalakshmi VK et al., 2010). Characterization of three mouse models where key miRNA pathway genes Dicer, Dgcr8, and the entire Argonaute gene family (Ago1, 2, 3, and 4) were inactivated, revealed that inhibition of miRNAs in CDs spontaneously evokes a renal tubule injury-like response, which culminates in progressive tubulointerstitial fibrosis (TIF) and renal failure (Hajarnis S et al., 2018).

Inactivation of Drosha or Dicer in podocytes produced dysplasia in early developing glomeruli and caused proteinuria and glomerulosclerosis (Harvey SJ et al., 2008; Ho JJ and Marsden PA, 2008; Shi S et al., 2008; Zhdanova O et al., 2011). *Bai et al.* combining the expression profiles of microRNAs in young (3-month) and old (24-month) rat kidneys together with senescence study in mesangial cells confirmed the

regulatory importance of microRNAs in renal aging by inhibiting intracellular pathways such as those involving the mitochondrial antioxidative enzymes SOD2 and Txnrd2 (Bai XY et al., 2011).

(ii) miRNAs' are predicted to act in kidney homeostasis and maintenance by modulating the expression of different proteins. They regulate water re-absorption thorough the control of aquaporin (AQPs) channels expression (Sepramaniam S et al., 2010 and 2011), and they modulate osmotic response targeting Sodium-hydrogen antiporter 3 regulator 1 (Nherf1) (Flynt AS et al., 2009) or the osmotic response element binding protein (OREBP) (Huang W et al., 2011). microRNAs maintain also the renin-producing juxtaglomerular cells and the morphologic integrity and function of the kidney (Sequeira-Lopez ML et al., 2010).

(iii) miRNAs' involvement have been identified also in a variety of renal diseases (reviewed by Ichii O et al., 2017; Ma L and Qu L, 2013), including diabetic nephropathy (Dewanjee S et al., 2018), acute kidney injury (AKI) (Jones TF et al., 2018), chronic kidney disease (CKD) (Lv W et al., 2018), polycystic kidney disease (Tran U et al., 2010; Duan J et al., 2012; Phua YL and Ho J, 2015), cancer (Juan D et al., 2010; Catto JW et al., 2011) and others. A schematic representation of the renal pathogenic role of microRNAs is illustrated below (**Figure 31**).

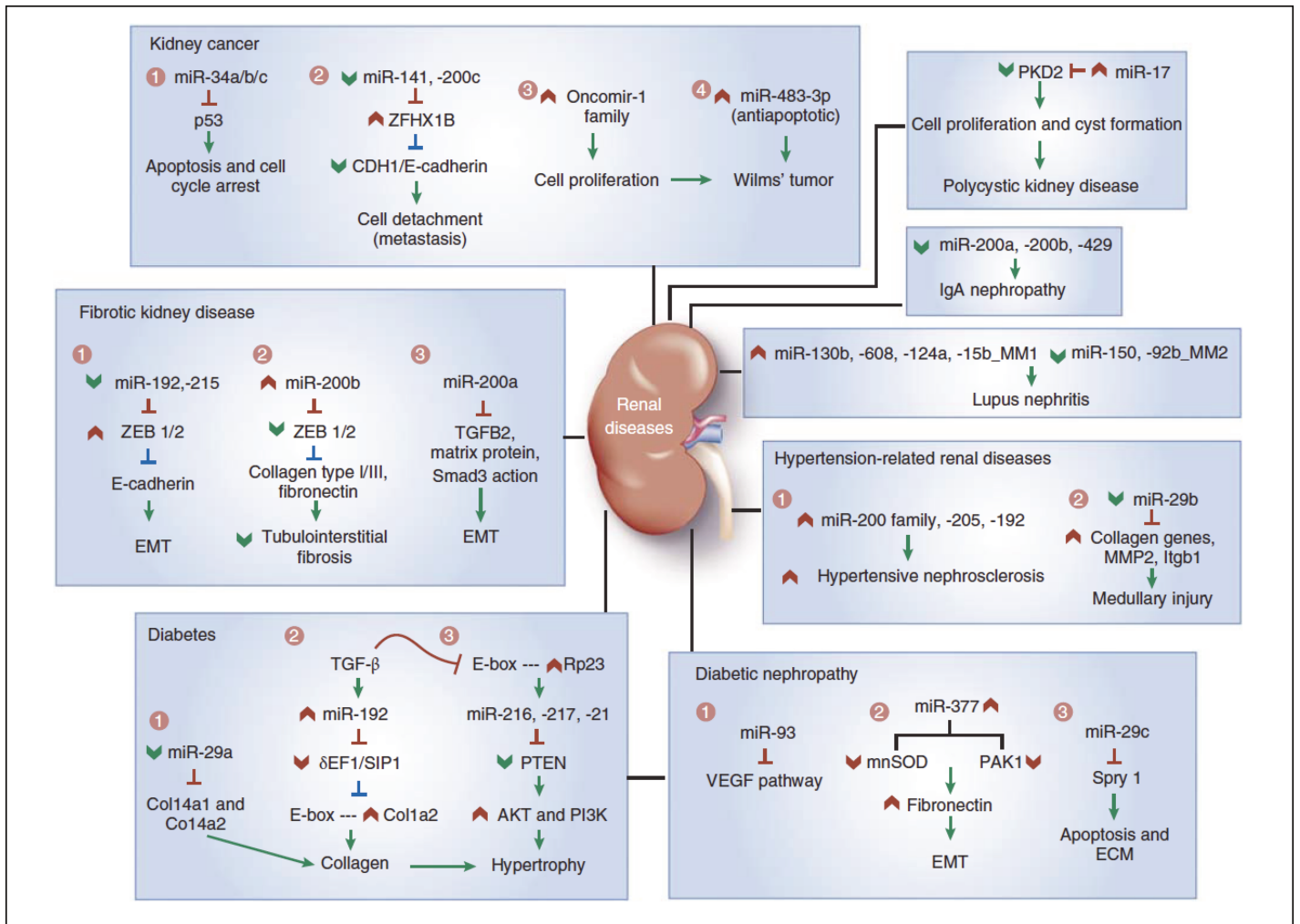


Figure 31. MicroRNAs (miR) in renal diseases. Possible miRNA-regulatory networks involved in renal pathophysiology. Col1, collagen type 1; ECM, extracellular matrix; δEF1, delta 1–crystallin enhancer binding protein; EMT, epithelial–mesenchymal transition; Ig, immunoglobulin; Itgb1, integrin beta 1; miRNA, microRNA; MMP2, matrix metalloproteinase 2; mnSOD, manganese superoxide dismutase; PI3K, phosphoinositide kinase-3; PKD, polycystic kidney disease; PTEN, phosphatase and tensin homolog; SIP1, smad-interacting protein; TGF-β, transforming growth factor beta; VEGF, vascular endothelial growth factor; ZEB, zinc finger E-box-binding homeobox (Adapted from Chandrasekaran K et al., 2012).

3.5 HNF1B and microRNAs

Different studies performed in cell lines and mouse models suggest a fine regulation between HNF1B and some microRNAs. First, HNF1B was recently shown to be able to regulate the expression of different microRNAs as the long noncoding RNA (lncRNA) containing the miR-200 cluster (Hajarnis SS et al., 2015) or miR-194-2/192 cluster (Jenkins RH et al., 2012). A decreased expression of miR-200 has been observed in kidney tubule-specific deletion of *Hnf1b*, and in turn, knockdown of miR-200 in cultured renal epithelial cells inhibits tubulogenesis and produces cyst-like structures (Hajarnis SS et al., 2015). Knockdown of *Hnf1b* in HK-2 proximal tubule cell line inhibited mature miR-192 and miR-194 expression and the transcriptional factor was found to bind their promoter sequences (Jenkins RH et al., 2012).

Different microRNAs (miRNAs) have been found to control *Hnf1b* mRNA abundance in mouse kidneys as miR-17~92, miR-92a or miR-802. *Patel et al.* reported that the miR-17~92 miRNA cluster regulates the posttranscriptional expression of PKD genes, including *Pkd1*, *Pkd2*, and *Hnf1b* (Patel V et al., 2013): kidney-specific transgenic overexpression of this oncogenic miRNA cluster seems to produce kidney cysts in mice, while a kidney-inactivation in a mouse model of PKD retards kidney cyst growth, and improve renal function. Within this cluster, miR-92a repressed the 3' UTR of *Hnf1b*. Moreover, *Hnf1b* was shown to be a target of miR-802-dependent silencing in hepatocytes potentially reducing its transcript and causing glucose intolerance, and impairing insulin signalling in humans and mice (Kornfeld JW et al., 2013).

In the result section (Topic II) we present our last findings about a potential autoregulatory loop regulation between HNF1B and three microRNAs in the RCAD mouse model (miR-802, miR-192/194-2 and miR-30a), which may be essential during the last stages of kidney development.

CHAPTER 4. The urinary proteome as research tool

4.1 The urinary proteome

Proteomics is one of the main challenges of the post-genomic era consisting in the identification, expression, and characterization of proteins. Derived from the fusion of the words “protein” and “genome”, proteomic evaluates the complete set of proteins encoded in the genome of a specific cell or organism. The researched information in a proteome corresponds to the sequence, structure, and localization of each protein, as well as the interaction with other proteins (Ideker T et al., 2001). In doing so, proteomic analysis provides informative data related to the biological mechanisms, which can be useful for a better readout of the physiological and pathological processes affecting the life of organisms (Latterich M et al., 2008; Wright PC et al., 2012). Biological specimens, such as tissue, blood (plasma and serum) or urine are valuable sources of information. In particular, urinary proteomics represents an enlarging field of interest for biologists and physicians and proteomic analysis have been employed for the discovery and the validation of biomarkers of several kidney diseases (Mischak H et al., 2015; Magalhães P et al., 2016). Urine represents an easy accessible biological fluid, which can be obtained in large quantities via a non-invasive procedure and may provides insights about different organs because it results from glomerular filtration via blood (Thongboonkerd V et al., 2005). Moreover, its proteome is originated 70% from the kidney and the urinary tract along with 30% from the circulation, which allows the study of different renal diseases and consequently associated events such as extracellular matrix (ECM) remodelling or fibrosis (Schaub S et al., 2004; Klein J et al., 2014; Magalhães P et al., 2017). Oppositely, its limitation is due to daily variability caused by circadian rhythms, physical activity, diet and metabolic or catabolic processes (Weissinger E et al., 2004; Decramer S et al., 2008), which can be corrected by different adjustment or calibration/normalization methods (Jantos-Siwy J et al., 2009). In the following manuscript we performed the first clinical proteomic analysis of the RCAD syndrome in a pediatric cohort of patients to provide new insights of this multisystem disorder identifying novel urinary biomarkers.

4.2 Analytic approaches

Proteomic analysis may require complex analytical steps to separate the mixture of all the proteins in accordance with their mass/charge ratio (m/z). Subsequently, these molecules are determined by mass spectrometry (Resing, KA et al., 2005; Züribig, P et al., 2008). While in a bottom-up approach proteins are cleaved into short peptides by the usage of a synthetic enzyme (usually trypsin) (Resing, KA et al., 2005; Züribig, P et al., 2008), top-down methods allow the identification of naturally occurring peptides, which does not require any prior proteolytic procedure. These peptides are stable and soluble biomolecules ranging from 0.5 to 20 kDa, not requiring any protein digestion before MS analysis, and being usually derived by the activity of endogenous proteases/peptidases (Züribig, P et al., 2008; Finoulst I et al., 2011). For the analysis of pediatric RCAD urinary proteome we performed capillary electrophoresis coupled to mass spectrometry (CE-MS), which is one of the most relevant top-down approach that can be clinically applicable.

4.3 CE-MS workflow

Capillary electrophoresis (CE) coupled to mass spectrometry (MS) has been employed in body fluids for the detection and identification of biomarkers for many diseases (Coon JJ et al., 2008; Mischak H et al., 2011; Klein J et al., 2016). The workflow of CE-MS normally comprises different steps. First, a step of protein separation is performed based on the electrophoretic mobility (dependent on size and charge of molecules) by CE, followed by a detection step using a MS (*Figure CE-MS*). Subsequently, after CE-MS run, data are processed through the use of a software that translates the mass spectral ion peaks representing molecules at different charge states into singles masses. Following calibration and normalization step, values of molecular masses and CE-migration time are assigned to each peptide (Coon JJ et al., 2008). Afterwards, all detected peptides are deposited, matched, and annotated in a database, enabling digital data compilation. In our study, after biomarker discovery, we combined the significant peptides of RCAD children in a mathematical classifier via support vector machine (SVM), an algorithm that allows a separation of features via multiple independent parameters in a high-dimensional hyperplane (Mischak H et al., 2013). This mathematical classifier was further validated using a blinded cohort, encompassing RCAD patients along with patients suffering from cystic kidney disease,

chronic kidney disease and nephrotic syndromes. The results revealed high accuracy, sensitivity and specificity.

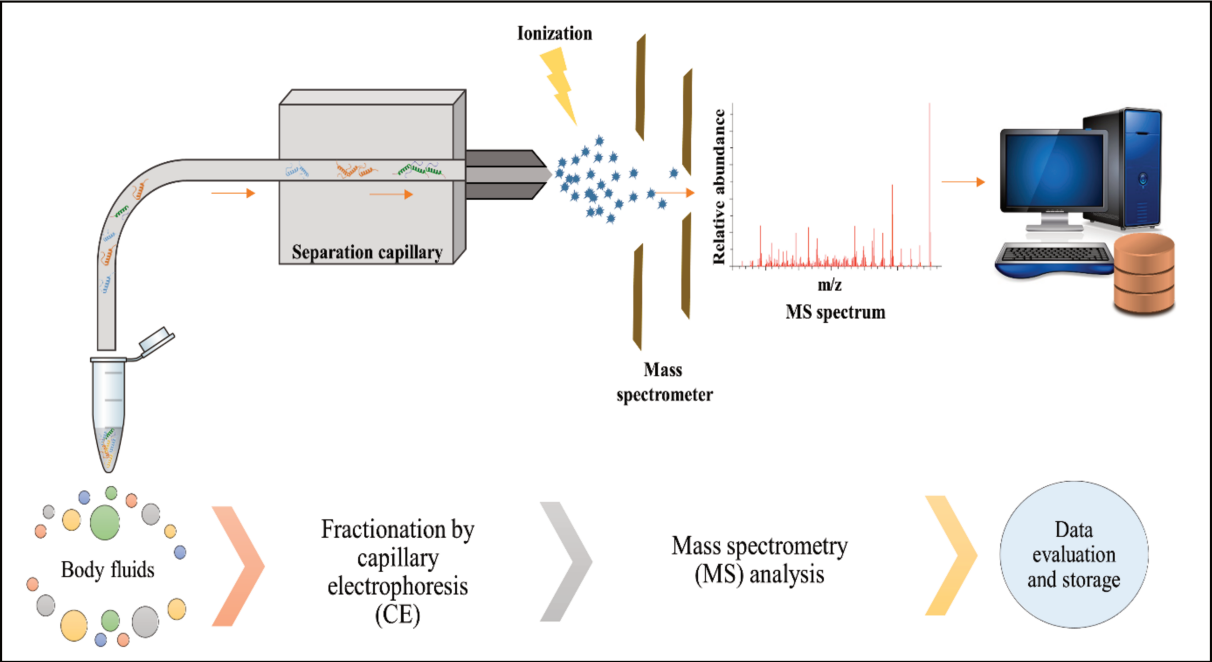


Figure 32. CE-MS workflow: after sample preparation, peptides are separated based on their size and charge by capillary electrophoresis. Subsequently, peptides are ionized and analysed in the mass spectrometer. A relative identification/quantification of a peptide is determined, i.e. mass, CE-migration time, and relative peptide abundance are assessed along with further evaluation and match to a SQL database. (Adapted from Krochmal M et al., 2018)

RESULTS

TOPIC I. A novel mouse model of the Renal Cysts and Diabetes disease uncovers HNF1B gene dosage targets during kidney development

I.1. Context of the study

I.2. Results and discussion

I.3. Conclusions

SCIENTIFIC ARTICLE 1

I.1. Context of the study

The transcription factor HNF1B is an important regulator of early liver, pancreas and kidney development in vertebrates. In humans, heterozygous mutations in *HNF1B* cause a complex syndrome, known as Renal Cysts and Diabetes, characterized by developmental abnormalities of kidney, genital tracts and pancreas as well as several disorders, including hyperuricaemia, hypomagnesemia, early onset of diabetes and liver dysfunctions. Renal abnormalities are the most prominent features, including single kidneys, hypoplasia and glomerulocystic dysplasia. There is no clear genotype-phenotype correlation with haploinsufficiency being the main disease mechanism. The pathogenesis underlying this disease remained unclear since mice with heterozygous mutations in *Hnf1b* have no phenotype, while constitutive or conditional *Hnf1b*-ablation led to more severe phenotypes without reflecting the human disease.

To better understand the pathogenesis of RCAD, the lab has previously developed a mouse model carrying an identified human mutation at the intron 2 splice donor site, referred as splicing mutation intron-2 (Sp2). At the time I arrived at the lab the embryonic phenotype of this mouse model was already characterized and I was initially involved in the embryonic transcriptional profiling, which I subsequently used also for the microRNA study presented in Topic II. I was also involved into postnatal analyses in particular basal urinary/plasma analyses and into the urinary proteome analyses at postnatal stages as well as immunostaining evaluations.

I.2. Results and discussion

Heterozygous *Hnf1b*^{Sp2/+} mutant embryos exhibited bilateral renal cysts from E15.5, originated primarily from proximal tubules (PT) and intermediate nephron segments and

glomeruli. They also exhibited apico-basal polarity defects in different renal tubules as well as delayed differentiation and unequal distribution of PT. Hydronephrosis and genital tract anomalies were also observed at later stages and postnatal life.

Combined mRNA-seq and ChIP-sequencing analyses at different embryonic stages (E14.5, E15.5, E17.5 and P1) identified more than 200 genes down-regulated at both E17.5 and P1, primarily expressed in early proximal tubules and to a lesser extent in loops of Henle and collecting ducts and involved in transport, lipid and organic acid metabolic processes. Several of these genes were putative HNF1B targets. Notably, among the different regulators, *Hnf4a* expressed in PT, and an HNF1B target, was the strongest down-regulated, while the expression of other previously identified targets, including the cystic disease genes (*Pkh1*, *Pdk2*, *Bicc1*) or *Pax2*, *Wnt9b* were slightly or not affected.

Postnatal analyses revealed a range of renal abnormalities ranged from few clusters of glomerular cysts, micro cysts, hydronephrosis and rare cases of multi cystic dysplasia. Partially urinary concentration defects were observed and investigating the urinary proteome of this mice we found a particular signature composed of several differentially excreted peptides in *Hnf1b*^{Sp2/+} versus WT mice including down-excretion of Uromodulin (*Umod*) and Epidermal Growth Factor (EGF) and up-excretion of collagen fragments.

I.3. Conclusions

Together these data suggest that reduced expression of HNF1B below a critical level results in kidney abnormalities such as cyst initiation and hydronephrosis, associated with the deregulation of a subset of target genes. HNF1B impairment leads to progressive urinary system physiology dysfunctions consistent with a pathological state that mirror RCAD syndrome in different features.

This work is presented in the following pages as a manuscript.

SCIENTIFIC ARTICLE 1

A novel mouse model of the Renal Cysts and Diabetes (RCAD) syndrome uncovers functional HNF1B dosage-sensitive genes during kidney development contributing to the disease

Leticia L Niborski^{1#}, Mélanie Paces-Fessy^{1#}, Pierbruno Ricci^{1#}, Adeline Bourgeois¹, Pedro Magalhães^{2,3}, Maria Kuzma-Kuzniarska¹, Celine Lesaulnier¹, Martin Rezko⁴, Edwige Declercq¹, Petra Zürlbig², Alain Doucet⁵ and Silvia Cereghini^{1*}

¹-Institut de Biologie Paris Seine (IBPS) - UMR7622 CNRS- Sorbonne Université - Université Pierre et Marie Curie. Paris- France

²- Mosaiques Diagnostics Hannover, Germany

³-Department of Pediatric Nephrology, Hannover Medical School, Hannover, Germany

⁴-BSRC Al. Fleming, Division of Molecular Biology & Genetics Genomics Facility- Athens Greece

⁵-Sorbonne Universités, Université Paris Descartes, UMRS 1138; CNRS, ERL 8228, Centre de Recherche des Cordeliers, Paris, France.

These authors contributed equally to the work

* Silvia Cereghini corresponding author

ABSTRACT

Heterozygous mutations in *HNF1B* cause the complex syndrome Renal Cysts and Diabetes, characterized by developmental abnormalities of the kidney, genital tracts and pancreas and a variety of renal, pancreas and liver dysfunctions. The pathogenesis underlying this syndrome remains unclear as mice with *Hnf1b* heterozygous null mutations have no phenotype, while constitutive or conditional *Hnf1b*-ablation led to more severe phenotypes without reflecting the disease.

We generated a novel mouse model carrying a human splice-site mutation. Unlike previously developed models, heterozygous mutant embryos exhibited bilateral renal cysts from E15.5 originated from glomeruli, intermediate nephron segments and proximal tubules (PT), together with delayed differentiation and unequal PT clusters and pelvic dilatations.

mRNA-sequencing at different embryonic stages show that most down-regulated included several putative HNF1B target genes primarily expressed in developing PTs and Henle's Loop and involved in ion/drug transport, organic acid and metabolic processes. Unexpectedly, the established targets upon *Hnf1b*-ablation, including the cystic disease genes, were slightly or no affected, thus revealing an unappreciated differential dosage-sensitivity in the HNF1B target genes.

Adult heterozygous mutants exhibited several renal abnormalities ranging from microcysts, glomerular cysts, hydronephrosis to occasional multicystic-hypoplasia as well as genital tract anomalies. Urine proteomics uncovered a specific signature of differentially excreted peptides, particularly a strong decrease of Epidermal Growth Factor and uromodulin and an increase of collagen fragments. In conclusion, mice haploinsufficient for *Hnf1b* exhibit a disease phenotype reproducing several of the characteristic features of the RCAD syndrome and further suggests it represents a unique clinical/pathological viable model of the human disease.

Key words: HNF1B, RCAD, gene-dosage sensitivity, kidney development, transcriptomics

INTRODUCTION

The transcription factor HNF1B is an important regulator of kidney, liver and pancreas organogenesis either at the specification stage or during branching morphogenesis {Haumaitre, 2005 #3}{Coffinier, 2002 #9}{Lokmane, 2008 #2}{Lokmane, 2010 #12}{Gresh, 2004 #10}{Heliot, 2013 #7}{Massa, 2013 #11}{De Vas, 2015 #8}. In humans heterozygous germ- line mutations in the *HNF1B* gene cause a complex and heterogeneous syndrome, known as Renal Cysts and Diabetes (RCAD, OMIM #137920) and characterized by early onset of Diabetes and developmental abnormalities of the kidney, genital tract and pancreas as well as a variety of liver, biliary, pancreas and renal dysfunctions {Chen, 2010 #40} {Clissold, 2015 #68}. This pattern of clinical features is consistent with the broad expression profile of *HNF1B* in the human developing metanephric kidney, urogenital tract and endodermal derived tissues {Haumaitre, 2006 #4}{Kato, 2009 #14}, which is remarkably conserved in vertebrates {Sun, 2001 #15}{Lokmane, 2008 #2}{Naylor, 2017 #16}{Kaminski, 2016 #17}.

To date, more than one hundred fifty heterozygous mutations in *HNF1B* have been described, including missense, nonsense, frameshift, splice site mutations and insertion/deletions as well as whole gene deletions {Stenson, 2003 #18}{Edghill, 2006 #19}{Heidet, 2010 #20}{Chen, 2010 #40}. The phenotype of HNF1B carriers is highly variable both between and within families. No clear genotype-phenotype correlations were observed neither for the type or location of mutations, and haploinsufficiency has been the main underlying disease mechanism proposed.

Heterozygous mutations in *HNF1B* are as well one the most common monogenic causes of developmental kidney disease. A large spectrum of renal abnormalities has been observed including unilateral or bilateral cysts, severe multicystic dysplasia, oligomeganonephronia, hypoplastic Glomerulocystic Kidney Disease (GCKD), solitary or horseshoe kidney (reviewed by {Bingham, 2004 #31}{Heidet, 2010 #20}{Chen, 2010 #40} {Clissold, 2015 #68}.

Despite the increasing number of mutations identified, the molecular mechanisms by which heterozygous mutations in the HNF1B gene cause this broad spectrum of clinical symptoms remains poorly understood. Unlike humans, heterozygous mice for an *Hnf1b* null

allele have no apparent phenotype, while the homozygous deletion results in early embryonic death due to defective visceral endoderm formation {Barbacci, 1999 #26}, thus delaying our understanding of the pathogenic mechanisms of *HNF1B*-mutations. Likewise, constitutive inactivation of *Hnf1b* in the entire mouse epiblast {Haumaitre, 2005 #3}{Lokmane, 2008 #2}{Lokmane, 2010 #12} or specific inactivation of *Hnf1b* either in renal tubules, liver or pancreas {Gresh, 2004 #10}{Coffinier, 2002 #9} {Heliot, 2013 #7}{Desgrange, 2017 #5}{De Vas, 2015 #8} results either in early embryonic or perinatal death along with far more severe phenotypes than those observed in humans. Regarding renal development, mouse genetic studies have shown that HNF1B acts at multiple and sequential steps during early metanephric development. Initially required for early ureteric bud branching and the induction of nephrogenesis {Lokmane, 2010 #12}, specific deletion in nephron progenitors uncovered a crucial role in early nephron segmentation {Heliot, 2013 #7} {Massa, 2013 #11}. Additionally, *Hnf1b*-ablation in the collecting ducts resulted into massively mispatterned ureteric tree network, defective collecting duct differentiation and disrupted tissue architecture leading to cystogenesis and perinatal death {Desgrange, 2017 #5}, while deletion at relatively later stages in medullar tubules led to cystic kidneys after birth associated with downregulation of several cystic disease genes, including *Pkhd1*, *Pkd2* and *Umod* {Gresh, 2004 #10}{Hiesberger, 2005 #33}.

Molecular characterization of fetuses carrying different *HNF1B* heterozygous mutations demonstrated that HNF1B plays in humans, as in mice, an important role in both kidney and pancreas morphogenesis {Haumaitre, 2006 #4}. However, the cystic renal phenotype either in these fetuses {Haumaitre, 2006 #4} or in adult mutant carriers {Faguer, 2012 #34}{Casemayou, 2017 #35} was not associated with the decreased expression of the renal cystic disease genes previously identified as HNF1B targets in mice {Gresh, 2004 #10}. These observations together led to the suggestion that mice are either less sensitive to haploinsufficiency or alternatively the mouse mutant models so far generated do not correctly represent the mutations identified in humans.

To explore these possibilities and obtain a more comprehensive view of HNF1B function in organ development and disease in the context of the whole animal, we generated a novel mouse RCAD model by introducing a previously identified human point mutation at the intron-2 splice donor site (<IVS2nt+1G>T, {Bingham, 2003 #36}{Harries, 2004 #37}). Five different mutations have already been identified at this splice site indicating that it is a putative hotspot mutation. Moreover, patients with these mutations exhibited the typical features *HNF1B* mutations (renal cysts, diabetes, hyperuricaemia) {Bingham, 2003 #36}

(Adalat et al, 2008) and could therefore be representative of a large number of *HNF1B* intragenic disease causing mutations.

We present here a comprehensive analysis of the renal phenotype of heterozygous mutants for the splicing mutation at different developmental stages and a preliminary characterization of the progression of the renal disease phenotype in adulthood. Heterozygous mutants (referred as splicing mutation intron-2 (Sp2) *Hnf1b*^{Sp2/-}) exhibited bilateral cysts and tubular dilatations as well as glomerular cysts from E15, along with rare cases of genital tract abnormalities and other extra renal manifestations that have been described in human *HNF1B* mutant carriers.

Unlike heterozygous mouse mutants for a null allele, in which the HNF1B protein levels remained essentially unchanged {Kornfeld, 2013 #39}, in the *Hnf1b*^{Sp2/+} heterozygous mutants the HNF1B protein levels were strongly reduced, in particular during development, without correlating with the more modest reduction of *Hnf1b* transcript levels.

Further molecular and global transcriptional profiling indicate that only a subset of target genes was sensitive to reduced levels of HNF1B protein at different embryonic stages, whereas the previously identified targets strongly downregulated in the absence of *Hnf1b*, including the cystic disease genes, were relatively insensitive to reduced levels of HNF1B protein. Postnatal analyses revealed a range of renal abnormalities ranging from few clusters of glomerular cysts, micro cysts, and hydronephrosis to rare cases of hypoplastic-glomerulocystic kidney. Thus, this novel mouse model exhibits at the heterozygous state a disease phenotype reproducing several features of the RCAD syndrome and therefore represents a unique clinical/pathological viable model of the human disease.

RESULTS

Generation of a mouse model reproducing a clinical *HNF1B* splicing mutation

The mouse model carrying a point mutation at the intron-2 splice donor site, was generated by homologous recombination by introducing a G to T point mutation (Fig.1 A) thus mimicking the c.544+1G>T (<IVS2nt+1G>T) mutation identified in humans {Bingham, 2003 #36}. The *LoxP*-flanked neomycin-resistance cassette located within intron-1 was subsequently excised by breeding heterozygous mutant mice with a “Cre deleter” mouse line (Materials and Methods). Thus, the *Hnf1b* mutant allele encompassed the human splicing

point mutation and a unique LoxP site within the intron-1.

To precisely define the consequences of this mutation, we performed semiquantitative RT-PCR using RNA from heterozygotes for the splicing mutation (*Hnf1b*^{sp2/+}) and wild type (*WT*) kidneys using primers located in exon-1 and exon-3. Sequence of the PCR products obtained indicated the expected production in heterozygous mutants of the two *Hnf1b* spliced isoforms A and B. Four additional novel transcripts were detected, corresponding to isoforms A and B in which exon 2 was deleted and the isoforms A and B deleting respectively the last 32 bp of exon 2 through the use of a novel cryptic splice donor site (Fig.1 B). This pattern of alternative splicing from the mutant allele was observed at different stages and in other tissues expressing *Hnf1b* (not shown). The detection of *HNF1B* variants lacking the exon 2 was consistent with previous analysis in human patients {Harries, 2004 #37}. Yet the variants lacking the last 32 bp of exon 2 has not been described in humans.

The predicted consequences of deleting either the entire or part of exon 2 is the production of putative truncated HNF1B proteins encompassing the N-terminal dimerisation domain, but lacking the DNA binding domain and the C-terminal transactivation domain. Moreover and consistent with the absence of the NLS, upon transient expression in different cell-lines, these truncated proteins remained mainly in the cytoplasm (Supplementary Fig.S1). Therefore, if these putative truncated proteins are expressed they would be non functional (see below). In agreement with these observations, analysis of embryos from heterozygous intercrosses at different developmental stages indicated that the homozygous *Hnf1b*^{Sp2/Sp2} mutation was lethal soon after implantation similarly to the *Hnf1b* homozygous mutants for a null allele previously described {Barbacci, 1999 #26}, thus confirming that the splice mutation generate nonfunctional *Hnf1b* transcripts (data not shown).

Heterozygous embryos for the *Hnf1b*^{Sp2/+} allele exhibit bilateral tubular dilatations, glomerular cysts and hydronephroses

To evaluate the onset and progression of the mutant phenotype, histological analyses of heterozygous mutants and WT littermates were performed at different embryonic stages in a mixed background C57BL/6N x 129/sv. Up to E14.5, heterozygous and WT embryos developed normally (Supplementary Fig.S2). However from E15, we reproducibly observed bilateral cystic kidneys, including glomerular and tubular cysts predominantly in the cortical and medullar regions, respectively (Fig. 2). A similar phenotype was observed at E16.5 (not shown). As kidney growth progressed, by E17.5 there was an apparent reduction of the

volume of cystic structures relative to whole kidney volume, while glomerular cyst exhibited similar distribution all throughout development (Fig. 2).

To examine the influence of mouse strain susceptibility into the disease phenotype we backcrossed the *Hnf1b*^{sp2/+} mutant mice into two inbred backgrounds: C57BL/6N and 129/sv. We observed similar tubular dilatations and glomerular cysts from E15 in the two inbred backgrounds (Fig. 2). However, in the C57BL/6N background the *Hnf1b*^{sp2/+} embryonic kidneys exhibited a more severe and variable renal phenotype, in particular at later stages and newborn pups with higher numbers of both medullar and glomerular cysts frequent pelvic dilatations and hydronephroses, which in some cases occurred bilaterally as well as duplicated kidneys (Fig.2 and Supplementary Fig.S3: E-F C57BL/6N).

Heterozygous mutant embryos or newborns were obtained at the expected Mendelian ratio in different background; however in the C57BL/6N background 10-15% of heterozygous mutants die between P1-25 days of age (Supplementary Table S1), in general without being able to define the causes due to cannibalism. Heterozygous mutants in both backgrounds were able to reproduce, but they were less fertile than WT littermates. Further postnatal analysis revealed rare cases of genital tract abnormalities (agenesis of an uterine horn, epididymis cysts, abnormal branched and dilated seminal vesicles) in either C57BL/6N or 129/sv backgrounds. Heterozygous mutants exhibited also pancreatic dysfunction with glucose intolerance, a phenotype that will be described elsewhere by C. Haumaitre's laboratory (IBPS, UMR7622). Other associated phenotypes, but only in the C57BL/6N background were unilateral or bilateral absence of eyes (30% of n: 36 *Hnf1b*^{Sp2/+} males and n=20 *Hnf1b*^{Sp2/+} females), which is manifested from embryo stages along with a higher susceptibility to eye infections. This ocular phenotype could eventually be linked to the mutation Rd8 mutation of the *Crb1* gene present in the strain C57BL/6N {Mattapallil, 2012 #70}. Unless otherwise indicated the following analysis were mainly performed in the C57BL/6N background.

Altogether, these data show the heterozygous mutants exhibited several of the urogenital phenotypes described in RCAD patients and further suggest that genetic modifiers may either aggravate (C57BL/6N) or attenuate (129/sv) the phenotype.

Relative expression of normal *Hnf1b* transcript and protein levels in *Hnf1b*^{Sp2/+} mutant kidneys at different stages

To further understand the molecular mechanism by which the heterozygous mutants for the splicing mutation exhibited a RCAD like disease phenotype, a finding that contrasts with the absence of phenotype in heterozygous mutants for a null allele (*Hnf1b*^{lacZ/+} {Barbacci, 1999 #26}), we first examined the transcript levels produced by the normal allele in *Hnf1b*^{Sp2/+} heterozygous kidneys relative to *WT*. We used primers located in the ATG translational site and in the last 32bp of the exon 2, which encompassed sequences absent in the abnormal spliced transcripts produced by the mutant allele (Supplementary Table S2). Unexpectedly and similarly to heterozygous mutants for a null allele, in our heterozygous mutants, the *Hnf1b* transcripts were decreased by only 20-25% relative to *WT*, instead of the expected 50% reduction (Fig. 3 A). We therefore hypothesized that the HNF1B protein levels produced by the normal allele were either decreased under lower levels than those of transcripts or alternatively, the functional protein levels were decreased by heterodimerization with the putative truncated proteins produced by the mutant allele (depicted in Fig. 1B)

HNF1B immunostainings at different embryonic stages revealed a global decrease in nuclear staining in *Hnf1b*^{Sp2/+} mutants, although dilated tubules did exhibit nuclear staining without any evidence of a further decrease or a focal lack of expression as reported in other autosomal dominant polycystic kidney diseases (Fig. 3 B).

To obtain a quantitative evaluation of the levels of HNF1B protein and of the putative truncated variants, Western blot analyses were performed using whole cell extracts from at least 4 independent mice/embryo kidneys microdissected at different stages. In contrast to the moderate decrease of transcript levels, in heterozygous mutants we observed a stronger decrease in the HNF1B protein levels, in particular at earlier stages (Fig. 3 C, D). This finding provides further evidence of a posttranscriptional and/or translational control of HNF1B protein by a not yet identified mechanism. We also confirmed that in *Hnf1b*^{LacZ/+} mice, the HNF1B protein levels were actually increased (Fig. 3 D) consistent with the absence of a disease phenotype as previously reported {Kornfeld, 2013 #39}). More importantly, we were unable to detect any truncated protein encoded by abnormally spliced *Hnf1b* transcripts, under conditions the endogenous *WT* HNF1B protein was easily detected, thus suggesting that they were either very unstable or not produced.

Altogether these results suggest that decreased levels in the HNF1B functional protein are likely responsible of the cystic disease phenotype of our mutants, rather than through a dominant negative effect via the formation of nonfunctional heterodimers between HNF1B and the truncated proteins encoded by the abnormal spliced transcripts.

Embryos heterozygous for the splicing mutation display glomerular cysts, early proximal tubule dilatations and delayed differentiation of proximal tubules and collecting ducts

We previously reported that *Hnf1b*, expressed in the ureteric bud (UB), the entire collecting system and nascent nephrons, is required for early ureteric bud branching and initiation of nephrogenesis {Lokmane, 2010 #12}. We therefore began the phenotypic analysis by examining the expression of Calbindin-D-28K, a protein first expressed in the emerging UB branches of the metanephric kidney and found that it showed a similar expression profile in E14.5 heterozygous mutants and *WT* (Fig. 4 A, A'). Likewise, the expression of the key regulator PAX2, whose transcription in the collecting system has been shown to depend on *Hnf1b* {Lokmane, 2010 #12} {Desgrange, 2017 #5} {Paces-Fessy, 2012 #1} was not affected neither at E14.5 and E15.5 (compare Fig 4 B, C with B', C') nor at later stages (not shown). Thus, in *Hnfl^{Sp2/+}* mutants decreased HNF1B protein levels did not affect branching of the UB, nor the expression of the early HNF1B targets previously identified. WT1 was also normally expressed in heterozygous both in the condensed mesenchyme around the ureteric buds and in the podocytes. Moreover, nephrogenesis appeared normally induced as indicated by the glomeruli stained by WT1 and the presence of normally shaped S-shaped bodies, in contrast to the abnormal S-shaped bodies observed upon *Hnf1b*-conditional inactivation in nephron progenitors {Heliot, 2013 #7} (Fig. 4 D, D').

We next examined the origin of cystic structures by staining with different nephron and collecting ducts markers at different stages (E14.5-16.5 in Fig. 4; E17.5 and P1 in Fig. 5). For these analyses we selected mutant kidneys without overt hydronephrosis in order to visualize the collecting duct network and medullar nephron tubules. Interestingly, using the marker of early proximal tubules (PTs) HNF4A we observed not only decreased expression of this transcription factor, but also a decrease in the number of labeled structures (Fig. 4 E, E'). Notably, the mature PT marker LTA was not expressed up to the E16.5 stage (Fig. 4 F') and

began to be expressed by E17.5 (Fig. 5 A'). However, the *Hnf1b*^{Sp2/+} PT clusters were consistently reduced in size and exhibited an unequal distribution both at E17.5 and P1 (Fig. 5 B'). Interestingly, most of the *Hnf1b*^{Sp2/+} medullar cysts and tubular dilatations observed, both at E17.5 and P1, were stained by the Na-K-Cl cotransporter (NKCC2), which is expressed in the thick ascending Loop of Henle (Fig. 5 C'; D'). Distal tubules labeled by SLC12a3 (NCC) showed only rare and mild dilatations (data not shown).

Surprisingly, *Hnf1b*^{Sp2/+} collecting ducts were normally stained by either AQP2 (Fig. 5 E', F') or pancytokeratin (CK) (Fig. 4 G'; Fig. 5 G'; H') and mainly devoid of dilatations. However, they were not stained by the lectin DBA, neither during development nor in postnatal life suggesting defective maturation of collecting duct cells (Fig. 4 H'; Fig. 5 I'; L').

In summary, in addition to cortical glomerular cysts, cysts and tubular dilatations in *Hnf1b*^{Sp2/+} appear to predominate initially in early proximal tubules and subsequently from E17.5 in the thick Loop of Henle, while neither nascent nor mature collecting ducts appeared significantly affected (see below).

***Hnf1b*^{Sp2/+} tubular dilatations of developing nephrons are associated with apical polarity defects**

Cystogenesis in embryonic kidneys has been reported to be associated with several cellular defects, including abnormal cell-polarity changes in cell-cell and cell-matrix interactions as well as increased proliferation and apoptosis {Wilson, 2011 #46}.

We found that the PT brush border marker villin was normally expressed in *Hnf1b*^{Sp2/+} nondilated tubules, but it was interrupted in cystic proximal tubules (Fig. 6). PTs also exhibited lower expression of HNF4A with a far stronger decrease in cystic PTs (compare Fig. 6 B, insert B' and A). The expression of HNF1B was moderately decreased in these dilated PTs as compared to its expression in other renal tubules (Fig. 6 C, D, insert D'). Interestingly, the basal membrane marker Laminin (Lam) exhibited a global decrease and partial disorganization in E15.5 heterozygous kidney tubules (both nondilated and dilated) (Fig. 6 F, H). In medullar cystic tubules, the NKCC2 apical staining of epithelial cells of the thick ascending limb of the Loop of Henle (TAL) was also decreased in a proximo-distal gradient and disorganized (Fig. 6 J). At later stages most of the tubular dilatations were found in the TAL, while PTs exhibited rare dilatations.

Consistent with the lack of dilatations/cysts in *Hnf1^{Sp2/+}* collecting system, the apical markers of collecting ducts Muc1 and CK, were both correctly expressed (Fig. 6 E, F, K, L). As previously reported in other *Hnf1b*-deficient kidneys {Gresh, 2004 #10} {Desgrange, 2017 #5}, staining with α -acetylated tubulin, a component of cilia, showed a reduction of cells with cilia in cystic tubules, but a rather similar distribution in non-dilated heterozygous mutants.

Further analysis of proliferation and apoptosis using respectively, the mitosis marker phosphorylated histone H3 and Tunel assay, did not detect significant changes in the tubular structures of heterozygous mutants as compared with WT at E15.5 (data not shown). Together these results show that decreased levels of HNF1B appear to affect basal membrane organization without affecting apical cell polarity markers in nondilated tubules. The decreased expression of apical and brush border markers as well as the defects in cilia integrity in cystic tubules of *Hnf1^{Sp2/+}* mutants appear to be secondary to tubular dilations. These observations contrast our previous results showing that lack of *Hnf1b* results in disrupted apico-basal cell-polarity and epithelial organization of both non dilated and dilated collecting duct tubules {Desgrange, 2017 #5}.

Transcriptomic analyses at different stages uncover common genes sensitive to reduced levels of HNF1B protein

We initially focused our expression analysis on cystic disease genes previously identified as HNF1B targets {Gresh, 2004 #10} {Verdeguer, 2010 #45} as well as additional putative target genes involved in cystogenesis (see {De Vas, 2015 #8}). The expression of most of these genes was however, only slightly or not affected (Supplementary Fig. S4), suggesting that a more complex process is involved in the disease phenotype. To further elucidate the cellular and molecular components sensitive to HNF1B levels, we performed RNA-sequencing on *WT* and heterozygous mutant kidneys at E14.5 (considered as pre-disease kidneys) and at disease stages (E17.5 and P1). Microdissected kidneys from embryos/newborns of the same litter were used. We also included in these analysis deep RNA-sequencing at E15.5 on pools of the two kidneys from n=3 WT and n=3 heterozygous embryos (6 kidneys/sample) (Supplementary Material and Methods).

Since WT mice were compared with heterozygous mutants still expressing HNF1B we did not expected differentially expressed genes at very high levels and therefore considered an

absolute fold-change cutoff value $>$ or $<$ 0.70 log, instead of 1 with an adjusted p-value $<$ 0.05. At E17.5 an additional list of genes with a cutoff value of $<$ -0,6 log was included since contained many known HNF1B target genes that were significantly downregulated (Supplementary Table S3 provide the lists of up- and down-regulated at each stage). Remarkably, the RNA-seq data identified several genes differentially expressed with fold-changes $>$ 1 at all stages. From E14.5 the number of differentially downregulated genes was increased (51, 37, 241 and 127 genes at E14.5, E15.5, E17.5 and P1, respectively consistent with the growth and further morphogenesis of the kidney,

Only a reduced number of UP-regulated genes differentially expressed were observed with no common genes between stages neither putative HNF1B targets among them. In contrast, the number of shared downregulated genes increased from 10 at E14.5 and E15.5 to reach 91 genes at E17.5 and P1 (Supplementary Table S3, File 5). The down regulated genes with greater fold-changes were expressed predominantly in developing PTs and to lesser extent in primitive Loops of Henle and S-shaped bodies and in the cortical and medullary collecting ducts. GO-term analysis {Chen, 2009 #71} highlighted transporter activity, active trans-membrane transporter activity, organic acid and lipid metabolic processes and metabolism terms as well as an association with abnormal renal/urinary system physiology, renal reabsorption, aminoaciduria, decreased urine osmolality and nephrocalcinosis (Table 1, Supplementary Table S4). From E17.5 and consistent with the onset of mature cell-types in the developing nephrons, the pathways enriched included SLC-active transmembrane transport, transport of glucose and small molecules and metabolism (Supplementary Table S4).

It is of interest that among the 25 identified anchor genes of early proximal tubule (EPT) and predicted to be controlled by HNF1B and HNF4A {Thiagarajan, 2011 #72}, 18 genes were found down-regulated at E17.5 and 15 genes at P1 (Supplementary Table S3, File 6). While nine EPT-anchor genes were downregulated at both stages, others were specific to either E17.5 or P1 suggesting a dynamic temporal control of these genes. It is worth noting that the expression of other EPT anchor genes was either not affected, such as *Cml1*, *AI317395*, *Ugt2b37* or only modestly downregulated (*Mogat2*, *Bdha2*, *Aqp11*, *C2*, *Sord*, *Cry11*) thus indicating that the observed down regulations are not simple due to a reduction in proximal tubule structures.

Similarly, both at E17 and P1, the downregulated genes included drug-metabolizing enzymes (*Abcc2*, *Ggt1*, *Fmo2*, *Akr1c1*) and more than fifty *SLC-transmembrane-transporter*

genes (organic cation (the Slc22a family) and sodium glucose transporters gene, see Table S3, File 7) that have been shown to be transcriptionally controlled in postnatal proximal tubules by HNF4A along with HNF1A {Martovetsky, 2013 #73}. Unexpectedly, *Hnf1a* expression, which is restricted to developing and adult PTs was only moderately decreased at E17.5 but remained comparable to *WT* levels at P1 and postnatal mutant kidneys (not shown), further indicating that during development HNF1A was unable to compensate for the decreased protein levels of HNF1B.

It is worth noting that ChIP-PCR/ChIP-seq assays in kidney cell-lines and adult kidneys (reviewed by {Ferre, 2018 #69} or E14.5 kidney ChIP-seq ({Desgrange, 2017 #5}; C. Heliot and S.C. unpublished data) detected specific recruitment of HNF1B to most of the consensus binding sites found in the regulatory sequences of these downregulated genes. The mRNA-seq data showed however that the expression of these targets was not similarly affected. Amongst those HNF1B targets strongly downregulated at most of the stages in our mutants we can mention *Hnf4a*, *Pdzk1*, *Pah*, *Tmem27*, *Cubn*, *Spp1*, *Spp2*, *Kcnj* as well as many *SLC-transmembrane transporters*, thus indicating that these genes represent a subset of targets that appeared to be the most sensitive to reduced levels of HNF1B protein (Supplementary Table S3, see below Fig.7). Intriguingly, *Pdzk1*, a HNF1A target in adult kidneys, encodes a scaffolding protein involved in the normal localization and function to the brush border of the PT of several transporters {Thomson, 2005 #74}, further suggesting additional indirect roles of HNF1B/HNF1A in renal tubule transport via its transcriptional regulation.

Remarkably and confirming our initial Q-RTPCRs (Supplementary Fig S7) the mRNA-seq data showed that the expression of several known HNF1B targets strongly reduced in the absence of *Hnf1b*, including *Wnt9b* and *Pax2* {Lokmane, 2010 #12}, *Pkd2*, *Cdh16*, *Crb3*, *Kif12* {Verdeguer, 2010 #45}, *Cys1*, *Glis2*, *Glis3*, *Fgfr4* {De Vas, 2015 #8}, were indeed either not affected or modestly and not significantly decreased (Supplementary Table S3).

We further confirmed the mRNA-seq data by in situ hybridization (ISH), immunostaining and additional Q-RTPCR analyses. Consistent with the mRNA-seq data, ISH of *Fbp1* and *Spp2*, two early proximal tubule anchor genes {Thiagarajan, 2011 #72}, showed a strong downregulation of *Fbp1* transcript levels and to a lesser degree of *Spp2* both at E17.5 and P0 *Hnf1b*^{Sp2/+} kidneys (Supplementary Fig. S5), while as expected ISH for *Wnt9b*, *Pax2* and *Pkhd1* showed similar expression to *WT* littermates (not shown). Similarly, immunofluorescence analysis for SPP1 (osteopontin), CUBN and LRP2 in E17.5 and P0 *Hnf1b*^{Sp2/+} kidneys, showed a strong downregulation of SPP1 and CUBN, and a more modest

decrease of LRP2 (Fig. 7A).

While in the mRNA-seq analysis the known targets *Umod*, *Tmem27* and *Pkhd1* were significantly downregulated at E17.5, but not at P1 (Supplementary Table S3), further validations by Q-RT-PCR at different stages and adult kidneys showed a significant downregulation of *Umod* and *Tmem27* from E16.5 to adults in heterozygous mutants (Fig.7 E; Fig.S7). The additional targets examined *Hnf4a*, *Kcnj1* (*RomK*), *Lrp2*, *Ihh*, exhibited a preferential downregulation during development up to P0, whereas *Umod* and *Tmem27* remained significantly downregulated in adult mice (Fig.7 E). In addition, we examined the expression of *Aqp2*, a gene found downregulated during development in collecting ducts lacking *Hnf1b* {Desgrange, 2017 #5} and upregulated in postnatal kidneys of *Hnf1b* conditional inactivated medullar renal tubules {Gresh, 2004 #10}. We found that *Aqp2* expression was indeed downregulated throughout development, whereas it was only modestly and not significantly increased in adult mutant kidneys (Fig. 7 E).

Together these results show differential dosage sensitivity among the HNF1B-activated genes during metanephric kidney development. Our data reveal that among the various metanephric kidney developmental processes known to be controlled by HNF1B, the genes participating to proximal tubule differentiation and the onset of nephron cellular maturation are those exhibiting a unique response to the levels of HNF1B protein.

Preliminary postnatal characterization of heterozygous *Hnf1b*^{sp2/+} mutant mice

As mentioned above (Supplementary TableS1), a fraction of heterozygous died between P1 and P25, yet the renal phenotype in these cases could not be studied owing cannibalism. Otherwise, mice lived more than one year, beginning to manifest disease symptoms approximately after 12 months. In few cases, disease symptoms were manifested already in 5 month-old mice and required euthanasia (Fig.8 D).

Body weight curve analyses showed approximately 20% reduction in weight of heterozygous mice relative to *WT*, with males and females behaving rather similarly (Supplementary Fig S6). Analysis of kidney weight/body weight ratio of males at different ages did not show significant differences as compared to *WT* littermates (Supplementary Fig. S6). Yet, one month-old heterozygous mutants exhibited lower kidney weight/body weight ratios than *WT* reflecting mild hypoplastic kidneys.

Further histological analysis of adult *Hnf1b*^{sp2/+} mice revealed variability in the severity of the renal phenotype with increased abnormalities observed both in aged males and females. They usually exhibited unilateral hydronephrosis while the other kidney less affected, displayed mainly cortical or medullar glomerular cysts with collapsed or rudimentary capillary tufts (Fig.8, B, C, H, I) as well as microcysts (Fig.8 B, I). Dilated of Bowmann's spaces were often filled with finely granular proteinaceous material (Fig. 8 B', E', I'). A rare case (1/48 heterozygous mutants) exhibited severely bilateral affected kidneys: one kidney was highly multicystic/hypoplastic and nonfunctional and the other was severely hydronephrotic (Supplementary Fig. S6 H, H'). This mouse exhibited obvious symptoms of severe renal dysfunction, including bloody urines, at the time of dissection (12-month-old), but at 6 months its renal functions were similar heterozygous littermates indicative of progressive hydronephrosis with age. Accordingly, some old mice (males or females) developed giant hydronephrosis.

We then performed preliminary urinary analyses at different ages under basal conditions. Three month-old *Hnf1b*^{sp2/+} mutant mice exhibited normal physiological parameters. However, by 6 month-old they exhibited defective urine concentrating ability with polyuria, and reduced urine osmolality (Table 2). Reduced urine osmolality was also observed after 22hs of water deprivation (data not shown). By 12 months, although urine volumes remained higher than *WT*, urine osmolality was more modestly and non-significantly decreased (Table 2). A similar increase in 24-hour urine output and daily water consumed was observed in three independent groups of mice in 5-6 month-old mutant mice, followed by an attenuation of these parameters in 12 month-old mice (Supplementary Table S6). Furthermore, impaired urinary concentration ability was also observed in 8-months *Hnf1b*^{sp2/+} mice in a mixed genetic background, but not in 6-month-old in the 129/sv background (not shown).

In agreement with the lower urine osmolality, 6-month-old *Hnf1b*^{sp2/+} mice had significantly lower urinary magnesium, sodium and potassium concentrations. However, the total excretion of these solutes was increased as compared to *WT* (Table 2); this tendency was maintained in 12-month-old mice, although did not reach significance. Interestingly, urinary calcium concentration was significantly increased despite decreased osmolality. Further, plasma analysis in a separate group of mice revealed an increase of creatinine levels, although non-significant, while the levels of Mg were similar to *WT*. We have also observed a significant increase in the levels of the alanine aminotransferase ALT and a tendency of higher levels aspartate aminotransferase (AST), reflecting potential liver dysfunctions in our

heterozygous mutant mice as previously reported in some RCAD mutant carriers {Iwasaki, 1998 #77}.

To gain further insight into the pathophysiology of the renal disease we also performed urinary proteome analysis. Urinary low molecular weight proteomes were investigated from urine samples of 17 *Hnflb*^{sp2/+} mutant and 18 *WT* mice with an age ranging from 3 months to 17 months, using Capillary electrophoresis-mass spectrometry (CE-MS) and tandem mass spectrometry (MS/MS). We identified 40 significant differentially excreted peptides (Supplementary Table S7A). The most prominent findings associated to our mouse model were a substantial decrease of Epidermal Growth Factor (EGF), uromodulin (UMOD) and the kidney androgen-regulated protein (KAP) and a tendency of an increase of collagen fragment urinary excretion. Amongst the collagen fragments (e.g. collagen type I alpha-1, type I alpha-2 and type III), 23 were increased and only 4 displayed a decrease in the urine of heterozygous mutant mice (Supplementary Table S7A). Interestingly, no significant differences were detected in the peptides excreted by younger and older *Hnflb*^{sp2/+} mice (data are not shown). Subsequently, we performed a peptide-based *in silico* protease analysis based on the N- and C-terminal and on the mean intensities (peptide amplitudes) of the 40 sequenced naturally occurring peptides and found both downregulated proteases, such as cathepsins and matrix-metalloproteinases and upregulated proteases, such as granzymes and collagenases potentially responsible for generation of the urinary peptides in our mouse model (Supplementary Table S7B).

The urinary proteomic profile of *Hnflb*^{sp2/+} is consistent with the HNF1B-dependent regulation of both *Umod* {Gresh, 2004 #10; Fig. 7) and of the *Kap* gene, found strongly downregulated at all stages examined (Supplementary Table S3). In this context, mutations in the *Umod* gene lead to autosomal dominant tubule interstitial diseases, a rare disease characterized by progressive tubulointerstitial damage, impaired urinary concentrating ability, hyperuricemia, renal cysts, and progressive renal failure (Rampoldi et al, 2011), thus sharing some of the features exhibited by our mouse model as well as RCAD patients. The function of the *Kap* gene, although encoding one of the most abundant proteins in the mouse PT, remains mainly unknown and no orthologous was found in humans. Of note, a decreased EGF urinary concentration has been reported in several kidney injury rodent models (reviewed {Klein, 2016 #80} {Kok, 2014 #81}) and low urinary excretion of EGF was found in ADPKD patients at an early stage in the disease {Weinstein, 1997 #82}.

In conclusion, heterozygous *Hnflb*^{sp2/+} exhibit progressive renal abnormalities associated with a tendency to defective urinary concentration ability under basal conditions, associated with increased excretion of certain solutes and hypercalcuria, followed by a partial recovery in old animals. Interestingly, urinary proteome analysis uncovers a particular profile of our heterozygous mutants predictive of progressive decline in kidney function, kidney injury and fibrosis.

DISCUSSION

We report here the generation of a novel mouse model of the RCAD disease by replicating a previously identified human splicing mutation and show that at the heterozygous state reproduces several of the urogenital defects described in *HNF1B* mutant carriers. These observations show that not only humans but also mice are sensitive to haploinsufficiency for HNF1B.

Our findings highlight the importance to precisely replicate the human disease mutations within the *Hnf1b* locus. Although previous mouse *Hnf1b* mutations (Barbacci, 1999 #26; Coffinier, 1999) generated a loss of function alleles as our new model, the levels of the HNF1B protein at the heterozygous state did not decrease and were even increased (Kornfeld, 2013 #39}, Fig. 3 C, D). In these previous knock out models one of the major difference with our model was the presence of the neomycin resistance cassette with its regulatory elements, which may impact severely the genomic structure of the locus.

An additional important observation is that the levels of HNF1B protein in heterozygous mutants were strongly reduced, in particular during development, without correlating with the corresponding transcript levels. Thus, HNF1B activity appears to be highly regulated at the post-transcriptional and/or translational level. Previous analyses have also reported the apparent non-correlation between the transcript levels and HNF1B binding activity during mouse development (Cereghini et al, 1992). Further studies of our mouse model are required to fully define the underlying molecular mechanisms involved and eventually uncover how the HNF1B protein levels could be manipulated. The ubiquitin proteasome pathway and miRNA-mediated regulation of HNF1B are, amongst others, possible mechanisms mediating tightly regulation of HNF1B protein levels and potentially deregulated in our model. This knowledge will certainly have potential implications for disease therapy.

The high variability in the phenotype of *HNF1B* mutant carriers has been explained by diverse mechanisms ranging from modifier genes, environmental factors, epigenetic influences, interacting cofactors and potential dominant negative function of certain mutations. We show that heterozygous mouse mutants, similar to RCAD patients develop heterogeneous urogenital abnormalities. Moreover, they exhibited a more severe phenotype in the C56BL/6N background than in the 129/sv background with 10% of C57BL/6N *Hnf1b*^{Sp2/+} mutants dying during the first month of life. Thus, genetic modifiers may indeed either

aggravate or attenuate the disease phenotype. Interestingly, even in these two inbred backgrounds we still observed variability in the phenotype presentation of heterozygous *Hnf1b*^{Sp2/+} notably at later stages of development and postnatal life. In particular, in the C57BL/6N background very often one kidney was more severely affected and hydronephrotic while the other was moderately affected mainly with glomerular cysts and microcysts. This variability was also observed in *Hnf1b*^{Sp2/+} mutants from the same litter and raised together reducing different environmental exposition. One possible explanation of this variability could be the known inherent stochasticity in transcription and translation processes (Bar-Even A et al, 2006) or epigenetic modifications that may also underlie the observed variability in *HNF1B* mutant carriers.

Our results also show that although transcripts from the mutated allele are transcribed at relative lower levels than those from the *WT* allele, there were no evidences of nonsense mediated mRNA decay (Fig.1 B), thus confirming previous observations of a differential susceptibility to mRNA decay of naturally occurring *HNF-1B* mutations (Harries et al. 2005). However, we did not detect any of the potential truncated proteins encoded by the alternative spliced transcripts, thus excluding a proposed dominant negative action. It is possible that these truncated proteins are misfolded and degraded by ubiquitin-mediated protein quality control system (Rousseau A, Bertolotti 2018). These observations further suggest that intragenic *HNF1B* mutations leading to premature stop codons do not necessarily encode the respective truncated proteins thus excluding, at least in these cases, the hypothesis that function as dominant negative via heterodimerisation with the *WT* protein.

Owing the developmental character of the RCAD disease, we focused our analysis throughout embryogenesis. Global transcriptional profiling at different embryonic stages indicate that only a subset of the established target genes was sensitive to reduced levels of HNF1B protein. Unexpectedly, most of the targets strongly decreased in the absence of *Hnf1b*, most notably the cystic genes considered the major downstream effectors of the *HNF1B*- associated cystic renal disease, were relatively insensitive to HNF1B dosage. Remarkably, the most downregulated genes were primarily involved in proximal tubule differentiation and onset of nephron tubule mature functions. Consistent with these findings, analyses of human fetuses carrying heterozygous mutations in *HNF1B* showed decreased numbers of nascent nephron structures {Haumaitre, 2006 #4}.

Accordingly, the HNF1B target gene *Hnf4a* {Heliot, 2013 #7}, involved in proximal tubule differentiation and function {Martovetsky, 2013 #73} (A. Desgrange and S.C. unpublished data), is the unique transcriptional regulator strongly reduced in our mutants at all developmental stages, further suggesting that the transcription factor HNF4A cooperate with HNF1B in the observed developmental renal phenotype. Such a functional interaction between HNF1A and HNF4A has already been described in pancreatic islets (Boj et al, 2010).

Despite a global increase in the number of downregulated genes from E14.5 to E17.5, we also observed dynamic and temporal regulation patterns (i.e. some genes were strongly downregulated at an early stage but not at a later stage) suggesting an increasing complexity in the regulatory network involved in the differentiation and maturation of nephron segments. It is tempting to speculate that similar changes in promoter occupancy patterns during development involving new recruitments, release, and exchange of specific factors as described during hepatocyte differentiation (Kyrnizi et al, 2006), take also place during renal development.

Not unexpectedly since HNF1B and the structurally related transcription factor HNF1A bind to the same sequences either as dimers or heterodimers, several of the proximal tubule genes strongly downregulated during development in our mutants have also been shown to be targets of HNF1A or HNF1A/HNF1B heterodimers in adult kidneys (Saji et al, 2007; Kikuchi et al.2007; David-Silva et al 2013). In our mutants, the expression of *Hnf1a* in the PT was only moderately decreased at E17.5 and not affected at P1 and P21 (Supplementary Table S3 and data not shown), indicating that HNF1A was unable to compensate for HNF1B decreased levels during development. However, it appears, at least partially, to compensate in postnatal life as indicated the observed restoration of the expression of some proximal tubule markers such as *Lrp2* and *Spp2* in *Hnf1b*^{Sp2/+} adult kidneys. In this context, heterozygous *Hnf1b*^{Sp2/+} did not show glycosuria, suggesting that HNF1A replaced HNF1B in the control of *Sglt2* (*Slc5a2*), a gene strongly downregulated in our mutants at both E17.5 and P1. Other targets however were found strongly downregulated at all stages in both our mutants and *Hnf1a*^{-/-} mice, such as the phenylalanine hydroxylase (*Pah*) and the PDZ Domain-Containing Protein 1 (*Pdzk1*), suggesting their transcriptional dependence on HNF1A/HNF1B heterodimers. Unexpectedly, the renal expression of other known HNF1 targets, including *Tmem27* and the cationic amino acid exchanger *Slc7a9* were not affected in *Hnf1a*-deficient mice (Bonzo et al, 2010) and remained downregulated in our heterozygous mutants (Fig.7), highlighting the complexity in the regulatory networks of these two transcription factors in the cells they coexpress.

Adult *Hnf1b*^{sp2/+} mice often exhibited unilateral hydronephrosis (40% n: 45). One the most common cause of hydronephrosis is ureter obstruction. Although we did not observed ureter obstruction in our mutants, occasionally we observed dilated ureters at the ureteropelvic junction (Sup. Fig. 3-C57BL/6N). Of note, hydronephrosis and hydroureter have been already described in some RCAD patients (Adalat et al, 2008) as well as in different mouse models of *Hnf1b*-inactivated in the collecting ducts {Desgrange, 2017 #5} {Aboudehen, 2017 #75}. Interestingly, compound heterozygotes for *Pax2* and *Hnf1b* null alleles displayed hydronephroses and megaureters, which appeared to result from a functional defect in the ureter smooth muscle differentiation {Paces-Fessy, 2012 #1}. Further analyses of *Hnf1b*^{sp2/+} mutant are required to define whether hydronephrosis is due to similar perturbations of smooth muscle differentiation of the ureter and/or through other proposed mechanisms, such as polyuria (see below, {Aboudehen, 2017 #75}). In this context, we have also shown that heterozygous *Hnf1b*^{sp2/+} exhibited progressive renal abnormalities associated with defective urinary concentration ability under basal conditions and hypercalcuria by 6 month-old followed by a partial restoration by 12-month-old. Similar defects in urine concentration have recently been described in mice with specific *Hnf1b* inactivation in the collecting ducts at later stages {Aboudehen, 2017 #75}, which were associated with increased expression and abnormal apical localization of AQP2, indirect downregulation of the PT urea transporter *UT-A1* (*Slc22a12*) and the direct control of the HNF1B target *Fxr*. Although additional analyses are required, included urinary concentration ability under different conditions along with transcriptomics and urinary metabolomics, we have not observed misexpression of AQP2 in our mutant mice (data not shown). It is worth noting that the defects observed in *Hnf1b*^{sp2/+} mutant mice are not restricted to the collecting ducts. Indeed, the combined decreased expression of *Tmem27* and *Umod* found in heterozygous mutant mice (Fig.7 E) may at least in part, explain the observed urinary concentration defects since reduced urinary concentrating ability has been described in both *Umod*- and *Tmem27*-deficient mice (Bachmann et al., 2005; Mutig et al., 2011; Malakauskas SM et al 2007. Interestingly, *Tmem27*-deficiency leads also to defective renal amino acid uptake in mice and generalized aminoaciduria (Malakauskas et al 2007), which it would be important to further explore in our model.

We recently reported a metabolic profiling of different organs, including kidney, pancreas and liver as well as plasma of adult *Hnf1b*^{sp2/+} mice (8-months, mixed genetic

background). Although urinary metabolomics was not performed, we found evidences of impaired amino acid renal metabolism in kidneys and reduced levels of total free amino acids and increased myo-inositol in plasma samples that are metabolic parameters reflecting impaired renal function (Torrel et al, 2018). The metabolomic analyses also suggested that *Hnflb*^{sp2/+} mice exhibited disturbed hepatic lipid metabolism and endocrine pancreas alterations. Likewise, and as previously been reported in RCAD mutant carriers, we also observed in our mutants a significant increase in the plasma levels of the alanine aminotransferase (ALT) and a tendency of higher levels aspartate aminotransferase (AST) reflecting liver dysfunctions (Table 2). Unlike humans, however adult mice did not exhibit hypo-magnesemia and/or hyper-magnesuria (Table 2) reported in more than 40% of *HNF1B* mutant patients. We do not have a mechanistic explanation for the normal urine and plasma Mg levels in our mutants, which may reflect differences between mouse and humans in ion transport regulation and/or adaptive mechanisms. For instance, the lack of hyperuricaemia observed in *Umod* transgenic mice despite the defective transport in the TAL, is likely due to the uricase activity that catalyses the conversion of uric acid to allantoin and is present in rodents but not in humans (Rampoldi et al, 2011).

More importantly, our urinary proteome analysis uncovered a particular profile in our heterozygous mutants, with a substantial decrease of uromodulin (UMOD) and epidermal growth factor (EGF) peptides, predictive of progressive decline in kidney function and kidney injury, as well as UP-excreted collagen fragments, which are consistent with an excessive extracellular matrix (ECM) turnover. Interestingly, a subsequent analysis in a pediatric cohort of RCAD patients revealed a similar signature with a majority of peptides collagen type I or type III fragments enriched in the urine of RCAD patients and a down-excretion of uromodulin fragments, together with other additional de-regulated peptides (Ricci P, Magalhães P, et al., Submitted (#footnote))

In summary, the *Hnflb*^{sp2/+} heterozygous mutant mouse model represents a unique clinical/pathological viable model of the human disease and promises to be important in the integrative evaluation of the broad facets of this disease ranging from various developmental abnormalities to kidney, pancreas and liver dysfunctions in the context of the whole animal.

Ricci P^{1*}, Magalhães P^{2,3*}, Krochmal M², Pejchinovski M², Daina E⁴, Caruso MR⁴, Goea L¹, Iwona Belczacka I^{2,5}, Remuzzi G⁴, Umbhauer M¹, Drube J³, Pape L³, Mischak H², Decramer S⁶, Schaefer F⁷, Schanstra JP⁶, Cereghini S¹, Züribig P². **Urinary proteome signature of Renal Cysts and Diabetes syndrome in children (submitted)**

MATERIAL AND METHODS

Generation of a mouse model carrying a point mutation at the intron 2 splice donor site

The knock-in mouse carrying a human splicing point mutation was generated according to a project presented by S. Cereghini with the support of the GIS Maladies Rares and the Mouse Clinical Institute. The splice mutation into the *Hnf1b* locus was introduced by homologous recombination. The WT sequence GAC/g taagtgtttaacctt was mutated to GAC/t taagtgtttaagcctt sequence (Capital letters show end Exon2 bases, lower letters indicates the intron2-Exon2 junction sequence, in bold the point mutations). The *LoxP*-flanked neomycin-resistance cassette was located within intron-1 and subsequently excised by breeding heterozygous mutant mice with a “Cre deleter” mouse line, in this way the mutated allele encompassed the point mutation at the splice donor site in addition to a single *LoxP* site and *HindIII* restriction site aagcct (underlined) within intron 2. Mice heterozygous for the *Hnf1b* null allele (*Hnf1b*^{lacZ/+}), with the *lacZ* gene replacing the first exon of *Hnf1b* {Barbacci, 1999 #26}, were maintained as heterozygotes.

Animal care and the experimental protocols were approved by and conducted in accordance with French and European ethical legal guidelines and the local ethical committee for animal care (Comité d'éthique en Expérimentation Animale Charles Darwin N°5, approval number N° 04817.02), respecting the 3R rule.

RNA extraction and real-time PCR analysis

Both metanephroi of each embryo were dissected in ice cold Dulbecco Modified Medium (DMEM), washed in PBS. Total RNA was extracted using the miRNase Mini Kit (Qiagen), Dnase1 treated on the columns and 250 ng was reverse-transcribed using the high capacity cDNA reverse transcription kit (Applied Biosystems). Real-time PCR was performed using Fast SYBR Green master mix (Applied Biosystems) and the Step-One Plus system (Applied Biosystems) as described (Paces-Fessy, 2012 #1). The method of relative quantification ($2^{-\Delta\Delta CT}$) was used to calculate the expression levels of each target gene, normalized to cyclophilin A (Livak and Schmittgen, 2001), and relative to WT cDNA from E15.5 embryonic kidney. The primers used are listed in Supplementary Table S2. All PCR reactions were run in duplicate. Number of kidney samples is indicated in the figures. The mean and SEM were calculated by genotypes and the statistical significance was determined using Student's t-test (significance at * $P < 0.05$, ** $P < 0.01$, *** $P < 0.001$).

Semiquantitative RT-PCR

Total RNA from microdissected kidneys was extracted and subjected to semiquantitative RT-PCR as described {Lokmane, 2008 #2} with the following modifications. The conditions were chosen so the RNAs analyzed were in the exponential phase of amplification by performing different PCR cycles indicated in Fig. 1. PCR products were resolved in 2% agarose/TBE ethidium bromide gels and photographed using GELDOC documentation system. Densitometry quantification was performed in ImageJ software. Primer sequences used were *Gapdh* for normalization and for *Hnf1b*, vATG and v695 (Supplementary Table S2)

Western blots

The two kidneys of each embryo from at least three (n=3) different embryos were pooled, snap-frozen in liquid N₂ and reduced to a fine powder under Liquid N₂. They were lysed in ice-cold buffer (10% glycerol, 50 mM Tris-HCl pH 7.4, 150 mM NaCl, 10 mM EDTA, 1% NonidetP-40 with complete protease inhibitor cocktail ROCHE) using a dounce-homogenizer. Samples were centrifuged for 15 minutes at 13,000 rpm 4°C, and the supernatant kept in

Liquid N₂ until use. Whole cell extracts containing 30µg of protein were prepared in SDS sample buffer and subjected to SDS-PAGE (4–15% Mini-PROTEAN® TGX™ Precast Protein Gels, Biorad). After transfer to PVDF membrane and blocking with TBST (50 mM Tris-HCl pH 7.4, 150 mM NaCl, 0.1 % Tween), 5% skim milk, immunostaining was performed by overnight incubation in TBST 1% skim milk buffer with a rabbit polyclonal antibody against HNF1B (1:500) raised in the laboratory against residues 39–89 of the mouse HNF1b protein {Haumaitre, 2005 #3}; α -Actin was subsequently used as a loading control (monoclonal antibody A4700, 1:1,000; Sigma-Aldrich). Secondary antibodies are listed in Supplementary Table S8. Positive bands were detected by chemiluminescence (ECL, Pierce; SuperSignal West Dura, Thermo Scientific). Images were captured with a Fusion Fx7 and quantified with Bio-1D software (Vilbert-Lourmat).

Plasma and urine analyses

Urine and plasma were obtained on age- and gender-matched heterozygous and *WT* mice (males). They were housed in light- and temperature-controlled room with *ad libitum* access to tap water and standard chow (Diet AO4, SAFE, France). 24-h urine samples collected under mineral oil to avoid evaporation were obtained at baseline in individual metabolic cages, after 2-3 days habituation. Each 24-h, animals were weighed and the food, water intake, urine volume and fecal weight recorded. Blood was sampled by retro-ocular puncture in general 2 weeks after being in the metabolic cages and plasma samples were kept at -80°C . The urinary concentrating ability was tested after 22h water deprivation. Urinary creatinine, urea and electrolytes, plasma urea, creatinine, magnesium, ASAT, ALAT and were measured on Olympus AU400 Chemistry Analyzer (ICB-IFR2, Laboratoire de Biochimie UFR de Médecine Paris 7, Bichat. Osmolality was measured using a vapor pressure osmometer (Wescor 5500, USA).

Statistical

Data are represented as mean \pm standard error of mean (SEM). Comparisons between groups were performed using with a two-tailed test of significance. $P < 0.05$ was considered to be significant with $*P < 0.05$, $**P < 0.01$, $***P < 0.001$.

Immunofluorescence on transfected cells, In situ hybridization (ISH) and immunohistochemistry

The human epithelial C33 cell line was transiently transfected with reporter constructs of WT-HNF1B and truncated HNF1B proteins lacking the exon 2 and immunofluorescence analysis on glass-slides was carried out as described {Barbacci, 2004 #25}, using rabbit anti-HNF1B (Supplementary Table S2),

In situ hybridization (ISH) on paraffin sections was performed as described {Lokmane, 2008 #2}. The *Fbp*, *Spp2* cRNA probes were generated by PCR (GUDMAP database). Embryos and postnatal kidneys up to 2 month-old were fixed with 60% ethanol/11% formaldehyde and 10% acetic acid. Adult kidneys (> 2months) were fixed in alcoholic Bouin (Duboscq-Brasil) solution and paraffin sections were used for H&E histological analysis and immunohistochemistry. Antibody staining on paraffin sections was performed as described {Lokmane, 2010 #12} {Desgrange, 2017 #5}. For each probe (ISH) or antibody sections from at least three different embryos were used. The primary and secondary antibodies are listed in supplementary Table S7. Terminal deoxynucleotidyl transferase, mediated digoxigenin-deoxyuridine nick-end labelling (TUNEL) was performed on E15.5 kidney sections as described {Paces-Fessy, 2012 #1} {Heliot, 2013 #7}.

ACKNOWLEDGMENTS

We thank Daniel Darby and Adrian S. Woolf for critical reading of the manuscript, Eduard Manzoni for animal care. We also thank Pantelis Hatzis (Alexander Fleming Institute, Genomics Facility, Greece) for mRNA sequencing, Christophe Antoniewsky (IBPS UMR7622) for help in mRNA-seq statistical analyses, Mark Knepper (Bethesda USA), Renata Kozyraki (Institut Cordeliers, France) and Sylvie Robine (Institut Curie, Paris) for kindly providing antibodies.

FUNDINGS

L.N and M. K were early researchers (ER) supported by the by the Biology of Liver and Pancreatic Development and Disease (BOLD) Marie Curie Initial Training Network (MCITN) EU- FP7 programme (No. 238821); P. R. and P.M. were recipients of PhD student fellowships from ITN RENALTRACT MSCA-ITN-2014-642937. C. L. was a postdoctoral researcher supported by Agence National de la Recherche (ANR) Blan06-2_139420. This work was supported by the GIS- Institut Maladies Rares Paris France & Institut Clinique de la Souris, Ilkirch, France, the Agence National de la Recherche (ANR) Blan06-2_139420 ; the Institut National de la Santé et de la Recherche Médicale (INSERM, France); the BOLD Marie Curie Initial Training Network (MCITN) EU-FP7 programme (No. 238821); by the European Union's Horizon 2020 Research and Innovation Programme under the Marie Skłodowska-Curie grant agreement No. 642937 (RENALTRACT; MSCA-ITN-2014-642937); the by the Centre National de la Recherche Scientifique (CNRS, France) and the Université Pierre et Marie Curie (to S.C.). P.M. and P.Z. were supported by RENALTRACT MSCA-ITN-2014-642937

REFERENCES

Aboudehen K, Noureddine L, Cobo-Stark P, Avdulov S, Farahani S, Gearhart MD, Bichet DG, Pontoglio M, Patel V, Igarashi P: Hepatocyte Nuclear Factor-1beta Regulates Urinary Concentration and Response to Hypertonicity. *J Am Soc Nephrol* 2017, 28:2887-2900.

Adalat S, Woolf AS, Johnstone KA, Wirsing A, Harries LW, Long DA, Hennekam RC, Ledermann SE, Rees L, van't Hoff W, Marks SD, Trompeter RS, Tullus K, Winyard PJ, Cansick J, Mushtaq I, Dhillon HK, Bingham C, Edghill EL, Shroff R, Stanescu H, Ryffel GU, Ellard S, Bockenhauer D. HNF1B mutations associate with hypomagnesemia and renal magnesium wasting. *J Am Soc Nephrol*. 2009 May;20(5):1123-31. doi: 10.1681/ASN.2008060633. Epub 2009 Apr 23.

Bachmann S, Mutig K, Bates J, Welker P, Geist B, Gross V, Luft FC, Alenina N, Bader M, Thiele BJ, Prasad K, Raffi HS, Kumar S. Renal effects of Tamm-Horsfall protein (uromodulin) deficiency in mice. *Am J Physiol Renal Physiol*. 2005 Mar;288(3):F559-67. Epub 2004 Nov 2.

Bar-Even A, Paulsson J, Maheshri N, Carmi M, O'Shea E, Pilpel Y, Barkai N. Noise in protein expression scales with natural protein abundance. *Nat Genet*. 2006 Jun;38(6):636-43. Epub 2006 May 21.

Barbacci E, Reber M, Ott MO, Breillat C, Huetz F, Cereghini S: Variant hepatocyte nuclear factor 1 is required for visceral endoderm specification. *Development* 1999, 126:4795-4805.

Barbacci E, Chalkiadaki A, Masdeu C, Haumaitre C, Lokmane L, Loirat C, Cloarec S, Talianidis I, Bellanne-Chantelot C, Cereghini S: HNF1beta/TCF2 mutations impair transactivation potential through altered co-regulator recruitment. *Hum Mol Genet* 2004, 13:3139-3149.

Bellanne-Chantelot C, Chauveau D, Gautier JF, Dubois-Laforgue D, Clauin S, Beaufils S, Wilhelm JM, Boitard C, Noel LH, Velho G, et al.: Clinical spectrum associated with hepatocyte nuclear factor-1beta mutations. *Ann Intern Med* 2004, 140:510-517.

Bellanne-Chantelot C, Clauin S, Chauveau D, Collin P, Daumont M, Douillard C, Dubois-Laforgue D, Dusselier L, Gautier JF, Jadoul M, et al.: Large genomic rearrangements in the hepatocyte nuclear factor-1beta (TCF2) gene are the most frequent cause of maturity-onset diabetes of the young type 5. *Diabetes* 2005, 54:3126-3132.

Bingham C, Ellard S, van't Hoff WG, Simmonds HA, Marinaki AM, Badman MK, Winocour PH, Stride A, Lockwood CR, Nicholls AJ, et al.: Atypical familial juvenile hyperuricemic nephropathy associated with a hepatocyte nuclear factor-1beta gene mutation. *Kidney Int* 2003, 63:1645-1651.

Bingham C, Hattersley AT: Renal cysts and diabetes syndrome resulting from mutations in hepatocyte nuclear factor-1beta. *Nephrol Dial Transplant* 2004, 19:2703-2708.

Boj SF, Petrov D, Ferrer J. Epistasis of transcriptomes reveals synergism between transcriptional activators Hnf1alpha and Hnf4alpha. *PLoS Genet.* 2010 May 27;6(5):e1000970. doi: 10.1371/journal.pgen.1000970.

Bonzo JA, Patterson AD, Krausz KW, Gonzalez FJ. Metabolomics identifies novel Hnf1alpha-dependent physiological pathways in vivo. *Mol Endocrinol.* 2010 Dec;24(12):2343-55.

Casemayou A, Fournel A, Bagattin A, Schanstra J, Belliere J, Decramer S, Marsal D, Gillet M, Chassaing N, Huart A, et al.: Hepatocyte Nuclear Factor-1beta Controls Mitochondrial Respiration in Renal Tubular Cells. *J Am Soc Nephrol* 2017, 28:3205-3217.

Cereghini S, Ott MO, Power S, Maury M. Expression patterns of vHNF1 and HNF1 homeoproteins in early postimplantation embryos suggest distinct and sequential developmental roles. *Development.* 1992 Nov;116(3):783-97.

Chen J, Bardes EE, Aronow BJ, Jegga AG: ToppGene Suite for gene list enrichment analysis and candidate gene prioritization. *Nucleic Acids Res* 2009, 37:W305-311.

Chen YZ, Gao Q, Zhao XZ, Chen YZ, Bennett CL, Xiong XS, Mei CL, Shi YQ, Chen XM: Systematic review of TCF2 anomalies in renal cysts and diabetes syndrome/maturity onset diabetes of the young type 5. *Chin Med J (Engl)* 2010, 123:3326-3333.

Clissold RL, Hamilton AJ, Hattersley AT, Ellard S, Bingham C: HNF1B-associated renal and extra-renal disease-an expanding clinical spectrum. *Nat Rev Nephrol* 2015, 11:102-112.

Coffinier C, Gresh L, Fiette L, Tronche F, Schutz G, Babinet C, Pontoglio M, Yaniv M, Barra J: Bile system morphogenesis defects and liver dysfunction upon targeted deletion of HNF1beta. *Development* 2002, 129:1829-1838.

David-Silva A, Freitas HS, Okamoto MM, Sabino-Silva R, Schaan BD, Machado UF. Hepatocyte nuclear factors 1 α /4 α and forkhead box A2 regulate the solute carrier 2A2 (Slc2a2) gene expression in the liver and kidney of diabetic rats. *Life Sci.* 2013 Nov 19;93(22):805-13. doi: 10.1016/j.lfs.2013.10.011.

Desgrange A, Heliot C, Skovorodkin I, Akram SU, Heikkila J, Ronkainen VP, Miinalainen I, Vainio SJ, Cereghini S: HNF1B controls epithelial organization and cell polarity during ureteric bud branching and collecting duct morphogenesis. *Development* 2017, 144:4704-4719.

De Vas MG, Kopp JL, Heliot C, Sander M, Cereghini S, Haumaitre C: Hnf1b controls pancreas morphogenesis and the generation of Ngn3⁺ endocrine progenitors. *Development* 2015, 142:871-882.

Edghill EL, Bingham C, Ellard S, Hattersley AT: Mutations in hepatocyte nuclear factor-1beta and their related phenotypes. *J Med Genet* 2006, 43:84-90.

Faguer S, Decramer S, Devuyst O, Lengele JP, Fournie GJ, Chauveau D: Expression of renal cystic genes in patients with HNF1B mutations. *Nephron Clin Pract* 2012, 120:c71-78.

Ferre S, Igarashi P: New insights into the role of HNF-1beta in kidney (patho)physiology. *Pediatr Nephrol* 2018.

Gresh L, Fischer E, Reimann A, Tanguy M, Garbay S, Shao X, Hiesberger T, Fiette L, Igarashi P, Yaniv M, et al.: A transcriptional network in polycystic kidney disease. *EMBO J* 2004, 23:1657-1668.

Haldorsen IS, Vesterhus M, Raeder H, Jensen DK, Sovik O, Molven A, Njolstad PR: Lack of pancreatic body and tail in HNF1B mutation carriers. *Diabet Med* 2008, 25:782-787.

Harries LW, Ellard S, Jones RW, Hattersley AT, Bingham C: Abnormal splicing of hepatocyte nuclear factor-1 beta in the renal cysts and diabetes syndrome. *Diabetologia* 2004, 47:937-942.

Harries LW, Bingham C, Bellanne-Chantelot C, Hattersley AT, Ellard S. The position of premature termination codons in the hepatocyte nuclear factor -1 beta gene determines susceptibility to nonsense-mediated decay. *Hum Genet.* 2005 Nov;118(2):214-24. Epub 2005 Nov 15.

Haumaitre C, Barbacci E, Jenny M, Ott MO, Gradwohl G, Cereghini S: Lack of TCF2/vHNF1 in mice leads to pancreas agenesis. *Proc Natl Acad Sci U S A* 2005, 102:1490-1495.

Haumaitre C, Fabre M, Cormier S, Baumann C, Delezoide AL, Cereghini S: Severe pancreas hypoplasia and multicystic renal dysplasia in two human fetuses carrying novel HNF1beta/MODY5 mutations. *Hum Mol Genet* 2006, 15:2363-2375.

Heidet L, Decramer S, Pawtowski A, Moriniere V, Bandin F, Knebelmann B, Lebre AS, Faguer S, Guignonis V, Antignac C, et al.: Spectrum of HNF1B mutations in a large cohort of patients who harbor renal diseases. *Clin J Am Soc Nephrol* 2010, 5:1079-1090.

Heliot C, Desgrange A, Buisson I, Prunskaitė-Hyyryläinen R, Shan J, Vainio S, Umbhauer M, Cereghini S: HNF1B controls proximal-intermediate nephron segment identity in vertebrates by regulating Notch signalling components and *Irxf1/2*. *Development* 2013, 140:873-885.

Hiesberger T, Shao X, Gourley E, Reimann A, Pontoglio M, Igarashi P: Role of the hepatocyte nuclear factor-1beta (HNF-1beta) C-terminal domain in *Pkhd1* (ARPKD) gene transcription and renal cystogenesis. *J Biol Chem* 2005, 280:10578-10586.

Iwasaki N, Ogata M, Tomonaga O, Kuroki H, Kasahara T, Yano N, Iwamoto Y: Liver and kidney function in Japanese patients with maturity-onset diabetes of the young. *Diabetes Care* 1998, 21:2144-2148.

Kaminski MM, Tosic J, Kresbach C, Engel H, Klockenbusch J, Muller AL, Pichler R, Grahmmer F, Kretz O, Huber TB, et al.: Direct reprogramming of fibroblasts into renal tubular epithelial cells by defined transcription factors. *Nat Cell Biol* 2016, 18:1269-1280.

Kato N, Motoyama T: Expression of hepatocyte nuclear factor-1beta in human urogenital tract during the embryonic stage. *Anal Quant Cytol Histol* 2009, 31:34-40.

Kettunen JLT, Parviainen H, Miettinen PJ, Farkkila M, Tamminen M, Salonen P, Lantto E, Tuomi T: Biliary Anomalies in Patients With HNF1B Diabetes. *J Clin Endocrinol Metab* 2017, 102:2075-2082.

Kikuchi R, Kusuhara H, Hattori N, Kim I, Shiota K, Gonzalez FJ, Sugiyama Y. Regulation of tissue-specific expression of the human and mouse urate transporter 1 gene by hepatocyte nuclear factor 1 alpha/beta and DNA methylation. *Mol Pharmacol.* 2007 Dec;72(6):1619-25. Epub 2007 Sep 13.

Kok HM, Falke LL, Goldschmeding R, Nguyen TQ: Targeting CTGF, EGF and PDGF pathways to prevent progression of kidney disease. *Nat Rev Nephrol* 2014, 10:700-711. 48.

Kornfeld JW, Baitzel C, Konner AC, Nicholls HT, Vogt MC, Herrmanns K, Scheja L, Haumaitre C, Wolf AM, Knippschild U, et al.: Obesity-induced overexpression of miR-802 impairs glucose metabolism through silencing of *Hnf1b*. *Nature* 2013, 494:111-115.

Lindner TH, Njolstad PR, Horikawa Y, Bostad L, Bell GI, Sovik O: A novel syndrome of diabetes

mellitus, renal dysfunction and genital malformation associated with a partial deletion of the pseudo-POU domain of hepatocyte nuclear factor-1beta. *Hum Mol Genet* 1999, 8:2001-2008.

Livak K. J. and Schmittgen T. D. (2001). Analysis of relative gene expression data using real-time quantitative PCR and the 2^{(-Delta Delta C(T))} method. *Methods* 25, 402-408 10.1006/meth.2001.1262 [PubMed] [Cross Ref]

Lokmane L, Haumaitre C, Garcia-Villalba P, Anselme I, Schneider-Maunoury S, Cereghini S: Crucial role of vHNF1 in vertebrate hepatic specification. *Development* 2008, 135:2777-2786.

Lokmane L, Heliot C, Garcia-Villalba P, Fabre M, Cereghini S: vHNF1 functions in distinct regulatory circuits to control ureteric bud branching and early nephrogenesis. *Development* 2010, 137:347-357.

Malakauskas SM, Quan H, Fields TA, McCall SJ, Yu MJ, Kourany WM, Frey CW, Le TH. Aminoaciduria and altered renal expression of luminal amino acid transporters in mice lacking novel gene collectrin. *Am J Physiol Renal Physiol*. 2007 Feb;292(2):F533-44. Epub 2006 Sep 19.

Martovetsky G, Tee JB, Nigam SK: Hepatocyte nuclear factors 4alpha and 1alpha regulate kidney developmental expression of drug-metabolizing enzymes and drug transporters. *Mol Pharmacol* 2013, 84:808-823.

Massa F, Garbay S, Bouvier R, Sugitani Y, Noda T, Gubler MC, Heidet L, Pontoglio M, Fischer E: Hepatocyte nuclear factor 1beta controls nephron tubular development. *Development* 2013, 140:886-896.

Mattapallil MJ, Wawrousek EF, Chan CC, Zhao H, Roychoudhury J, Ferguson TA, Caspi RR: The Rd8 mutation of the *Crb1* gene is present in vendor lines of C57BL/6N mice and embryonic stem cells, and confounds ocular induced mutant phenotypes. *Invest Ophthalmol Vis Sci* 2012, 53:2921-2927.

Mutig K, Kahl T, Saritas T, Godes M, Persson P, Bates J, Raffi H, Rampoldi L, Uchida S, Hille C, Dosche C, Kumar S, Castañeda-Bueno M, Gamba G, Bachmann S. Activation of the bumetanide-sensitive Na⁺,K⁺,2Cl⁻ cotransporter (NKCC2) is facilitated by Tamm-Horsfall protein in a chloride-sensitive manner. *J Biol Chem*. 2011 Aug 26;286(34):30200-10. doi: 10.1074/jbc.M111.222968. Epub 2011 Jul 7.

Nakayama M, Nozu K, Goto Y, Kamei K, Ito S, Sato H, Emi M, Nakanishi K, Tsuchiya S, Iijima K: HNF1B alterations associated with congenital anomalies of the kidney and urinary tract. *Pediatr Nephrol* 2010, 25:1073-1079.

Naylor RW, Qubisi SS, Davidson AJ: Zebrafish Pronephros Development. *Results Probl Cell Differ* 2017, 60:27-53.

Paces-Fessy M, Fabre M, Lesaulnier C, Cereghini S: Hnf1b and Pax2 cooperate to control different pathways in kidney and ureter morphogenesis. *Hum Mol Genet* 2012, 21:3143-3155.

Rampoldi L, Scolari F, Amoroso A, Ghiggeri G, Devuyst O. The rediscovery of uromodulin (Tamm-Horsfall protein): from tubulointerstitial nephropathy to chronic kidney disease. *Kidney Int*. 2011 Aug;80(4):338-47. Review.

Rousseau A, Bertolotti A. Regulation of proteasome assembly and activity in health and disease. *Nat Rev Mol Cell Biol*. 2018 Jul 31. doi: 10.1038/s41580-018-0040-z. [Epub ahead of print] Review.

Saji T, Kikuchi R, Kusuhara H, Kim I, Gonzalez FJ, Sugiyama Y.J. Transcriptional regulation of human and mouse organic anion transporter 1 by hepatocyte nuclear factor 1 alpha/beta. *Pharmacol Exp Ther*. 2008 Feb;324(2):784-90. Epub 2007 Nov 20.

Stenson PD, Ball EV, Mort M, Phillips AD, Shiel JA, Thomas NS, Abeyasinghe S, Krawczak M, Cooper DN: Human Gene Mutation Database (HGMD): 2003 update. *Hum Mutat* 2003, 21:577-581.

Sun Z, Hopkins N: vhnf1, the MODY5 and familial GCKD-associated gene, regulates regional specification of the zebrafish gut, pronephros, and hindbrain. *Genes Dev* 2001, 15:3217-3229.

Thomson RB, Wang T, Thomson BR, Tarrats L, Girardi A, Mentone S, Soleimani M, Kocher O, Aronson PS: Role of PDZK1 in membrane expression of renal brush border ion exchangers. *Proc Natl Acad Sci U S A* 2005, 102:13331-13336.

Thiagarajan RD, Georgas KM, Rumballe BA, Lesieur E, Chiu HS, Taylor D, Tang DT, Grimmond SM, Little MH: Identification of anchor genes during kidney development defines ontological relationships, molecular subcompartments and regulatory pathways. *PLoS One* 2011, 6:e17286.

Torell F, Bennett K, Cereghini S, Fabre M, Rännar S, Lundstedt-Enkel K, Moritz T, Haumaitre C, Trygg J, Lundstedt T. Metabolic Profiling of Multiorgan Samples: Evaluation of MODY5/RCAD Mutant Mice. *J Proteome Res.* 2018 Jul 6;17(7):2293-2306. doi: 10.1021/acs.jproteome.7b00821. Epub 2018 Jun

Verdeguer F, Le Corre S, Fischer E, Callens C, Garbay S, Doyen A, Igarashi P, Terzi F, Pontoglio M: A mitotic transcriptional switch in polycystic kidney disease. *Nat Med* 2010, 16:106-110.

Weinstein T, Hwang D, Lev-Ran A, Ori Y, Korzets A, Levi J: Excretion of epidermal growth factor in human adult polycystic kidney disease. *Isr J Med Sci* 1997, 33:641-642.

Wilson PD: Apico-basal polarity in polycystic kidney disease epithelia. *Biochim Biophys Acta* 2011, 1812:1239-1248.

Zaffanello M, Brugnara M, Franchini M, Fanos V: TCF2 gene mutation leads to nephro-urological defects of unequal severity: an open question. *Med Sci Monit* 2008, 14:RA78-86.

SUPPLEMENTARY MATERIAL AND METHODS

Transcriptional profiling at different stages by mRNA-sequencing

The two kidneys from heterozygous for the *Hnf1b* splicing mutation and WT embryos were microdissected from the same litter. This requirement limited the number of samples used in general to 2 controls and 2 mutants, independently of the sex. Note that we found a similar phenotype in males and females. The stages analyzed included E14.5 (when morphologically the mutant kidneys were morphological normal and considered as pre-disease and at disease stages E15.5, E17.5 and postnatal day 1 (P1). Note that at E15.5 we performed deep sequencing from pooled samples of 3 WT and 3 *Hnf1b*^{Sp2/+} (6 kidneys each sample)

Stade	WT	WT	<i>Hnf1b</i> ^{Sp2/+}	<i>Hnf1b</i> ^{Sp2/+}
E14.5	SCR10-E145-4wt	SCR13-E145-4wt	SCR12-E145 HET	SCR15-E145-HET
E15.5	WT (Pool n=3)		TR (Pool n=3)	
E17.5 *	GZS 17	GZS 35 (n=3)	GSZ 3 4 (n=3)	GSZ 36 (n=3)
P1	SCR20_P1_	SCR21_P1_	SCR22 P1	SCR23_P1

RNA was prepared from the 2 kidneys of each embryo, except when the n is indicated (i.e. E15.5 and E17.5)

** RNA from 2 litters born the same day in the same cage (Pool n=3, 6 kidneys)*

RNA from microdissected kidneys was extracted by Tryzol, using the miRNA mini kit Qiagen for the extraction of total and miRNAs. The quality of the RNA samples was assessed on the Agilent Bioanalyzer system using the Agilent RNA 6000 Nano Kit (Agilent Technologies) and RNA with a Ring higher than 8 was used. 1-2 µg of total RNA were used for mRNA isolation using the Dynabeads® mRNA DIRECT™ Micro Kit (ThermoFisher Scientific). mRNA was digested with RNase III, purified, hybridized and ligated to Ion Adaptors, reverse transcribed, barcoded and amplified, using the Ion Total RNA-Seq Kit v2 (ThermoFisher Scientific).

RNA sequencing was performed on an Ion Proton™ System, according to the manufacturer's instructions. The prepared libraries were quantified and pooled together in duplicates at the required concentration. The pools were then processed on an OneTouch 2 instrument and enriched on a One Touch ES station. Templating was performed using the Ion PI™ Template OT2 200 Kit (ThermoFisher Scientific) and sequencing with the Ion PI™ Sequencing 200 Kit on Ion Proton PI™ chips (ThermoFisher Scientific) according to commercial protocols.

The resulting RNA-Seq BAM files were analyzed with the Bioconductor package metaseqR {Moulos, 2015 #60} and applying the edgeR (<http://www.bioconductor.org/packages/release/bioc/html/edgeR.html>) methodology for differential expression analysis with default settings.

Urinary proteomic analysis

Urines from wild-type (WT) and *Hnf1b*^{Sp2/+} mutant mice (males) were collected by spontaneous voiding and kept frozen at -80°C or after being placed individually in metabolic cages as described in Material and Methods. The total volume of 24-hs urines was aliquoted and frozen at -80°C. A 150 µl sample of mouse urine was diluted with the same volume of urea buffer (2 M urea, 10 mM NH₄OH, 0.2% sodium dodecylsulfate). The total volume of urines was aliquoted and frozen at -80°C. 150 µl of urine samples were ultrafiltrated, desalted, lyophilized and resuspended for proteomics analysis as described {von zur Muhlen, 2012 #61}.

CE-MS analysis and data processing.

Capillary electrophoresis-mass spectrometry (CE-MS) analysis was performed using a Beckman Coulter Proteome Lab PA800 capillary electrophoresis system (Fullerton, CA) online coupled to a

microTOF II MS (Bruker Daltonic, Bremen, Germany) as described {Coon, 2008 #59}{Mischak, 2013 #58}. For normalization caused by analytical variances and differences in urine dilution, MS signal intensities were normalized relative to 41 internal standard peptides generally present in at least 90% of all urine samples, with small relative standard deviation (SD) {von zur Muhlen, 2012 #61}. The peak lists obtained characterized each peptide by its molecular mass (in daltons), normalized CE migration time (in minutes) and normalized signal intensity. The data of all detected peptides were deposited, matched, and annotated in a Microsoft SQL database as previously described allowing further analysis and comparison of multiple samples {Siwy, 2011 #62}.

Peptide sequencing and In silico protease prediction.

For sequencing peptides, tandem mass spectrometry was performed as described {Klein, 2014 #66}. Concisely, MS/MS analysis were performed using a Dionex Ultimate 3000 RSLC nano flow system (Dionex, Camberly, UK) coupled to an Orbitrap Velos MS instrument (Thermo Fisher Scientific). Data files were analyzed using Proteome Discoverer 1.2 and searched against the Swiss-Prot *Mus Musculus* database {Nkuipou-Kenfack, 2017 #63}. To link the urinary peptide fragments to the proteases involved, in silico protease mapping was generated using Proteasix software as described by {Klein, 2013 #65}.

Statistical analysis. The main peptidomic differences between the WT and *Hnf1^{Sp2/+}* urines were obtained using the P-values based on Wilcoxon rank-sum test. Statistical adjustment of P-values due to multiple testing was performed by Benjamini and Hochberg method. Peptides that were detectable in >90% of mice and reached an adjusted P value of <0.05 were further considered as relevant.

LEGENDS TO FIGURES

Figure 1: Structure and generation of the *Hnf1b* intron-2 spliced mutant mice

A- Genomic organization of the *Hnf1b* locus, illustrating the 9 coding exons and the main functional domains (N-terminal Dimerization, POU-specific (POU_S) and POU-homeodomain (POU_H) and C-terminal transactivation domain). Also indicated are the mutation G to T introduced at the intron-2 splice donor site, the cryptic splicing site within Exon 2 (ss); the Nuclear Localization Signal (NLS) and the location of the alternative exon of 78 bp present in the *Hnf1b* isoform A.

B- Characterization of abnormal spliced *Hnf1b* transcripts generated by the *HNF1b*^{Sp2/+} mutant allele. Representative semiquantitative RT-PCR from P1- kidney RNA of *WT* (lanes a, b) and *HNF1b*^{Sp2/+} (lanes c, d), using primers located in exon 1 and exon 3 (Material and Methods). Amplifications were performed for different cycles ranging 27 to 36 for *Hnf1b* (lanes a, c and lanes b, d correspond respectively to 30 and 33 cycles) and for *Gapdh*, used to normalize for RNA amount for 24 to 30 cycles, (e, f, show 28 cycles). Sequence of PCR products indicated that *WT* express *Hnf1b* variants A and B, while *Hnf1b*^{Sp2/+} mice express four additional abnormal spliced transcripts corresponding to variants A and B lacking either exon 2 or the last 32bp of exon2. The structure of these spliced products and putative encoded proteins are depicted in the middle and right panels. Right panel: grey shows the dimerization and DNA-binding domains, checkerboard box represent the new protein sequences encoded by abnormal spliced transcripts.

Figure 2: *Hnf1b* heterozygous for the splicing mutation *Hnf1b*^{Sp2/+} exhibit renal cysts and hydronephrosis during embryogenesis

(A-F) Representative Hematoxylin and Eosin (H&E) staining sections of embryo kidneys show glomerular cysts and tubular dilatations in the medulla at E15.5 and E17.5 (arrows in E' higher magnification of E). Cystic glomeruli are shown in F' (arrows in F' higher magnification of F). (G-N) Backcrosses to inbred C57BL/6N and 129/Sv backgrounds show different severity of phenotype. Note in C57BL/6N background pelvic dilatations at E17.5 (H) and hydronephrosis and duplicated kidney at P0 (J, see also supplementary Fig S3), in addition to cystic glomeruli and medullar tubules dilatations also observed in 129/sv background (L, N). Images are representative of *n* = 6 for each genotype. See also Supplementary Fig.S3. Scale bar: 200µm.

Figure 3: Expression levels of *Hnf1b* transcripts and protein from WT and heterozygous mutants *Hnf1b*^{Sp2/+}

A- Q-RT PCR of normal *Hnf1b* transcripts at the indicated stages from *WT* and *Hnf1b*^{Sp2/+} kidneys. Number of samples were: at E14.5: 2 *WT* and 5 *Hnf1b*^{Sp2/+}; at E15.5: 3 *WT* and 6 *Hnf1b*^{Sp2/+} (2 litters), at E16.5: 3 *WT* and 8 *Hnf1b*^{Sp2/+} (2 litters); at E17.5: 3 *WT*, 4 *Hnf1b*^{Sp2/+}; at P0: 5 *WT*, 10 *Hnf1b*^{Sp2/+} (2 litters) and adults: 3 *WT* and 3 *Hnf1b*^{Sp2/+}. The 2 kidneys of each embryo/mice were pooled. *Hnf1b* WT transcripts were amplified by primers located in the ATG translational site and in the last 32bp of the Exon 2. Asterisk show significant values *p*<0,05 (*) and *p*<0,001 (**). Error bars represent standard error of the mean (SEM). B- HNF1B immunostaining of E15.5 embryo sections show a partial decrease in nuclear staining in *Hnf1b*^{Sp2/+}. Note HNF1B nuclear staining in both nondilated and dilated *Hnf1b*^{Sp2/+} tubules. C- Representative western blot of WT and *Hnf1b*^{Sp2/+} kidney extracts at the indicated stages from WT and *Hnf1b*^{Sp2/+}. The two HNF1b variant A and B are visible on blot. α -actin was used to normalize for protein amount. D- Quantification of western blots show more than 50% reduction in HNF1B protein levels in *Hnf1b*^{Sp2/+} relative to WT particularly at earlier stages. A decrease of 55% and 67% is observed respectively at E15.5 and E17.5, while at P0

is decreased by 30% and in adults by 60%, with some variability. In adult heterozygous for the null allele of *Hnf1b* (*Hnf1b^{Lac/+Z}*) we observe an increase of 98% in HNF1B levels. N= 4 to 6 WT and *Hnf1b^{Sp2/+}* embryo /mouse kidneys were used per stage and 2 independent experiments were performed. Significant differences between mutants and WT (**P** < 0.05) are indicated (*).

Figure 4: ***Hnf1b^{Sp2/+}* exhibit normal branching of the ureteric bud but delayed differentiation of proximal tubules and collecting duct maturation.** Immunohistochemical analyses of E14.5 to E16.5 WT and *Hnf1b^{Sp2/+}* kidney embryos from the same litter, with Calbindin-D-28K (A, A') and PAX2 (B, B') and (C, C'), WT1 (D, D'), the early proximal tubule marker HNF4A (E, E'), the proximal tubule LTA (F, F'), the collecting duct markers pancytokeratin CK (G, G') and DBA (H, H') at the indicated embryo stages. Note decreased expression of HNF4A (E'), and the absence of LTA (F') and DBA (H') in *Hnf1b^{Sp2/+}* sections, while the other markers express similar to WT. Sections (except C, C') are co-stained with DAPI.

Figure 5: **Immunohistochemical analyses of nephron segment and collecting duct markers of E17.5 -E18.5 and P0 kidney sections**

In *Hnf1b^{Sp2/+}* kidneys LTA staining shows decreased and unequal clusters of proximal tubules both at E17.5 (compare A and A') and P0 (compare B and B'), NKCC2 a marker of the thick ascending Loop of Henle, stains predominantly medullar–cortical cystic structures (compare C and C'; D and D') and DBA is absent in *Hnf1b^{Sp2/+}* collecting ducts at E17.5 (I'), P0 (L'). Sections (except C, C', E, E') are co-stained with DAPI.

Figure 6: **Cystic and tubular dilations of proximal tubule and thick Loop of Henle cells exhibit abnormal apico-basal polarity and reduced number of cells with cilia**

Confocal microscopy of co-stained sections with Villin (Vil1) and HNF4A (A, B, B' magnification in B') and Vil1 and HNF1B (C, D, magnification D') revealed that the expression of Villin, specifically localized on the brush border of proximal tubules, is interrupted in several regions of cystic structures of *Hnf1b^{Sp2/+}* indicative of brush border loss, as highlighted in B' and D' magnifications. Confocal images of Muc1 and Lam1 (E, F) and Lam1 and ZO1 ((G, H) co-immunohistochemistry show that the collecting duct apical marker Muc1 in E15.5 *Hnf1b^{Sp2/+}* (F) is expressed similar to WT (E), while the basement membrane Lam1 exhibit a partial disorganized pattern in *Hnf1b^{Sp2/+}* (F and H) compared to WT kidneys (E, G). The tight junction ZO1 is normally expressed (compare G and H). Co-stained P0 kidney sections with NKCC2 and pancytokeratin (CK) with only NKCC2 in I, J and merged NKCC2 and CK in K, L, show strong decreased staining of NKCC2 in cystic medullar Loops of Henle of *Hnf1b^{Sp2/+}* (compare WT I, K with J, L), while the apical expression of collecting ducts with CK (K, L) is not affected in *Hnf1b^{Sp2/+}* kidneys. Acetylated tubulin cilium staining (M, N, N' magnification) shows partial loss of primary cilia in cystic structures in E15.5 mutant cysts, while non-dilated tubules have apparent normal cilia distribution of cilia (compare M (WT) with N, N' (*Hnf1b^{Sp2/+}*)).

Figure 7: **Reduced expression of a subset of HNF1B targets in *Hnf1b^{Sp2/+}* kidneys**

Representative Immunostainings of E17.5 WT and *Hnf1b^{Sp2/+}* kidneys with TMEM27 (Collectrin) (A, A') and CUBN (B, B'), SPP1 (Osteopontin) (C, C') and LRP2 (Megalin) (D, D') showing strongly reduced expression of TMEM27, CUBN and SPP1 (A', B', C'), in *Hnf1b^{Sp2/+}* mutant kidneys while the expression of LRP2 is only moderately reduced (compare D with D'). E: QRTPCR analysis of selected HNF1B targets at different stages show significant and strong downregulation of *Hnf4a*, *Ihh*, *Lrp2*, *Kcnj1*, *Tmem27* and *Umod* during

embryo stages up to P0, consistent with mRNA-seq data (Sup Table S3). Also included *Aqp2*, which is not a HNF1B target. *Aqp2*, *Lrp2* and *Ihh* while downregulated during development are either slightly upregulated or expressed similarly to WT in adult mice. In adults, *Umod* and *Tmem 27* remained downregulated.

Figure 8: Representative histological sections of the renal phenotypes of adult kidneys from *Hnfl^{Sp2/+}* males and females (A- F) H&E stained sections of male kidneys of WT 12 months (A) and *Hnflb^{Sp2/+}* (B- F) showing kidney sections of 2month (B), 11 month- (C) 5 month- (D), 17 month- (E), 12 month-old (F). H&E stained sections (G, J, K, L) and trichrome Masson (H, I) stained sections of female kidneys. G: *WT*; H to L of *Hnflb^{Sp2/+}* of 2-months (H), 12 months (I), 17 months (J), 15 months (K, L). Note clusters of glomerular cysts (magnifications shown in B', E', F', I', I''), microcysts (B, H, I), severe hydronephrosis both in old males (E) and females (L) and rare cases of a severe dysplastic kidney (F; see also supplementary Figure S6). Note no evidences of fibrosis in trichrome Masson stained sections (H, I).

TABLE 1: Selected Gene ontology (GO) terms of differentially expressed genes at different embryonic stages

TABLE 2: Urine and plasma parameters of *WT* and *Hnflb^{Sp2/+}* mice

Values are the mean \pm SEM and correspond to the average of measurements from 2 or 3 days of urine sample collection under basal conditions at the indicated ages. Urine samples at 3 and 6-months were from the same series of mice, while at 12-months as well as the plasma analysis were from separate groups of mice.

SUPPLEMENTARY MATERIAL

Supplementary Figure S1: Truncated mutant proteins encoded by alternative spliced transcripts lacking the Exon2 are located primarily in the cytoplasm. Immunofluorescence of the human cell line C33 transiently expressing the WT HNF1B (isoform A) and the putative truncated proteins encoded by mutant alternative spliced isoforms A and B lacking the Exon2. Note the restricted nuclear expression of WT HNF1B in contrast to mutant truncated proteins detected both in the cytoplasm and to lesser degree into the nuclei. HNF1B (green), Dapi (nuclei, blue), middle panels (merged).

Supplementary Figure S2: Hematoxylin and Eosin (H&E) stained sections of E14.5 embryo kidneys. Upper panel F1 background (mixed genetic background C57BL/6Nx129/sv), middle panel C57BL/6N and Lower panel 129/sv background, showing in each case one E14.5 WT kidney and the two *Hnflb^{Sp2/+}* kidneys of the same litter. Scale bar: 200 μ m

Supplementary Figure S3: Representative Hematoxylin and Eosin (H&E) stained sections of P0 kidneys in the 129/sv and C57BL/6N backgrounds exhibiting increasing severity in the renal phenotype. Note frequent pelvic dilatations and /or hydronephrosis in the C57BL/6N background (lower panels). The last two C57BL/6N kidney sections correspond to the same *Hnflb^{Sp2/+}* embryo indicating bilateral severely affected kidneys (duplication, hydronephrosis) that would likely be incompatible with life.

Supplementary Figure S4: Comparison of mRNA levels of previously identified *Hnflb*

target genes in WT and *Hnf1b*^{sp2/+} at different embryonic stages and at P0. mRNA levels of the indicated genes at E14.5, E15.5, E17.5 and P0 stages were determined by qRT-PCR and normalized by cyclophilin A expression. The indicated number of WT and *Hnf1b*^{sp2/+} samples were used with n being a pool of the 2 kidneys of each embryo. Values are represented as percentage of WT controls. Note the modest and non-significant downregulation of few genes. Significant differences between WT and *Hnf1b*^{sp2/+} (p<0.05 (*)) and p <0.01 (**)) are indicated. Error bars represent standard error of the mean (SEM)

Supplementary Figure S5: In situ hybridization of early proximal tubule anchor genes *Fbp* and *Spp2*. In situ hybridization at E17.5 and P0 of WT and *Hnf1b*^{sp2/+} kidneys show a strong decrease of *Fbp* at both stages (*Left panels*), and a more modest decrease of *Spp2* (*Right panels*).

Supplementary Figure S6: Representative histological sections of the Left and Right kidneys of *Hnf1b*^{Sp2/+} adult males and females, illustrating the variable severity and body weight curve analyses. H&E stained sections of the Left and Right kidneys of males (left panel) and females (right panel). **Male Age:** A, A': 17-months; B, B': 13-months, C, C': 10-months; D, D': 16-months; E, E': 9-months; F, F': 17-months; G, G': 17-months; H, H': 12 months. **Female Age:** A, A': 2 months; B, B': 13-months; C, C': 17-months. The right lower panel shows body weight curves of males (at the left) and females (at the right) at different ages. Note the tendency of 20% reduction in body weight of both *Hnf1b*^{Sp2/+} males and females, although lower numbers of females were examined.

Supplementary Figure S7: Representation of urinary peptides significantly altered between *Hnf1b*^{sp2/+} and WT male mice. Each peak corresponds to an identified peptide using capillary electrophoresis coupled to mass-spectrometry (CE-MS), and is characterized by specific mass (kDa), migration time (min) and abundance in the samples.

SUPPLEMENTARY TABLES

Table S1: Mendelian inheritance in the offspring of *Hnf1b*^{Sp2/+} and WT intercrosses in different mouse backgrounds. Are indicated the number of embryos and/or animals of WT and heterozygous *Hnf1b*^{sp2/+} mutant obtained from *Hnf1b*^{Sp2/+} males x WT females in the indicated genetic backgrounds, the total embryos or animals (TOT) and percentages of heterozygotes. Numbers with * in C57BL/6N background mice indicate that 7 *Hnf1b*^{Sp2/+} mice died from P1 and P25.

Table S2: Primers used for Q- RT-PCR and semi-Q- RT-PCR

Table S3: Transcriptomic profiles at E14.5, E15.5, E17.5 and P1. Venn's diagram of shared differentially expressed genes between stages. Differentially anchor early proximal tubules and SLC transmembrane differentially expressed

Table S4: Gene ontology enrichment analysis of downregulated genes at E14.5, E15.5, E17.5 and P1

GO term enrichment analysis using using ToppGene informatics at different stages {Chen, 2009 #71}, showing the most important GO-terms at each stage

Table S5: Kidney-to-body weight ratio of *Hnf1b*^{Sp2/+} and WT males in the C57BL/6N background

Values represent the mean +/- SEM of the indicated numbers (n) of male mice. Animals with the 2 kidneys to total body weight ratio lower than 1.4 are considered as low. Note also that there is a bias in these ratios in cases of pelvic dilations of *Hnflb*^{sp2/+}. One month-old *Hnflb*^{sp2/+} kidneys exhibit a moderate hypoplasia relative to the WT littermates as manifested by the low kidney-to-body ratio.

Table S6: Basal Parameters of adult *Hnflb*^{sp2/+} and WT mice

Values are the mean ± SEM and are the average of measurements from 2 days of urine sample collection under basal conditions at the indicated ages.. Urine samples were from 3 different groups of mice at both 5-6 months and 12-months.

Table S7: Urinary proteomic analysis A- differentially excreted urinary peptides

between *Hnflb*^{sp2/+} and WT mice. Data were obtained from 17 *Hnflb*^{sp2/+} and 18 WT mice from 3, 8, 12, 17 months. 40 peptides with different abundance in urine between the two groups were selected after multiple testing (Supplementary **Material and Methods**). No differences were observed among different ages. *P* values were defined using Wilcoxon rank-sum test followed by adjustment for multiple testing. Peptides are separated according to *Hnflb*^{sp2/+} mice urinary results (up- and down-excreted).

B- Proteases potentially responsible for generation of the urinary peptides associated with RCAD mouse model. Using the 40 sequenced urinary peptides associated-proteases were predicted for N and C-terminal cleavage sites. Only proteases with ≥ 2 cleavage sites association and predicted as a high and medium prediction score were used for further analysis Mann-Whitney test with adjusted p-values <0.05 was applied to identify the proteases with a significant proteolytic activity responsible for protein/peptide fragmentation.

Table S8: List primary and secondary antibodies

Figure 1.

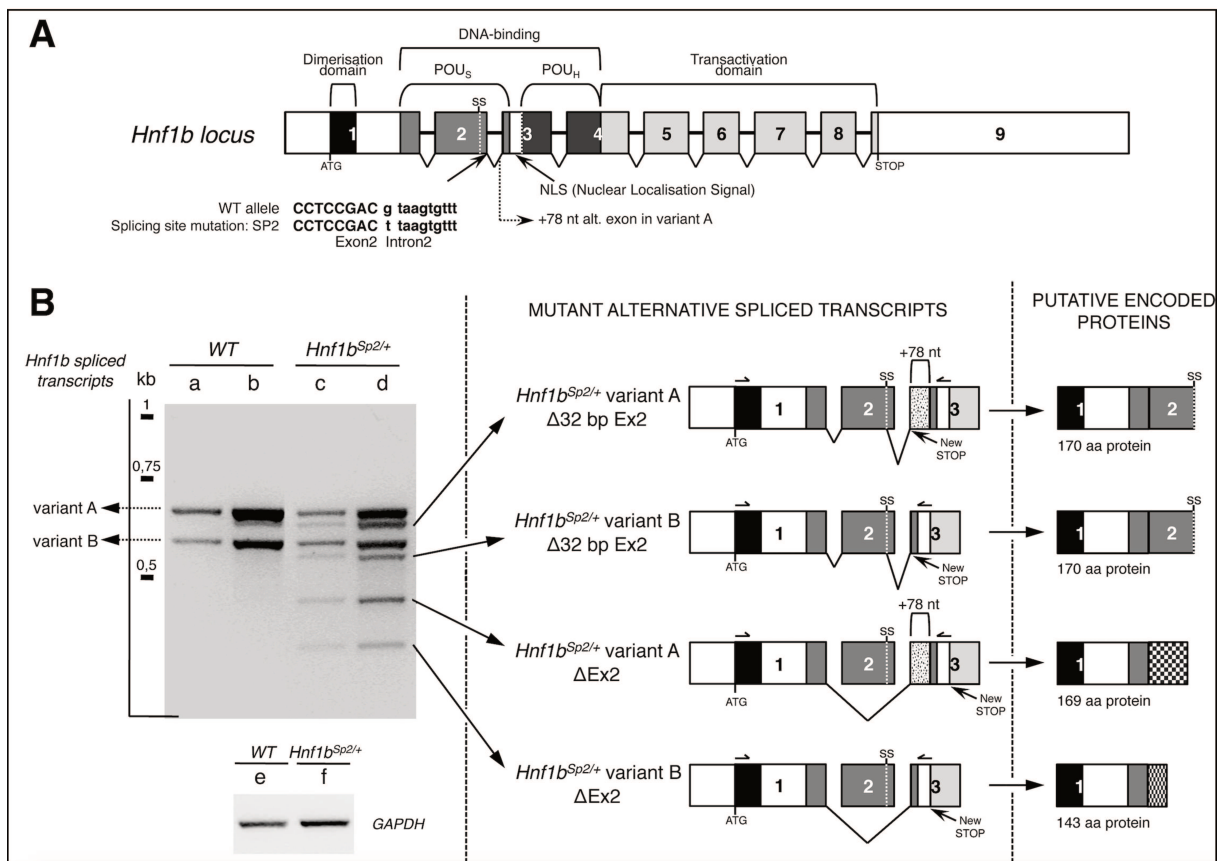


Figure 2.

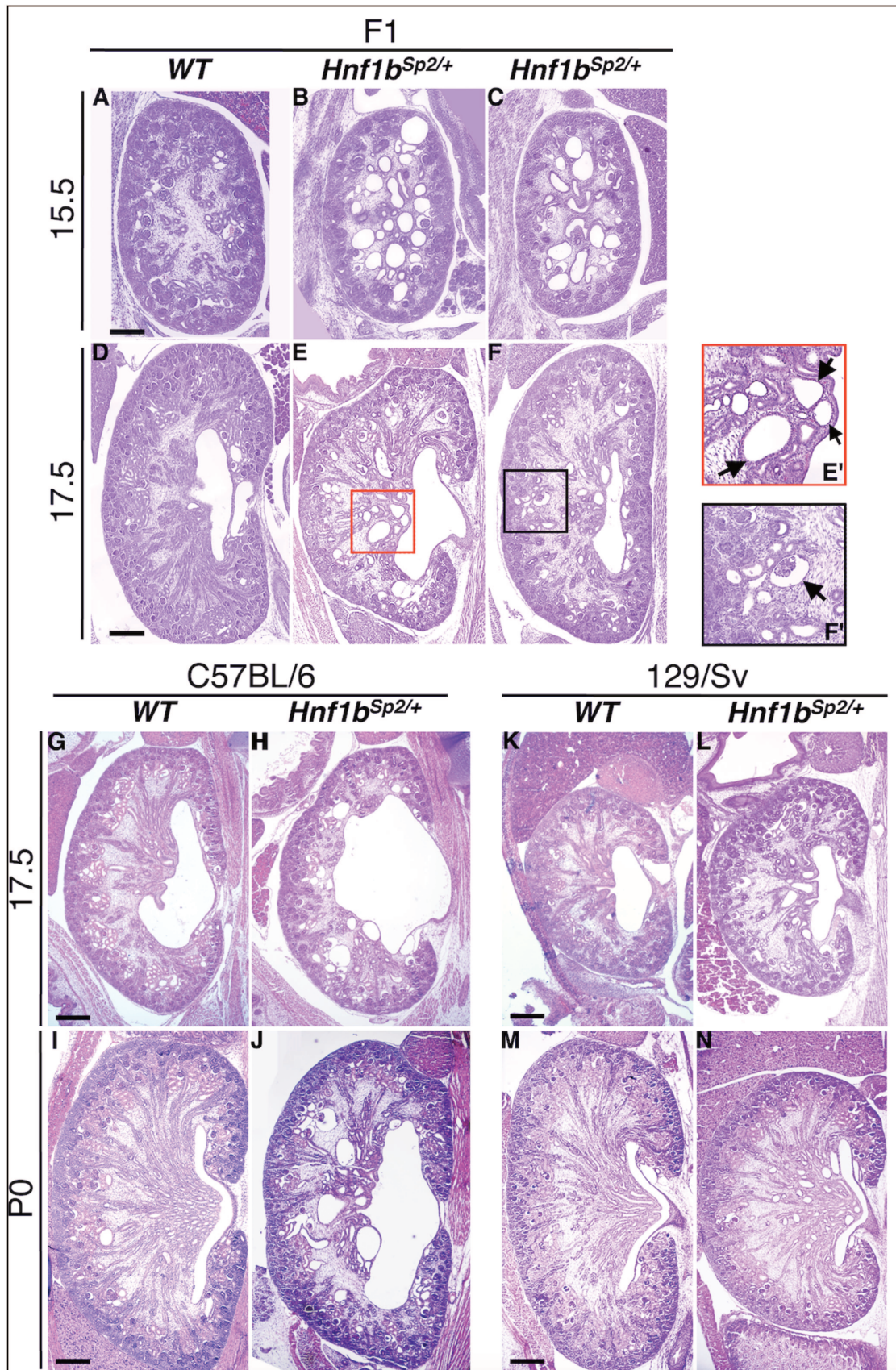


Figure 3.

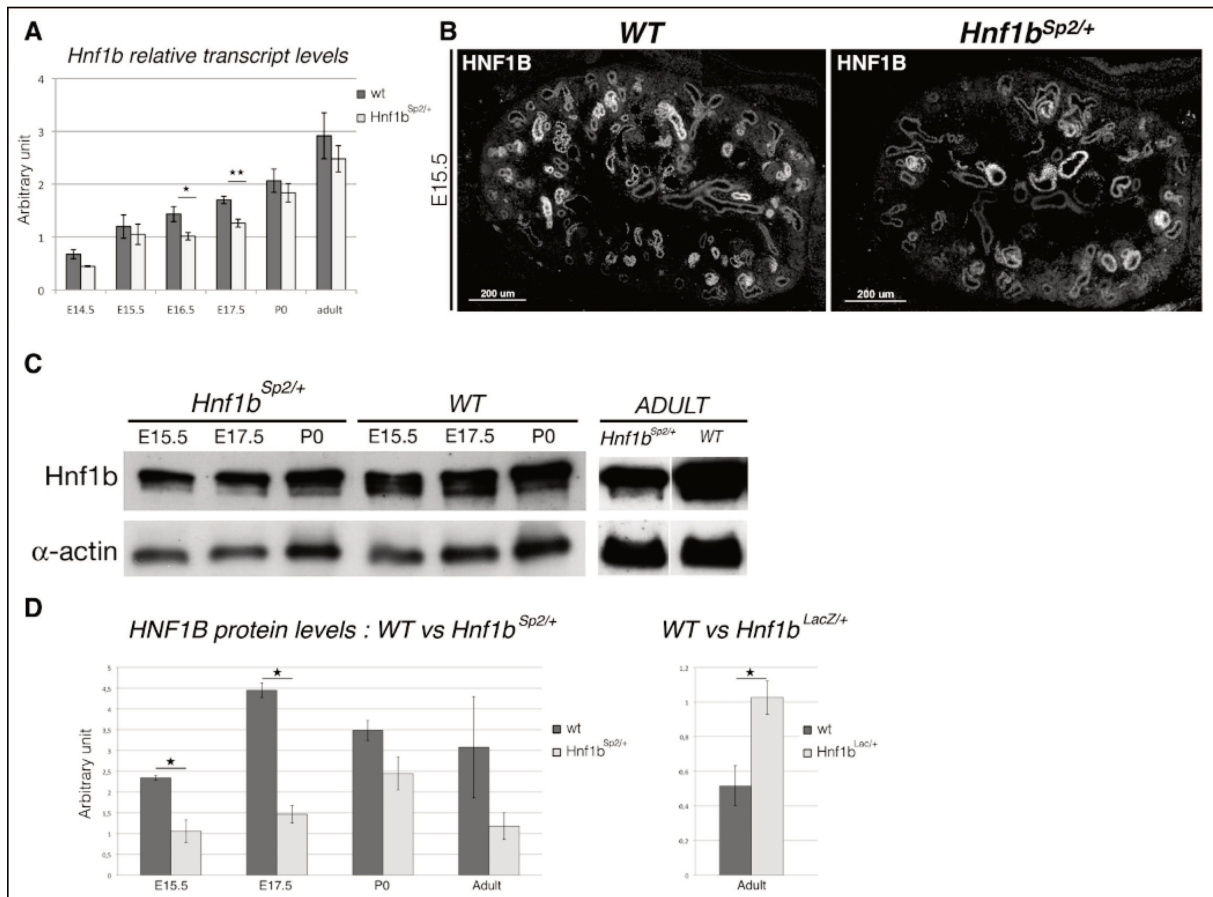


Figure 4.

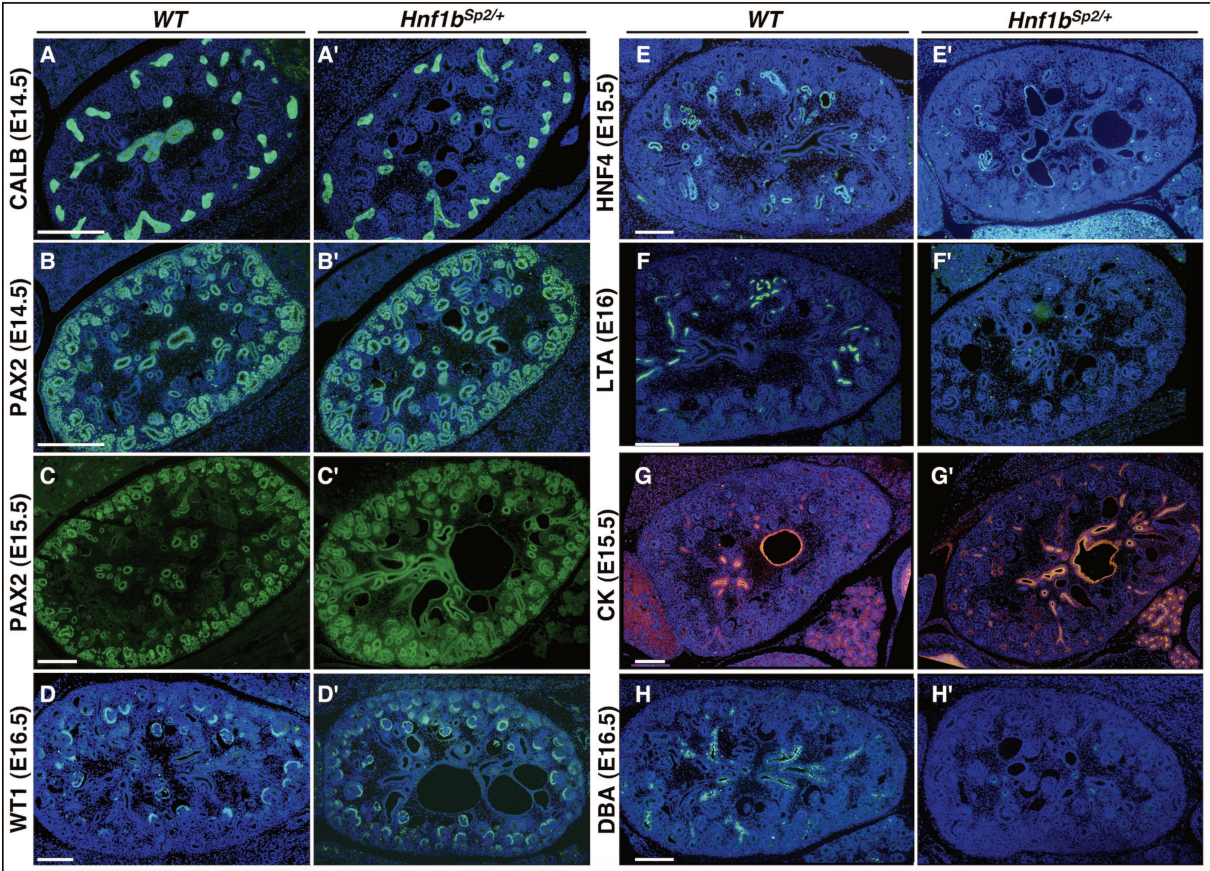


Figure 5.

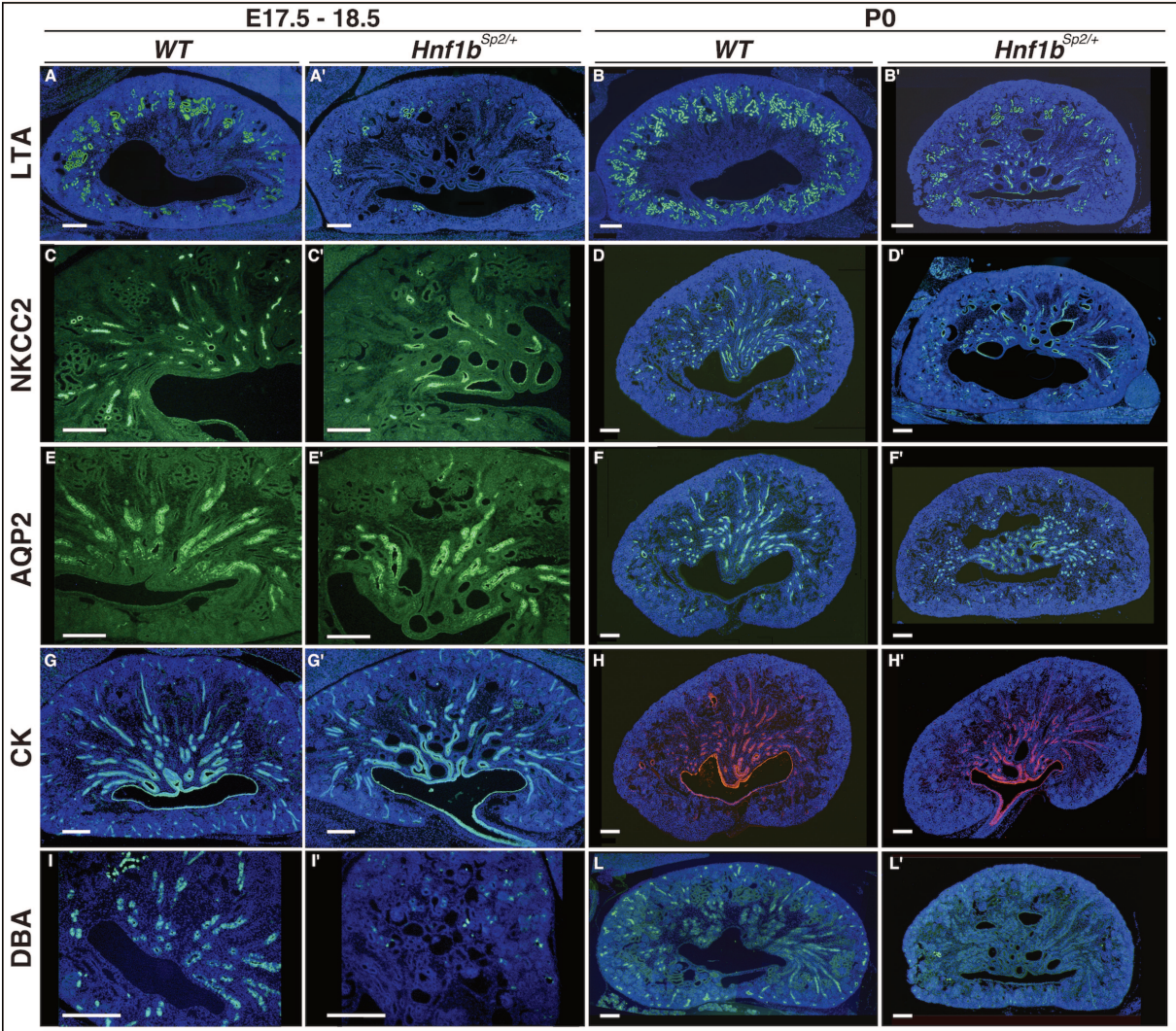


Figure 6.

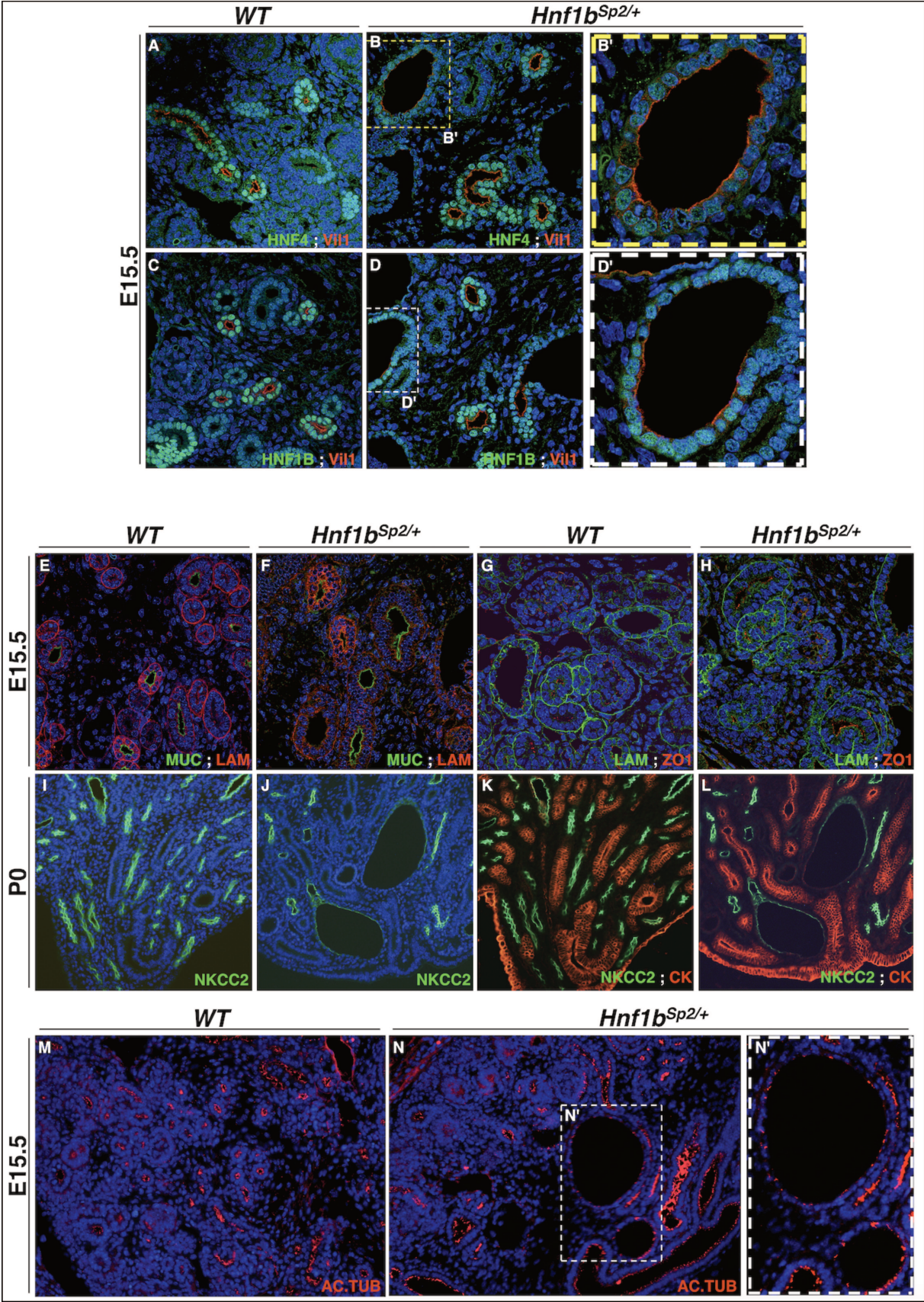


Figure 7.

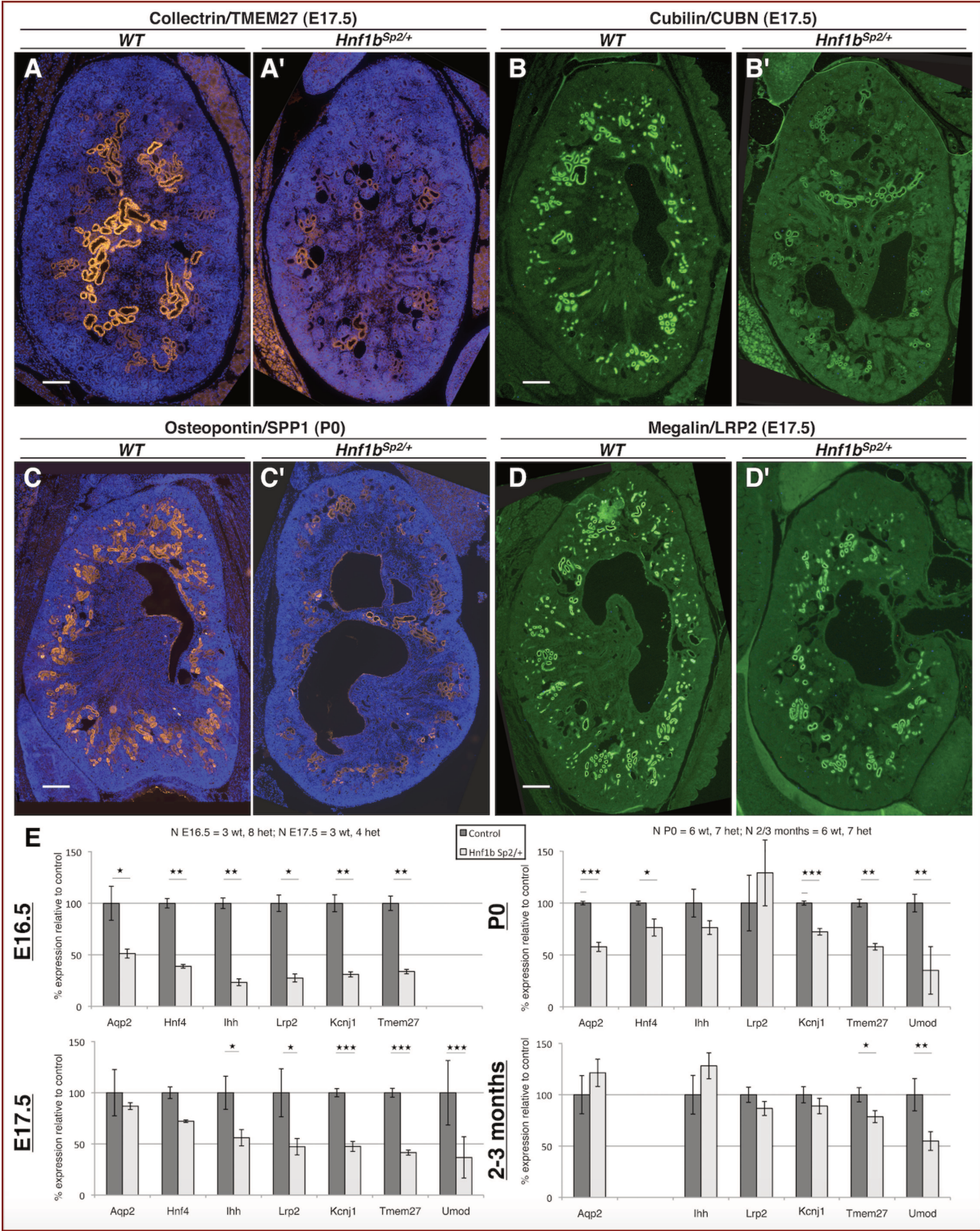


Figure 8.

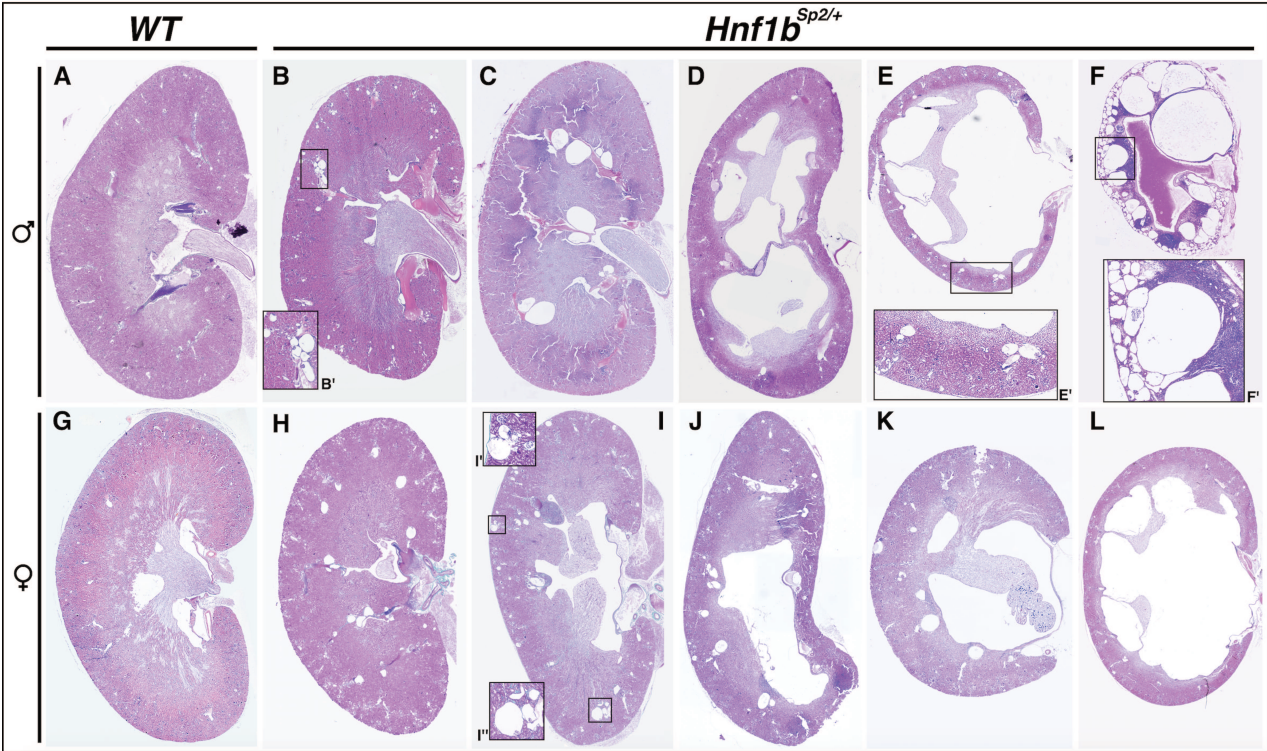


Table 1. Gene ontology

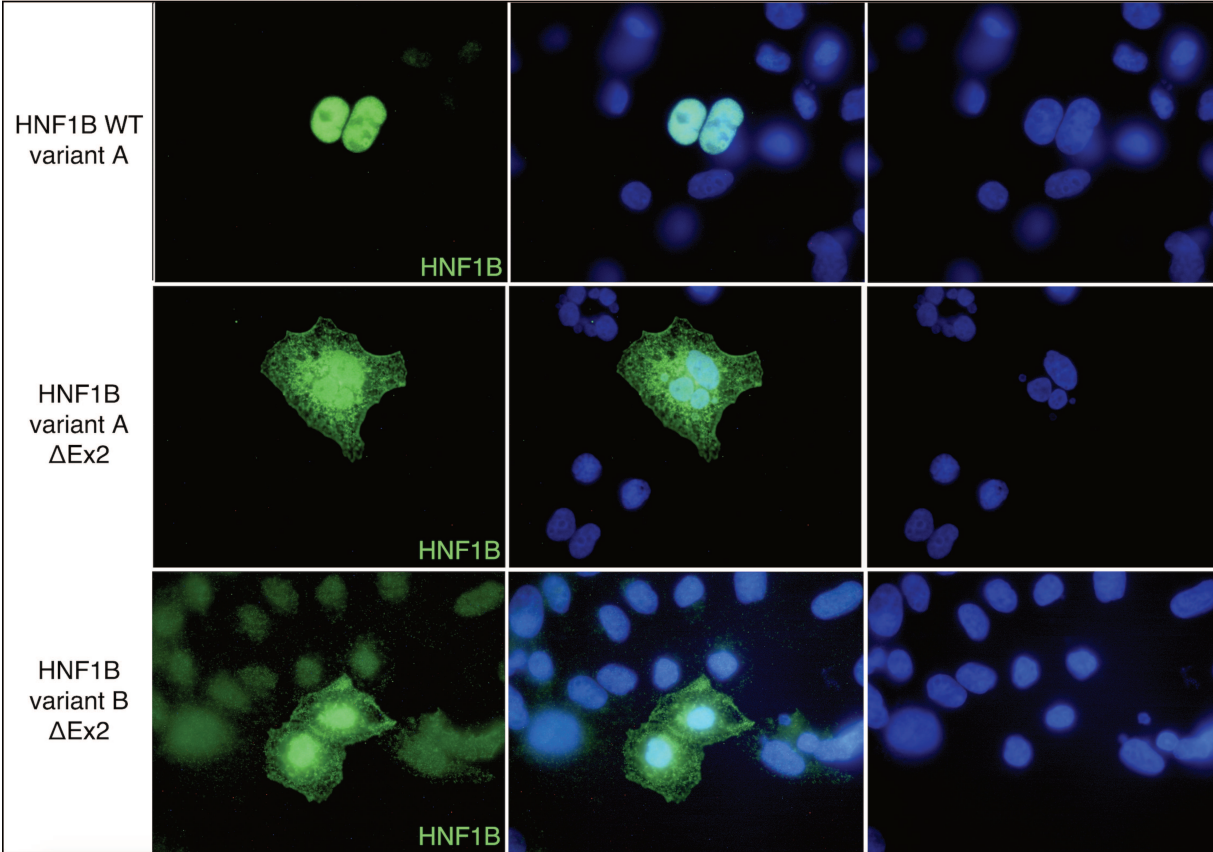
ID	p-value	E15.5 Query List	p-value	E17.5 Query List	p-value	P1 Query List	TOTAL Genome
GO: Molecular Function							
active transmembrane transporter activity	3.541E-4	5	7.008E-28	40	3.669E-20	25	363
secondary active transmemb. transp.activity	5.181E-3	3	1.134E-27	34	5.284E-22	23	236
symporter activity			2.192E-21	24	4.164E-15	15	143
ion transmembrane transporter activity			1.504E-18	46	3.259E-12	26	873
active ion transmemb. transporter activity	2.235E-3	3	2.645E-10	15	2.632E-11	13	175
GO: Biological Process							
organic acid metabolic process			3.053E-26	62	1.239E-20	39	1131
ion transport			7.069E-23	69	6.042E-13	36	1627
carboxylic acid metabolic process	5.620E-4	7	2.466E-22	54	1.019E-16	33	1003
organic anion transport	5.638E-4	5	5.971E-22	38	2.070E-13	21	462
oxoacid metabolic process	1.049E-3	7	9.222E-22	56	3.841E-17	35	1114
lipid metabolic process			6.790E-12	47	5.749E-8	26	1377
drug transport			9.965E-10	8	3.224E-8	6	33
GO: Cellular Component							
brush border membrane	1.050E-9	6	2.867E-22	19	1.634E-15	12	65
apical part of cell	3.577E-4	5	1.664E-18	33	4.548E-4	7	244
cluster of actin-based cell projections	4.086E-7	6	4.308E-17	22	2.011E-10	14	175
PATHWAYS							
SLC-mediated transmembrane transport			2.996E-20	32	7.207E-17	22	287
Transport of glucose bile salts organic acids			1.643E-17	20	3.643E-17	16	106
Transmembrane transport small molecules.			5.674E-16	41	7.207E-17	22	287
Metabolic pathways			4.304E-15	55	2.849E-9	30	1272
Biological oxidations			7.984E-13	22	1.059E-8	13	229
Human Phenotype							
Abnormality of urine homeostasis	4.968E-8	9	4.178E-12	40	7.408E-9	22	751
Abnormal urinary system physiology			6.201E-11	46	4.563E-6	22	1063
Abnormality of amino acid metabolism			2.749E-10	23	2.480E-8	14	285
Abnormality of carboxylic acid metabolism			3.906E-10	23	3.099E-8	14	290
Mouse Phenotype							
abnormal urine homeostasis	1.581E-8	10	1.005E-21	40	1.572E-14	22	457
abnormal renal/urinary system physiology			4.565E-19	45	1.119E-11	23	702
abnormal renal reabsorption	1.042E-6	4	2.763E-13	12	3.281E-12	9	42
abnormal amino acid level	9.569E-7	7	4.046E-11	23	4.670E-8	13	309
abnormal circulating amino acid level	4.528E-6	6	1.294E-9	19	2.758E-6	10	246
abnormal lipid homeostasis			3.637E-8	40			
increased urine calcium level			1.528E-6	6	2.649E-5	4	28
aminoaciduria	2.480E-5	3			1.953E-5	4	26
Disease							
Glycosuria			1.164E-9	8	1.383E-8	6	29
Nephrolithiasis			1.420E-9	11			
Renal tubular disorder			1.640E-9	11	1.435E-8	8	77
Hyperphosphaturia			2.818E-8	7	1.102E-8	6	28
Diabetic Nephropathy			6.981E-8	23			
Fanconi Syndrome			9.665E-8	5	3.396E-7	4	11
Transcription Factor Binding Site							
V\$HNF1_Q6	1.424E-4	5	2.065E-17	26	2.842E-6	10	213
V\$HNF1_O1			4.216E-15	23	1.114E-5	9	196
V\$HNF1_C			1.801E-9	17	4.664E-4	7	192

Table 2. Urine and plasma parameters of WT and *Hnf1b*^{Sp2/+} mice

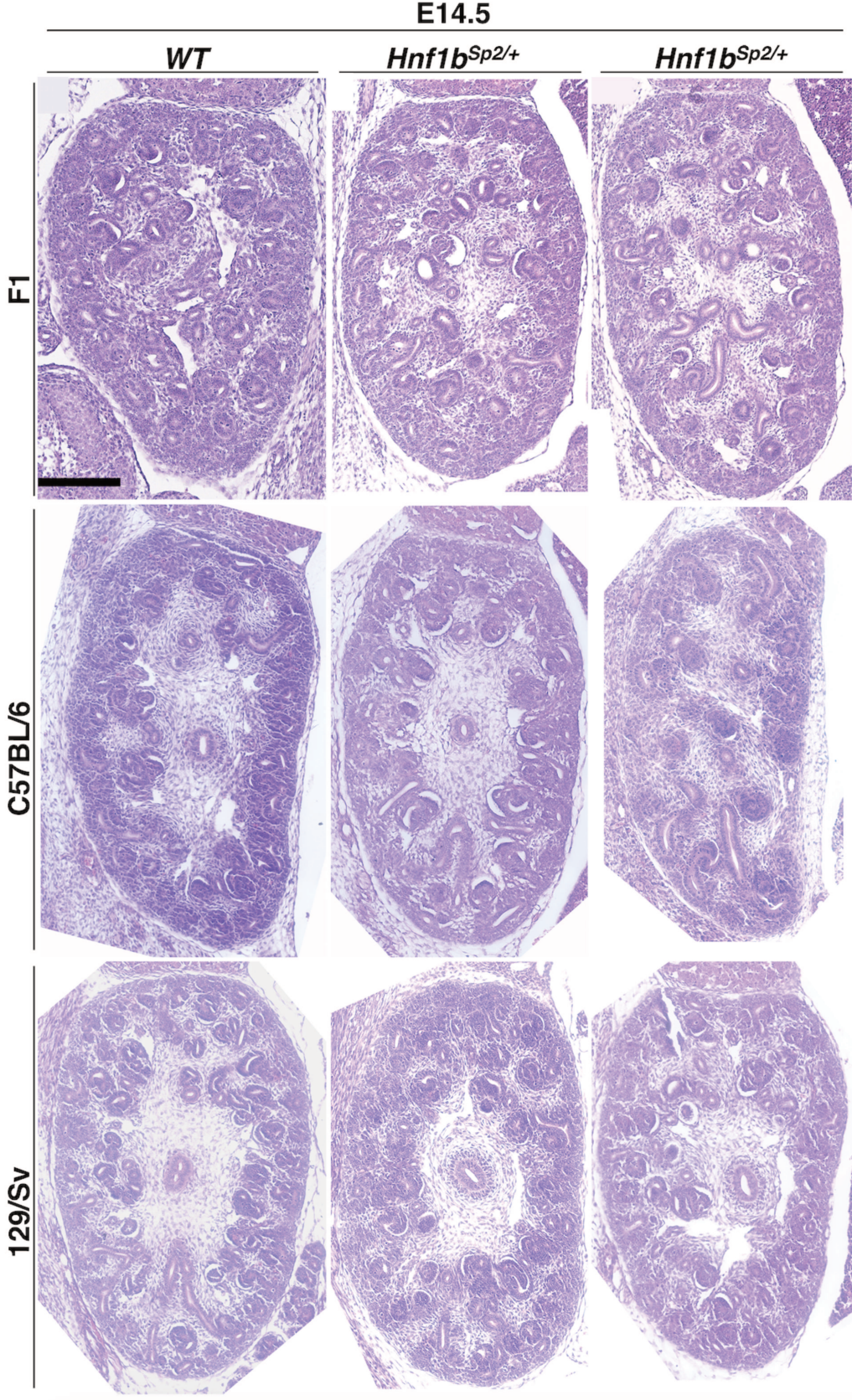
Age	3 months		6 months		10-11 months	
<i>Basal parameters</i>	<i>WT</i>	<i>Hnf1b</i> ^{Sp2/+}	<i>WT</i>	<i>Hnf1b</i> ^{Sp2/+}	<i>WT</i>	<i>Hnf1b</i> ^{Sp2/+}
Body weight (BW) (g)	26,1 ± 1,5	<u>23,4 ± 2,4*</u>	<u>29,5 ± 2,8</u>	<u>26,5 ± 3,13*</u>	36,5 ± 2,7	34,9 ± 3,12
Water intake (ml/day)	4,75 ± 0,67	5,01 ± 0,64	<u>3,90 ± 1,43</u>	<u>5,36 ± 1,81*</u>	2,51 ± 1,1	3,4 ± 1,71
Water intake day (20g BW)	3,63 ± 0,51	4,28 ± 0,54	<u>2,64 ± 0,96</u>	<u>4,04 ± 1,36*</u>	1,37 ± 0,6	1,95 ± 0,98
Urine volume (ml/day)	1,24 ± 0,41	1,23 ± 0,73	<u>0,79 ± 0,50</u>	<u>1,61 ± 1,18*</u>	0,72 ± 0,33	0,98 ± 0,38
Urine volume day (20g BW)	0,951 ± 0,31	1,05 ± 0,63	<u>0,535 ± 0,33</u>	<u>1,21 ± 0,89*</u>	0,394 ± 0,18	0,561 ± 0,217
Aliments (g/day)	4,24 ± 0,16	4,23 ± 0,31	3,91 ± 1,46	3,39 ± 0,58	1,22 ± 0,96	1,44 ± 0,9
<i>Urine parameters</i>						
U-Creat (mM)	4,48 ± 0,91	4,11 ± 0,40	5,94 ± 0,88	4,76 ± 1,53	4,29 ± 2,85	3,75 ± 1,84
U-Prot (g/L)	5 ± 2,67	4,7 ± 3,06	7,09 ± 0,85	4,5 ± 2,07	5,07 ± 1,91	5,71 ± 3,67
Mg ²⁺ (mM)	31,9 ± 7	29,4 ± 2,8	<u>35,9 ± 7,2</u>	<u>24,2 ± 2,3*</u>	18,6 ± 10,5	14,3 ± 4,64
Total Mg ²⁺ excreted day	30,33 ± 2,17	30,8 ± 1,76	<u>19,2 ± 2,43</u>	<u>29,2 ± 2*</u>	7,33 ± 3,45	8,03 ± 1
U-Urea (mM)	1376,8 ± 169	1440 ± 135	1264,5 ± 291	1269,3 ± 173	822,7 ± 530	837,7 ± 136
Total Urea excreted day	1309 ± 52	1512 ± 85,2	676,5 ± 98,5	324,14 ± 153	324,14 ± 95,4	469,94 ± 29,6
Na ⁺ (mM)	189 ± 26,1	152,2 ± 10,8*	188,4 ± 29,1	<u>132,3 ± 35,4*</u>	85,2 ± 48,13	98,5 ± 26,2
Total Na ⁺ excreted day	179,73 ± 8	159,8 ± 6,8*	100,79 ± 9,83	<u>160,08 ± 31*</u>	33,56 ± 8,66	55,25 ± 5,6
K ⁺ (mM)	311,3 ± 62,7	272,4 ± 38,6	<u>329,4 ± 41,5</u>	<u>231,8 ± 47*</u>	183,2 ± 88,3	170,2 ± 32,7
Total K ⁺ excreted day	296 ± 19,43	286 ± 24	<u>176,23 ± 14</u>	<u>280,47 ± 41*</u>	72,18 ± 15,9	95,48 ± 7,1
Ca ²⁺ (mM)	1,26 ± 0,41	1,43 ± 0,42	<u>0,94 ± 0,25</u>	<u>1,46 ± 0,18*</u>	1,71 ± 0,57	1,6 ± 0,45
Total Ca ²⁺ excreted day	1,198 ± 0,12	1,57 ± 0,26	<u>0,502 ± 0,08</u>	<u>1,766 ± 0,16*</u>	0,673 ± 0,1	0,897 ± 0,09
U-Pi (mM)	45,4 ± 12	47,9 ± 13,2	70,3 ± 14,2	52,5 ± 17,6	74,8 ± 43	52,5 ± 27,6
Total U-PI excreted day	43,17 ± 3,7	50,29 ± 8,3	37,6 ± 4,7	63,52 ± 15,6	29,47 ± 7,7	29,45 ± 5,9
Cl ⁻ (mM)	242,8 ± 36,0	221,5 ± 19,5	226,5 ± 42,4	224,3 ± 17,8	109,2 ± 73	150,2 ± 48
Total Cl ⁻ excreted day	158 ± 11	232,5 ± 12,2	121,1 ± 14,2	271,4 ± 15,8	43 ± 13	84,3 ± 10,4
Osmolality (mOsm/kg H ₂ O)	2377 ± 445	2196,2 ± 76,3	<u>2893,5 ± 166</u>	<u>2209 ± 271*</u>	1738 ± 751	1583 ± 225
	n=4	n=4	n=4	n=4	n=4	n=4

<i>Plasma parameters (7months)</i>	<i>WT</i>	<i>Hnf1b</i> ^{Sp2/+}
Creat (µM)	30,3 ± 2,44	33,3 ± 4,67
Mg ²⁺ (mM)	<u>0,77 ± 0,08</u>	<u>0,89 ± 0,09*</u>
Urea (mM)	7,16 ± 0,84	8,2 ± 1,65
Gluc (mM)	10,7 ± 1,78	11,7 ± 2,02
Ala (U/l)	<u>55,7 ± 14,5</u>	<u>136,3 ± 76,3*</u>
Asat (U/l)	155 ± 60,1	334 ± 282,9
	n=9	n=6

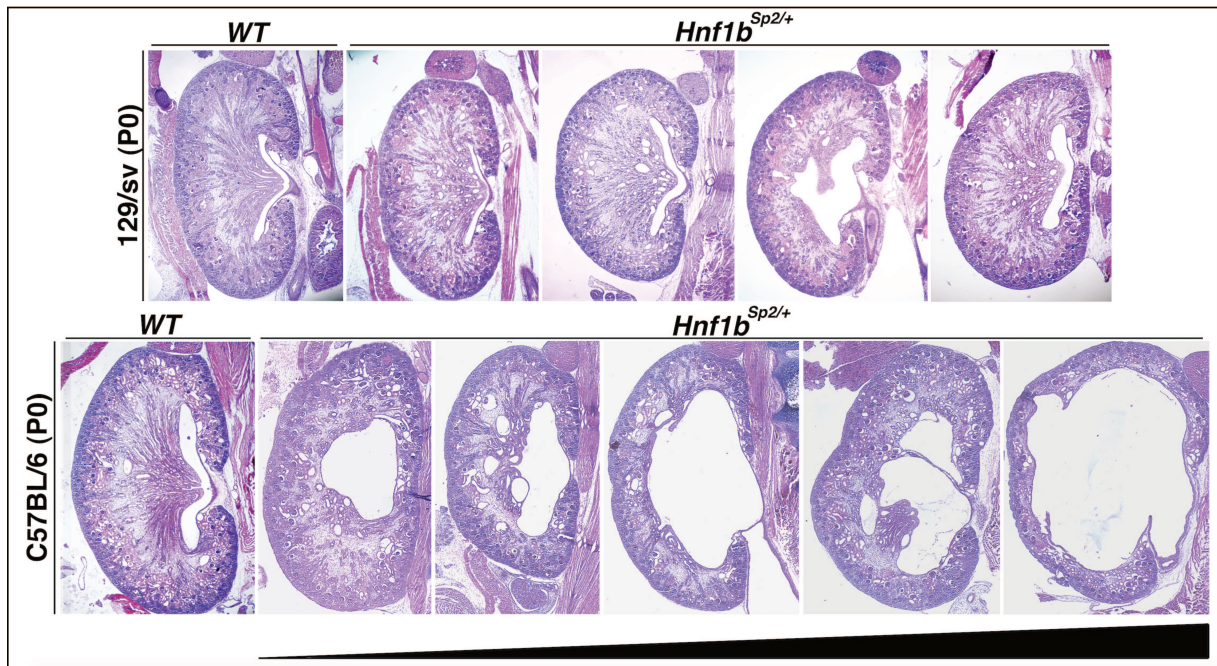
Supplementary Figure 1.



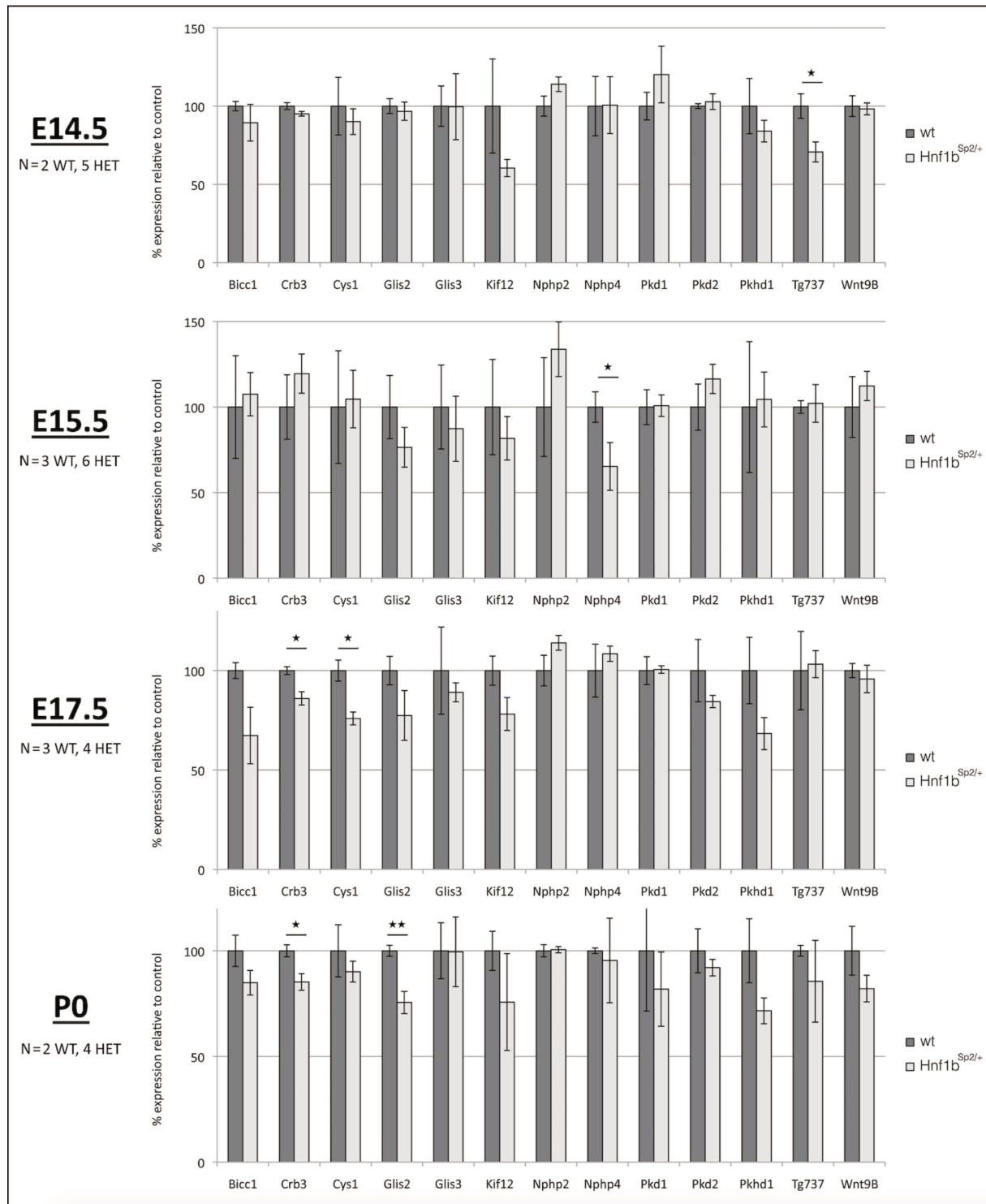
Supplementary Figure 2.



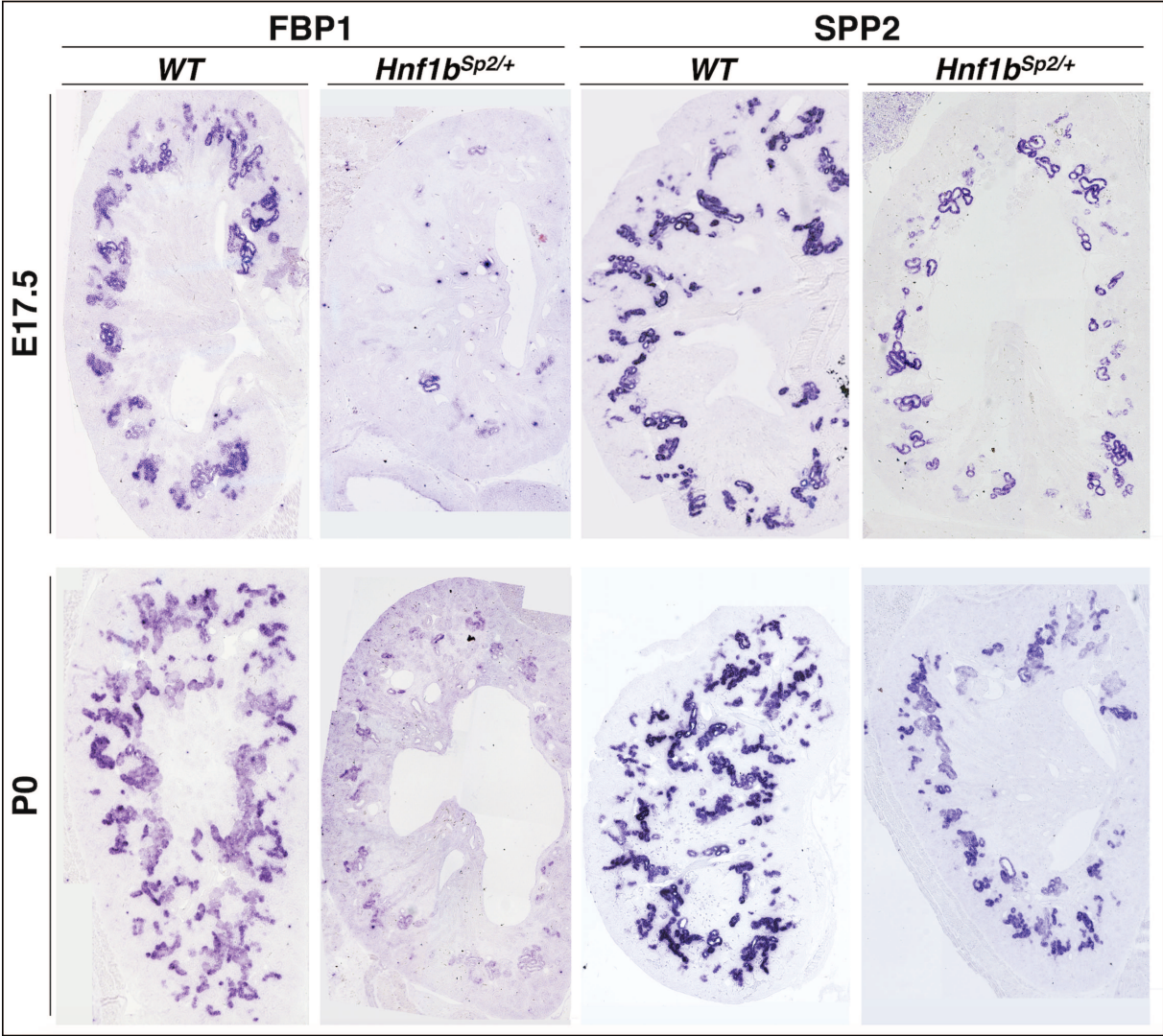
Supplementary Figure 3.



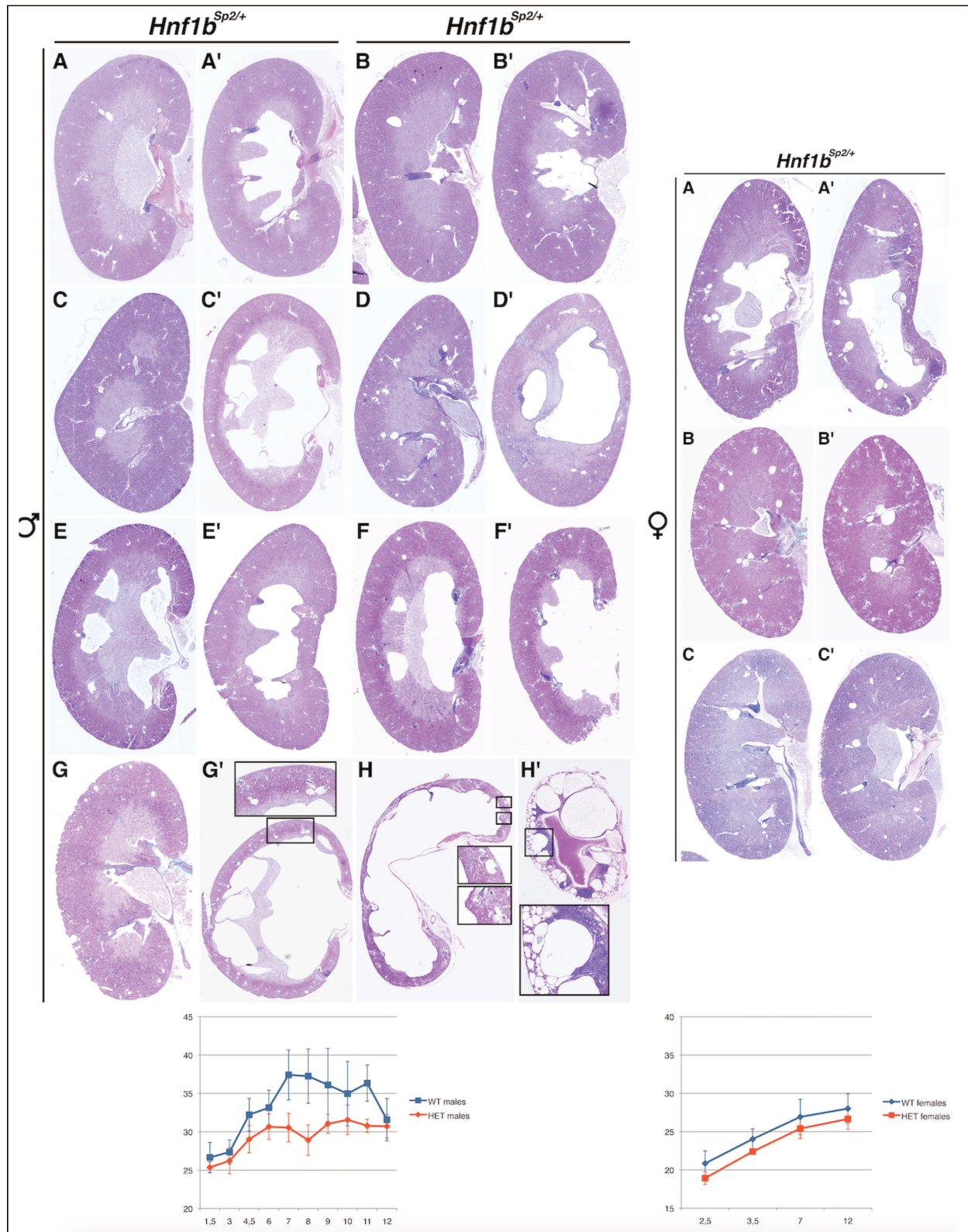
Supplementary Figure 4.



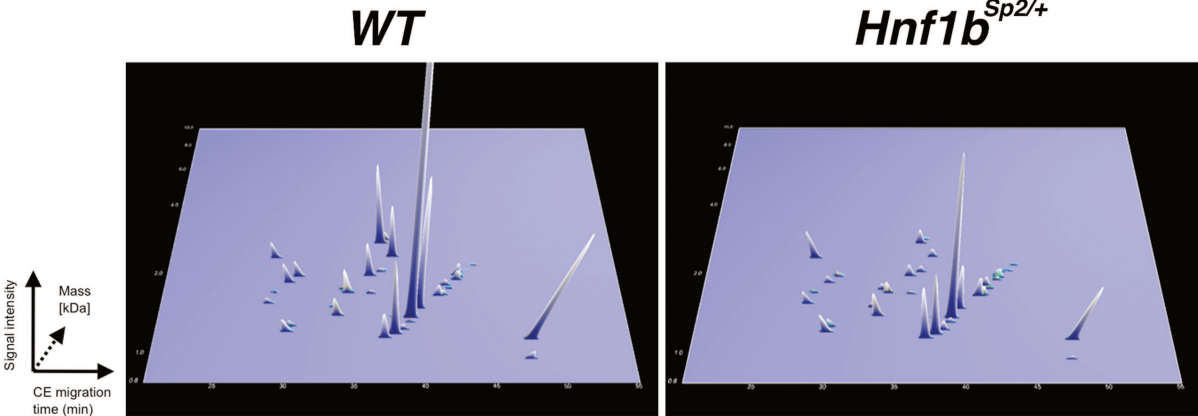
Supplementary Figure 5.



Supplementary Figure 6.



Supplementary Figure 7.



Supplementary Table S1: Mendelian inheritance in the offspring of *Hnf1b*^{Sp2/+} and *WT* intercrosses in different mouse backgrounds

Stage	C57BL/6				129/Sv				F1			
	<i>Hnf1b</i> ^{Sp2/+}	<i>WT</i>	TOT	%HET	<i>Hnf1b</i> ^{Sp2/+}	<i>WT</i>	TOT	%HET	<i>Hnf1b</i> ^{Sp2/+}	<i>WT</i>	TOT	%HET
E14.5	25	32	57	43,8					18	11	29	62
E15.5	13	15	28	46,4	9	9	18	50	9	10	19	47,3
E17.5	13	12	25	52	9	12	21	42,8	16	19	35	45,7
P0	10	12	22	45,4	10	8	18	55,5	20	21	41	48,7
Adult	(125)	223	348	(35,9)	241	265	506	47,6	99	133	232	42,6
	(118*)	223		(33,9)								

Supplementary Table S2: Primers used for quantitative and semiquantitative RT-qPCRs

Gene symbol	Gene name	RefSeq (NCBI)	Primers (5'-3')
<i>Aqp2</i>	aquaporin 2	NM_009699	CCATTGGTTTCTCTGTTACCCTG CGGTGAAATAGATCCCAAGGAG
<i>Bicc1</i>	protein bicaudal C homolog 1 isoform 2	NM_001347189	TGAGGTCAGAACACCTACGA AGTGCAGTGAAGACTGTCCA
<i>Crb3</i>	crumbs family member 3	NM_001347408	CCTGTCTTCAGGGGCTATTG TCGCATGAGCAGAAACAGTC
<i>Cyclo</i>	cyclophilin A	NM_120034.2	CAGGTCCTGGCATCTTGTC TTGCTGGTCTTGCCATTCT
<i>Cys1</i>	cystin 1	NM_001004455	AGAGGAGCTCATGGCGAGCATT CTGTGGCACAGATGCCAAGAGG
<i>Glis2</i>	GLIS family zinc finger 2	NM_031184	GACGAGCCCTCGACCTAA AGCTCTCGATGCAAAGCATGA
<i>Glis3</i>	GLIS family zinc finger 3	NM_001305671	TGTGGCATGAATCTCCACCG TGATGGGAGGGATATGTTGACC
<i>Hnf1a</i>	hepatocyte nuclear factor 1 (HNF-1), alpha	NM_009327.3	GTGTAAGTGCACAGGAGGCAAA TTCTCACGTGTCCAAGACCTA
<i>Hnf1b</i> : <i>WT</i> transcript in <i>Hnf1b</i> ^{Sp2/+} samples	hepatocyte nuclear factor 1 (HNF-1), beta	NM_001291268.1	CGAGGTGGACCGGATGCTCA TCGGAGGATCTCCCCTGTGCT
<i>Hnf4a</i>	hepatocyte nuclear factor 4 (HNF-4), alpha	NM_001312906.1	CCATCATCTTCTTGATCCAG CTCACTTGACCTGTGACC
<i>Ihh</i>	Indian hedgehog	NM_001313683	CCACGTGCATTGCTCTGTCA CACGCTCCCCGTTCTTAGG
<i>Kcnj1</i>	potassium inwardly-rectifying channel, subfamily J, member 1	NM_001168354	TGTCTCCACGTTTACCCAGCA CGTTGCCGAGAAGCCCAAATA
<i>Kif12</i>	kinesin family member 12	NM_001317352	GAGGCCAATAGCATCAACCG GGAGATGCAGTGGCCCAAT
<i>Lrp2</i>	low density lipoprotein receptor-related protein 2	NM_001081088	AAAATGAAAACGGGGTGA GGCTGCATACATTGGGTTTTC
<i>Nphp2</i>	inversin	NM_010569	ACTTGTACCAGCATATGTGGTC AGGAGAAAACATTTGAACCTGTCTT
<i>Nphp4</i>	nephronophthisis 4 (juvenile) homolog (human)	NM_153424	TTGGCAATAAGCCAGAATCTCC TGATACAGCCTCAACCGTTTGT
<i>Pkd1</i>	polycystic kidney disease 1 homolog	NM_013630	GCTGCATGCCAGTCTTTTG TTTTAAAGTGCAGAAGCCCA
<i>Pkd2</i>	polycystic kidney disease 2	NM_008861	CATGTCTCGATGTGCCAAAGA ATGGAGAACATTATGGTGAAGCC
<i>Pkhd1</i>	polycystic kidney and hepatic disease 1	NM_153179	ATGGAGAACATTATGGTGAAGCC ATGTTTCTGGTCAACAGCCC
<i>Tg737</i>	transgene insert site 737, insertional mutation, polycystic kidney disease	NM_009376	GCAGGCTTCAACCTCATCCTTA TTTCTCCCAGTCTCCAATGG
<i>Tmem27</i>	transmembrane protein 27	NM_001313719	TCTATCTGGAATCCGGCAAC CACTCCAGGTGGTCCTTTGT
<i>Wnt9B</i>	wingless-type MMTV integration site family, member 9B	NM_011719	GTGAGAAGGAAGATGGTGAGC GCAGAATCTGGAGAAGTGGC
<i>Umod</i>	uromodulin	NM_001278605.1	CTGCACCGATCCTAGTTCCG TCTACCCTGCATTCTTCGCAA

Oligonucleotides used for semiquantitative PCR experiments			
Gene symbol	Gene name	RefSeq (NCBI)	Primers (5'-3')
<i>vATG</i>	hepatocyte nuclear factor 1 (HNF-1), beta	NM_001291268.1	TGGTGTACAGCTCACGTC
<i>V695</i>	hepatocyte nuclear factor 1 (HNF-1), beta	NM_001291268.1	CAGTCGGAGGACACCTGCTC
<i>Gapdh</i>	glyceraldehyde-3-phosphate dehydrogenase	NM_001289726.1	TCCAGTATGACTCCACTCAC ACCTTGCCACAGCCTTG

Supplementary Table S3 in excel. Transcriptional profiling at E14.5 - E15.5 - E17.5 - P1

Supplementary Table S4 in excel. Gene ontology terms of downregulated genes at E14.5, E15.5, E17.5 and P1

Supplementary Table S5. Kidney-to-body weight ratios of WT and *Hnf1b*^{Sp2/+} males

Age	1 month		5 months		10 months	
	<i>WT</i>	<i>Hnf1b</i> ^{Sp2/+}	<i>WT</i>	<i>Hnf1b</i> ^{Sp2/+}	<i>WT</i>	<i>Hnf1b</i> ^{Sp2/+}
Parameter						
Body Weight (BW) (g)	20,2 ± 2,6	18,28 ± 0,83	35,1 ± 1,52	29,3 ± 6,46	31,2 ± 2,7	30,1 ± 1,5
Left Kidney Weight (KW) (g)	<u>0,14 ± 0,01</u>	<u>0,11 ± 0,02*</u>	0,2 ± 0,02	0,19 ± 0,03	0,22 ± 0,04	0,22 ± 0,04
Right Kidney Weight (KW) (g)	<u>0,14 ± 0,01</u>	<u>0,11 ± 0,02*</u>	0,22 ± 0,01	0,23 ± 0,04	0,24 ± 0,04	0,21 ± 0,04
%KW (left) / BW	<u>0,71 ± 0,05</u>	<u>0,58 ± 0,07*</u>	0,6 ± 0,09	0,66 ± 0,24	0,72 ± 0,07	0,74 ± 0,15
%KW (right) / BW	<u>0,69 ± 0,05</u>	<u>0,59 ± 0,05*</u>	0,65 ± 0,07	0,79 ± 0,03	0,78 ± 0,11	0,70 ± 0,15
%KW (left+right) / BW	<u>1,40 ± 0,1</u>	<u>1,16 ± 0,11*</u>	1,24 ± 0,17	1,45 ± 0,27	1,50 ± 0,15	1,44 ± 0,27
	n=3	n=5	n=2	n=2	n=6	n=5

Age	12 months		16-20 months	
	<i>WT</i>	<i>Hnf1b</i> ^{Sp2/+}	<i>WT</i>	<i>Hnf1b</i> ^{Sp2/+}
Parameter				
Body Weight (BW) (g)	37,7 ± 4,38	29,2 ± 1,77	33,1 ± 5,5	30,6 ± 6,2
Left Kidney Weight (KW) (g)	0,29 ± 0,05	0,17 ± 0,09	0,25 ± 0,06	0,22 ± 0,07
Right Kidney Weight (KW) (g)	0,26 ± 0,02	0,19 ± 0,001	0,27 ± 0,08	0,22 ± 0,06
%KW (left) / BW	0,77 ± 0,08	0,59 ± 0,13	0,75 ± 0,07	0,72 ± 0,19
%KW (right) / BW	0,72 ± 0,08	0,66 ± 0,05	0,82 ± 0,15	0,72 ± 0,13
%KW (left+right) / BW	1,49 ± 0,14	1,15 ± 0,18	1,58 ± 0,19	1,44 ± 0,23
	n=3	n=2	n=5	n=11

Supplementary Table S6. Basal Parameters of adult *Hnf1b*^{Sp2/+} and *WT* mice

AGE	5-6 months		12 months	
	<i>WT</i>	<i>Hnf1b</i> ^{Sp2/+}	<i>WT</i>	<i>Hnf1b</i> ^{Sp2/+}
Basal parameters				
Body weight (BW, g)	31,137 ± 5,622	29,683 ± 3,5	36,5 ± 5,39	35,87 ± 4,9
Water intake (ml/day)	<u>3,909 ± 1,43</u>	<u>5,361 ± 1,81*</u>	2,703 ± 1,196	3,409 ± 0,64
Water intake (20g BW)	<u>2,51 ± 0,91</u>	<u>3,61 ± 1,2*</u>	1,47 ± 0,65	1,9 ± 0,35
Urine volume (ml/day)	<u>0,79 ± 1,43</u>	<u>1,615 ± 1,187*</u>	0,79 ± 1,43	0,79 ± 1,43
Urine volume day (20g BW)	<u>0,507 ± 0,9</u>	<u>1,088 ± 0,79*</u>	9 ± 1,43	1 ± 1,43
Aliments (g/day)	3,91 ± 1,46	3,39 ± 0,58	1,15 ± 0,7	1,58 ± 0,9
	n=11	n=13	n=11	n=14

RATIO	5-6 months	12 months
	<i>Hnf1b</i> ^{sp2/+} / WT	<i>Hnf1b</i> ^{sp2/+} / WT
<i>Hnf1b</i> /+ / WT Urine vol 20g BW	<u>2.14*</u>	1,354
<i>Hnf1b</i> /+ / WT Water vol 20g BW	<u>1.43*</u>	1,45

Supplementary Table S7A: Differentially excreted urinary peptides between *Hnf1b*^{Sp2/+} and WT mice

Sequence	Protein name	Accession number	Start (aa position)	Stop	Adjusted p-value	Fold Change
DOWN-REGULATED						
WTDVGMSPRIESASLQGS DRV L	Pro-epidermal growth factor	P01132	620	641	0.0385	-6,27
GRMAHASmGNRPYGP NMANMP PQVGS	AT-rich interactive domain-containing protein 1A	A2BH40	857	882	0.0009	-5,02
PAAPGPAGSPANDNGNGNGNGN GNGNGGK GKPA	Striatin-interacting proteins 2	Q8C9H6	4	36	0.002	-4,95
LSSLKHPSNIAVDPIERL	Pro-epidermal growth factor	P01132	161	178	0.0028	-4,54
SSLKHPSNIAVDPIERLM	Pro-epidermal growth factor	P01132	162	179	0.0063	-3,7
ALDYDPVESKIYFAQTA	Pro-epidermal growth factor	P01132	522	538	0.0005	-3,7
SGNFIDQTRV LNLGPITR	Uromodulin	Q91X17	590	607	0.0385	-2,81
SSLKHPSNIAVDPIERL	Pro-epidermal growth factor	P01132	162	178	0.0114	-2,78
GAGLEQEA AAG	Heterogeneous nuclear ribonucleoprotein U	Q8VEK3	70	80	0.0494	-2,76
SINKELQNSIIDL	Kidney androgen-regulated protein	P61110	26	38	0.0385	-2,36
SPRIESASLQGS DRV L	Pro-epidermal growth factor	P01132	626	641	0.0304	-2,18
LVSINKELQNSIIDLLNS	Kidney androgen-regulated protein	P61110	24	41	0.0448	-2,16
PGApGAPGHPGPPGPV	Collagen alpha-1(III) chain	P08121	1039	1054	0.002	-1,9
GpPpGpGpGpGpG	Collagen alpha-1(XV) chain	O35206	704	716	0.0436	-1,71
SINKELQNSIID	Kidney androgen-regulated protein	P61110	26	37	0.0132	-1,58
DGQPGAKGEpGDTGVKGD	Collagen alpha-1(I) chain	P11087	809	826	0.0193	-1,54
SpGPDGKTGPpGP	Collagen alpha-1(I) chain	P11087	535	547	0.0117	-1,18
UP-REGULATED						
PGA KGEpGDTGVKGD	Collagen alpha-1(I) chain	P11087	812	826	0.0311	1,29
pGpPpGpRGPQGPNGADGPQgP	Collagen alpha-1(XI) chain	Q61245	1219	1239	0.0145	1,38
KpGERGLpGEF	Collagen alpha-2(I) chain	Q01149	575	585	0.0466	1,43
GpGERGEHGPpGP	Collagen alpha-1(III) chain	P08121	795	807	0.0212	1,53
GIpGTGGpPGENGKpGEpGP	Collagen alpha-1(III) chain	P08121	641	660	0.0032	1,62
NIGFpGPKGPSGDpGKpGERGHpG	Collagen alpha-2(I) chain	Q01149	497	520	0.0311	1,68
GpPpGTPGAGDKGD	Collagen alpha-1(III) chain	P08121	617	630	0.0348	1,69
GLPpAGPpGEAGKpGEQ	Collagen alpha-1(I) chain	P11087	633	650	0.0009	1,69
GQPGAKGEpGDTGVKGDAGPpGP	Collagen alpha-1(I) chain	P11087	810	832	0.0348	1,74
DGTpGpGpGIRGMpG	Collagen alpha-1(III) chain	P08121	526	539	0.0464	1,8
TGPIGpPGPAGApGDKGEA	Collagen alpha-1(I) chain	P11087	755	773	0.0287	1,87
GpPpGEAGKpGEQ	Collagen alpha-1(I) chain	P11087	639	650	0.0375	1,94
GPIGpPpGAGQpGDKGEGGSpGLpG	Collagen alpha-1(III) chain	P08121	764	788	0.0132	2
EAGKpGEQGVpGDLGApGP	Collagen alpha-1(I) chain	P11087	643	661	0.0348	2,04
GQpGAKGEpGDTGVKGDAGpGP	Collagen alpha-1(I) chain	P11087	810	832	0.0348	2,16
RDGApGAKGDRGETGP	Collagen alpha-1(I) chain	P11087	1015	1030	0.0032	2,26
GLpGAPGpPpGEAGKpGEQGVpG	Collagen alpha-1(I) chain	P11087	633	654	0.0231	2,31
TTGEVgKpGERGLpGEF	Collagen alpha-2(I) chain	Q01149	569	585	0.0375	2,48
GEpGAKGERGApGEKGEg	Collagen alpha-1(III) chain	P08121	818	835	0.002	2,72
AGQpGEKGPpGAQGPpGSpGPLG	Collagen alpha-1(III) chain	P08121	925	947	0.0054	3,06
EVGKpGERGLpGEF	Collagen alpha-2(I) chain	Q01149	572	585	0.002	3,13
pGPAGpPpGEAGKpGEQGVpGDLG	Collagen alpha-1(I) chain	P11087	635	657	0.0005	6,9
GpPpGEAGKpGEQGVpGDLGApGP	Collagen alpha-1(I) chain	P11087	639	661	0.0008	7,07

Supplementary Table S7B. Proteases potentially responsible for generation of the urinary peptides associated with RCAD mouse model

Protease	PROTEASE ID	nr of cleavage sites (#CS)	Cleaved Protein	Fold change	p-value
DOWN-REGULATED					
Cathepsin E	CTSE (P14091)	3	EGF	-3,95	P = 0,0003
Cathepsin D	CTSD (P07339)	4	EGF	-3,57	P = 0,0004
Granzyme M	GZMM (P51124)	2	EGF	-3,09	P = 0,0008
Cathepsin G	CTSG (P08311)	5	COL1A2, EGF	-1,22	P < 0,0001
Matrix metalloproteinase-2	MMP2 (P08253)	4	COL1A2, COL3A1, KAP	-1,09	P < 0,0001
Matrix metalloproteinase-9	MMP9 (P14780)	20	COL1A1, COL1A2, COL3A1, COL15A1, HNRNPU	-1,06	P < 0,0001
Cathepsin L1	CTSL1 (P07711)	10	COL1A1, COL3A1, COL15A1	-1,02	P < 0,0001
UP-REGULATED					
Collagenase 3	MMP13 (P45452)	9	COL1A1, COL1A2, COL3A1	1,11	P < 0,0001
Neutrophil collagenase	MMP8 (P22894)	7	COL1A1, COL1A2, COL3A1	1,14	P < 0,0001
Granzyme B	GZMB (P10144)	5	COL1A1, COL3A1	1,31	P = 0,0178
Caspase-1	CASP1 (P29466)	2	COL1A1	1,82	P = 0,0390
Interstitial collagenase	MMP1 (P03956)	5	COL1A1, COL1A2, COL3A1	1,86	P = 0,0041

Supplementary Table S8 in excel. List primary and secondary antibodies

TOPIC II. Analysis of HNF1B regulating microRNAs in the renal pathogenesis of a mouse model of the RCAD syndrome

II.1. Introduction

II.2. Summary of results

II.3. Discussion and conclusions

PROGRESS SCIENTIFIC REPORT (ongoing)

II.1. Introduction

microRNAs (miRNAs) are small non-coding RNA molecule of ~22 nucleotides that negatively regulates gene expression at post-transcriptional level of numerous organisms including fungi, algae, plants, insects and animals (Bartel DP 2004; Griffiths-Jones S et al., 2008). miRNAs induce gene silencing via base pairing to complementary sequences present on target molecules (mRNA or lncRNA) (Ameres SL and Zamore PD 2013) and recent analysis indicates the number of functional microRNAs in human at around 600 (Fromm B et al., 2015). Most of miRNAs are located within the cell, but some miRNAs (commonly known as circulating miRNAs), have been found in extracellular environment, including various biological fluids and cell culture media (Weber JA et al., 2010; Boeckel JN et al., 2014), thus potentially serving as powerful tools for diagnosis and treatment (Kaucsár T et al., 2010).

As different studies performed in cell lines and mouse models suggest a fine regulation between HNF1B and some microRNAs (Hajarnis SS et al., 2015; Jenkins RH et al., 2012; Patel V et al., 2013; Kornfeld JW et al., 2013) and the post-transcriptional regulation of HNF1B may be an undervalued factor related to RCAD syndrome, we performed genome wide transcriptomic analyses at different developmental stages from our RCAD mouse model and investigate the possible roles of miRNAs that may contribute to post-transcriptional regulation of *Hnf1b* and to the disease phenotype.

II.2. Summary of results

Performing mRNA and microRNA sequencing analysis made at three developmental stages (E14.5, E15.5 and E17.5) from kidney samples of *Hnf1b*^{Sp2/+} mutant mice and taking advantage from ChIP seq HNF1B (E14.5) analysis made by Heliot C. and Cereghini S.

(unpublished data), we performed a transcriptomic reverse correlation analysis presenting a list of genes potentially controlled by microRNAs in the RCAD phenotype during development.

Subsequently, we focalized the analysis in cell culture testing the capacity of HNF1B in transactivating three regulatory sequences coding for four microRNAs (miR-194-2, miR-192, miR-30a and miR-802). Luciferase assays in HEK293 cells demonstrated that HNF1B was able to transactivate the regulatory sequences upstream these microRNAs through specific binding. Moreover, luciferase assays showed also that miR-194-2, miR-192, and miR-802 were able to inhibit HNF1B transcript via binding its 3'UTR.

When I arrived in the lab, mRNA and microRNA sequencing at different developmental stages were just performed. I began all the analyses on microRNAs of interest and potential regulations with other mRNAs taking advantage of HNF1B ChIP sequencing data available in the lab, updated bibliography, and from the different databases available online. I performed all the bioinformatic analysis and with the help of my supervisors, we designed the project to analyze potential HNF1B-microRNAs regulatory networks. I subsequently performed the main experiments concerning this project including construction of vectors, cell-transfections, luciferase assays, site-directed mutagenesis, and q-RT-PCRs. Results interpretation was made with the help of Dr. Silvia Cereghini, who also suggested completing this study with additional data of ChIP seq at later embryonic stages done in collaboration with Dr. JS Park and Dr. Chung E.

II.3. Discussion and conclusions

Here we show that the transcriptional factor HNF1B is integrated into a microRNA regulatory network during kidney development. Our analyses suggest that Hnf1b de-regulation in the RCAD mouse model compromised the direct transcription of different microRNAs such as miR-802, the cluster miR-194-2/192 and miR-30a potentially altering the pathways involved in normal renal tubule differentiation and morphogenesis.

PROGRESS SCIENTIFIC REPORT (ongoing)

Analysis of HNF1B regulating microRNAs in the renal pathogenesis of a mouse model of the RCAD syndrome

2.2 Results

2.2.1 miRNAs of interest in the RCAD mouse model

To identify differentially expressed mRNAs and miRNAs high throughput miRNA sequencing and mRNA-sequencing from pre-diseased embryonic kidneys (at E14.5) and diseased kidneys (E15.5-17.5) from our RCAD mouse model was performed. We then confronted this transcriptomic data with the HNF1B-ChiP-Seq data on E14.5 kidneys available in the lab that identified more than 3.000 HNF1B putative binding sites in the regulatory sequences of both coding genes and genes encoding microRNAs.

miRNA seq analyses showed that the stage with the higher number of differentially expressed miRNAs was E15.5 (total 25). At E14.5 and at E17.5, 11 and 14 miRNAs were differentially expressed respectively (**Figure 1**).

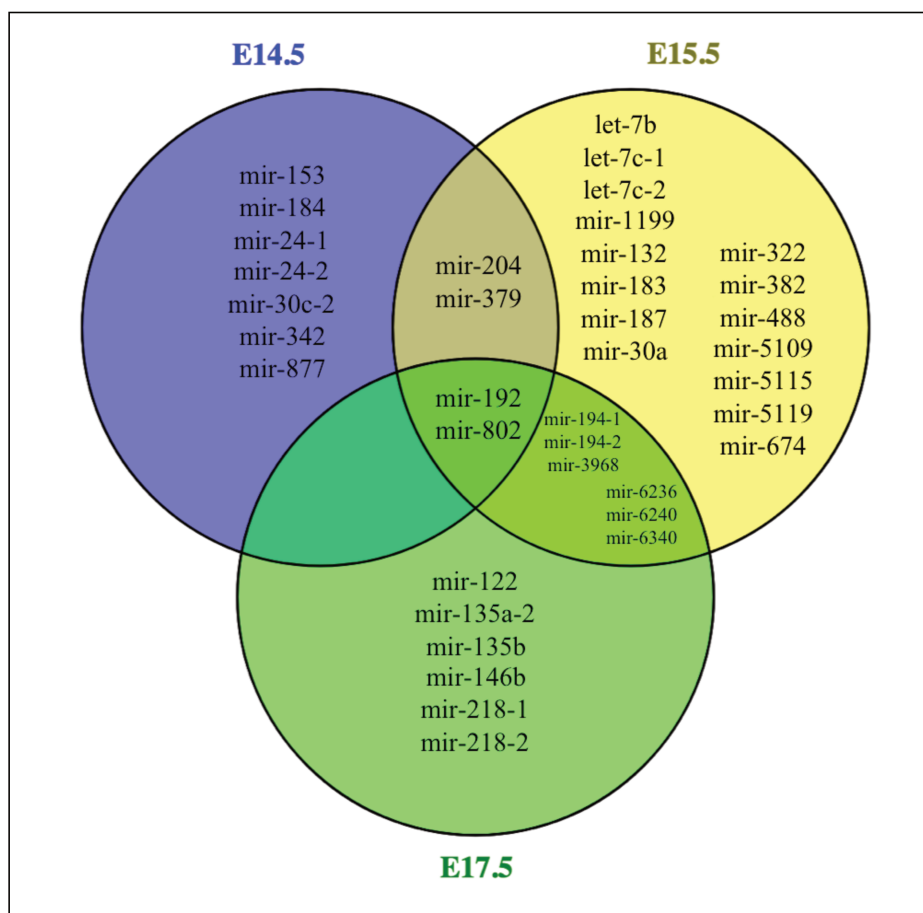


Figure 1. The differentially expressed microRNAs in the RCAD mouse model identified by stage. A complete table representing p-values and fold change for each microRNAs is integrated in the **Supplementary Table 1**.

As most microRNAs negatively regulate the levels of expression of their targets, miRNA-mRNA target pair should be inversely correlated for their expression levels. So, if the expression of a miRNA is UP-regulated, levels of its target genes should be DOWN-regulated and *vice-versa*. The predicted mRNAs target of each significant microRNA listed above were found from the major Internet databases (TargetScan, miRSystem, and miRDB) and crossed with the mRNAs from our mRNA seq at the selected stage. At E14.5, the expression of 11 microRNAs was inversely related to expression of 6 potential target genes and at the following stage the expression of 25 microRNAs was inversely related to expression of 22 potential target genes (**Table 1**). The number of mRNA potential targets increased to 67 at E17.5 linking their control to 14 microRNAs de-regulated in the RCAD mouse model at this stage.

E15.5				
Genes	log2FoldChange (E15.5) on mRNA seq	Target miRNA	log2FoldChange miRNA (E15.5) from microRNA seq	Prediction Algorithms
IL31RA	1.59	mmu-miR-1199, mmu-miR-322	-1.38, -0.28	TargetScan, miRDB
LARS2	1.62	mmu-miR-1199	-1.38	TargetScan
REST	1.61	mmu-miR-1199	-1.38	TargetScan
SCUBE3	1.54	mmu-miR-194-2	-0.76	TargetScan
ZFP791	1.87	mmu-miR-1199	-1.38	TargetScan
ASS1	-2.65	mmu-miR-488	0.47	TargetScan
CLRN3	-2.32	mmu-let-7b	0.54	miRDB
CPN1	-1.7	mmu-miR-488	0.47	TargetScan
FBP1	-5.29	mmu-let-7c-1	0.45	TargetScan
GPD1	-1.51	mmu-miR-379	1.32	miRSystem, miRDB
HAO2	-2.65	mmu-miR-183	0.27	miRDB
HNF4A	-1.63	mmu-miR-488, mmu-miR-5119	0.47, 2.53	TargetScan
KL	-1.8	mmu-let-7b, mmu-miR-488, mmu-miR-382	0.54, 0.47, 1.72	TargetScan
MT2	-2.24	mmu-let-7c-1	0.45	miRDB
PCK1	-3.52	mmu-miR-5119, mmu-miR-6240	2.53, 2.17	TargetScan
PDZK1	-2.17	mmu-miR-379	1.32	miRDB
SLC5A8	-4.23	mmu-miR-183, mmu-let-7b	0.27, 0.54	TargetScan
SULT1D1	-2.43	mmu-miR-183	0.27	miRDB
TMEM229A	-1.61	mmu-miR-5119	2.53	TargetScan
TMEM25	-1.49	mmu-let-7c-1	0.45	TargetScan, miRDB
TMEM27	-1.64	mmu-let-7b, mmu-let-7c-1	0.54, 0.45	TargetScan
UGT1A1	-1.5	mmu-miR-183, mmu-miR-5119	0.27, 2.53	TargetScan

Table 1. Several genes are predicted as targets of microRNAs showing a reciprocal relationship at E15.5. In the table, values of log2FoldChange for mRNAs and microRNAs are denoted as well as the algorithm that predicted the regulation. microRNAs or mRNAs are colored in blue if UP-regulated, in red if DOWN-regulated. A complete table including also E14.5 and E17.5 inverse regulation is integrated in the **Supplementary Table 2**.

Thus, despite our analysis suggests a potential important role for different microRNAs in the RCAD mouse model, we emphasize that these predicted miRNA:mRNA interaction pairs need to be further validated to uncover their functional meanings. This dataset will provide a useful resource for future investigations.

As our first aim was to highlight the role of HNF1B in this mRNAs-miRNAs regulatory network, we searched for miRNAs potentially regulated by this transcription factor and subsequently microRNAs targeting HNF1B. In fact, HNF1B not only could regulate mRNAs involved in RCAD pathogenesis via microRNAs, but could be regulated itself by microRNAs. We used the available HNF1B ChIP sequencing data looking for the nearest binding sequences of HNF1B for each de-regulated microRNA. The sequences recruited by HNF1B (called MACS PEAKs) by ChIP seq were further analyzed by mainly 2 databases (<http://jaspar.binf.ku.dk/>, <https://ecrbrowser.dcode.org/>) confirming the presence of consensus HNF1B binding sites (**Supplementary Table 1**).

In parallel, through the use of the same databases previously used (TargetScan, miRSystem, and miRDB), we identified microRNAs potentially able to regulate HNF1B transcripts (**Figure 2**).

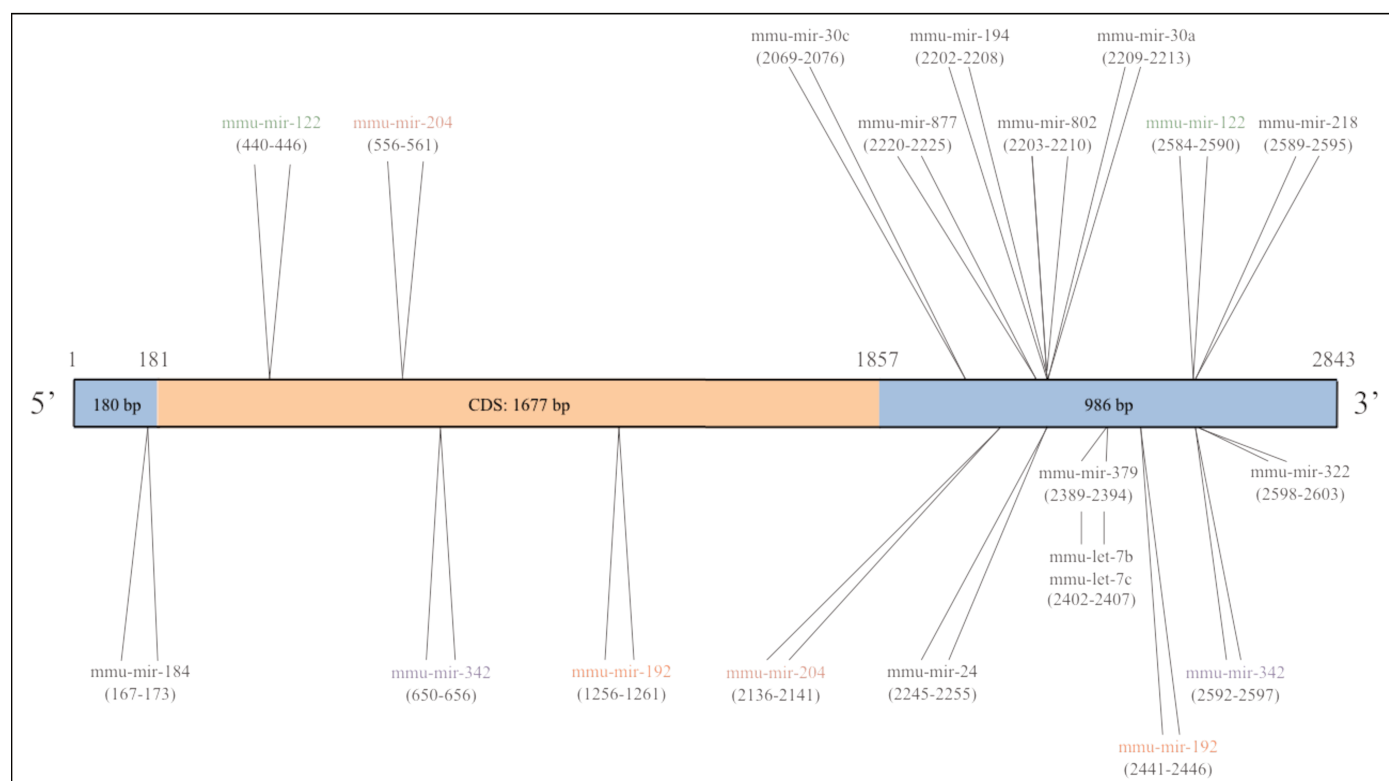


Figure 2. MicroRNAs potentially acting on *Hnf1b* mRNA in the RCAD mouse model. The majority of miRNA Recognition Elements (MREs, the miRNA-binding sequence in a given target) are found in the 3'UTR of *Hnf1b*. miR-122, miR-192, miR-204, and miR-342, which are colored, have two different MREs.

Following this double study approach “ChIP seq/miRNA seq”, together with the previous and recent studies on miRNA expression and function revision, we shorten the list of microRNAs focusing our attention on four microRNAs: **802, 192, 194, and 30a**.

miR-802 express in the same tissues of HNF1B (kidney, pancreas, liver) (Higuchi C et al., 2015) and it was the most strongly DOWN-regulated microRNA at all the 3 stages (E14.5, E15.5, E17.5). We found that HNF1B is recruited to the upstream sequence of its genomic locus within 1 kb of distance, thus potentially participating in its transactivation. Surprisingly, *Kornfeld et al.* have previously described a direct down-regulation of *Hnf1b* by miR-802 in Hepa1-6 cells (Kornfeld JW et al., 2013) and therefore we did not expect that miR802 be the most strongly downregulated miRNA in our mode.

As miR-802, miR-192 was DOWN-regulated at all the 3 stages (E14.5, E15.5, E17.5). HNF1B is recruited to the upstream sequence of its genomic locus within 1 kb of distance. It is co-transcribed with miR-194-2 and it is found DOWN-regulated at both E15.5 and E17.5 together with its isoform miR-194-1. miR-192 and miR-194 are among the most expressed miRNAs in kidney (preferentially in the renal cortex) (Bhatt K et al., 2011, Sun Y et al., 2004, Tian Z et al., 2008). Interestingly, *Jenkins et al.* have previously demonstrated that HNF1A was able to bind the miR-194-2/192 promoter in proximal tubule epithelial cell line (HK-2), whereas knockdown of HNF1 α and HNF1 β with siRNAs resulted in a decrease expression of miR-192 and miR-194 of -40% and -50% respectively (Jenkins RH et al., 2012). It has also been shown a correlation between low miR-192 expression and structural (tubulointerstitial fibrosis) and functional (reduced estimated glomerular filtration rate) indicators of renal damage (Krupa A et al., 2010).

miR-30a was DOWN-regulated at E15.5 and HNF1B is recruited 10 kb upstream to its sequences in a region without any other coding or non coding genes; miR-30 family showed a prominent kidney-restricted expression (Shi S et al., 2008; Wu J et al., 2014) and research on pronephros development in *Xenopus* demonstrated that miR-30 regulated normal renal development by targeting *Xlim/Lhx1* (Agrawal R et al., 2009). Microarrays in a PKD mouse model (PKD/Mhm(cy/+)) at P36 identified miR-30a as DOWN-regulated (Pandey P et al., 2008) and together with miR-194, and miR-802 it was reported in the published list of DOWN-regulated microRNAs in another PKD mouse model (Kif3a-KO) at P28 (Patel V et al., 2013).

Moreover, a loss of regulation of miR-192, miR-194, miR-802, and miR-30a could regulate epithelial to mesenchymal transition (EMT) (Khella et al. 2013, Kato et al. 2007, Dong P et

al. 2011, Wang D et al., 2017; Peng R et al. 2015), which is predicted to play a role in epithelial tubular morphogenesis and polycystic kidney disease (Togawa et al. 2011). A sequence comparison of miR-194-2/192, miR-30a and miR-802 among species using different databases (<https://genome.ucsc.edu/>, www.ensembl.org/ and <http://www.xenbase.org>) shows the high conservation of these miRNAs among more than 25 species. Conservation among species indicates that these miRNAs may have vital functions that are maintained during their evolution.

2.2.2 Validation of selected microRNAs by q-RT-PCR

We have performed q-RT-PCR analysis at developmental stage E17.5 and at post-natal stage P10 from kidney tissues from *Hnf1b*^{Sp2/+} mice to confirm the down-regulation of the miRNAs of interest during development and to assess their expression at a later stage. The results showed that miR-802, miR-192, miR-194-2 are down-regulated at E17.5 (-20%, -28%, -31% respectively) but not at P10, suggesting that their role is confined during kidney development in mice (data not shown). Interestingly, despite mRNA seq analysis restricts miR-30a down-regulation at E15.5, we observed its down-regulation (-30%) also at E17.5 and no de-regulation at P10 (**Figure 3**).

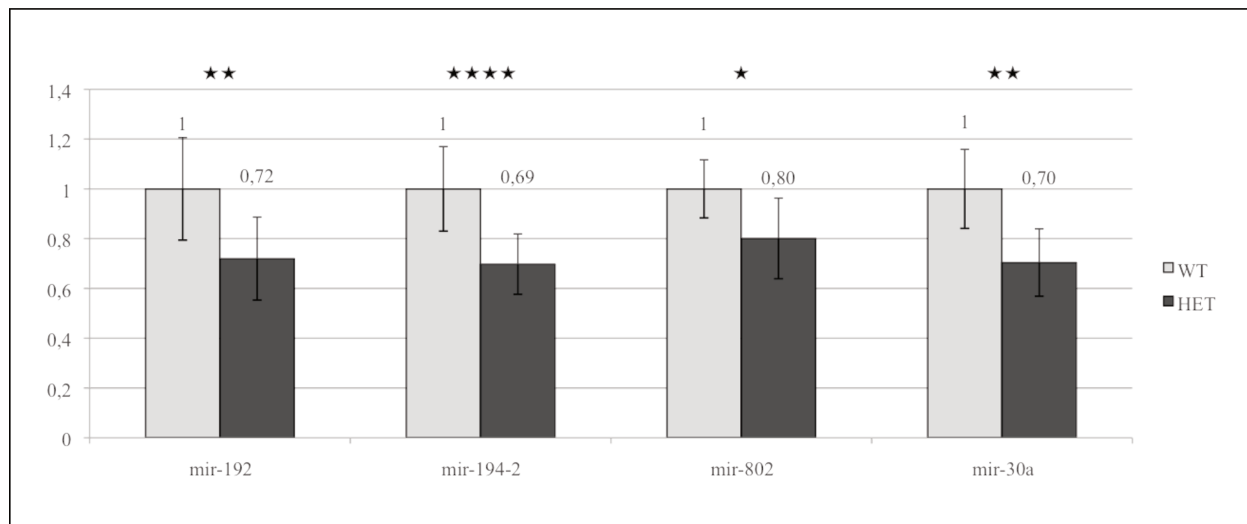


Figure 3. qRT-PCR analysis at E17.5 of the indicated miRNAs show a reduced down-regulation in *Hnf1b*^{Sp2/+} mouse kidney tissues in comparison to wt mice, confirming the miRNAseq data (n wt = 6, n het = 11).

2.2.3 HNF1B transactivate the miR-194-2/192, miR-30a and miR-802 through binding to regulatory promoter/enhancer upstream sequences

We cloned the genomic sequences upstream each microRNA obtained by HNF1B ChIP sequence (called MACS PEAK and referred from here as promoter or enhancer) upstream of the luciferase gene. To assess whether HNF1B can stimulate the regulatory sequences of miR-802, miR-194-2/192 and miR-30a we cotransfected the reporter luciferase constructs (pGL4.10[luc2]-802 or 194-2/192 or -30a) with increasing amounts of an expression vector of HNF1B into Human embryonic kidney cells (HEK-293), which are devoid of HNF1B.

HNF1B stimulates the luciferase activity of all the three constructs in a dose response mode (**Figure 4**). Moreover and supporting the specificity of HNF1B binding to the miRNA regulatory sequences coexpression of a mutant Q136E that abolish binding or of a HNF1B mutant encompassing a selective in phase deletion of exon 7 that abolish transcriptional activation (Barbacci E et al., 2004) fails to transactivate the regulatory sequences of miR802, 194 or 30a. Importantly, these regulatory sequences are conserved between mouse and human.

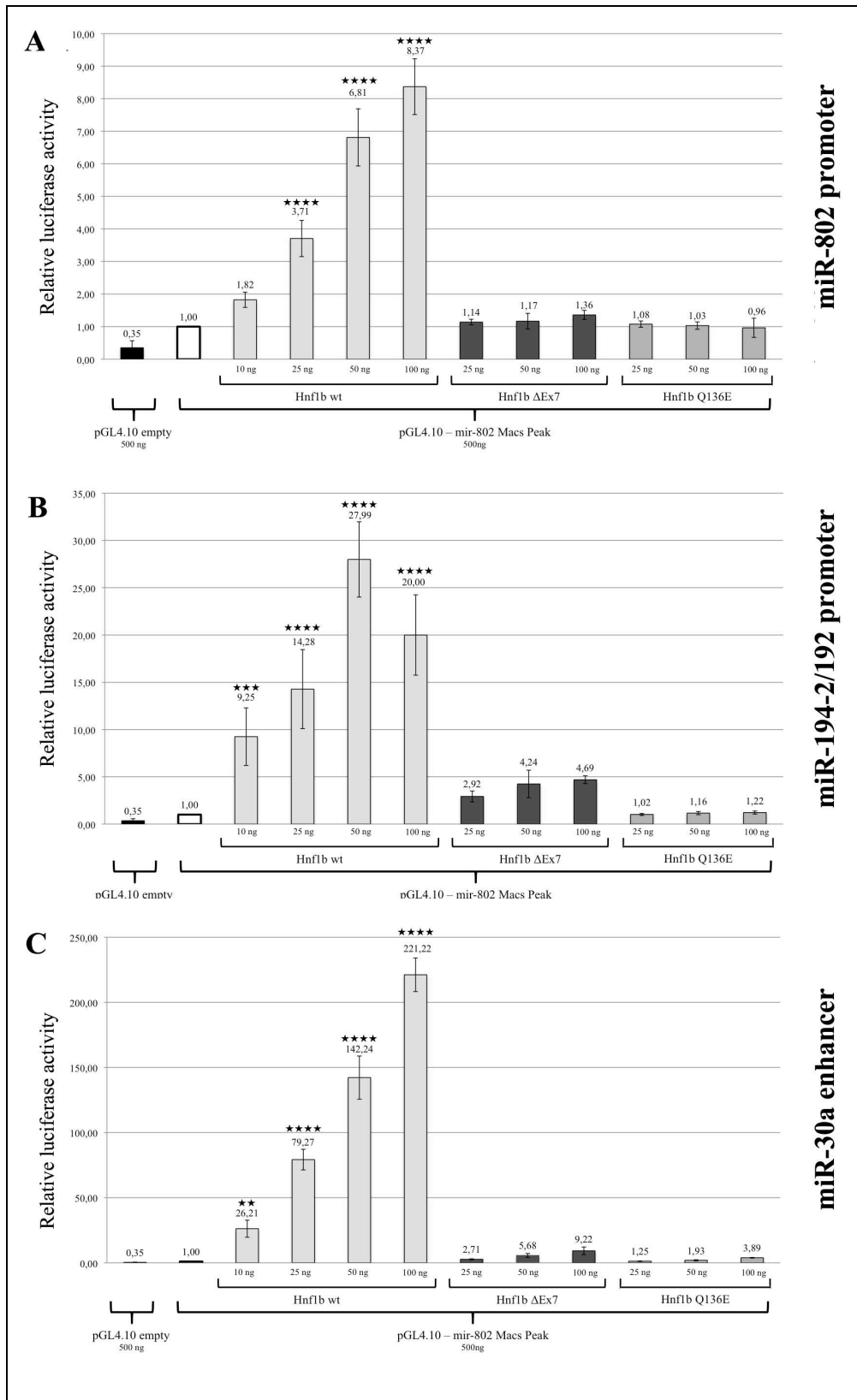


Figure 4: HEK293 cells were co-transfected with pGL4.10[luc2]vectors containing the indicated promoter/enhancer elements and either a human Hnfb expression vector, or “Hnfb ΔEx7” vector containing a deletion in the Exon7 in the transactivation domain or “Hnfb Q136E” vector containing a human missense mutation that abolish DNA binding (Barbacci E et al., 2004). HNF1B lacking binding or transactivation activities fails in transactivate the regulatory sequences efficiently. The normalized firefly luciferase activity was obtained by measuring firefly luciferase activity/Renilla luciferase activity. In each condition the amount DNA

transfected was 600 ng (500 ng pGL4.10 vector + different quantities of Hnf1b vectors adjusted with pCB6 empty vector). All experiments were performed at least three times. Statistical significance was analyzed by one-way ANOVA for multiple comparisons.

Subsequently, to further confirm the specificity of HNF1B binding we mutagenized HNF1B binding sites in miR-802 and miR-30a regulatory sequences (not in miR-194-2/192 promoter because already demonstrated by *Jenkins et al.*) (**Supplementary Figure 1, 2 and 3**). As a result of mutations, HNF1B was not anymore able to transactivate miR-802 promoter and miR-30a enhancer sequences. A summary of these results is shown in **Figure 5**.

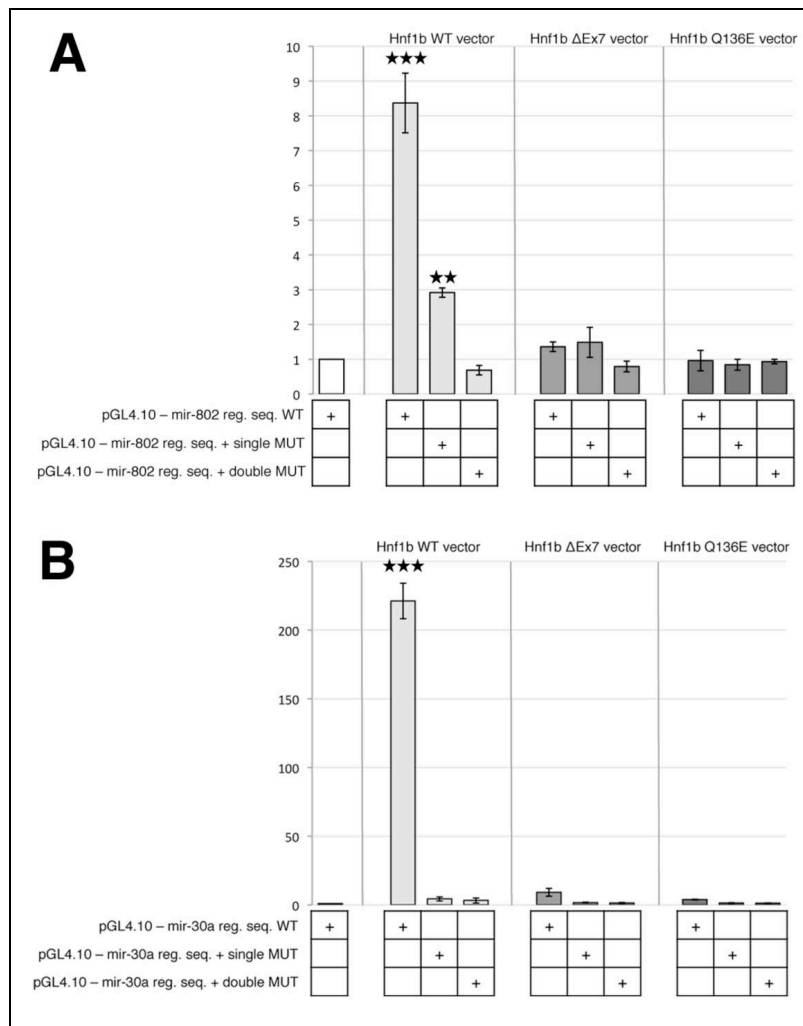


Figure 5. pGL4.10[luc2]-802 or -30a vectors containing single or double HNF1B binding site mutations in the promoter and enhancer elements. The normalized firefly luciferase activity was obtained by measuring firefly luciferase activity/Renilla luciferase activity. In each condition the amount of DNA reporter transfected was 500 ng and the amount of DNA expression vector was 100 ng. All experiments were performed at least three times. Statistical significance was analyzed by one-way ANOVA for multiple comparisons.

2.2.4 miR-194-2, miR-192, and miR-802 are able to inhibit HNF1B transcript via binding its 3'UTR

Co-expressing miRNA MIMICS with luciferase vectors containing wt versions of 3'UTR of Hnf1b, we have shown that miR-802 and miR-194-2 mimics are able to inhibit luciferase activity. Furthermore, mutating the miRNA regulatory elements (MRE) for miR-802 and miR-194-2 on HNF1B 3'UTR, did not lead to a down-regulation of the transcript, demonstrating the specificity of the regulation (**Figure 6 and Supplementary Figure 4**). Interestingly, also miR-192 is also able to inhibit luciferase activity by specific binding to the Hnf1b 3'UTR but the mutation of its MRE is lacking to confirm its specificity.

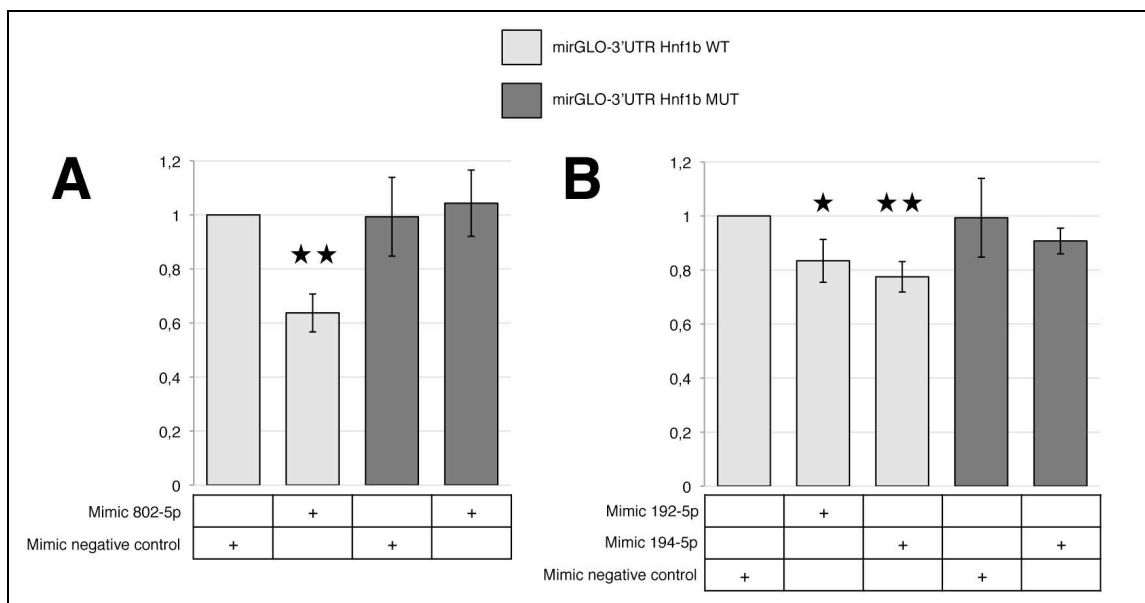


Figure 6. Luciferase assays were made co-transfecting 250 ng of mirGLO-Hnf1b-3'UTR vectors and 100 nM of the indicated miRNA mimics for each condition. mirGLO vectors was either WT or specifically mutated for miR-802 and miR-194-2 recognition elements (MRE) as shown in Supplementary Figure 4.

2.3 Discussion and conclusions

We have attempted to reveal microRNAs playing a role in the RCAD mouse model during kidney development. The results obtained so far demonstrated that HNF1B and the microRNAs -802 and -194-2 are linked by an autoregulatory-loop. Potentially, miR-192 also participates in this molecular autoregulation. We established an unknown transactivation capacity of HNF1B on miR-802 and miR-30a and we revealed for the first time a role of miR-802 in the kidney, thus showing a multi-organ regulation of this microRNA (**Figure 7**). We discovered that miR-194-2 and miR-192 are able to inhibit HNF1B transcripts through binding its 3'UTR, and confirmed *Jenkins et al.* studies on HNF1B transactivation activity on the cluster miR-194-2/192 (Jenkins RH et al., 2012) using a different cellular system.

Previous findings described a regulation between microRNAs and HNF1B in different models. For instance, *Hajarnis SS et al.* showed a direct transactivation by HNF1B of the miR-200b~429 cluster (Hajarnis SS et al., 2015), which is involved in tubular maturation and post-transcriptional control of *Pkd1* (Patel V et al., 2012). Moreover, it has been reported that the miR-17~92 miRNA cluster (Patel V et al., 2013) as well as the miR-375 (Hao J et al., 2017) regulates the posttranscriptionally the expression of Hnf1b.

In our RCAD mouse model we did not find a deregulation of these microRNAs. This may certainly be due to the differences in the models and to the differential effects of heterozygous mutations as compared *Hnf1b*-deficient mouse models. However, taking in consideration that deregulation of miR-802, miR-194-2 and miR-30a have been observed in other PKD mouse models, and the various annotation of some of these microRNAs in the kidney (see introduction), we strongly believe that they may have essential roles in HNF1B-associated syndrome. It still remains largely unclear how microRNAs act in this system and which other genes they control in addition to HNF1B. The reverse correlation mRNA:miRNA analysis may be an useful source for future functional studies and may highlight novel roles of these microRNAs as early biomarkers of the RCAD disease.

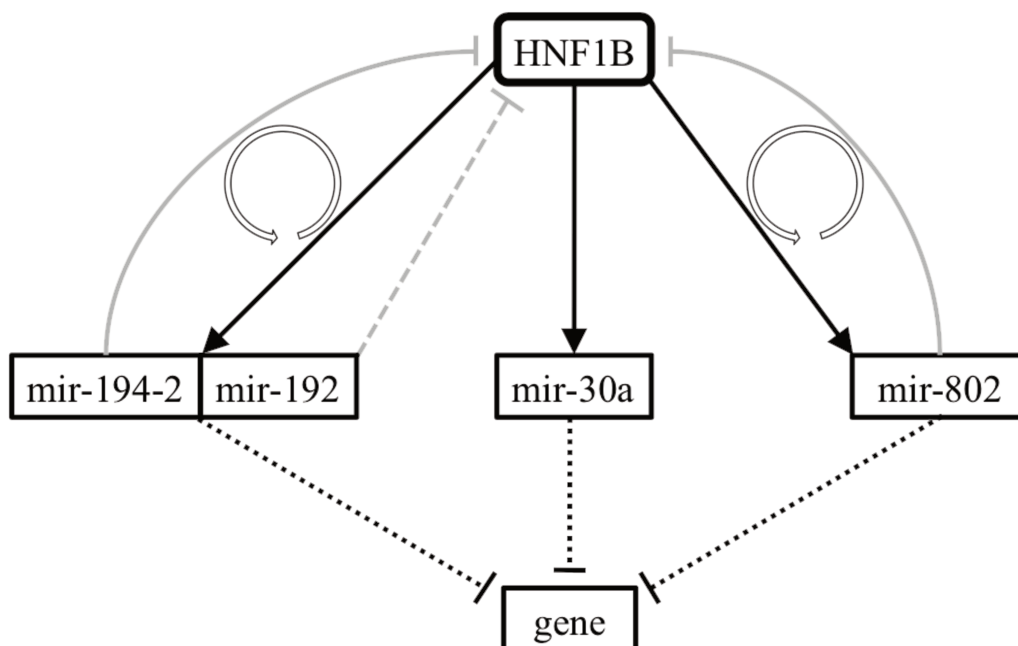


Figure 7. Autoregulatory loop between HNF1B and the selected microRNAs and potential indirect regulation of HNF1B on other genes through microRNAs. The continuous lines represent validated regulations, the dotted lines show potential regulations.

CONCISE METHODS

Cell Culture

Human embryonic kidney (HEK-293) cells were grown in DMEM (1X) + GlutaMAX medium supplemented with 10% BSA and maintained in 5% CO₂ atmosphere at 37°C.

Vector constructions

For Hnf1b transactivation analyses:

The regulatory sequences of each microRNA were amplified with PCR from mouse genome and inserted into pGEM®-T Easy vectors (PROMEGA). These sequences were confirmed by sequencing, removed from each plasmid with corresponding restriction sites and ligated into the pGL4.10[luc2]vector (PROMEGA) to form pGL4.10-miR-194-2/192, pGL4.10-miR-30a, and pGL4.10-miR-802 linked to luciferase cDNA. pGL4.10-miR-802 and pGL4.10-miR-30a point mutations variants were obtained by the use of a Site-Directed Mutagenesis using the QuikChange® II XL Site-Directed Mutagenesis Kit (Agilent Technologies) as depicted in **Supplementary Figure 1 and 2**. Primers used are listed below.

For microRNA targeting analyses:

The 3'UTR of mouse Hnf1b was cloned into a p-mirGLO Dual-Luciferase miRNA Target Expression Vector (Promega). A mirGLO-Hnf1b-3'UTR wt and a mutated version of these vectors were kindly provided by Dr. Jan-Wilhelm Kornfeld.

Chromatin immunoprecipitation (ChIP) assays

ChIP was performed on E14.5 kidneys using the rabbit HNF1B antibody (H85, Santa Cruz) as described by Heliot and Cereghini, 2012.

Dual Luciferase Reporter Assay

For Hnf1b transactivation analyses:

HEK-293 cells were plated into twelve-well plates at a density of 2.5×10^5 cells/well. After 24 hours transfection mixtures containing Opti-MEM® Reduced Serum Media (ThermoFisher), 500 ng of each reporter vector (pGL4.10[luc2] + regulatory sequence wt or mutated), 5 ng of pCMV-*renilla luciferase* normalization vector and from 25 to 100 ng of transactivation vector (Hnf1b wt, the mutated versions Δ Ex7 / Q136E or a pCB6 empty vector) were prepared. Subsequently, cells were transfected using 1.5 μ L of X-tremeGENE HP DNA Transfection Reagent (Roche) for each well according to manufacturer's protocol. Cells were harvested after 48 hours and luciferase activity was calculated.

For microRNA targeting analyses:

HEK-293 cells were plated into twenty-four-well plates at a density of 1.25×10^5 cells/well. After 24 hours, transfection mixtures containing Opti-MEM® Reduced Serum Media (ThermoFisher), 250 ng of reporter vector (mirGLO Hnf1B 3'UTR wt or mut) together with miRNA mimics (miRIDIAN microRNA Mimics Dharmacon) at the concentration of 100 nM for each condition were prepared. Subsequently, cells were transfected using 0.75 μ L of X-tremeGENE™ Hp Dna Transfection Reagent (Roche) for each well according to manufacturer's protocol. Cells were harvested after 24 hours and luciferase activity was calculated. In both experiments luciferase expression was assayed using a Dual Luciferase Assay Kit (Promega) according to the manufacturer's protocol, and the luminescence was recorded on a microplate reader (Berthold Tech TriStar² LB 942). The normalized firefly luciferase activity was obtained by measuring firefly luciferase activity/Renilla luciferase activity. All experiments were performed at least three times.

miRNA Isolation and Quantitative reverse transcription PCR (qRT-PCR)

miRNA sequencing results were confirmed by reverse transcription quantitative real-time PCR analysis for four different microRNAs. Total RNA was extracted from entire kidneys and reverse transcribed using miScript II RT kit (QIAGEN). The cDNA (diluted 10 times) was used for a 40-cycle Q-PCR reaction with miScript specific Primers (forward primer) and miScript Universal Primer (reverse primer, sequences copyright of QIAGEN). All reactions were performed using the Applied Biosystems StepONEPlus Real-Time system (ThermoFisher Scientific). All the amplifications were done using SYBR Green PCR Master Mix (Applied Biosystems). The control target SNORD61 (sequence copyright of QIAGEN) was used to normalize and the expression values of the respective miRNA were compared using $\Delta\Delta C_T$ method. The thermal cycling conditions included an initial holding stage of 20s, followed by the cycling stage composed by 40 cycles (95°C for 3sec, 60°C for 30s), followed by the melt curve stage (95°C for 15s, 60°C for 60 sec, temp increase of 0.3°C until 95°C for 15 sec). Melting curve analysis of every qPCR was conducted at the end of the cycling stage.

Primers

Name	Sequence
mmu-mir-802 promoter FW	C <i>CTCGAG</i> G TACTGGGAAGGCAGAGACG
mmu-mir-802 promoter RV	C <i>AAGCTT</i> CGTGGGCAGGCAGTATCCT
mmu-mir-802 promoter FW 1st mutation	CCGGGCCTTTAGCTTGCTAATCGGTTATGGATCCGGGAGTTAATAATTC
mmu-mir-802 promoter RV 1st mutation	GAATTATTAAC TCCCGGATCCATAACCGATTAGCAAGCTAAAGGCCCGG
mmu-mir-802 promoter FW 2nd mutation	CGGTTATGGATCCGGGAGTTGGTAATGGATGTTAATTGGTGCTATAAGC
mmu-mir-802 promoter RV 2nd mutation	GCTTATAGCACCAATTAACATCCATTACCAACTCCCGGATCCATAACCG
mmu-mir-194-2/192 promoter FW	C <i>CTCGAG</i> TTAGCTGTGGTCCGCTCCTCC
mmu-mir-194-2/192 promoter RV	CC <i>AAGCTT</i> ACTTGCTCAGAAGGGCTGATG
mmu-mir-30A enhancer FW	GA <i>AGATCT</i> CAGGGAGTAGCGACAAGC
mmu-mir-30A enhancer RV	CC <i>AAGCTT</i> TGCTAAGCACGACTGAACG
mmu-mir-30A enhancer FW 1st mutation	GCCCTGAAATTATAAGATGCTGTGGTCCAGGGACCAGACTTTAGGG
mmu-mir-30A enhancer FW 2nd mutation	CCCTAAAGTCTGGTCCCTGGACCACAGCATCTTATAATTTTCAGGGC
Hnf1b 3'UTR FW	CG GCTAGC CACACCATCAGTCTCTGGG
Hnf1b 3'UTR RV	GC TCTAGA GAGTCTGGCTGGCTTGC

Primers used are represented with restriction sites in *italic* and supplementary nucleotides in **bold**.

Bioinformatics

Prediction of miRs targets was performed using TargetScan mouse 5.0 (<http://targetscan.org>), miRDB (<http://www.mirdb.org/>), mirSystem (<http://mirsystem.cgm.ntu.edu.tw/>) (which integrates seven well known miRNA target gene prediction programs) and mirWalk 2.0 (<http://zmf.umm.uni-heidelberg.de/apps/zmf/mirwalk2/custom.html>). Prediction of HNF1B binding sites in regulatory sequences was performed using the JASPAR database (<http://jaspar.binf.ku.dk/>) and the ECR Browser (<https://ecrbrowser.dcode.org/>). A limitation of the bioinformatic study may be that focusing on the predicted targets also excludes potential previously unknown mRNA targets that are not recognized by any of the well-known algorithms. Using a negative miRNA-mRNA correlation method excludes more complicated miRNA regulatory mechanisms, such as the interaction with transcription factors, thus inducing or repressing the expression of multiple genes that are not a direct target of the respective miRNA.

Statistical Analyses

Data are shown as mean \pm standard error. Unless indicated otherwise, data sets were analysed for statistical significance using a two-tailed unpaired Student *t* test. *= $p < 0.05$, **= $p < 0.01$, ***= $p < 0.001$.

Supplementary Table 1

Listed below all the microRNAs significantly de-regulated in the RCAD mouse model. Data were obtained from microRNA seq at three different developmental stages from kidney samples. In addition to foldChange and p-values, the genomic sequence of each significantly de-regulated microRNA was examined through the use of HNF1B ChIP seq at E14.5; the nearest PEAK for each sequence was identified and evaluated for potential HNF1B binding sites. microRNAs are colored in blue if UP-regulated, in red if DOWN-regulated.

E14.5					
id	foldChange	log2FoldChange	pval	Putative seed sequence in Hnf1b mRNA	Nearest HNF1B Macs Peak from ChIP seq (kb)
mmu-mir-192-5p	0,76	-0,40	0,005522256	yes (CDS, 3'UTR)	1
mmu-mir-802-5p	0,15	-2,72	0,002401317	yes (3'UTR)	1
mmu-mir-342-5p	1,45	0,54	0,00066888	yes (CDS, 3'UTR)	16
mmu-mir-30c-2-3p	0,75	-0,42	0,006256346	yes (3'UTR)	30
mmu-mir-24-1-3p	0,73	-0,46	0,002983014	yes (3'UTR)	32
mmu-mir-204-5p	0,70	-0,52	0,000728916	yes (CDS, 3'UTR)	48
mmu-mir-24-2-3p	0,74	-0,44	0,004202491	yes (3'UTR)	58
mmu-mir-877-5p	1,35	0,43	0,00450893	yes (3'UTR)	144
mmu-mir-379-5p	0,68	-0,55	0,001397799	yes (3'UTR)	207
mmu-mir-153-3p	0,27	-1,90	0,000190631	no	540
mmu-mir-184-3p	0,18	-2,45	3,37E-20	yes (3'UTR)	2000

E15.5					
id	foldChange	log2FoldChange	pval	Putative seed sequence in Hnf1b mRNA	Nearest HNF1B Macs Peak from ChIP seq (kb)
mmu-mir-192-5p	0,51	-0,96	2,11E-20	yes (CDS, 3'UTR)	1
mmu-mir-194-2-5p	0,59	-0,76	1,77E-06	yes (3'UTR)	1
mmu-mir-802-3p	0,14	-2,81	0,002994326	yes (3'UTR)	1
mmu-mir-802-5p	0,13	-2,97	3,73E-07	yes (3'UTR)	1
mmu-mir-1199-5p	0,38	-1,38	0,005306279	no	10
mmu-mir-30a-3p	0,82	-0,28	0,005701507	yes (3'UTR)	10
mmu-mir-187-3p	0,62	-0,70	0,00015646	no	20
mmu-mir-204-5p	0,77	-0,38	0,000673598	yes (CDS, 3'UTR)	48
mmu-let-7c-2-5p	1,37	0,46	2,49E-06	yes (3'UTR)	64
mmu-let-7b-5p	1,46	0,55	4,86E-07	yes (3'UTR)	65
mmu-mir-183-3p	1,21	0,27	0,005037814	no	120
mmu-mir-132-3p	0,74	-0,43	0,002172258	no	123
mmu-mir-379-5p	2,50	1,32	6,40E-07	yes (3'UTR)	207
mmu-mir-382-5p	3,30	1,72	3,25E-12	no	232
mmu-mir-194-1-5p	0,68	-0,55	0,001660338	yes (3'UTR)	360
mmu-mir-322-3p	0,82	-0,29	0,003910507	yes (3'UTR)	408
mmu-mir-488-3p	1,39	0,47	0,004607872	no	425
mmu-let-7c-1-5p	1,37	0,45	3,08E-06	yes (3'UTR)	665
mmu-mir-674-3p	0,76	-0,40	0,001405383	no	1000
mmu-mir-3968-3p	0,74	-0,43	0,001363173	no	unknown
mmu-mir-5109-3p	4,92	2,30	9,40E-92	no	unknown
mmu-mir-5115-5p	5,17	2,37	7,47E-60	no	unknown
mmu-mir-5119-3p	5,79	2,53	4,84E-06	no	unknown
mmu-mir-6236-5p	3,69	1,89	6,49E-39	no	unknown
mmu-mir-6240-3p	4,51	2,17	1,91E-47	no	unknown
mmu-mir-6340-3p	Inf	Inf	1,50E-30	no	unknown

E17.5					
id	foldChange	log2FoldChange	pval	Putative seed sequence in Hnf1b mRNA	Nearest HNF1B Macs Peak from ChIP seq (kb)
mmu-mir-192-5p	0,49	-1,01	6,74E-09	yes (CDS, 3'UTR)	1
mmu-mir-802-3p	0,33	-1,58	0,001939792	yes (3'UTR)	1
mmu-mir-802-5p	0,35	-1,52	4,67E-09	yes (3'UTR)	1
mmu-mir-218-1-5p	1,47	0,56	0,001566905	yes (3'UTR)	24
mmu-mir-146b-5p	1,40	0,49	0,005244074	no	63
mmu-mir-122-5p	0,19	-2,36	7,07E-06	yes (CDS, 3'UTR)	117
mmu-mir-135a-2-3p	1,78	0,83	0,003657453	no	135
mmu-mir-218-2-5p	1,47	0,56	0,001539087	yes (3'UTR)	218

mmu-mir-135b-5p	1,96	0,97	0,008733622	no	313
mmu-mir-194-1-5p	0,57	-0,81	2,41E-05	yes (3'UTR)	360
mmu-mir-194-2-5p	0,64	-0,66	0,000570755	yes (3'UTR)	360
mmu-mir-3968-3p	0,67	-0,57	0,001026361	no	unknown
mmu-mir-6236-5p	2,84	1,51	2,78E-07	no	unknown
mmu-mir-6240-5p	0,16	-2,65	4,61E-13	no	unknown
mmu-mir-6240-3p	2,19	1,13	5,79E-06	no	unknown
mmu-mir-6340-3p	Inf	inf	3,80E-06	no	unknown

Supplementary table 2

Inverse gene-(predicted)miRNA relations. Several genes are predicted as targets of microRNAs showing a reciprocal relationship during the three stages analyzed. In the table, values of log2FoldChange for mRNAs and microRNAs are denoted as well as the algorithm that predicted the regulation. microRNAs or mRNAs are colored in blue if UP-regulated, in red if DOWN-regulated. A complete table including also E14.5 and E17.5 inverse regulation is integrated in the **Supplementary Table 2**.

E14.5				
Genes	log2FoldChange (E14.5) on mRNA seq	Targe miRNA	log2FoldChange miRNA (E14.5) from microRNA seq	Prediction Algorithms
CLDN2	-1.92	mmu-mir-877	0.43	TargetScan
GRHPR	-1.68	mmu-mir-877, mmu-mir-342	0.43, 0.54	TargetScan
HCLS1	-1.48	mmu-mir-342	0.54	TargetScan
HNF4A	-1.61	mmu-mir-342	0.54	TargetScan
LGALS9	-1.51	mmu-mir-342	0.54	TargetScan
PLCG2	-1.45	mmu-mir-342	0.54	TargetScan

E15.5				
Genes	log2FoldChange (E15.5) on mRNA seq	Targe miRNA	log2FoldChange miRNA (E15.5) from microRNA seq	Prediction Algorithms
IL31RA	1.59	mmu-mir-1199, mmu-mir-322	-1.38, -0.28	TargetScan, miRDB
LARS2	1.62	mmu-mir-1199	-1.38	TargetScan
REST	1.61	mmu-mir-1199	-1.38	TargetScan
SCUBE3	1.54	mmu-mir-194-2	-0.76	TargetScan
ZFP791	1.87	mmu-mir-1199	-1.38	TargetScan
ASS1	-2.65	mmu-mir-488	0.47	TargetScan
CLRN3	-2.32	mmu-let-7b	0.54	miRDB
CPN1	-1.7	mmu-mir-488	0.47	TargetScan
FBP1	-5.29	mmu-let-7c-1	0.45	TargetScan
GPD1	-1.51	mmu-mir-379	1.32	miRSystem, miRDB
HAO2	-2.65	mmu-mir-183	0.27	miRDB
HNF4A	-1.63	mmu-mir-488, mmu-mir-5119	0.47, 2.53	TargetScan
KL	-1.8	mmu-let-7b, mmu-mir-488, mmu-mir-382	0.54, 0.47, 1.72	TargetScan
MT2	-2.24	mmu-let-7c-1	0.45	miRDB
PCK1	-3.52	mmu-mir-5119, mmu-mir-6240	2.53, 2.17	TargetScan
PDZK1	-2.17	mmu-mir-379	1.32	miRDB
SLC5A8	-4.23	mmu-mir-183, mmu-let-7b	0.27, 0.54	TargetScan
SULT1D1	-2.43	mmu-mir-183	0.27	miRDB
TMEM229A	-1.61	mmu-mir-5119	2.53	TargetScan
TMEM25	-1.49	mmu-let-7c-1	0.45	TargetScan, miRDB
TMEM27	-1.64	mmu-let-7b, mmu-let-7c-1	0.54, 0.45	TargetScan
UGT1A1	-1.5	mmu-mir-183, mmu-mir-5119	0.27, 2.53	TargetScan

E17.5				
Genes	log2FoldChange (E17.5) on mRNA seq	Targe miRNA	log2FoldChange miRNA (E17.5) from microRNA seq	Prediction Algorithms
GABRP	0.88	mmu-mir-194-1, mmu-mir-194-2	-0.8, -0.65	TargetScan
PMAIP1	0.65	mmu-mir-192	-1.01	TargetScan, miRSystem
TCERG1L	0.59	mmu-mir-194-2	-0.8	TargetScan
TCHH	0.63	mmu-mir-192	-1.01	TargetScan
AICF	-1.05	mmu-mir-218-1	0.55	TargetScan

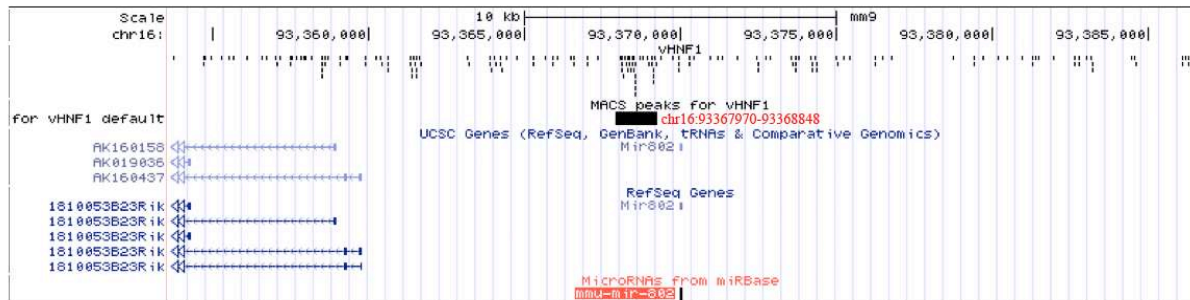
ABCC2	-1.6	mmu-mir-135a-2	0.83	TargetScan
ACSM5	-1.04	mmu-mir-135a-2, mmu-mir-135b	0.83, 0.96	TargetScan
AK4	-0.88	mmu-mir-218-2	0.55	TargetScan
ALDH1L1	-0.96	mmu-mir-218-2	0.55	TargetScan
ALDH4A1	-0.79	mmu-mir-135a-2, mmu-mir-135b, mmu-mir-218-1	0.83, 0.96, 0.55	TargetScan
ALDH6A1	-0.75	mmu-mir-6240, mmu-mir-135a-2, mmu-mir-218-1, mmu-mir-218-2	1.13, 0.83, 0.55, 0.55	TargetScan, miRDB
AQP1	-0.92	mmu-mir-218-1	0.55	TargetScan
ASS1	-0.72	mmu-mir-135b	0.96	TargetScan
B3GALT5	-0.7	mmu-mir-135a-2	0.83	TargetScan
CALML4	-0.7	mmu-mir-6240, mmu-mir-135a-2, mmu-mir-135b	1.13, 0.83, 0.96	TargetScan
CHDH	-0.75	mmu-mir-146b	0.48	TargetScan
CNDP1	-0.98	mmu-mir-135a-2, mmu-mir-135b	0.83, 0.96	TargetScan
CUBN	-1.61	mmu-mir-218-2	0.55	TargetScan
CYP27B1	-1.27	mmu-mir-146b, mmu-mir-135b, mmu-mir-218-1, mmu-mir-218-2	0.48, 0.96, 0.55, 0.55	TargetScan
CYP4A31	-1.4	mmu-mir-135a-2, mmu-mir-135b	0.83, 0.96	miRDB
ELOVL2	-0.71	mmu-mir-135b	0.96	miRSystem, miRDB
ENTPD5	-0.84	mmu-mir-6240, mmu-mir-135a-2, mmu-mir-218-1, mmu-mir-218-2	1.13, 0.83, 0.55, 0.55	miRDB, TargetScan
ERBB4	-0.72	mmu-mir-6240, mmu-mir-146b, mmu-mir-218-1, mmu-mir-218-2	1.13, 0.48, 0.55, 0.55	TargetScan
FMO1	-1.1	mmu-mir-146b, mmu-mir-218-2	0.48, 0.55	miRDB, TargetScan
FMO2	-1.37	mmu-mir-135a-2, mmu-mir-135b	0.83, 0.96	TargetScan
FUT9	-1.55	mmu-mir-135b	0.96	miRSystem
GCNT1	-0.96	mmu-mir-146b, mmu-mir-218-1, mmu-mir-218-2	0.48, 0.55, 0.55	TargetScan
GLYCTK	-0.92	mmu-mir-135b, mmu-mir-218-1	0.96, 0.55	TargetScan, miRSystem, miRDB
GPC5	-1	mmu-mir-135a-2, mmu-mir-135b	0.83, 0.96	TargetScan
GPM6A	-0.92	mmu-mir-6240	1.13	TargetScan
HAO2	-1.12	mmu-mir-135b	0.96	TargetScan
HNF4A	-0.9	mmu-mir-135b	0.96	miRDB
HNF4G	-0.9	mmu-mir-6240, mmu-mir-218-1, mmu-mir-218-2	1.13, 0.55, 0.55	miRDB, TargetScan
KCNJ1	-0.79	mmu-mir-135a-2, mmu-mir-135b	0.83, 0.96	TargetScan
KCNJ15	-1.44	mmu-mir-218-1	0.55	TargetScan
LRP2	-1.23	mmu-mir-218-2	0.55	TargetScan
LRRC19	-1.28	mmu-mir-135a-2	0.83	TargetScan
NCEH1	-0.81	mmu-mir-6240, mmu-mir-146b, mmu-mir-135a-2, mmu-mir-135b, mmu-mir-218-2	1.13, 0.48, 0.83, 0.96, 0.55	TargetScan, miRDB
OPCML	-0.76	mmu-mir-135a-2, mmu-mir-135b, mmu-mir-218-1, mmu-mir-218-2	0.83, 0.96, 0.55, 0.55	TargetScan
PAQR9	-0.85	mmu-mir-146b	0.48	TargetScan
PCK1	-0.97	mmu-mir-6240, mmu-mir-218-1, mmu-mir-218-2	1.13, 0.55, 0.55	miRDB, TargetScan
PKHD1	-0.84	mmu-mir-218-1	0.55	TargetScan
PRKAA2	-0.84	mmu-mir-6240, mmu-mir-218-1	1.13, 0.55	miRDB, TargetScan
PTER	-0.9	mmu-mir-218-1	0.55	TargetScan
RDH16	-1.33	mmu-mir-218-2	0.55	TargetScan
RDH19	-1.88	mmu-mir-6240	1.13	miRDB

SLC15A2	-0.86	mmu-mir-218-1, mmu-mir-218-2	0.55, 0.55	TargetScan
SLC16A12	-0.73	mmu-mir-218-1	0.55	TargetScan
SLC17A4	-1.19	mmu-mir-146b	0.48	TargetScan
SLC22A1	-1.75	mmu-mir-218-1	0.55	TargetScan
SLC22A13	-1.44	mmu-mir-135a-2	0.83	TargetScan
SLC22A2	-2.86	mmu-mir-218-2	0.55	TargetScan
SLC26A1	-0.74	mmu-mir-146b	0.48	TargetScan
SLC2A2	-1.32	mmu-mir-218-1	0.55	TargetScan
SLC4A4	-1.18	mmu-mir-135b, mmu-mir-218-1	0.96, 0.55	TargetScan
SLC5A12	-1.44	mmu-mir-218-2	0.55	TargetScan
SLC5A2	-1.09	mmu-mir-218-1	0.55	TargetScan
SLC5A8	-1.72	mmu-mir-218-1	0.55	TargetScan
SLC6A15	-1.79	mmu-mir-135b	0.96	TargetScan
SOD3	-1.14	mmu-mir-218-1	0.55	TargetScan
SUSD2	-0.79	mmu-mir-218-1	0.55	TargetScan
TFEC	-0.81	mmu-mir-146b, mmu-mir-218-1, mmu-mir-218-2	0.48, 0.55, 0.55	TargetScan
THRB	-0.7	mmu-mir-6240, mmu-mir-146b, mmu-mir-135b, mmu-mir-218-1	1.13, 0.48, 0.96, 0.55	TargetScan, miRDB, miRSystem
TMEM25	-0.74	mmu-mir-218-1	0.55	TargetScan
TMEM252	-1.14	mmu-mir-135a-2, mmu-mir-135b, mmu-mir-218-1	0.83, 0.96, 0.55	TargetScan
TYW3	-1.01	mmu-mir-135a-2, mmu-mir-135b	0.83, 0.96	TargetScan
XPNPEP2	-0.9	mmu-mir-135a-2, mmu-mir-135b	0.83, 0.96	TargetScan

Supplementary Figure 1

miR-802 regulatory sequence. **A.** miR-802 Macs peak from HNF1B ChIP seq with genomic location. **B.** miR-802 promoter sequence amplified in pGL4.10 vector. In red the predicted binding sites (Source: <http://jaspar.binf.ku.dk/>), in yellow the point mutations introduced by mutagenesis; in each case the nucleotides evidenced were changed with a guanine (G). **C.** Other potential Regulatory Elements (RE) controlling miR-802 Macs Peak. (Source: <http://linux1.softberry.com/cgi-bin/programs/promoter/nsite.pl>).

A



B

GTACTGGGAAGGCAGAGACGGCCAATGATGGACTCTGTCTTTATAAAACCAGCTACAAGTTTCATGAGGAATAGCTGAGATTCACCACTGCTGC
 ACACACACATATGAACATGCACATACCATACACATGTGCACACACACCAGCCAGACACACACATGTGCATACACACACTAGTTCAGT**GATAA**
TCATGAAGCAGAAATCCATATGAGCCCTTFCAGACAGAGGTTAATACAGTGAAGAGGTACAGAGATACCTGTAAAAGGAAAATTTAAAGGCCAA
 CATCCACATGAGTCAGTCTATGAATTATTTGTGACTTTTGGACTCTCCGGCCACATGACAGTAGAGGAGAAATAAGCAATCCTTTAAAAAGCCAA
 AATGTCATTACTTAAGCCAAGCCCTGCCTGAACCTGTTCTAATTGTATCTAAATTTGTTTCGTAGGTTCCCTCTCTCGATAGTGTGATGTGGCAGGT
 GCCCCGGGCTTTAGCTTGCTAA**TCAA****TTATTAAT**CCGGGAG**TTAATAATTCAT**GTTAATTGGTGCTATAAGCACTTTCTCTGGCAATGTGAG
 CAAAGGTCACAACCTTTTAAACAGCAAGGGGAAACATTCCTCAAGTTTCTTTTTCATGGCCATATCATGGAAATACCAAGATACGGAAG**ACAAAA**
TTTAAACCAGAAGTGGAAAGCAAGATAGCTCCACAGCTGAAAGATTAGACATCTCTCTGGGGACCAGCTCTGTTCACAGCCTGCTGGAAGGA
 GGAGAGGTTCTCCAGGGGACAAGGGACAGGACTTCAGCCCCACAGGAGCGCTCCACTCCGAGGATGCATCTCTAGGCAGGTTTGTGGACCTTTG
 TCAACAAGATGAGTAATATAAGTCTCTAGTCAGAAAAGCTT

C

RE: 326. AC: RSA00326//OS: human /GENE: LE/RE: PU.1 /BF: **PU.1; GABPalpha**
 Motifs on "-" Strand: Mean Exp. Number 0.00755 Up.Conf.Int. 1
 Found 1 448 **GAGAGGAA** 441 (Mism.= 0)

RE: 375. AC: RSA00375//OS: human /GENE: CD53/RE: Ets-1 /BF: **Ets-1/Pu.1**
 Motifs on "-" Strand: Mean Exp. Number 0.00998 Up.Conf.Int. 1
 Found 1 448 **GAGAGGAACC** 439 (Mism.= 1)

RE: 471. AC: RSA00471//OS: mouse /GENE: envoplakin/RE: E-box/Klf /BF: **unknown**
 Motifs on "-" Strand: Mean Exp. Number 0.00854 Up.Conf.Int. 1
 Found 2 292 **CATGTGGATGT** 282 (Mism.= 1) 160 CATGTGTGTGT 150 (Mism.= 1)

RE: 507. AC: RSA00507//OS: human /GENE: G6Pase/RE: HNF1 /BF: **HNF1**
 Motifs on "-" Strand: Mean Exp. Number 0.00107 Up.Conf.Int. 1
 Found 1 34 **AGTccATCATTGGCC** 20 (Mism.= 2)

RE: 584. AC: RSA00584//OS: human /GENE: v-erbA/RE: COUP BS /BF: **COUP**
 Motifs on "-" Strand: Mean Exp. Number 0.00883 Up.Conf.Int. 1
 Found 1 326 **GaGTCAAAGTCA** 314 (Mism.= 2)

RE: 656. AC: RSA00656//OS: mouse /GENE: IgH/RE: microE3 /BF: BF1: **NF-microE3**; BF2: **TFE3**
 Motifs on "+" Strand: Mean Exp. Number 0.00609 Up.Conf.Int. 1
 Found 1 331 **GCCACATGCa** 341 (Mism.= 1)

RE: 704. AC: RSA00704//OS: mouse /GENE: Amy 2A/RE: XPF BS /BF: **XPF-1**
 Motifs on "+" Strand: Mean Exp. Number 0.00322 Up.Conf.Int. 1
 Found 1 692 **CAGCTG** 697 --14-- 712 TCTC 715 (Mism.= 0/ 0)

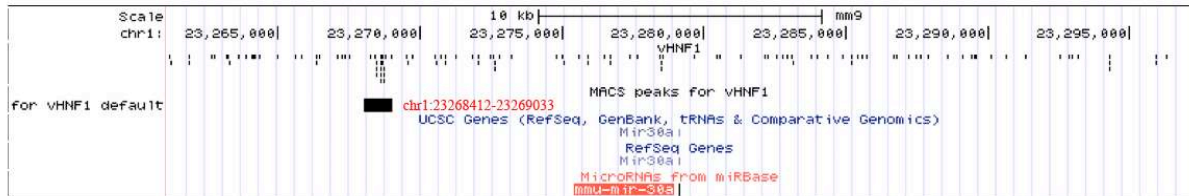
RE: 1419. AC: RSA01419//OS: human /GENE: IAPP/RE: A2 /BF: **PDX1**
 Motifs on "+" Strand: Mean Exp. Number 0.00316 Up.Conf.Int. 1
 Found 1 855 **ATGAGTAATaTAAG** 868 (Mism.= 2)

Totally 9 motifs of 8 different REs have been found

Supplementary Figure 2

miR-30a regulatory sequence. **A.** miR-30a Macs Peak from HNF1B ChIP seq with genomic location. **B.** miR-30a enhancer sequence amplified in pGL4.10 vector. In red the predicted binding sites (Source: <http://jaspar.binf.ku.dk/>), in yellow the first point mutations performed; nucleotides evidenced were changed with a guanine (G). The deletion performed in further experiments is underlined. **C.** Other potential Regulatory Elements (RE) controlling miR-30a Macs Peak. (Source: <http://linux1.softberry.com/cgi-bin/programs/promoter/nsite.pl>).

A



B

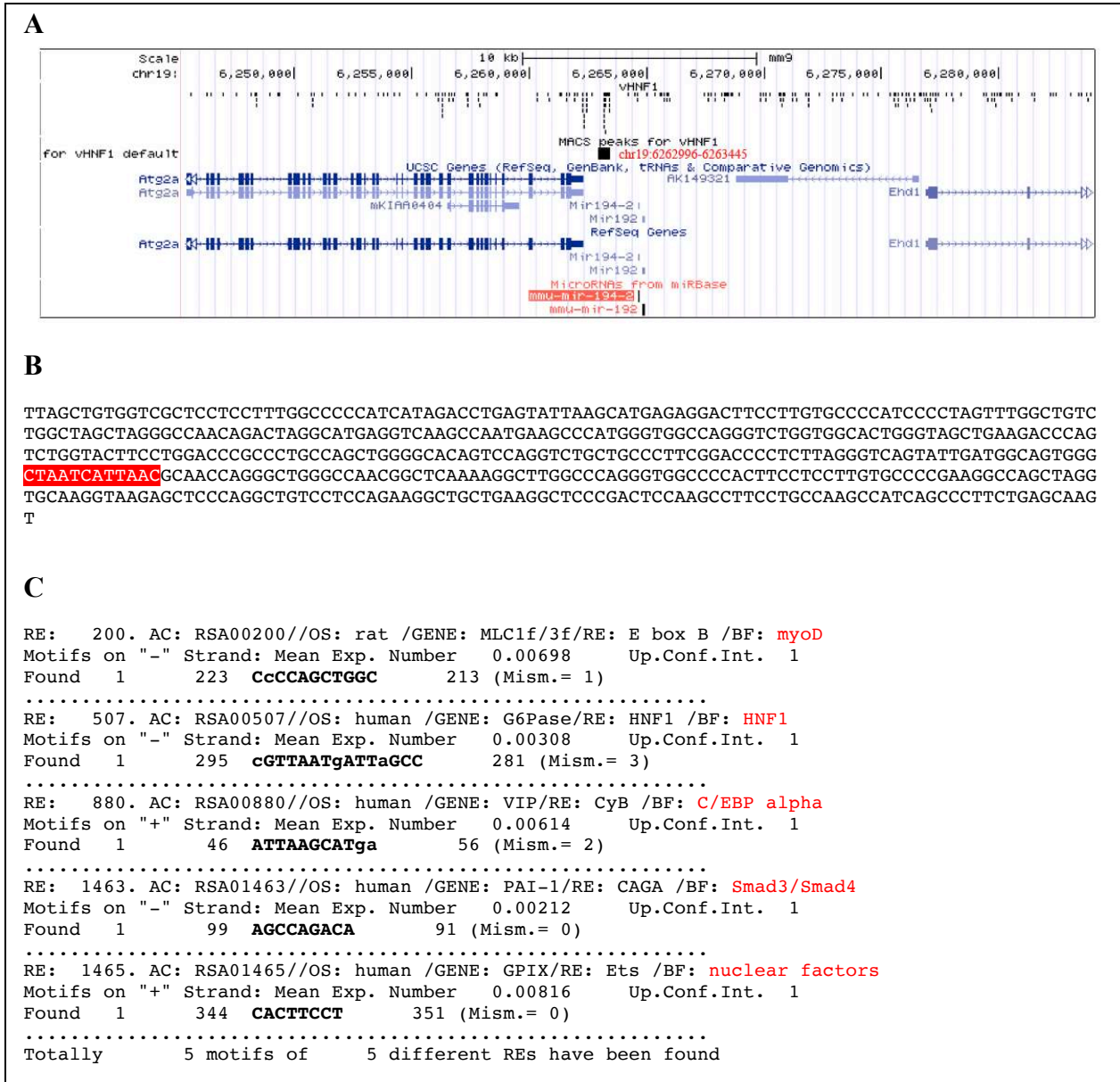
```
CAGGGAGTAGCGACAAGCTAAAGTTTATACATGCTTAATATTTAAATTAATATATTTGTTTGTGTTTATGTATTGAGACAAGGTATTGCATTAACC
CAATGTGGACTAGAACTTACTGTGTAGTCTATGCTGTCCTGAATTGATAATTCFCAGTTCAGCTTTACAAATTCGGAATTCGAGGCATGT
GGCATGGAGCTTGGCATACTTTTACACACACACACACACACACACACACACATGATCCATAGAAACTAGAATGTCATATGTGAAAACC
AAAGTTATTTTACATTTTATTTTATTGACTAATGCTGTGTAATACTTGGCTGTGTGTTCTTTTTTGAATCATTGTGTAACAAAGTCATAGATG
GAAAAAACTCTAGGTTAGATACAAGATGGACAGTCCACTAATCTGGCTGGTGTGAGTATTGTATAAACTGTGTGTGTGTGTGTGTGTGTGTG
TATGTGTGTGTGTGTGTATCTCACGTGCACATTATGCCTAAGTTAAGGATGCCCTGAAATTATAAGATGCTGTATCCATTGACCAGACTTTAG
GGATATCTCTTTAAAGTGTGTTGACATTTAATTGACATTTGAAGGTTTCATTCTGTTAATCATACTCAAAGTGCTAAAGCTATGGTTGACTGCTT
TGGAAATTTTACGTTTCAGTCGTGCTTAGCA
```

C

```
RE: 218. AC: RSA00218//OS: mouse /GENE: MLC-2/RE: HF-1a /BF: HF1a
Motifs on "+" Strand: Mean Exp. Number 0.00648 Up.Conf.Int. 1
Found 1 187 GTGGCATG 194 (Mism.= 0)
.....
RE: 252. AC: RSA00252//OS: rat /GENE: Cx32/RE: YY-1 /BF: YY-1
Motifs on "-" Strand: Mean Exp. Number 0.00384 Up.Conf.Int. 1
Found 1 270 TGACATTCT 262 (Mism.= 0)
.....
RE: 471. AC: RSA00471//OS: mouse /GENE: envoplakin/RE: E-box/Klf /BF: unknown
Motifs on "-" Strand: Mean Exp. Number 0.00142 Up.Conf.Int. 1
Found 1 248 CATGTGtGTGT 238 (Mism.= 1)
.....
RE: 944. AC: RSA00944//OS: human /GENE: TSG-6/RE: NF-IL6* BS /BF: NF-IL6
Motifs on "+" Strand: Mean Exp. Number 0.00553 Up.Conf.Int. 1
Found 1 355 TTGTGTAAC 363 (Mism.= 0)
.....
Totally 4 motifs of 4 different REs have been found
```

Supplementary Figure 3

miR-194-2/192 regulatory sequence. **A.** miR-194-2/192 Macs Peak from HNF1B ChIP seq with genomic location. **B.** miR-194-2/192 promoter sequence amplified in pGL4.10 vector. In red the predicted binding site (Source: <http://jaspar.binf.ku.dk/>). **C.** Other potential Regulatory Elements (RE) controlling miR-194-2/192 Macs Peak. (Source: <http://linux1.softberry.com/cgi-bin/programs/promoter/nsite.pl>).



Supplementary Figure 4

microRNAs alignment with HNF1B 3'UTR wt and mutant. **A.** miR-802 alignment with HNF1B 3'UTR. **B.** miR-194 alignment with HNF1B 3'UTR. **C.** miR-30a alignment with HNF1B 3'UTR. **D.** miR-192 alignment with HNF1B 3'UTR. While miR-802, miR-194 and miR-30a are sharing different common nucleotides in their miRNA regulatory elements (MRE) on 3'UTR of HNF1B, miR-192 is targeting another sequence.

miR-802 alignment with HNF1B 3'UTR wt and mutant

Human WT 3'UTR	5'	AAACUUGAAUC	UGUUACUGAAUAA	3'
WT 3'UTR	5'	aaacuUGAAUC--UGUUACUGAAUAA		3'
mmu-miR-802	3'	uuccuACUUAGAAACAAUGACUAAUAA		5'
Mutant 3'UTR	5'	AAACUguccga--guggcagucAAUAA		3'

miR-194 alignment with HNF1B 3'UTR wt and mutant

Human WT 3'UTR	5'	GAUGCGAAAACUUGAAUCUGUUACUG	3'
Mouse WT 3'UTR	5'	gaUGCAAAAACUUGAAUCUGUUACUG	3'
mmu-miR-194	3'	agGUGUACCUCAAC---GACAAUGu	5'
Mutant 3'UTR	5'	gaUGCAAAAACUguccgaguggcaguc	3'

miR-30a alignment with HNF1B 3'UTR wt and mutant

Human WT 3'UTR	5'	AACUUGAAUCUGUUACUGAAUAA	3'
Mouse WT 3'UTR	5'	aaacuUGAAUCUGUUACUGAAUAA	3'
mmu-miR-30a	3'	cgacGUUUGUAGGCUGACUUuc	5'
Mutant 3'UTR	5'	AACUguccgaguggcagucAAUAA	3'

miR-192 alignment with HNF1B 3'UTR wt and mutant

Human WT 3'UTR	5'	ACUUUUCUUUGUAAAGGUCAG	3'
Mouse WT 3'UTR	5'	acUUUUCUUUGUAAAGGUCag	3'
mmu-miR-192	3'	CCGACAGUUAAGUAUCCAGUc	5'

No mutant form tested

TOPIC III. Urinary proteome signature of Renal Cysts and Diabetes syndrome in children

III.1. Context of the study

III.2. Results and discussion

III.3. Conclusions

SCIENTIFIC ARTICLE 2

III.1. Context of the study

Urinary proteomics represents an enlarging field of interest for biologists and physicians and proteomic analysis have been employed for the discovery and the validation of biomarkers of several kidney diseases (Mischak H et al., 2015; Magalhães P et al., 2016). Urine represents an easy accessible biological fluid, which can be obtained in large quantities via a non-invasive procedure and may provides insights about different organs because it results from glomerular filtration via blood (Thongboonkerd V et al., 2005). Moreover, its proteome is originated 70% from the kidney and the urinary tract along with 30% from the circulation, which allows the study of different renal diseases and consequently associated events such as extracellular matrix (ECM) remodelling or fibrosis (Schaub S et al., 2004; Klein J et al., 2014; Magalhães P et al., 2017). Oppositely, its limitation is due to daily variability caused by circadian rhythms, physical activity, diet and metabolic or catabolic processes (Weissinger E et al., 2004; Decramer S et al., 2008), which can be corrected by different adjustment or calibration/normalization methods (Jantos-Siwy J et al., 2009).

Top-down methods, as Capillary electrophoresis–mass spectrometry (CE-MS), allow the identification of naturally occurring peptides, which does not require any prior proteolytic procedure. These peptides are stable and soluble biomolecules ranging from 0.5 to 20 kDa, not requiring any protein digestion before MS analysis, and being usually derived by the activity of endogenous proteases/peptidases (Zürbig, P et al., 2008; Finoulst I et al., 2011).

Following the promising results on the urinary proteome of *Hnflb*^{Sp2/+} mutant mice described in the Topic II, we decided to perform the first clinical proteomic analysis of the RCAD syndrome in a pediatric cohort of patients to provide new insights of this multisystem disorder identifying novel urinary biomarkers. For this analysis we performed capillary electrophoresis coupled to mass spectrometry (CE-MS).

Regarding my personal role in this study, in the context of the RENALTRACT consortium and in collaboration with the Mosaiques Diagnostic and Therapeutics AG (Hannover) company, I performed with the help of my colleague Pedro Magalhães the first

proteomic analysis on mouse urines. Following these results I thought with him to apply the same scientific approach to RCAD human patients and after a discussion with our supervisors we decided to contact nephrologists in different European Center. I was involved in the collection of samples and during my secondments in the Mosaiques Diagnostic and Therapeutics AG (Hannover) I performed urine preparation (ultrafiltration process) under the supervision of Pedro Magalhães and Dr Züribig. Subsequently, my role has been focused in experimental design deciding the different cohorts to use as discovery and validation along with data interpretation and writing the manuscript.

III.2. Results and discussion

Performing CE-MS we found 146 peptides associated with RCAD urines in 22 pediatric patients compared to 22 healthy age-matched controls. Interestingly, comparable results regarding collagen fragments (generally UP-excreted) and uromodulin fragments (DOWN-excreted) were obtained between RCAD human and RCAD mice proteome. Following the identification of RCAD urinary proteome signature, a classifier based on these peptides was generated and further tested on an independent blinded cohort, clearly discriminating RCAD patients from different groups of controls (ADPKD, nephrotic and CKD patients).

III.3. Conclusions

Our study demonstrates that the urinary proteome in children with RCAD syndrome differs from autosomal dominant polycystic kidney disease (*PKD1*, *PKD2*), congenital nephrotic syndrome (*NPHS1*, *NPHS2*, *NPHS4*, *NPHS9*), and also from chronic kidney disease conditions, suggesting differences between the pathophysiology behind these disorders. Future studies will further evaluate the performance of the RCAD panel in additional pediatric cohorts of disorders more closely related to RCAD such as autosomal recessive polycystic kidney disease (ARPKD), medullary cystic kidney disease (MCKD), autosomal dominant tubulointerstitial kidney disease (ADTKD) or diabetic patients. Moreover, and along with the evaluation of the performance of this classifier to predict the progression of RCAD, follow-up clinical data of the patients described in this study will be addressed.

SCIENTIFIC ARTICLE 2

Urinary proteome signature of Renal Cysts and Diabetes syndrome in children

Pierbruno Ricci^{1#}, Pedro Magalhães^{2,3#}, Magdalena Krochmal², Martin Pejchinovski², Erica Daina⁴, Maria Rosa Caruso⁵, Laura Goea¹, Iwona Belczacka^{2,6}, Giuseppe Remuzzi⁴, Muriel Umbhauer¹, Jens Drube³, Lars Pape³, Harald Mischak², Stéphane Decramer^{7,8,9,10}, Franz Schaefer¹¹, Joost P. Schanstra^{9,10}, Silvia Cereghini¹, Petra Zürgbig^{2*}

¹Sorbonne Université, CNRS, Institut de Biologie Paris-Seine, IBPS, Laboratoire de Biologie du Développement, UMR7622, 9 quai Saint-Bernard, Paris F-75005, France

²Mosaïques Diagnostics GmbH, Hannover, Germany

³Department of Pediatric Nephrology, Hannover Medical School, Hannover, Germany

⁴IRCCS – Istituto di Ricerche Farmacologiche Mario Negri – Clinical Research Center for Rare Diseases Aldo e Cele Daccò, Ranica Bergamo, Italy

⁵Unit of Nephrology, ASST Papa Giovanni XXIII, Bergamo, Italy

⁶University Hospital RWTH Aachen, Institute for Molecular Cardiovascular Research (IMCAR), Aachen, Germany

⁷Service de Néphrologie Pédiatrique, Hôpital des Enfants, CHU Toulouse, Toulouse, France

⁸Centre De Référence des Maladies Rénales Rares du Sud Ouest (SORARE), Toulouse, France

⁹Institut National de la Santé et de la Recherche Médicale (INSERM), U1048, Institut of Cardiovascular and Metabolic Disease, Toulouse, France

¹⁰Université Toulouse III Paul-Sabatier, Toulouse, France

¹¹University Children Hospital, Pediatric Nephrology, Heidelberg, Germany

#P.R. and P.M. contributed equally to this work.

Corresponding author:

Dr. Petra Zürgbig

Mosaïques diagnostics GmbH

Rotenburger Str. 20

30659 Hannover

Germany

Phone: +49 511 554744 15

FAX: + 49 511 554744 31

E-mail: zuerbig@mosaiques-diagnostics.com

(Submitted the 30th of July to Scientific Reports)

Abstract

Renal Cysts and Diabetes Syndrome (RCAD) is an autosomal dominant disorder caused by mutations in the *HNF1B* gene encoding for the transcriptional factor hepatocyte nuclear factor-1B. RCAD is characterized as a multi-organ disease, with a broad spectrum of symptoms including kidney abnormalities (renal cysts, renal hypodysplasia, single kidney, horseshoe kidneys, hydronephrosis), early-onset diabetes mellitus, abnormal liver function, pancreatic hypoplasia and genital tract malformations. In the present study, using capillary electrophoresis coupled to mass spectrometry (CE-MS), we investigated the urinary proteome of a pediatric cohort of RCAD patients and different controls to identify peptide biomarkers and obtain novel insights into the pathophysiology of this disorder. As a result, 146 peptides were found to be associated with RCAD in 22 pediatric patients compared to 22 healthy age-matched controls. A classifier based on these peptides was generated and further tested on an independent blinded cohort, clearly discriminating RCAD patients from different groups of controls. This study demonstrates that the urinary proteome in children with RCAD syndrome differs from autosomal dominant polycystic kidney disease (*PKD1*, *PKD2*), congenital nephrotic syndrome (*NPHS1*, *NPHS2*, *NPHS4*, *NPHS9*), and also from chronic kidney disease conditions, suggesting differences between the pathophysiology behind these disorders.

Introduction

Renal Cysts and Diabetes (RCAD) syndrome is caused by heterozygous mutations in the *HNF1B* gene, encoding the transcriptional factor hepatocyte nuclear factor-1B. RCAD syndrome (RCAD, OMIM #137920)¹ can also be referred as MODY5 (Maturity Onset Diabetes of the Young type 5)². The wide spectrum of clinical features in RCAD patients is due to the multisystem role of HNF1B, which is involved in normal morphogenesis of several organs, including kidneys, pancreas, liver, and genitourinary tract³. Consistent with its broad developmental expression pattern^{4,5}, studies on fetuses carrying *HNF1B* mutations revealed a fundamental function during kidney, urogenital tract and pancreas development^{4,6-8}.

RCAD disease is inherited in an autosomal dominant pattern⁹. To date, more than 150 mutations have been described in the *HNF1B* gene, including missenses, nonsense, frameshifts, splice site mutations, insertions/deletions as well as whole gene deletions that represent approximately 50% of all mutations found in patients¹⁰.

The most prominent clinical feature in HNF1B-associated syndrome is the renal disease, usually characterized by congenital anomalies of the kidney and urinary tract (CAKUT) including such as renal cysts, renal dysplasia, solitary or horseshoe kidney, hydronephrosis, and hyperuricaemic nephropathy¹¹. In addition, cases of otherwise unexplained chronic kidney disease (CKD) have been reported both in children¹² and adults^{13,14}. Tubular dysfunction manifesting by hypomagnesemia, hypocalciuria¹⁵⁻¹⁷, and hyperuricemia^{13,18} has also been described. Extrarenal features comprise maturity-onset diabetes of the young, pancreatic hypoplasia, abnormal liver function, and genital tract malformations. The phenotype of *HNF1B* mutant carriers is indeed highly variable within and between families¹⁹. These observations led to the hypothesis that non-allelic factors, as well as stochastic variation in temporal *HNF1B* gene expression and environmental factors, could cause the strong intrafamilial variability of RCAD patients^{3,20}.

Urinary proteomics is increasingly being employed in kidney disease research. Several studies have demonstrated that capillary electrophoresis coupled to mass spectrometry (CE-MS) enables the identification and validation of several biomarkers or peptide signatures classifying the diagnosis and prognosis of various kidney diseases²¹⁻²⁴. In addition to their diagnostic and prognostic usefulness, proteomics derived biomarkers may advance the understanding of the molecular pathways involved in the pathogenesis of a specific condition.

In this study, we aimed to obtain more insights of the RCAD syndrome by applying urinary proteomics to discover peptides that can be used to characterize RCAD patients' proteome.

Results

Identification of RCAD-related urinary peptides and development of a urinary peptide-based classifier

Urine samples from RCAD patients obtained from three European centers were analyzed with CE-MS. Furthermore, data from previously measured samples were extracted from the Human Urinary Proteome Database²⁵⁻²⁷. The data of those samples were separated in two different groups: a discovery cohort ($n=44$) and an independent cohort for validation ($n=230$) (**Figure 1A**). For the identification of significant urinary peptides related to RCAD syndrome, we compared the urinary proteome profiles of 22 RCAD patients with a group of 22 age- and gender-matched healthy patients (discovery cohort) (**Table 2A** and **Supplementary Table 1**). The selection of the peptides was adjusted for multiple testing following the concept described by Benjamini and Hochberg²⁸ and following the clinical proteomics guidelines²⁹. This led to the identification of 294 differentially excreted peptides (corrected $p<0.05$) between these two groups. For 146 out of the 294, high-confidence sequence information could be assigned. Fragments of uromodulin, osteopontin and mucin, as well as a large number of collagen fragments were identified. Moreover, peptides associated to cystic conditions as annexin A1 and unc-119 homolog A were de-regulated (details such as the sequence information as well as the fold-change are described in detail in **Supplementary Table 2**). The difference in abundance of these 146 peptides between RCAD patients and healthy controls is shown in **Figure 1B**. These 146 peptides were combined into a classifier termed “RCAD146” using a support vector machine (SVM), defining a cut-off score based on the classification of the patients in the discovery cohort. Based on the cut-off score 0.30, the RCAD classifier discriminated RCAD from healthy controls with 90.9% sensitivity and 100% specificity and an AUC of 0.99 in the discovery cohort (**Figure 1C**).

Validation of RCAD146 in an independent group

The mathematical RCAD146 model was validated in an independent group of samples (**Table 2B**), consisting of 24 RCAD and 20 healthy controls. The analysis revealed an AUC of 1.00 [0.92 to 1.00 (95% CI); $p<0.0001$]. At the pre-defined cut-off level of 0.30 based on the discovery cohort, the classifier displayed a sensitivity of 91.67% and specificity of 100%. To obtain confirmation about the performance of the RCAD146 in differentiating pediatric RCAD patients from patients suffering from other kidney diseases, we further selected a group of patients with chronic kidney disease (CKD) ($n=85$). This control group of children

was particularly interesting as i) 40% of adults with HNF1B mutations develop CKD¹³, ii) it represents a condition with severe chronic kidney damage and, iii) to confirm that the performance of the RCAD146 classifier is independent of proteinuria in RCAD patients. This analysis showed a specificity of 97.7% and an AUC of 0.99 [0.949 to 1.00 (95% CI); $p < 0.0001$] for the classification of children with CKD as non RCAD. To further evaluate the specificity and validity of the pediatric RCAD urinary proteomic pattern, the classifier was subsequently tested in patients with different monogenic kidney diseases, including ADPKD and nephrotic syndrome subjects. In the case of ADPKD, 53 out of 55 patients were scored as non RCAD corresponding to a specificity of 96.4% [AUC: 0.974] (**Figure 2A**). On the other hand, in the group of patients with nephrotic syndrome, 39 of 46 patients were scored by RCAD146 as non-RCAD displaying a specificity of 84.8 [AUC: 0.952] (**Figure 2A**). When evaluating all data sets combined the overall sensitivity and specificity were 91.7% and 91.1%, respectively. Furthermore, this receiver operating characteristic (ROC) analysis revealed an AUC of 0.978 [0.950 to 0.993 (95% CI); $p < 0.0001$] (**Figure 2B**).

Discussion

In this study, we aimed to identify urinary peptides related to RCAD syndrome with the goal of providing a non-invasive readout together with molecular changes that can be significant and specific of this disease. This is the first study showing a unique proteome profile, which distinguishes RCAD children from healthy controls and patients with different renal diseases. To demonstrate the RCAD pediatric proteome specificity from genetic point-of-view, patients with more than ten different heterozygous mutations in the *HNF1B* gene were evaluated in our study. Considering that more than 150 heterozygous mutations in *HNF1B* have so far been shown to be pathogenic (**Figure 3**), this study covered a distinct range of exonic and intronic variations.

The most prominent finding of the study was the identification of 294 differentially excreted peptides potentially related to RCAD syndrome, where sequence information was obtained for 146 peptides. Due to the fact that changes in the kidney and genitourinary tract are reflected by modifications of the urinary proteome³⁰, peptides may display a particular signature/feature, providing better insights of RCAD syndrome pathophysiology. Interestingly, as previously shown in the ADPKD urinary proteome³¹, the majority of peptides enriched in the urine of RCAD patients were collagen type I or type III fragments. This may reflect active extracellular matrix (ECM) remodeling, which could be related to ECM modifications due to cyst expansion, which affects modifications in the ECM³².

In contrast, other peptides, previously associated with cystic conditions, were downregulated in RCAD. These included annexin A1 (ANXA1), a key protein in cystic fibrosis pathogenesis and a prognostic marker of glomerular injury^{33,34}; hemoglobin subunit delta (HBD), which was found downregulated in arachnoid cysts fluids compared with cerebrospinal fluids³⁵; the protein unc-119 homolog A (UNC119) that play a crucial role in proper ciliary targeting of the cystic gene nephrocystin-3.

In the RCAD urinary proteome we observed altered of several peptides with calcium binding or calcium regulating properties, such as sarcalumenin (SRL), and annexin A1 (ANXA1), gelsolin (GSN), short transient receptor potential channel 4-associated protein (TRPC4AP) and the direct target of *HNF1B* osteopontin (SPP1)³⁶. This may be related to the role of *HNF1B* as a mediator of the urinary reabsorption of calcium^{15,37}.

Following the identification of the proteomic signature, the urinary peptides were combined into a classifier, RCAD146, predicting and positively differentiating RCAD syndrome from other kidney diseases. The performance of RCAD146 in differentiating

RCAD patients from children affected by CKD was evaluated. The RCAD146 classifier correctly identified the majority of CKD patients as non-RCAD (97.6%) demonstrating that the RCAD signature is clearly different from the CKD background peptide excretion, which is conversely characterized by a down excretion of collagen peptides²². The increased excretion of collagen fragments in the RCAD urinary samples may reflect the cystic phenotype and the still non-fibrotic status of patients' kidneys, whereas tubulointerstitial fibrosis determines the peptide excretion pattern in CKD³⁸. Since CKD is a rare condition in RCAD children¹², it would be of interest testing a cohort of adult RCAD patients suffering from CKD, in order to investigate the performance of the RCAD146 classifier.

The other disorders used as diseased controls in this study were biologically related (e.g ADPKD) or non-related (e.g. nephrotic syndrome) to the RCAD syndrome. In particular, a group of patients affected by autosomal dominant polycystic kidney disease (ADPKD) appears relevant as there are genotypic and phenotypic correlations with the RCAD syndrome. *HNF1B* was shown to regulate *Pkd2* in mouse³⁹ and mutations in *HNF1B* can mimic polycystic kidney disease especially in prenatal setting and early childhood^{40,41}. Notably, the RCAD146 classifier precisely discriminated RCAD from ADPKD.

We then selected other patients with monogenic mutations sharing a common nephrotic syndrome phenotype. In this case too, RCAD146 classifier identified subjects carrying mutations in *NPHS1*, *NPHS2*, *WT1* (*NPHS4*), and *ADCK4* (*NPHS9*) as non-RCAD. This result may highlight that RCAD146 is not just reflecting proteinuria, which has been found in almost one of three RCAD patients¹³, but reflecting a specific pathophysiological state.

Interestingly, in a parallel test, the urinary proteome of a patient with *Pax2* mutation was misrecognized by RCAD146 (data not shown). This observation suggests that the RCAD pediatric proteome can potentially be closer to patients with mutations in the gene encoding the transcription factor PAX2, known to cooperate with HNF1B in kidney morphogenesis and ureter differentiation⁴², than patients with either polycystic or nephrotic syndrome. Additional samples are required to further validate this common feature.

A limitation of the current study is related to the ADPKD cohort, which were not children, but adults. This is due to the difficulty in recruiting children with ADPKD because the average age at the diagnosis is approximately 30 years old⁴³. Another issue that could be a limitation is that this study included post hoc analysis, due to the selection of the diseased control population from previous studies. Overall, the study, performed in agreement with all guidelines for clinical proteomics demonstrates a significant value of the urinary proteome

analysis in the detection of RCAD, highlighting some proteins that potentially participate in the development of cysts and may be useful for early diagnosis.

In conclusion, the urinary proteome of pediatric patients with *HNFI1B* mutations was investigated here, providing novel insights into the pathophysiology of the RCAD phenotype. The urinary peptide signature of pediatric RCAD patients is mainly characterized by the upregulation of collagens peptides (especially type I or type III fragments), and osteopontin along with the downregulation of uromodulin. Including the 146 peptides differentially excreted between RCAD and healthy patients in a diagnostic biomarker panel, we demonstrated that RCAD pediatric urinary proteome is different from the proteome of patients with *Pkd1-2* and *Nphs1-2-4-9* mutations, and also from the urinary proteome of CKD patients.

Future studies will further evaluate the performance of the RCAD panel in additional pediatric cohorts of disorders more closely related to RCAD such as autosomal recessive polycystic kidney disease (ARPKD), medullary cystic kidney disease (MCKD), autosomal dominant tubulointerstitial kidney disease (ADTKD) or diabetic patients. Moreover, and along with the evaluation of the performance of this classifier to predict the progression of RCAD, follow-up clinical data of the patients described in this study will be addressed.

Methods

Patient recruitment

RCAD urine samples were collected from three different clinical centers: Children's Hospital, CHU-Toulouse (France, $n=33$), University Children Hospital, Heidelberg (Germany; $n=11$), Clinical Research Center for Rare Diseases Aldo e Cele Daccò, Ranica (Italy, $n=2$). RCAD patients' average age was 8.4 years. Baseline characteristics of the RCAD patients used in this study are summarized in the **Table 1** and extended in **Supplementary Table 1**. After collection, urine samples were stored at -20°C and shipped frozen for subsequent proteome analysis. In addition, all non-RCAD samples were retrieved from the Human Urinary Proteome database²⁵⁻²⁷. This group of samples included healthy patients ($n=42$), and patients suffering from kidney diseases and carrying different genetic mutations, such as: *PKD1* ($n=46$); *PKD2* ($n=9$), *NPHS1* ($n=2$), *NPHS2* ($n=35$), *WT1* ($n=6$), *ADCK4* ($n=3$). Additionally, a group of samples from a pediatric cohort with chronic kidney disease was tested ($n=85$). This wider group of negative controls (non-RCAD) presented an average age of 16.5 years.

This study was designed and performed in compliance with all the regulations regarding the protection of subjects participating in medical research. Collection, storage and analysis of urine samples have been approved by the local ethics committees of the three participating centers (Comité de Protection des Personnes Sud-Ouest et Outre Mer III, Ethikkommission der Medizinischen Fakultät Heidelberg, and Comitato Etico di Bergamo, respectively). All participating subjects or legal guardians of patients provided written informed consent to the use of urine samples. This study was performed in accordance with the Helsinki Declaration.

Urine sample preparation and CE-MS analysis

Urine sample collection and CE-MS analysis were performed as reported previously^{44,45}. Briefly, immediately before preparation, urine samples aliquots stored at -20°C were thawed and 700 μl were diluted with the same volume of 2 M urea, 10 mM NH_4OH comprising 0.02 % SDS. Then, samples were filtered via a Centrinstat 20-kDa cut-off centrifugal filter device (Sartorius, Goettingen, Germany) at 2,600 g for one hour at 4°C in order to remove high molecular weight compounds. The obtained filtrate was desalted using a PD-10 column (GE Healthcare, Sweden) equilibrated in 0.01% aqueous NH_4OH to eliminate urea, electrolytes and salts. Finally, samples were lyophilized and stored at 4°C prior to CE-MS analysis. The samples were re-suspended in 10 μL of HPLC-grade H_2O shortly before CE-MS analysis, as

described⁴⁵. CE-MS analyses were accomplished using a P/ACE MDQ capillary electrophoresis system (Beckman Coulter, Fullerton, USA) online coupled to a MicroTOF MS (BrukerDaltonic, Bremen, Germany)⁴⁵. The electro-ionization sprayer (Agilent Technologies) was grounded, and the ion spray interface potential was defined between -4 and -4.5 kV. Spectra were accumulated every 3s along with over a range of m/z to 350-3000. Detailed information on accuracy, precision, selectivity, sensitivity, reproducibility and stability of the CE-MS method have been described previously⁴⁵.

CE-MS data processing

A proprietary software (MosaiquesVisu) was used to deconvolute mass spectral ion peaks demonstrating identical molecules at different charge states into single masses⁴⁶. The achieved peak list allows the characterization of each polypeptide according to its CE-migration time (in minutes), molecular mass (in Daltons), and ion signal intensity. Subsequently, normalization of the amplitude of the urinary peptides was conducted on twenty-nine 'housekeeping' peptides (peptides varied slightly between samples, generally present in at least 90% of all urine), similarly to previous studies⁴⁷. All detected peptides were deposited, clustered, matched and annotated in a Microsoft SQL database²⁵⁻²⁷, allowing further statistical analysis.

Peptide sequencing

Candidate peptides for the RCAD-classifier were identified and sequenced by the use of tandem mass spectrometry (MS/MS) analysis and searched against human entries in the UniProt database, as previously described previously^{48,49}. Briefly, to acquire the sequence information, urine samples were separated on a Dionex Ultimate 3000 RSLC nano flow system (Dionex, Camberly, UK) or a Beckman CE systems (PACE MDQ) coupled to an Orbitrap Velos MS instrument (Thermo Fisher Scientific)^{48,49}. Thereafter, data files were examined against the UniProt human non-redundant database using Proteome Discoverer 1.2 (Thermo) and the SEQUEST search engine. No fixed modifications were selected, hydroxylation of proline and lysine and oxidation of methionine were enabled as optional modification, nor enzyme specificity were specified in the settings⁴⁸. The matching of the peptide sequence obtained by MS/MS analysis to the CE-MS peaks were based on molecular mass [Da] and theoretical migration time, calculated using the number of basic amino acids⁵⁰. Peptides were accepted only if they had a mass deviation below ± 5 ppm and < 50 mDa for the fragment ions.

Peptide identification and statistical analysis

For the identification of potential RCAD-related urinary peptide biomarkers, a comparison between RCAD cases and healthy controls was performed. Only peptides that were detected in at least 70% (frequency threshold) of the samples in at least one of the two groups were further considered for statistical analysis. Adjusted P-values were calculated based on the comparison between RCAD cases and healthy controls, using the Wilcoxon rank-sum test followed by adjustment for multiple testing with the false-discovery rate method presented by Benjamini and Hochberg²⁸. Only peptides with a P-value less than 0.05 were considered as statistically significant. The area under the curve (AUC), and sensitivity and specificity values of the receiver operating characteristic (ROC) curves of the classifier were determined using R-based statistical software (version 3.3.3) and confirmed using MedCalc version 12.7.5.0 (MedCalc Software bvba, Ostend, Belgium). Graphs related to ROC curves and Box-and-Whisker plot were generated with R-based statistic software (packages ggplot2, plotly).

Data availability

The datasets generated during and/or analyzed during the current study are available from the corresponding author on reasonable request.

References

- 1 Bingham C, B. M., Ellard S, Allen LI, Lipkin GW, Hoff WG, Woolf AS, Rizzoni G, Novelli G, Nicholls AJ, Hattersley AT. Mutations in the hepatocyte nuclear factor-1beta gene are associated with familial hypoplastic glomerulocystic kidney disease. *Am J Hum Genet* **Jan;68(1):219-24**, (2001).
- 2 Horikawa, Y. *et al.* Mutation in hepatocyte nuclear factor-1 beta gene (TCF2) associated with MODY. *Nature Genetics* **17**, 384-385, (1997).
- 3 Clissold, R. L., Hamilton, A. J., Hattersley, A. T., Ellard, S. & Bingham, C. HNF1B-associated renal and extra-renal disease-an expanding clinical spectrum. *Nature Reviews Nephrology* **11**, 102-112, (2015).
- 4 Haumaitre, C. *et al.* Severe pancreas hypoplasia and multicystic renal dysplasia in two human fetuses carrying novel HNF1 beta/MODY5 mutations. *Human Molecular Genetics* **15**, 2363-2375, (2006).
- 5 Kato, N. & Motoyama, T. Expression of Hepatocyte Nuclear Factor-1 beta in Human Urogenital Tract During the Embryonic Stage. *Analytical and Quantitative Cytology and Histology* **31**, 34-40, (2009).
- 6 Body-Bechou, D. *et al.* TCF2/HNF-1beta mutations: 3 cases of fetal severe pancreatic agenesis or hypoplasia and multicystic renal dysplasia. *Prenatal Diagnosis* **34**, 90-93, (2014).
- 7 Duval, H. *et al.* Fetal anomalies associated with HNF1B mutations: report of 20 autopsy cases. *Prenatal Diagnosis* **36**, 744-751, (2016).
- 8 Haldorsen, I. S. *et al.* Lack of pancreatic body and tail in HNF1B mutation carriers. *Diabetic Medicine* **25**, 782-787, (2008).
- 9 Bingham C, H. A. Renal cysts and diabetes syndrome resulting from mutations in hepatocyte nuclear factor-1beta. *Nephrol Dial Transplant.* **Nov;19(11):2703-8.**, (2004).
- 10 Stenson, P. D. *et al.* Human gene mutation database (HGMD (R)): 2003 update. *Human Mutation* **21**, 577-581, (2003).
- 11 Nakayama, M. *et al.* HNF1B alterations associated with congenital anomalies of the kidney and urinary tract. *Pediatric Nephrology* **25**, 1073-1079, (2010).
- 12 Verbitsky, M. *et al.* Genomic imbalances in pediatric patients with chronic kidney disease. *Journal of Clinical Investigation* **125**, 2171-2178, (2015).

- 13 Dubois-Laforgue D, C. E., Saint-Martin C, Coste J, Bellanné-Chantelot C, Timsit J. Diabetes, Associated Clinical Spectrum, Long-term Prognosis, and Genotype/Phenotype Correlations in 201 Adult Patients With Hepatocyte Nuclear Factor 1B (HNF1B) Molecular Defects. *Diabetes Care*. **Nov;40(11):1436-1443**, (2017).
- 14 Musetti C, Q. M., Mellone S, Pagani A, Fusco I, Monzani A, Giordano M, Stratta P. Chronic renal failure of unknown origin is caused by HNF1B mutations in 9% of adult patients: a single centre cohort analysis. *Nephrology (Carlton)*. **Apr;19(4):202-9**, (2014).
- 15 Adalat, S. *et al.* HNF1B Mutations Associate with Hypomagnesemia and Renal Magnesium Wasting. *Journal of the American Society of Nephrology* **20**, 1123-1131, (2009).
- 16 Heidet, L. *et al.* Spectrum of HNF1B Mutations in a Large Cohort of Patients Who Harbor Renal Diseases. *Clinical Journal of the American Society of Nephrology* **5**, 1079-1090, (2010).
- 17 Verhave JC, B. A., Wetzels JF, Nijenhuis T2. Hepatocyte Nuclear Factor 1 β -Associated Kidney Disease: More than Renal Cysts and Diabetes. *J Am Soc Nephrol*. **Feb;27(2):345-53**, (2016).
- 18 Bingham C, E. S., van't Hoff WG, Simmonds HA, Marinaki AM, Badman MK, Winocour PH, Stride A, Lockwood CR, Nicholls AJ, Owen KR, Spyer G, Pearson ER, Hattersley AT. Atypical familial juvenile hyperuricemic nephropathy associated with a hepatocyte nuclear factor-1beta gene mutation. *Kidney Int*. **May;63(5):1645-51**., (2003).
- 19 Decramer, S. *et al.* Anomalies of the TCF2 gene are the main cause of fetal bilateral hyperechogenic kidneys. *Journal of the American Society of Nephrology* **18**, 923-933, (2007).
- 20 Edghill, E. L., Bingham, C., Ellard, S. & Hattersley, A. T. Mutations in hepatocyte nuclear factor-1 beta and their related phenotypes. *Journal of Medical Genetics* **43**, 84-90, (2006).
- 21 Drube, J. *et al.* Urinary Proteome Analysis to Exclude Severe Vesicoureteral Reflux. *Pediatrics* **129**, E356-E363, (2012).
- 22 Good, D. M. *et al.* Naturally Occurring Human Urinary Peptides for Use in Diagnosis of Chronic Kidney Disease. *Molecular & Cellular Proteomics* **9**, 2424-2437, (2010).

- 23 Kistler, A. D. *et al.* Urinary Proteomic Biomarkers for Diagnosis and Risk Stratification of Autosomal Dominant Polycystic Kidney Disease: A Multicentric Study. *Plos One* **8**, (2013).
- 24 Klein, J. *et al.* Fetal Urinary Peptides to Predict Postnatal Outcome of Renal Disease in Fetuses with Posterior Urethral Valves (PUV). *Science Translational Medicine* **5**, (2013).
- 25 Coon, J. J. *et al.* CE-MS analysis of the human urinary proteome for biomarker discovery and disease diagnostics. *Proteomics Clinical Applications* **2**, 964-973, (2008).
- 26 Siwy, J., Mullen, W., Golovko, I., Franke, J. & Zuerbig, P. Human urinary peptide database for multiple disease biomarker discovery. *Proteomics Clinical Applications* **5**, 367-374, (2011).
- 27 Stalmach, A., Albalat, A., Mullen, W. & Mischak, H. Recent advances in capillary electrophoresis coupled to mass spectrometry for clinical proteomic applications. *Electrophoresis* **34**, 1452-1464, (2013).
- 28 Benjamini, Y. & Hochberg, Y. CONTROLLING THE FALSE DISCOVERY RATE - A PRACTICAL AND POWERFUL APPROACH TO MULTIPLE TESTING. *Journal of the Royal Statistical Society Series B-Methodological* **57**, 289-300, (1995).
- 29 Mischak, H. *et al.* Clinical proteomics: A need to define the field and to begin to set adequate standards. *Proteomics Clinical Applications* **1**, 148-156, (2007).
- 30 Mischak, H., Julian, B. A. & Novak, J. High-resolution proteome/peptidome analysis of peptides and low-molecular-weight proteins in urine. *Proteomics Clinical Applications* **1**, 792-804, (2007).
- 31 Kistler, A. D. *et al.* Identification of a unique urinary biomarker profile in patients with autosomal dominant polycystic kidney disease. *Kidney International* **76**, 89-96, (2009).
- 32 Norman, J. Fibrosis and progression of Autosomal Dominant Polycystic Kidney Disease (ADPKD). *Biochimica Et Biophysica Acta-Molecular Basis of Disease* **1812**, 1327-1336, (2011).
- 33 Bensalem, N. *et al.* Down-regulation of the anti-inflammatory protein annexin A1 in cystic fibrosis knock-out mice and patients. *Molecular & Cellular Proteomics* **4**, 1591-1601, (2005).
- 34 Ka, S. M. *et al.* Urine Annexin A1 as an Index for Glomerular Injury in Patients. *Disease Markers*, (2014).

- 35 Berle M, K. A., Garberg H, Aarhus M, Haaland OA, Wester K, Ulvik RJ, Helland C, Berven F. Quantitative proteomics comparison of arachnoid cyst fluid and cerebrospinal fluid collected perioperatively from arachnoid cyst patients. *Fluids Barriers CNS*. **10(1):17**, (2013).
- 36 Senkel, S., Lucas, B., Klein-Hitpass, L. & Ryffel, G. U. Identification of target genes of the transcription factor HNF1 beta and HNF1 alpha in a human embryonic kidney cell line. *Biochimica Et Biophysica Acta-Gene Structure and Expression* **1731**, 179-190, (2005).
- 37 Aboudehen, K. *et al.* Hepatocyte Nuclear Factor-1 beta Regulates Urinary Concentration and Response to Hypertonicity. *Journal of the American Society of Nephrology* **28**, 2887-2900, (2017).
- 38 Magalhães P, P. M., Markoska K, Banasik M, Klinger M, Švec-Billá D *et al.* Association of kidney fibrosis with urinary peptides: a path towards non-invasive liquid biopsies? *Sci Rep*. **20 5;7(1):16915**, (2017).
- 39 Gresh, L. *et al.* A transcriptional network in polycystic kidney disease. *Embo Journal* **23**, 1657-1668, (2004).
- 40 Bergmann, C. ARPKD and early manifestations of ADPKD: the original polycystic kidney disease and phenocopies. *Pediatric Nephrology* **30**, 15-30, (2015).
- 41 Faguer, S. *et al.* The HNF1B score is a simple tool to select patients for HNF1B gene analysis. *Kidney International* **86**, 1007-1015, (2014).
- 42 Paces-Fessy, M., Fabre, M., Lesaulnier, C. & Cereghini, S. Hnf1b and Pax2 cooperate to control different pathways in kidney and ureter morphogenesis. *Human Molecular Genetics* **21**, 3143-3155, (2012).
- 43 Dell, K. M. The Spectrum of Polycystic Kidney Disease in Children. *Advances in Chronic Kidney Disease* **18**, 339-347, (2011).
- 44 Metzger, J. *et al.* Urine proteomic analysis differentiates cholangiocarcinoma from primary sclerosing cholangitis and other benign biliary disorders. *Gut* **62**, 122-130, (2013).
- 45 Mischak, H., Vlahou, A. & Ioannidis, J. P. A. Technical aspects and inter-laboratory variability in native peptide profiling: The CE-MS experience. *Clinical Biochemistry* **46**, 432-443, (2013).
- 46 Kaiser T, H. A., Kielstein JT. Conference: 16th International Symposium on Microscale Separation and Analysis Location: San Diego, California. *Journal of Chromatography* **1013**, 157-171, (2003).

- 47 Jantos-Siwy, J. *et al.* Quantitative Urinary Proteome Analysis for Biomarker Evaluation in Chronic Kidney Disease. *Journal of Proteome Research* **8**, 268-281, (2009).
- 48 Klein, J., Papadopoulos, T., Mischak, H. & Mullen, W. Comparison of CE-MS/MS and LC-MS/MS sequencing demonstrates significant complementarity in natural peptide identification in human urine. *Electrophoresis* **35**, 1060-1064, (2014).
- 49 Magalhães, P. *et al.* Comparison of Urine and Plasma Peptidome Indicates Selectivity in Renal Peptide Handling. *Proteomics. Clinical applications*, e1700163-e1700163, (2018).
- 50 Zurbig, P. *et al.* Biomarker discovery by CE-MS enables sequence analysis via MS/MS with platform-independent separation. *Electrophoresis* **27**, 2111-2125, (2006).

Acknowledgments

The research presented in this manuscript was supported by the European Union's Horizon 2020 Research and Innovation Programme under the Marie Skłodowska-Curie grant agreement No. 642937 (RENALTRACT; MSCA-ITN-2014-642937). P.R., P.M. and L.G. were recipients of PhD student fellowships from ITN RENALTRACT MSCA-ITN-2014-642937. Furthermore, J.D. and L.P. were supported by the NEOCYST consortium, which is funded by the German Federal Ministry of Research and Education (BMBF, grant 01GM1515).

Author Contributions

P.R. and P.M. wrote the main manuscript text, performed CE-MS analysis, data analysis and interpretation, and prepared figures and tables. M.K. contributed to data interpretation, statistical analysis and preparation of figures and tables. M.P., I.B. and L.G. contributed to data analysis and results interpretation. E.D., M.R.C., G.R., L.P. and J.D. contributed to clinical data and urine sample collection, and supported results interpretation. S.D., F.S. and J.P.S. contributed to clinical data and urine sample collection as well as for the writing of the manuscript along with supervising the study. H.M., M.U., S.C. and P.Z. supervised experiments and results interpretation and provided critical reading and editing of the manuscript and supervising the study. All authors reviewed and approved the manuscript.

Additional Information

Competing financial interests

H.M. is the founder and co-owner of Mosaiques Diagnostic GmbH, who developed the CE-MS technology for clinical application. P.M., M.K., M.P., I.B., and P.Z. are employees of Mosaiques Diagnostic GmbH.

Figure 1

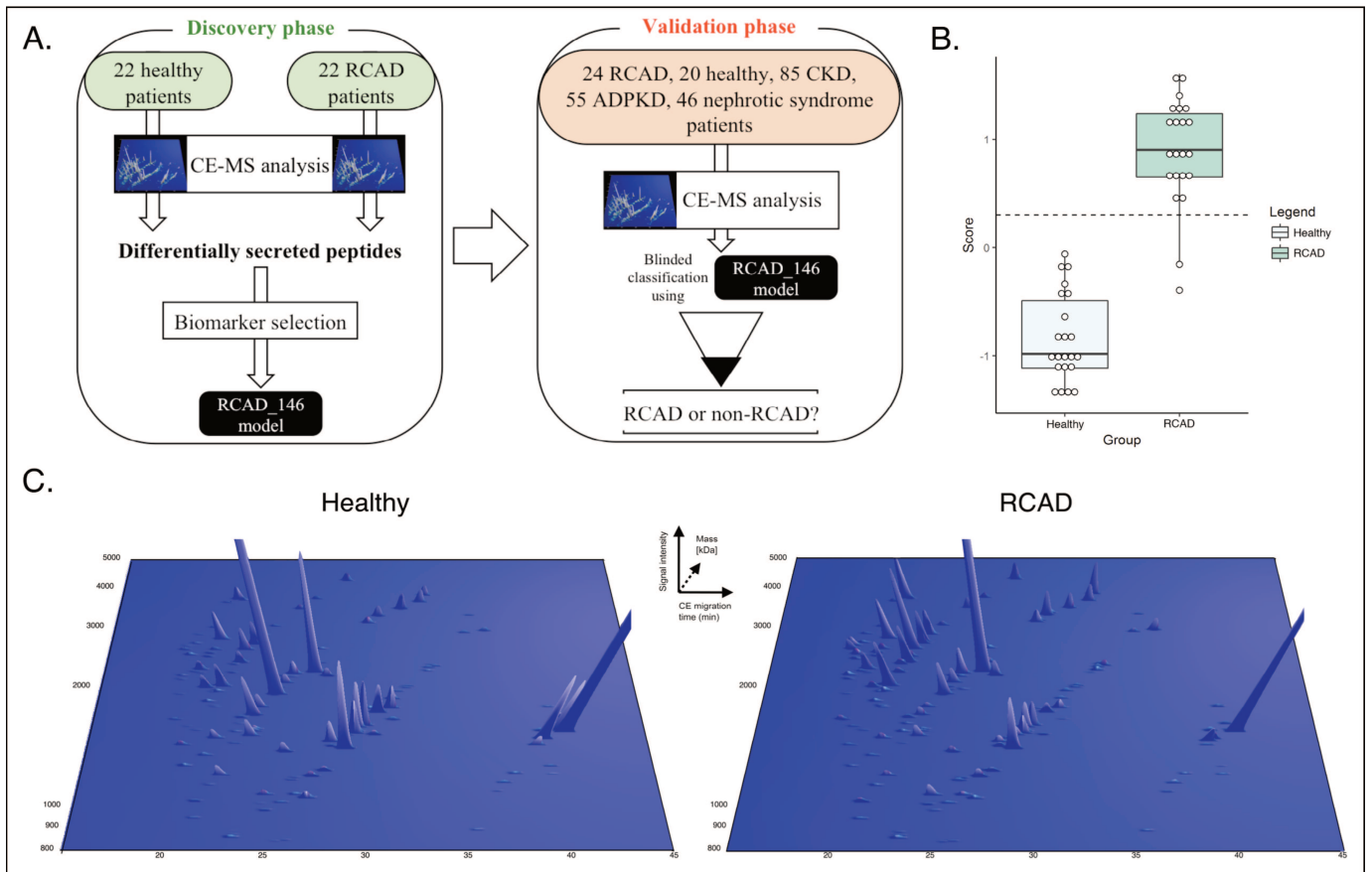


Figure 2

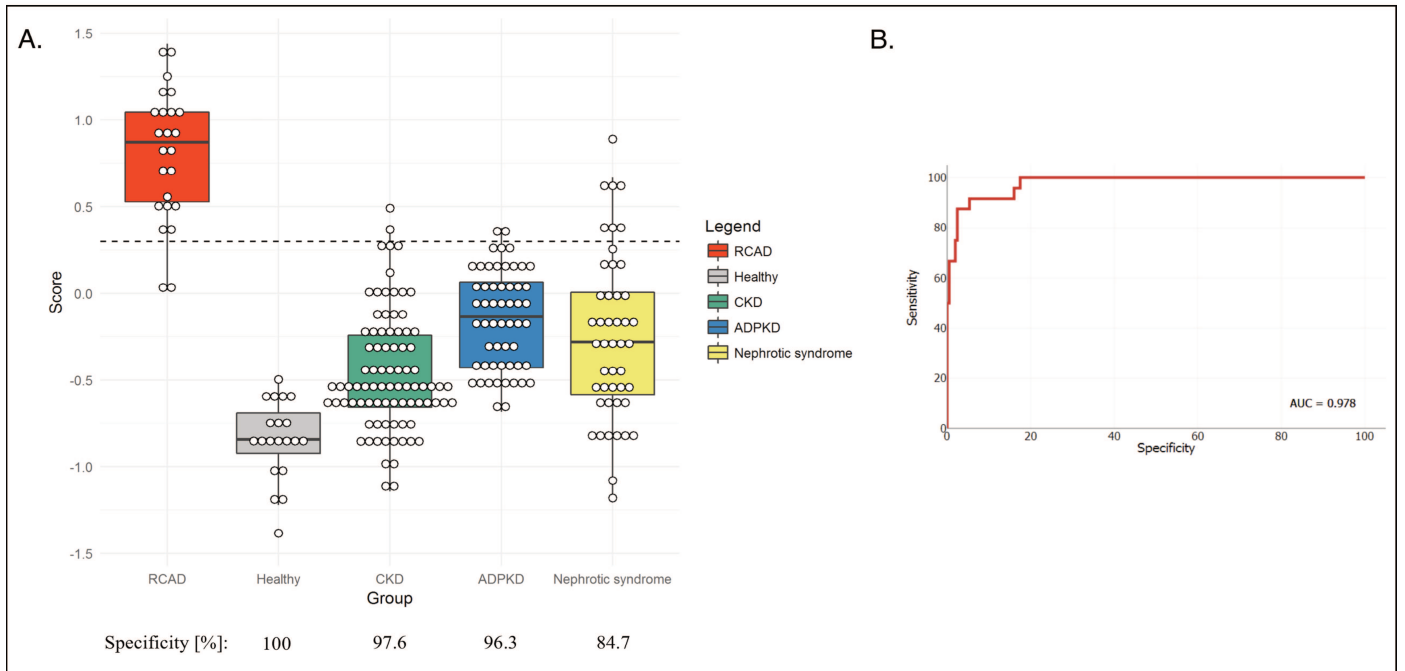


Figure 3

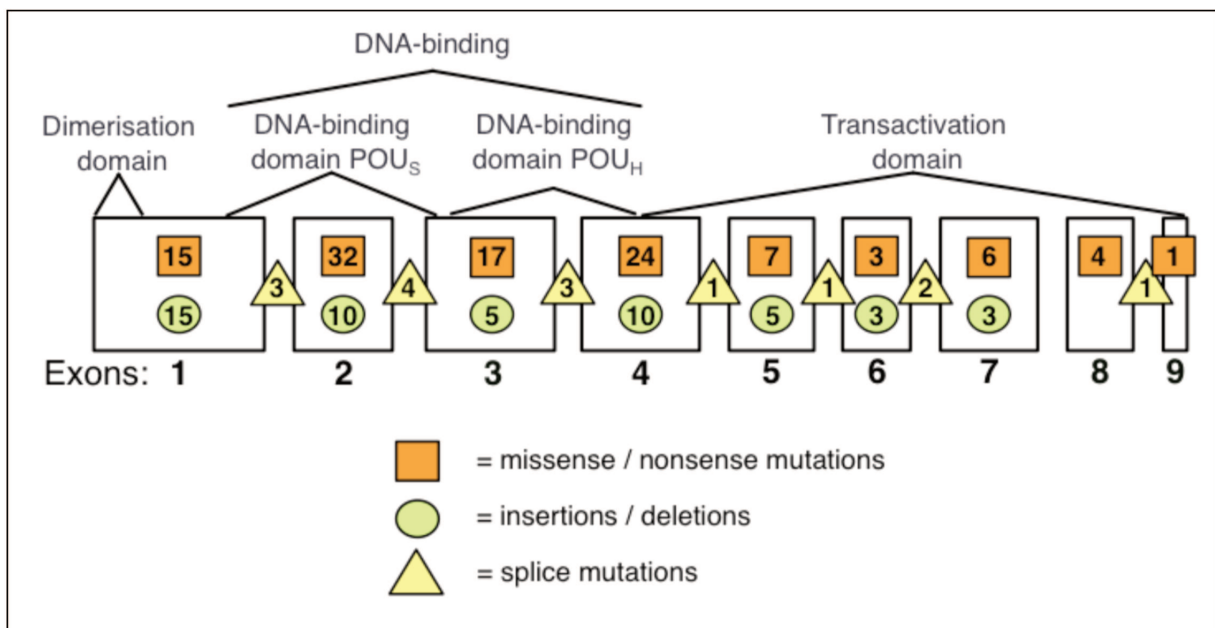


Figure Legends

Figure 1. Study design and CE-MS analysis in urine of patients with RCAD. **A.** This study was performed in two phases: a discovery phase, where the urinary proteome of 44 pediatric subjects (22 healthy, 22 RCAD) was analyzed leading to the identification of 146 sequenced urinary peptides that were further modelled in a SVM-classifier, termed RCAD146. In the next step, the validation phase, we evaluated the discriminatory ability of the panel RCAD146 panel in a new cohort of RCAD patients ($n=24$) as well as individuals with CKD or patients carrying monogenic mutations associated with different renal diseases. **B.** Representation of the 146 urinary peptides significantly modified between RCAD and healthy controls. Normalized molecular mass (kDa) was plotted against normalized capillary electrophoresis (CE)-migration time (min). Mean signal intensity was given in 3-dimensional depiction. **C.** Box-and-Whisker plot of cross-validation scores of the RCAD146 model from the analysis of the discovery cohort along with the definition of the cut-off 0.3 (dashed line).

Figure 2. Independent validation of urinary peptide classifier RCAD146 in a separate RCAD patient population together with healthy controls and patients suffering from other kidney diseases. **A.** Box-and-Whisker plot for the classification of all patient cohorts (RCAD subjects, non-RCAD groups) of the validation set according to the RCAD146 scores. **B.** ROC curve for the RCAD146 classifier based on all samples used in the validation cohort.

Figure 3. HNF1B gene transcript with known mutations. The mutations shown in the graph are registered in the Human Gene Mutation Database (Stenson PD 2003, accessed on 20 February 2018). They are grouped by three mutation type within the nine exons and splice sites of the transcript: missense/nonsense mutations, insertions/deletions, and splice mutations. The numbered white boxes correspond to the exons, and the different functional domains are shown above the gene transcript. The colored boxes correspond to the number of registered mutations up to date. The whole gene deletions are not depicted. Abbreviations: POU_S, POU specific domain; POU_H, POU homeodomain.

Table 1. Clinical characteristics of children with RCAD syndrome.

All	
<i>n</i>	46
Male, <i>n</i> (%)	37 (80.4)
Female, <i>n</i> (%)	9 (19.6)
Age, years	8.4 ± 5.7
Renal phenotypes	
kidney cysts, <i>n</i> (%)	34 (73.9)
bilateral hyperechoic kidneys, <i>n</i> (%)	24 (52.1)
hypo/dysplastic kidneys, <i>n</i> (%)	21 (45.6)
single kidneys, <i>n</i> (%)	1 (2.1)
vesicoureteral reflux, <i>n</i> (%)	2 (4.3)
horseshoe kidneys, <i>n</i> (%)	1 (2.1)
renal agenesis, <i>n</i> (%)	2 (4.3)
chronic renal failure, <i>n</i> (%)	1 (2.1)
Extrarenal phenotypes	
diabetes, <i>n</i> (%)	3 (6.5)
pancreatic hypoplasia, <i>n</i> (%)	3 (6.5)
uterine malformations, <i>n</i> (%)	2 (4.3)
unilateral ectopic testis, <i>n</i> (%)	2 (4.3)
hyperechoic liver, <i>n</i> (%)	1 (2.1)
cholestasis, <i>n</i> (%)	1 (2.1)
megabladder, <i>n</i> (%)	1 (2.1)
hyperuricemia, <i>n</i> (%)	5 (10.8)

Table 2. Baseline characteristics of the subjects used in the A. discovery set and B. validation set.

A. Discovery Set					
Group of subjects	Mutation	Sample size (<i>n</i>)	Gender		Age (years)
			Male	Female	
RCAD	HNF1B	22	17	5	9.4 ± 6.3
Healthy	----	22	17	5	9.3 ± 4.1
B. Validation Set					
Group of subjects	Mutation	Sample size (<i>n</i>)	Gender		Age (years)
			Male	Female	
RCAD	HNF1B	24	20	4	7.5 ± 5.1
Healthy	----	20	15	5	9.3 ± 2.4
CKD	----	85	40	45	11.1 ± 5.7
ADPKD	PKD1	46	20	26	34.3 ± 6
	PKD2	9	3	6	40.2 ± 3.3
Nephrotic Syndrome	NPHS1	2	2	-	6.5 ± 8.8
	NPHS2	35	14	21	10.5 ± 6.4
	NPSH4 (WT1)	6	1	5	13.3 ± 3.7
	NPHS9 (ADCK4)	3	1	2	13.6 ± 3.1

Table 3. Proteins origin of the 146 differentially excreted urinary peptides obtained by the comparison between RCAD patients and healthy controls.

Protein name	Gene symbol	N° of protein fragments	P-value (adjusted)	Mean fold change
Mucin-3a	MUC3A	1	1.10E-05	-56.9
Gelsolin	GSN	1	1.66E-05	105.4
Microfibrillar-associated protein 5	MFAP5	1	4.32E-05	308.3
Interleukin-1 receptor-associated	IL-1R	1	1.27E-04	43.2
Ig kappa chain C region	IGKC	1	1.88E-04	2.64
Collagen alpha-6 (IV) chain	COL4A6	1	5.61E-04	3
Collagen alpha-3 (V) chain	COL5A3	1	7.70E-04	-6.25
Collagen alpha-4 (IV) chain	COL4A4	1	1.46E-03	4
Collagen alpha-1 (XXVI) chain	COL26A1	1	1.72E-03	-11.2
Collagen alpha-1 (XVII) chain	COL17A1	1	3.14E-03	-2.03
Collagen alpha-1 (XI) chain	COL11A1	1	4.21E-03	1.19
Protein unc-119 homolog A	UNC119	1	4.95E-03	-7.05
Ephrin-A1	EFNA1	1	5.46E-03	5.55
Fibrinogen alpha chain	FGA	2	5.87E-03	4.79 (± 0.48)
Cystatin-A	CSTA	1	5.88E-03	-3.67
Annexin A1	ANXA1	1	6.44E-03	-2.68
Retinol binding protein 4	RBP4	1	7.78E-03	3.11
Mucin-1 subunit alpha	MUC1	1	9.90E-03	2.4
Beta-2-microglobulin	B2M	1	1.04E-02	-1.17
Sarcolumenin	SRL	1	1.05E-02	-2.21
Ig lambda-2 chain C regions	IGLC2	1	1.45E-02	-1.92
Osteopontin	OPN	2	1.56E-02	3.85 (± 2.21)
Collagen alpha-2 (V) chain	COL5A2	3	1.67E-02	0.22 (± 2.9)
Kininogen-1	KNG1	1	1.69E-02	1.53
Short transient receptor potential channel 4-associated protein	TRPC4AP	1	1.74E-02	1.98
Immunoglobulin kappa variable 4-1	IGKV4-1	1	1.88E-02	56.7
Collagen alpha-1 (XXVII) chain	COL27A1	1	2.04E-02	-5.66
Collagen alpha-5 (IV) chain	COL4A5	1	2.88E-02	2.86
Actin, cytoplasmic 1	ACTB	1	2.88E-02	3.3
Collagen alpha-1 (II) chain	COL2A1	7	3.05E-02	4.45 (± 5.37)
Protein scribble homolog	SCRIB	1	3.51E-02	3.15
Collagen alpha-1 (XVI) chain	COL16A1	1	3.53E-02	2.24
Collagen alpha-1 (VIII) chain	COL8A1	1	3.61E-02	1.29
Hemoglobin subunit delta	HBD	1	3.65E-02	-3.38
Neurosecretory protein VGF	VGF	1	3.80E-02	3.45
Collagen alpha-1 (III) chain	COL3A1	21	3.89E-02	3.71 (± 4.37)
Collagen alpha-1 (V) chain	COL5A1	2	4.36E-02	180.32 (± 253)
Uromodulin	UMOD	4	4.82E-02	-5.7 (± 2.33)
Collagen alpha-2 (I) chain	COL1A2	20	4.84E-02	3.28 (± 6.86)
Serum amyloid A protein	SAA1	2	4.87E-02	-0.81 (± 2.95)
Collagen alpha-1 (I) chain	COL1A1	52	4.97E-02	1.6 (± 3.44)

*Information described are the number of significant protein fragments for each protein origin, the highest observed *P-value* as well as the estimated mean fold change (± standard deviation).

CONCLUSION AND DISCUSSION

Conclusions and discussion

As shown in the introduction, HNF1B has a multiorgan role during mammalian development and heterozygous mutations in this gene are at the basis of a rare human syndrome called Renal Cysts and Diabetes (RCAD). The understanding of the molecular misregulation of HNF1B in patients carrying these mutations is essential for an early diagnosis and a potential cure.

One of the main limits to study the RCAD syndrome was the lacking of a mouse model, as heterozygous mutations in *Hnf1b* did not present phenotype. For the first time the lab developed a mouse model able to mimic different features of RCAD syndrome allowing to perform functional and molecular examinations. In sharp contrast with previous studies we introduced a human mutation, which was able to overcome the mouse strengthness in resist to diseases prompted by haploinsufficiency. Mirroring the human disease, heterozygous *Hnf1b*^{Sp2/+} mutant mice mainly exhibited bilateral renal cysts (originated primarily from proximal tubules (PT) and intermediate nephron segments and glomeruli), renal hydronephrosis and genital tract anomalies. Moreover, a partial urinary concentration defect was observed, thus further validating this model as a valuable instrument to investigate the RCAD disease.

Interestingly, the canonical cystic diseases genes (*Pkh1*, *Pdk2*, *Bicc1*) and branching genes (*Pax2*, *Wnt9b*) were slightly or not affected, and mRNA-seq analysis at different embryonic stages (E14.5, E15.5, E17.5 and P1) revealed a de-regulation of more than 300 hundred genes. These results demonstrate that i) cysts and morphological anomalies do not derived from the misregulation of classical cystic/branching genes and that ii) HNF1B de-regulation impairs several other genes expressed primarily in proximal tubules and mostly involved in transport, and lipid and organic acid metabolic processes.

In this context we strongly believe that the severity of de-regulated gene network together with the other causes characterizing RCAD features both in human and mouse is the failure to reach a minimal threshold value of HNF1B protein during development and potentially postnatally. The etiologies of the strong intrafamilial variability, found also in our RCAD model littermates, have been previously attributed to stochastic variation in temporal gene expression as well as environmental factors. We do not distance from this assumption, but we insisted on the fact that the only reason at the basis of the RCAD pathology is a failure to reach a minimum level of HNF1B protein, which can be also organ-specific.

Related to this, it is tempting to speculate that a significant number of patients with *HNF1B* heterozygous mutations do not show pathological RCAD features because, somehow, HNF1B minimal level for correct development and maintenance was achieved during their life (at least in the most of organs where HNF1B accomplish its functions). In this perspective, a dominant negative role of HNF1B-truncated mutant proteins at the basis of RCAD syndrome is unlikely.

If our theory is correct, the modulation of HNF1B protein during development may be at the basis of a treatment to ensure a proper development of kidney, pancreas, liver and genital tract in *HNF1B* heterozygous patients.

Taking into consideration that miRNAs regulation during kidney development, homeostasis and disease is dependent on transcription factors, the understanding of microRNAs involved in RCAD syndrome and controlled by HNF1B is a priority for molecular biology and medicine. In fact, microRNAs may be a tool to modulate transcription factor expression as HNF1B or at least to early predict diseases as RCAD (Christopher AF et al., 2016; Metzinger-Le Meuth V et al., 2018). We demonstrated that HNF1B and the microRNAs -802 and -194-2 and very likely miR-192 are linked by an autoregulatory-loop, and that HNF1B transactivates in a dose response mode an upstream enhancer likely controlling miR-30a expression. As these microRNAs are de-regulated in the RCAD mouse model, it is conceivable that they have an important role in RCAD pathogenesis but further studies on their other potential targets are required. Moreover, to add further value to this discovery, analyses in human kidney tissues may be done to show the conservation of this regulation.

Another analysis reinforces the value of the RCAD mouse model as consistent with the human disease: the urinary proteomic study. The first results obtained comparing wt and *Hnf1b*^{Sp2/+} mutant mice urinary proteome revealed a particular signature of the RCAD urinary proteome consisting mainly of UP-excreted collagen fragments, and DOWN-excreted uromodulin (UMOD) and epidermal growth factor (EGF) peptides. The results were coherent with an excessive extracellular matrix (ECM) turnover. Interestingly, a subsequent analysis in a pediatric cohort of RCAD patients revealed a similar signature with a majority of peptides collagen type I or type III fragments enriched in the urine of RCAD patients and a down-excretion of uromodulin fragments, together with other de-regulated peptides. Following studies in human, we hypothesize that this active extracellular matrix (ECM) remodeling may

be also related to cyst expansion/presence, which affects modifications in the ECM (Norman J, 2011). In addition, in the pediatric RCAD urinary proteome we observed altered of several peptides with calcium binding or calcium regulating properties as sarcalumenin (SRL), annexin A1 (ANXA1), gelsolin (GSN), short transient receptor potential channel 4-associated protein (TRPC4AP) and osteopontin (SPP1).

Furthermore, this proteomic analysis highlighted that RCAD syndrome has a unique urinary signature, which is different from the urinary proteome of patients from different groups of controls as Autosomal Dominant Polycystic Kidney Disease (ADPKD), nephrotic syndrome and chronic kidney disease CKD patients. This discovery is attractive as differentiates the biological events leading to the RCAD syndrome from other cystic diseases and conditions and open the possibilities to an early tool of diagnosis as well as a better understanding of the molecular basis underlying HNF1B regulation and so the RCAD syndrome. Future studies will further evaluate the performance of the RCAD panel in additional pediatric cohorts of disorders more closely related to RCAD such as autosomal recessive polycystic kidney disease (ARPKD), medullary cystic kidney disease (MCKD), autosomal dominant tubulointerstitial kidney disease (ADTKD) or diabetic patients. Moreover, and along with the evaluation of the performance of this classifier to predict the progression of RCAD, follow-up clinical data of the patients described in this study should be addressed.

The combined analysis of a unique RCAD mouse model together with urinary proteomic approaches provided new interesting means to comprehend the disease as well as revealed new insights on this disorder mainly related to the kidney phenotype, the urinary proteome and the post-transcriptional regulation of HNF1B transcriptional factor.

BIBLIOGRAPHY

BIBLIOGRAPHY

- (Aboudehen K et al., 2015) Aboudehen K, Kim MS, Mitsche M, Garland K, Anderson N, Noureddine L, Pontoglio M, Patel V, Xie Y, DeBose-Boyd R, Igarashi P. Transcription Factor Hepatocyte Nuclear Factor-1 β Regulates Renal Cholesterol Metabolism. *J Am Soc Nephrol*. 2016 Aug;27(8):2408-21. doi: 10.1681/ASN.2015060607. Epub 2015 Dec 28.
- (Aboudehen K et al., 2017) Aboudehen K, Noureddine L, Cobo-Stark P, Avdulov S, Farahani S, Gearhart MD, Bichet DG, Pontoglio M, Patel V, Igarashi P. Hepatocyte Nuclear Factor-1 β Regulates Urinary Concentration and Response to Hypertonicity. *J Am Soc Nephrol*. 2017 Oct;28(10):2887-2900. doi: 10.1681/ASN.2016101095. Epub 2017 May 15.
- (Adalat S et al., 2009) Adalat S, Woolf AS, Johnstone KA, Wirsing A, Harries LW, Long DA, Hennekam RC, Ledermann SE, Rees L, van't Hoff W, Marks SD, Trompeter RS, Tullus K, Winyard PJ, Cansick J, Mushtaq I, Dhillon HK, Bingham C, Edghill EL, Shroff R, Stanescu H, Ryffel GU, Ellard S, Bockenbauer D. HNF1B mutations associate with hypomagnesemia and renal magnesium wasting. *J Am Soc Nephrol*. 2009 May;20(5):1123-31. doi: 10.1681/ASN.2008060633. Epub 2009 Apr 23.
- (Akasaka J et al., 2012) Akasaka J, Uekuri C, Shigetomi H, Koike M, Kobayashi H. Hepatocyte nuclear factor (HNF)-1 β and its physiological importance in endometriosis. *Biomed Rep*. 2013 Jan;1(1):13-17. Epub 2012 Oct 11.
- (Alvelos MI et al., 2015) Alvelos MI, Rodrigues M, Lobo L, Medeira A, Sousa AB, Simão C, Lemos MC. A novel mutation of the HNF1B gene associated with hypoplastic glomerulocystic kidney disease and neonatal renal failure: a case report and mutation update. *Medicine (Baltimore)*. 2015 Feb;94(7):e469. doi: 10.1097/MD.0000000000000469
- (Ameres SL and Zamore PD, 2013) Ameres SL, Zamore PD. Diversifying microRNA sequence and function. *Nat Rev Mol Cell Biol*. 2013 Aug;14(8):475-88. doi: 10.1038/nrm3611. Epub 2013 Jun 26.
- (Avni FE and Hall M, 2010) Avni FE, Hall M. Renal cystic diseases in children: new concepts. *Pediatr Radiol*. 2010 Jun;40(6):939-46. doi: 10.1007/s00247-010-1599-5. Epub 2010 Apr 30.
- (Bach I et al., 1991) Bach I, Mattei MG, Cereghini S, Yaniv M. Two members of an HNF1 homeoprotein family are expressed in human liver. *Nucleic Acids Res*. 1991 Jul 11;19(13):3553-9.
- (Bach I and Yaniv M, 1993) Bach I, Yaniv M. More potent transcriptional activators or a transdominant inhibitor of the HNF1 homeoprotein family are generated by alternative RNA processing. *EMBO J*. 1993 Nov;12(11):4229-42.
- (Bai XY et al., 2011) Bai XY, Ma Y, Ding R, Fu B, Shi S, Chen XM. miR-335 and miR-34a Promote renal senescence by suppressing mitochondrial antioxidative enzymes. *J Am Soc Nephrol*. 2011 Jul;22(7):1252-61. doi: 10.1681/ASN.2010040367. Epub 2011 Jun 30.
- (Bai Y et al., 2002) Bai Y, Pontoglio M, Hiesberger T, Sinclair AM, Igarashi P. Regulation of kidney-specific Ksp-cadherin gene promoter by hepatocyte nuclear factor-1beta. *Am J Physiol Renal Physiol*. 2002 Oct;283(4):F839-51.
- (Barbacci E et al., 1999) Barbacci E, Reber M, Ott MO, Breillat C, Huetz F, Cereghini S. Variant hepatocyte nuclear factor 1 is required for visceral endoderm specification. *Development*. 1999 Nov;126(21):4795-805.
- (Barbacci E et al., 2004) Barbacci E, Chalkiadaki A, Masdeu C, Haumaitre C, Lokmane L, Loirat C, Clorec S, Talianidis I, Bellanne-Chantelot C, Cereghini S. HNF1beta/TCF2 mutations impair transactivation potential through altered co-regulator recruitment. *Hum Mol Genet*. 2004 Dec 15;13(24):3139-49. Epub 2004 Oct 27.
- (Bartel DP 2004) Bartel DP. MicroRNAs: genomics, biogenesis, mechanism, and function. *Cell*. 2004 Jan 23;116(2):281-97.
- (Bartel DP 2009) Bartel DP. MicroRNAs: target recognition and regulatory functions. *Cell*. 2009 Jan 23;136(2):215-33. doi: 10.1016/j.cell.2009.01.002.
- (Bartkowski S et al., 1993) Bartkowski S, Zapp D, Weber H, Eberle G, Zoidl C, Senkel S, Klein-Hitpass L, Ryffel GU. Developmental regulation and tissue distribution of the liver transcription factor LFB1 (HNF1) in *Xenopus laevis*. *Mol Cell Biol*. 1993 Jan;13(1):421-31.
- (Baumhueter S et al., 1988) Baumhueter S, Courtois G, Crabtree GR. A variant nuclear protein in dedifferentiated hepatoma cells binds to the same functional sequences in the beta fibrinogen gene promoter as HNF-1. *EMBO J*. 1988 Aug;7(8):2485-93.
- (Bai XY et al., 2011) Bai XY, Ma Y, Ding R et al. miR-335 and miR-34a promote renal senescence by suppressing mitochondrial antioxidative enzymes. *J Am Soc Nephrol* 2011; 220: 1252–1261.
- (Beards F et al., 1998) Beards F, Frayling T, Bulman M, Horikawa Y, Allen L, Appleton M, Bell GI, Ellard S, Hattersley AT. Mutations in hepatocyte nuclear factor 1beta are not a common cause of maturity-onset diabetes of the young in the U.K. *Diabetes*. 1998 Jul;47(7):1152-4.
- (Beckers D et al., 2007) Beckers D, Bellanné-Chantelot C, Maes M. Neonatal cholestatic jaundice as the first symptom of a mutation in the hepatocyte nuclear factor-1beta gene (HNF-1beta). *J Pediatr*. 2007 Mar;150(3):313-4.
- (Bellanné-Chantelot C et al., 2004) Bellanné-Chantelot C, Chauveau D, Gautier JF, Dubois-Laforgue D, Clauin S, Beaufils S, Wilhelm JM, Boitard C, Noël LH, Velho G, Timsit J. Clinical spectrum associated with hepatocyte nuclear factor-1beta mutations. *Ann Intern Med*. 2004 Apr 6;140(7):510-7.
- (Bellanné-Chantelot C et al., 2005) Bellanné-Chantelot C, Clauin S, Chauveau D, Collin P, Daumont M, Douillard C, Dubois-Laforgue D, Dusselier L, Gautier JF, Jadoul M, Laloi-Michelin M, Jacquesson L, Larger E, Louis J, Nicolino M, Subra JF, Wilhem JM, Young J, Velho G, Timsit J. Large genomic rearrangements in the hepatocyte nuclear factor-1beta (TCF2) gene are the most frequent cause of maturity-onset diabetes of the young type 5. *Diabetes*. 2005 Nov;54(11):3126-32.

- (Bender FC 2000) Bender FC, Reymond MA, Bron C and Quest AF: Caveolin-1 levels are down-regulated in human colon tumors, and ectopic expression of caveolin-1 in colon carcinoma cell lines reduces cell tumorigenicity. *Cancer Res* 60: 5870-5878, 2000.
- (Benjamini Y 1995) Benjamini Y, Hochberg Y. Controlling the false discovery rate: a practical and powerful approach to multiple testing. *J R Stat Soc B (Methodological)* 1995; 57: 125–133
- (Bernardini L 2009) Bernardini L, Gimelli S, Gervasini C, Carella M, Baban A, Frontino G, Barbano G, Divizia MT, Fedele L, Novelli A, Béna F, Lalatta F, Miozzo M, Dallapiccola B. Recurrent microdeletion at 17q12 as a cause of Mayer-Rokitansky-Kuster-Hauser (MRKH) syndrome: two case reports. *Orphanet J Rare Dis.* 2009 Nov 4;4:25. doi: 10.1186/1750-1172-4-25.
- (Berndt SI et al., 2011) Berndt SI, Sampson J, Yeager M, Jacobs KB, Wang Z, Hutchinson A, Chung C, Orr N, Wacholder S, Chatterjee N, Yu K, Kraft P, Feigelson HS, Thun MJ, Diver WR, Albanes D, Virtamo J, Weinstein S, Schumacher FR, Cancel-Tassin G, Cussenot O, Valeri A, Andriole GL, Crawford ED, Haiman C, Henderson B, Kolonel L, Le Marchand L, Siddiq A, Riboli E, Travis RC, Kaaks R, Isaacs W, Isaacs S, Wiley KE, Gronberg H, Wiklund F, Stattin P, Xu J, Zheng SL, Sun J, Vatten LJ, Hveem K, Njølstad I, Gerhard DS, Tucker M, Hayes RB, Hoover RN, Fraumeni JF Jr, Hunter DJ, Thomas G, Chanock SJ. Large-scale fine mapping of the HNF1B locus and prostate cancer risk. *Hum Mol Genet.* 2011 Aug 15;20(16):3322-9. doi: 10.1093/hmg/ddr213. Epub 2011 May 16.
- (Berner HS et al., 2003) Berner HS, Suo Z, Risberg B, Villman K, Karlsson MG and Nesland JM: Clinicopathological associations of CD44 mRNA and protein expression in primary breast carcinomas. *Histopathology* 42: 546-554, 2003.
- (Bernstein E et al., 2003) Bernstein E, Kim SY, Carmell MA, Murchison EP, Alcorn H, Li MZ, Mills AA, Elledge SJ, Anderson KV, Hannon GJ. Dicer is essential for mouse development. *Nat Genet.* 2003 Nov;35(3):215-7. Epub 2003 Oct 5.
- (Bertram JF et al., 2011) Bertram JF, Douglas-Denton RN, Diouf B, Hughson MD, Hoy WE: Human nephron number: Implications for health and disease. *Pediatr Nephrol* 26: 1529–1533, 2011
- (Bhatt K et al., 2011) Bhatt K, Mi QS, Dong Z. microRNAs in kidneys: biogenesis, regulation, and pathophysiological roles. *Am J Physiol Renal Physiol.* 2011 Mar;300(3):F602-10. doi: 10.1152/ajprenal.00727.2010. Epub 2011 Jan 12.
- (Bingham C 2000) Bingham C, Ellard S, Allen L, Bulman M, Shepherd M, Frayling T, Berry PJ, Clark PM, Lindner T, Bell GI, Ryffel GU, Nicholls AJ, Hattersley AT. Abnormal nephron development associated with a frameshift mutation in the transcription factor hepatocyte nuclear factor-1 beta. *Kidney Int.* 2000 Mar;57(3):898-907.
- (Bingham C 2001) Bingham C, Bulman MP, Ellard S, Allen LI, Lipkin GW, Hoff WG, Woolf AS, Rizzoni G, Novelli G, Nicholls AJ, Hattersley AT. Mutations in the hepatocyte nuclear factor-1beta gene are associated with familial hypoplastic glomerulocystic kidney disease. *Am J Hum Genet.* 2001 Jan;68(1):219-24. Epub 2000 Nov 20.
- (Bingham C 2002) Bingham C, Ellard S, Cole TR, Jones KE, Allen LI, Goodship JA, Goodship TH, Bakalinova-Pugh D, Russell GI, Woolf AS, Nicholls AJ, Hattersley AT. Solitary functioning kidney and diverse genital tract malformations associated with hepatocyte nuclear factor-1beta mutations. *Kidney Int.* 2002 Apr;61(4):1243-51.
- (Bingham C 2003) Bingham C, Ellard S, van't Hoff WG, Simmonds HA, Marinaki AM, Badman MK, Winocour PH, Stride A, Lockwood CR, Nicholls AJ, Owen KR, Spyer G, Pearson ER, Hattersley AT. Atypical familial juvenile hyperuricemic nephropathy associated with a hepatocyte nuclear factor-1beta gene mutation. *Kidney Int.* 2003 May;63(5):1645-51.
- (Bingham C 2004) Bingham C, Hattersley AT. Renal cysts and diabetes syndrome resulting from mutations in hepatocyte nuclear factor-1beta. *Nephrol Dial Transplant.* 2004 Nov;19(11):2703-8.
- (Body-Bechou D 2014) Body-Bechou D, Loget P, D'Herve D, Le Fiblec B, Grebille AG, Le Guern H, Labarthe C, Redpath M, Cabaret-Dufour AS, Sylvie O, Fievet A, Antignac C, Heidet L, Taque S, Patrice P. TCF2/HNF-1beta mutations: 3 cases of fetal severe pancreatic agenesis or hypoplasia and multicystic renal dysplasia. *Prenat Diagn.* 2014 Jan;34(1):90-3. doi: 10.1002/pd.4264.
- (Boeckel JN et al., 2014) Boeckel JN, Reis SM, Leistner D, Thomé CE, Zeiher AM, Fichtlscherer S, Keller T. From heart to toe: heart's contribution on peripheral microRNA levels. *Int J Cardiol.* 2014 Apr 1;172(3):616-7. doi: 10.1016/j.ijcard.2014.01.082. Epub 2014 Jan 24.
- (Bohn S 2003) Bohn S, Thomas H, Turan G, Ellard S, Bingham C, Hattersley AT, Ryffel GU. Distinct molecular and morphogenetic properties of mutations in the human HNF1beta gene that lead to defective kidney development. *J Am Soc Nephrol.* 2003 Aug;14(8):2033-41.
- (Bohnsack MT et al., 2004) Bohnsack MT, Czaplinski K, Gorlich D. Exportin 5 is a RanGTP-dependent dsRNA-binding protein that mediates nuclear export of pre-miRNAs. *RNA.* 2004 Feb;10(2):185-91.
- (Boj SF et al., 2001) Boj SF, Parrizas M, Maestro MA, Ferrer J. A transcription factor regulatory circuit in differentiated pancreatic cells. *Proc Natl Acad Sci U S A.* 2001 Dec 4;98(25):14481-6. Epub 2001 Nov 20.
- (Boyle S et al., 2008) Boyle S, Misfeldt A, Chandler KJ, Deal KK, Southard-Smith EM, Mortlock DP, Baldwin HS, de Caestecker M: Fate mapping using Cited1-CreERT2 mice demonstrates that the cap mesenchyme contains self-renewing progenitor cells and gives rise exclusively to nephronic epithelia. *Dev Biol* 313: 234–245, 2008
- (Brackenridge A 2006) Brackenridge A, Pearson ER, Shojaee-Moradie F, Hattersley AT, Russell-Jones D, Umphey AM. Contrasting insulin sensitivity of endogenous glucose production rate in subjects with hepatocyte nuclear factor-1beta and -1alpha mutations. *Diabetes.* 2006 Feb;55(2):405-11.
- (Briand N 2011) N. Briand, S. Le Lay, W. C. Sessa, P. Ferré, and I. Dugai. Distinct roles of endothelial and adipocyte caveolin-1 in macrophage infiltration and adipose tissue metabolic activity. *Diabetes*, vol. 60, no. 2, pp. 448–53, Feb. 2011.

- (Brunskill EW et al., 2008) Brunskill EW, Aronow BJ, Georgas K, Rumballe B, Valerius MT, Aronow J, Kaimal V, Jegga AG, Yu J, Grimmond S, McMahon AP, Patterson LT, Little MH, Potter SS. Atlas of gene expression in the developing kidney at microanatomic resolution. *Dev Cell*. 2008 Nov;15(5):781-91. doi: 10.1016/j.devcel.2008.09.007.
- (Cai X et al., 2004) Cai X, Hagedorn CH, Cullen BR. Human microRNAs are processed from capped, polyadenylated transcripts that can also function as mRNAs. *RNA*. 2004 Dec;10(12):1957-66. Epub 2004 Nov 3.
- (Calabrese JM et al., 2007) Calabrese JM, Seila AC, Yeo GW, Sharp PA. RNA sequence analysis defines Dicer's role in mouse embryonic stem cells. *Proc Natl Acad Sci U S A*. 2007 Nov 13;104(46):18097-102. Epub 2007 Nov 7.
- (Cao G et al., 2003) Cao G, Yang G, Timme TL, Saika T, Truong LD, Satoh T, Goltsov A, Park SH, Men T, Kusaka N, Tian W, Ren C, Wang H, Kadmon D, Cai WW, Chinault AC, Boone TB, Bradley A, Thompson TC. Disruption of the caveolin-1 gene impairs renal calcium reabsorption and leads to hypercalciuria and urolithiasis. *Am J Pathol* 162: 1241–1248, 2003.
- (Carroll TJ et al., 2005) Carroll TJ, Park JS, Hayashi S, Majumdar A, McMahon AP. Wnt9b plays a central role in the regulation of mesenchymal to epithelial transitions underlying organogenesis of the mammalian urogenital system. *Dev Cell*. 2005 Aug;9(2):283-92.
- (Cereghini S et al., 1987) Cereghini S, Raymondjean M, Carranca AG, Herbomel P, Yaniv M. Factors involved in control of tissue-specific expression of albumin gene. *Cell*. 1987 Aug 14;50(4):627-38.
- (Cereghini S et al., 1988) Cereghini S, Blumenfeld M, Yaniv M. A liver-specific factor essential for albumin transcription differs between differentiated and dedifferentiated rat hepatoma cells. *Genes Dev*. 1988 Aug;2(8):957-74.
- (Cereghini S et al., 1990) Cereghini S, Yaniv M, Cortese R. Hepatocyte dedifferentiation and extinction is accompanied by a block in the synthesis of mRNA coding for the transcription factor HNF1/LFB1. *EMBO J*. 1990 Jul;9(7):2257-63.
- (Cereghini S et al., 1992) Cereghini S, Ott MO, Power S, Maury M. Expression patterns of vHNF1 and HNF1 homeoproteins in early postimplantation embryos suggest distinct and sequential developmental roles. *Development*. 1992 Nov;116(3):783-97.
- (Cereghini S 1996) Cereghini S. Liver-enriched transcription factors and hepatocyte differentiation. *FASEB J*. 1996 Feb;10(2):267-82.
- (Casemayou A et al., 2017) Casemayou A, Fournel A, Bagattin A, Schanstra J, Belliere J, Decramer S, Marsal D, Gillet M, Chassaing N, Huart A, Pontoglio M, Knauf C, Bascands JL, Chauveau D, Faguer S. Hepatocyte Nuclear Factor-1 β Controls Mitochondrial Respiration in Renal Tubular Cells. *J Am Soc Nephrol*. 2017 Nov;28(11):3205-3217. doi: 10.1681/ASN.2016050508. Epub 2017 Jul 24.
- (Catto JW et al., 2011) Catto JW, Alcaraz A, Bjartell AS et al. MicroRNA in prostate, bladder, and kidney cancer: a systematic review. *Eur Urol* 2011; 59: 671–681
- (Ceska TA et al., 1993) Ceska TA, Lamers M, Monaci P, Nicosia A, Cortese R, Suck D. The X-ray structure of an atypical homeodomain present in the rat liver transcription factor LFB1/HNF1 and implications for DNA binding. *EMBO J*. 1993 May;12(5):1805-10.
- (Chandrasekaran K et al., 2012) Chandrasekaran K, Karolina DS, Sepramaniam S, Armugam A, Wintour EM, Bertram JF, Jeyaseelan K. Role of microRNAs in kidney homeostasis and disease. *Kidney Int*. 2012 Apr;81(7):617-27. doi: 10.1038/ki.2011.448. Epub 2012 Jan 11.
- (Cheng HT et al., 2007) Cheng HT, Kim M, Valerius MT, Surendran K, Schuster-Gossler K, Gossler A, McMahon AP, Kopan R. Notch2, but not Notch1, is required for proximal fate acquisition in the mammalian nephron. *Development*. 2007 Feb;134(4):801-11. Epub 2007 Jan 17.
- (Chen YZ et al., 2010) Chen YZ, Gao Q, Zhao XZ, Chen YZ, Bennett CL, Xiong XS, Mei CL, Shi YQ, Chen XM. Systematic review of TCF2 anomalies in renal cysts and diabetes syndrome/maturity onset diabetes of the young type 5. *Chin Med J (Engl)*. 2010 Nov;123(22):3326-33.
- (Chi YI et al., 2002) Chi YI, Frantz JD, Oh BC, Hansen L, Dhe-Paganon S, Shoelson SE. Diabetes mutations delineate an atypical POU domain in HNF-1 α . *Mol Cell*. 2002;10:1129–1137. doi: 10.1016/S1097-2765(02)00704-9.
- (Chouard T et al., 1990) Chouard T, Blumenfeld M, Bach I, Vandekerckhove J, Cereghini S, Yaniv M. A distal dimerization domain is essential for DNA-binding by the atypical HNF1 homeodomain. *Nucleic Acids Res*. 1990 Oct 11;18(19):5853-63.
- (Choi YH et al., 2013) Choi YH, McNally BT, Igarashi P. Zyxin regulates migration of renal epithelial cells through activation of hepatocyte nuclear factor-1 β . *Am J Physiol Renal Physiol*. 2013 Jul 1;305(1):F100-10. doi: 10.1152/ajprenal.00582.2012. Epub 2013 May 8.
- (Christopher AF et al., 2016) Christopher AF, Kaur RP, Kaur G, Kaur A, Gupta V, Bansal P. MicroRNA therapeutics: Discovering novel targets and developing specific therapy. *Perspect Clin Res*. 2016 Apr-Jun;7(2):68-74. doi: 10.4103/2229-3485.179431.
- (Chung AC et al., 2010) Chung AC, Huang XR, Meng X, Lan HY. miR-192 mediates TGF-beta/Smad3-driven renal fibrosis. *J Am Soc Nephrol*. 2010 Aug;21(8):1317-25. doi: 10.1681/ASN.2010020134. Epub 2010 May 20.
- (Clissold RL et al., 2014) Clissold RL, Hamilton AJ, Hattersley AT, Ellard S, Bingham C. HNF1B-associated renal and extra-renal disease—an expanding clinical spectrum. *Nat Rev Nephrol*. 2015 Feb;11(2):102-12. doi: 10.1038/nrneph.2014.232. Epub 2014 Dec 23.
- (Clissold RL et al., 2016) Clissold RL, Shaw-Smith C, Turnpenny P, Bunce B, Bockenbauer D, Kerecuk L, Waller S, Bowman P, Ford T, Ellard S, Hattersley AT, Bingham C. Chromosome 17q12 microdeletions but not intragenic HNF1B mutations link developmental kidney disease and psychiatric disorder. *Kidney Int*. 2016 Jul;90(1):203-11. doi: 10.1016/j.kint.2016.03.027. Epub 2016 May 24.
- (Clotman F et al., 2002) Clotman F, Lannoy VJ, Reber M, Cereghini S, Cassiman D, Jacquemin P, Roskams T, Rousseau GG, Lemaigre FP. The onecut transcription factor HNF6 is required for normal development of the biliary tract. *Development*. 2002 Apr;129(8):1819-28.

- (Coffinier C et al., 1999a) Coffinier, C., Thépot, D., Babinet, C., Yaniv, M., and Barra, J. (1999a). Essential role for the homeoprotein vHNF1/HNF1beta in visceral endoderm differentiation. *Dev. Camb. Engl.* 126, 4785–4794.
- (Coffinier C et al., 1999b) Coffinier C, Barra J, Babinet C, Yaniv M. Expression of the vHNF1/HNF1beta homeoprotein gene during mouse organogenesis. *Mech Dev.* 1999 Dec;89(1-2):211-3.
- (Coffinier C et al., 2002) Coffinier C, Gresh L, Fiette L, Tronche F, Schütz G, Babinet C, Pontoglio M, Yaniv M, Barra J. Bile system morphogenesis defects and liver dysfunction upon targeted deletion of HNF1beta. *Development.* 2002 Apr;129(8):1829-38.
- (Couet J et al., 1997) J. Couet, S. Li, T. Okamoto, T. Ikezu, and M. P. Lisanti, “Identification of peptide and protein ligands for the caveolin-scaffolding domain. Implications for the interaction of caveolin with caveolae-associated proteins.” *J. Biol. Chem.*, vol. 272, no. 10, pp. 6525–33, Mar. 1997.
- (Courtois G et al., 1987) Courtois G, Morgan JG, Campbell LA, Fourel G, Crabtree GR. Interaction of a liver-specific nuclear factor with the fibrinogen and alpha 1-antitrypsin promoters. *Science.* 1987 Oct 30;238(4827):688-92.
- (Cutting GR 2010) Cutting GR. Modifier genes in Mendelian disorders: the example of cystic fibrosis. *Ann N Y Acad Sci.* 2010 Dec;1214:57-69. doi: 10.1111/j.1749-6632.2010.05879.x.
- (D'Angelo A et al., 2010) D'Angelo A, Bluteau O, Garcia-Gonzalez MA, Gresh L, Doyen A, Garbay S, Robine S, Pontoglio M. Hepatocyte nuclear factor 1alpha and beta control terminal differentiation and cell fate commitment in the gut epithelium. *Development.* 2010 May;137(9):1573-82. doi: 10.1242/dev.044420.
- (Decramer S et al., 2007) Decramer S, Parant O, Beaufile S, Clauin S, Guillou C, Kessler S, Aziza J, Bandin F, Schanstra JP, Bellanné-Chantelot C. Anomalies of the TCF2 gene are the main cause of fetal bilateral hyperechogenic kidneys. *J Am Soc Nephrol.* 2007 Mar;18(3):923-33. Epub 2007 Jan 31.
- (Decramer S et al., 2008) Decramer, S., Gonzalez de, P. A., Breuil, B., Mischak, H. et al. Urine in clinical proteomics. *Mol Cell Proteomics* 2008, 7 (10), 1850-1862.
- (Demartis A et al., 1994) Demartis A, Maffei M, Vignali R, Barsacchi G, De Simone V. Cloning and developmental expression of LFB3/HNF1 beta transcription factor in *Xenopus laevis*. *Mech Dev.* 1994 Jul;47(1):19-28.
- (Deryckere F et al., 1995) Deryckere F, Byrnes L, Wagner A, McMorro T, Gannon F. Salmon HNF1: cDNA sequence, evolution, tissue specificity and binding to the salmon serum albumin promoter. *J Mol Biol.* 1995 Mar 17;247(1):1-10.
- (Desgrange A and Cereghini S, 2015) Desgrange A, Cereghini S. Nephron Patterning: Lessons from *Xenopus*, Zebrafish, and Mouse Studies. *Cells.* 2015 Sep 11;4(3):483-99. doi: 10.3390/cells4030483.
- (Desgrange A et al., 2017) Desgrange A, Heliot C, Skovorodkin I, Akram SU, Heikkilä J, Ronkainen VP, Miinalainen I, Vainio SJ, Cereghini S. HNF1B controls epithelial organization and cell polarity during ureteric bud branching and collecting duct morphogenesis. *Development.* 2017 Dec 15;144(24):4704-4719. doi: 10.1242/dev.154336. Epub 2017 Nov 20.
- (De Simone V et al., 1991) De Simone V, De Magistris L, Lazzaro D, Gerstner J, Monaci P, Nicosia A, Cortese R. LFB3, a heterodimer-forming homeoprotein of the LFB1 family, is expressed in specialized epithelia. *EMBO J.* 1991 Jun;10(6):1435-43.
- (De Vas MG et al., 2015) De Vas MG, Kopp JL, Heliot C, Sander M, Cereghini S, Haumaitre C. Hnf1b controls pancreas morphogenesis and the generation of Ngn3+ endocrine progenitors. *Development.* 2015 Mar 1;142(5):871-82. doi: 10.1242/dev.110759.
- (Dewanjee S et al., 2018) Dewanjee S, Bhattacharjee N2. MicroRNA: A new generation therapeutic target in diabetic nephropathy. *Biochem Pharmacol.* 2018 Jun 22;155:32-47. doi: 10.1016/j.bcp.2018.06.017. [Epub ahead of print]
- (Diaz LK et al., 2005) Diaz LK, Zhou X, Wright ET, et al: CD44 expression is associated with increased survival in node-negative invasive breast carcinoma. *Clin Cancer Res* 11: 3309-3314, 2005
- (Dietzen DJ et al., 1995) D. J. Dietzen, W. R. Hastings, and D. M. Lublin. Caveolin is palmitoylated on multiple cysteine residues. Palmitoylation is not necessary for localization of caveolin to caveolae. *J. Biol. Chem.*, vol. 270, no. 12, pp. 6838–42, Mar. 1995.
- (Donatello S et al., 2012) Donatello S, Babina IS, Hazelwood LD, Hill AD, Nabi IR, Hopkins AM. Lipid raft association restricts CD44-ezrin interaction and promotion of breast cancer cell migration. *Am J Pathol.* 2012 Dec;181(6):2172-87. doi: 10.1016/j.ajpath.2012.08.025. Epub 2012 Sep 29.
- (Dong P et al., 2011) Dong P, Kaneuchi M, Watari H, Hamada J, Sudo S, Ju J, Sakuragi N. MicroRNA-194 inhibits epithelial to mesenchymal transition of endometrial cancer cells by targeting oncogene BMI-1. *Mol Cancer.* 2011 Aug 18;10:99. doi: 10.1186/1476-4598-10-99.
- (Dressler GR 2004) Dressler GR. The cellular basis of kidney development. *Annu Rev Cell Dev Biol.* 2006;22:509-29.
- (Dressler GR 2009) Dressler GR. Advances in early kidney specification, development and patterning. *Development.* 2009 Dec;136(23):3863-74. doi: 10.1242/dev.034876.
- (Duan J et al., 2012) Duan J, Huang H, Lv X, Wang H, Tang Z, Sun H, Li Q, Ai J, Tan R, Liu Y, Chen M, Duan W, Wei Y, Zhou Q. PKHD1 post-transcriptionally modulated by miR-365-1 inhibits cell-cell adhesion. *Cell Biochem Funct.* 2012 Jul;30(5):382-9. doi: 10.1002/cbf.2795. Epub 2012 Mar 13.

- (Dubois-Laforgue D et al., 2017) Dubois-Laforgue D, Cornu E, Saint-Martin C, Coste J, Bellanné-Chantelot C, Timsit J; Monogenic Diabetes Study Group of the Société Francophone du Diabète. Diabetes, Associated Clinical Spectrum, Long-term Prognosis, and Genotype/Phenotype Correlations in 201 Adult Patients With Hepatocyte Nuclear Factor 1B (HNF1B) Molecular Defects. *Diabetes Care*. 2017 Nov;40(11):1436-1443. doi: 10.2337/dc16-2462. Epub 2017 Apr 18.
- (Dudziak K et al., 2008) Dudziak K, Mottalebi N, Senkel S, Edghill EL, Rosengarten S, Roose M, Bingham C, Ellard S, Ryffel GU. Transcription factor HNF1beta and novel partners affect nephrogenesis. *Kidney Int*. 2008 Jul;74(2):210-7. doi: 10.1038/ki.2008.149. Epub 2008 Apr 16.
- (Echiburú-Chau C et al., 2011) Echiburú-Chau C, Roy D, Calaf GM. Metastatic suppressor CD44 is related with oxidative stress in breast cancer cell lines. *Int J Oncol*. 2011 Dec;39(6):1481-9. doi: 10.3892/ijo.2011.1154. Epub 2011 Aug 9.
- (Eckardt KU et al., 2015) Eckardt KU, Alper SL, Antignac C, Bleyer AJ, Chauveau D, Dahan K, Deltas C, Hosking A, Kmoch S, Rampoldi L, Wiesener M, Wolf MT, Devuyt O; Kidney Disease: Improving Global Outcomes. Autosomal dominant tubulointerstitial kidney disease: diagnosis, classification, and management--A KDIGO consensus report. *Kidney Int*. 2015 Oct;88(4):676-83. doi: 10.1038/ki.2015.28. Epub 2015 Mar 4.
- (Edghill EL et al., 2006) Edghill EL, Bingham C, Ellard S, Hattersley AT. Mutations in hepatocyte nuclear factor-1beta and their related phenotypes. *J Med Genet*. 2006 Jan;43(1):84-90. Epub 2005 Jun 1.
- (Edghill EL et al., 2006 beta) Edghill EL, Bingham C, Slingerland AS, Minton JA, Noordam C, Ellard S, Hattersley AT. Hepatocyte nuclear factor-1 beta mutations cause neonatal diabetes and intrauterine growth retardation: support for a critical role of HNF-1beta in human pancreatic development. *Diabet Med*. 2006 Dec;23(12):1301-6.
- (Edghill EL et al., 2008) Edghill EL, Oram RA, Owens M, Stals KL, Harries LW, Hattersley AT, Ellard S, Bingham C. Hepatocyte nuclear factor-1beta gene deletions--a common cause of renal disease. *Nephrol Dial Transplant*. 2008 Feb;23(2):627-35. Epub 2007 Oct 30.
- (Edghill EL et al., 2013) Edghill EL, Stals K, Oram RA, Shepherd MH, Hattersley AT, Ellard S. HNF1B deletions in patients with young-onset diabetes but no known renal disease. *Diabet Med*. 2013 Jan;30(1):114-7. doi: 10.1111/j.1464-5491.2012.03709.x.
- (El-Khairi R et al., 2016) El-Khairi R, Vallier L. The role of hepatocyte nuclear factor 1β in disease and development. *Diabetes Obes Metab*. 2016 Sep;18 Suppl 1:23-32. doi: 10.1111/dom.12715.
- (Elvira-Matlot E et al., 2010) Elvira-Matlot E, Zhou XO, Farman N, Beaurain G, Henrion-Caude A, Hadchouel J, Jeunemaitre X. Regulation of WNK1 expression by miR-192 and aldosterone. *J Am Soc Nephrol*. 2010 Oct;21(10):1724-31. doi: 10.1681/ASN.2009111186. Epub 2010 Sep 2.
- (Faguer S et al., 2011) Faguer S, Decramer S, Chassaing N, Bellanné-Chantelot C, Calvas P, Beaufils S, Bessenay L, Lengelé JP, Dahan K, Ronco P, Devuyt O, Chauveau D. Diagnosis, management, and prognosis of HNF1B nephropathy in adulthood. *Kidney Int*. 2011 Oct;80(7):768-76. doi: 10.1038/ki.2011.225. Epub 2011 Jul 20.
- (Faguer S et al., 2012) Faguer S, Decramer S, Devuyt O, Lengelé JP, Fournié GJ, Chauveau D. Expression of renal cystic genes in patients with HNF1B mutations. *Nephron Clin Pract*. 2012;120(2):c71-8. doi: 10.1159/000334954. Epub 2012 Jan 21.
- (Faguer S et al., 2014) Faguer S, Chassaing N, Bandin F, Prouheze C, Garnier A, Casemayou A, Huart A, Schanstra JP, Calvas P, Decramer S, Chauveau D. The HNF1B score is a simple tool to select patients for HNF1B gene analysis. *Kidney Int*. 2014 Nov;86(5):1007-15. doi: 10.1038/ki.2014.202. Epub 2014 Jun 4.
- (Ferrè S et al., 2011) Ferrè S, Veenstra GJ, Bouwmeester R, Hoenderop JG, Bindels RJ. HNF-1B specifically regulates the transcription of the γ -subunit of the Na⁺/K⁺-ATPase. *Biochem Biophys Res Commun*. 2011 Jan 7;404(1):284-90. doi: 10.1016/j.bbrc.2010.11.108. Epub 2010 Dec 2.
- (Ferrè S et al., 2013) Ferrè S, Bongers EM, Sonneveld R, Cornelissen EA, van der Vlag J, van Boekel GA, Wetzels JF, Hoenderop JG, Bindels RJ, Nijenhuis T. Early development of hyperparathyroidism due to loss of PTH transcriptional repression in patients with HNF1B mutations? *J Clin Endocrinol Metab*. 2013 Oct;98(10):4089-96. doi: 10.1210/jc.2012-3453. Epub 2013 Aug 26.
- (Ferrè S et al., 2014) Ferrè S, de Baaij JH, Ferreira P, Germann R, de Klerk JB, Lavrijsen M, van Zeeland F, Venselaar H, Kluijtmans LA, Hoenderop JG, Bindels RJ. Mutations in PCBD1 cause hypomagnesemia and renal magnesium wasting. *J Am Soc Nephrol*. 2014 Mar;25(3):574-86. doi: 10.1681/ASN.2013040337. Epub 2013 Nov 7.
- (Ferrè S et al., 2018) Ferrè S, Igarashi P. New insights into the role of HNF-1β in kidney (patho)physiology. *Pediatr Nephrol*. 2018 Jul 1. doi: 10.1007/s00467-018-3990-7.
- (Finoulst I et al., 2011) Finoulst I, Pinkse M, Van D W, Verhaert P. Sample preparation techniques for the untargeted LC-MS-based discovery of peptides in complex biological matrices. *J Biomed Biotechnol*. 2011, 2011, 245291.
- (Fischer E et al., 2006) Fischer E, Legue E, Doyen A, Nato F, Nicolas JF, Torres V, Yaniv M, Pontoglio M. Defective planar cell polarity in polycystic kidney disease. *Nat Genet*. 2006 Jan;38(1):21-3. Epub 2005 Dec 11.
- (Flynt AS et al., 2009) Flynt AS, Thatcher EJ, Burkewitz K et al. miR-8 microRNAs regulate the response to osmotic stress in zebrafish embryos. *J Cell Biol* 2009; 185:115–127.
- (Frain M et al., 1989) Frain M, Swart G, Monaci P, Nicosia A, Stämpfli S, Frank R, Cortese R. The liver-specific transcription factor LF-B1 contains a highly diverged homeobox DNA binding domain. *Cell*. 1989 Oct 6;59(1):145-57.

- (Frank F et al., 2010) Frank F, Sonenberg N, Nagar B Structural basis for 5'-nucleotide base-specific recognition of guide RNA by human AGO2. *Nature*. 2010 Jun 10;465(7299):818-22. doi: 10.1038/nature09039. Epub 2010 May 26..
- (Friedman RC et al., 2009) Friedman RC, Farh KK, Burge CB, Bartel DP. Most mammalian mRNAs are conserved targets of microRNAs. *Genome Res*. 2009 Jan;19(1):92-105. doi: 10.1101/gr.082701.108. Epub 2008 Oct 27.
- (Fromm B et al., 2015) Fromm B, Billipp T, Peck LE, Johansen M, Tarver JE, King BL, Newcomb JM, Sempere LF, Flatmark K, Hovig E, Peterson KJ. A Uniform System for the Annotation of Vertebrate microRNA Genes and the Evolution of the Human microRNAome. *Annu Rev Genet*. 2015;49:213-42. doi: 10.1146/annurev-genet-120213-092023. Epub 2015 Oct 14.
- (Fu WH et al., 2002) W.H. Yu, J.F. Woessner, J.D. McNeish, and I. Stamenkovic. CD44 anchors the assembly of matrilysin/MMP-7 with heparin-binding epidermal growth factor precursor and ErbB4 and regulates female reproductive organ remodeling. *Genes Dev.*, vol. 16, no. 3, pp. 307–23, Feb. 2002.
- (Fujigaki Y 2007) Fujigaki Y, Sakakima M, Sun Y, Goto T, Ohashi N, Fukasawa H, Tsuji T, Yamamoto T, Hishida A. Immunohistochemical study on caveolin-1alpha in regenerating process of tubular cells in gentamicin-induced acute tubular injury in rats. *Virchows Arch* 450: 671–681, 2007
- (Fujimoto T 1993) Fujimoto T. Calcium pump of the plasma membrane is localized in caveolae. *J Cell Biol* 120: 1147–1157, 1993.
- (Georges SA et al., 2008) Georges SA, Biery MC, Kim SY, Schelter JM, Guo J, Chang AN, Jackson AL, Carleton MO, Linsley PS, Cleary MA, Chau BN. Coordinated regulation of cell cycle transcripts by p53-Inducible microRNAs, miR-192 and miR-215. *Cancer Res*. 2008 Dec 15;68(24):10105-12. doi: 10.1158/0008-5472.CAN-08-1846.
- (Ghildiyal M and Zamore PD 2009) Ghildiyal M, Zamore PD. Small silencing RNAs: an expanding universe. *Nat Rev Genet*. 2009 Feb;10(2):94-108. doi: 10.1038/nrg2504.
- (Godwin JG et al., 2010) Godwin JG, Ge X, Stephan K, Jurisch A, Tullius SG, Iacomini J. Identification of a microRNA signature of renal ischemia reperfusion injury. *Proc Natl Acad Sci U S A*. 2010 Aug 10;107(32):14339-44. doi: 10.1073/pnas.0912701107. Epub 2010 Jul 22.
- (Gong HY et al., 2004) Gong HY, Lin CJ, Chen MH, Hu MC, Lin GH, Zhou Y, Zou LI, Wu JL. Two distinct teleost hepatocyte nuclear factor 1 genes, hnf1alpha/tcf1 and hnf1beta/tcf2, abundantly expressed in liver, pancreas, gut and kidney of zebrafish. *Gene*. 2004 Aug 18;338(1):35-46.
- (Gong Y et al., 2008) Gong Y, Ma Z, Patel V, Fischer E, Hiesberger T, Pontoglio M, Igarashi P. HNF-1beta regulates transcription of the PKD modifier gene Kif12. *J Am Soc Nephrol*. 2009 Jan;20(1):41-7. doi: 10.1681/ASN.2008020238. Epub 2008 Nov 12.
- (Granberg CF 2011) Granberg CF, Harrison SM, Dajusta D, Zhang S, Hajarnis S, Igarashi P, Baker LA. Genetic basis of prune belly syndrome: screening for HNF1β gene. *J Urol*. 2012 Jan;187(1):272-8. doi: 10.1016/j.juro.2011.09.036. Epub 2011 Nov 23.
- (Gresh L et al., 2004) Gresh L, Fischer E, Reimann A, Tanguy M, Garbay S, Shao X, Hiesberger T, Fiette L, Igarashi P, Yaniv M, Pontoglio M. A transcriptional network in polycystic kidney disease. *EMBO J*. 2004 Apr 7;23(7):1657-68. Epub 2004 Mar 18.
- (Griffiths-Jones S et al., 2008) Griffiths-Jones S, Saini HK, van Dongen S, Enright AJ. miRBase: tools for microRNA genomics. *Nucleic Acids Res*. 2008 Jan;36(Database issue):D154-8. Epub 2007 Nov 8.
- (Gudmundsson J et al., 2007) Gudmundsson J, Sulem P, Steinthorsdottir V, Bergthorsson JT, Thorleifsson G, Manolescu A, Rafnar T, Gudbjartsson D, Agnarsson BA, Baker A, Sigurdsson A, Benediktsdottir KR, Jakobsdottir M, Blondal T, Stacey SN, Helgason A, Gunnarsdottir S, Olafsdottir A, Kristinsson KT, Birgisdottir B, Ghosh S, Thorlacius S, Magnusdottir D, Stefansdottir G, Kristjansson K, Bagger Y, Wilensky RL, Reilly MP, Morris AD, Kimber CH, Adeyemo A, Chen Y, Zhou J, So WY, Tong PC, Ng MC, Hansen T, Andersen G, Borch-Johnsen K, Jorgensen T, Tres A, Fuertes F, Ruiz-Echarri M, Asin L, Saez B, van Boven E, Klaver S, Swinkels DW, Aben KK, Graif T, Cashy J, Suarez BK, van Vierssen Trip O, Frigge ML, Ober C, Hofker MH, Wijmenga C, Christiansen C, Rader DJ, Palmer CN, Rotimi C, Chan JC, Pedersen O, Sigurdsson G, Benediktsson R, Jonsson E, Einarsson GV, Mayordomo JI, Catalona WJ, Kiemenev LA, Barkardottir RB, Gulcher JR, Thorsteinsdottir U, Kong A, Stefansson K. Two variants on chromosome 17 confer prostate cancer risk, and the one in TCF2 protects against type 2 diabetes. *Nat Genet*. 2007 Aug;39(8):977-83. Epub 2007 Jul 1.
- (Guo H et al., 2010) Guo H, Ingolia NT, Weissman JS, Bartel DP. Mammalian microRNAs predominantly act to decrease target mRNA levels. *Nature*. 2010 Aug 12;466(7308):835-40. doi: 10.1038/nature09267.
- (Ha M and Kim VN 2014) Ha M, Kim VN. Regulation of microRNA biogenesis. *Nat Rev Mol Cell Biol*. 2014 Aug;15(8):509-24. doi: 10.1038/nrm3838. Epub 2014 Jul 16.
- (Haeri S 2010) Haeri S, Devers PL, Kaiser-Rogers KA, Moylan VJ Jr, Torchia BS, Horton AL, Wolfe HM, Aylsworth AS. Deletion of hepatocyte nuclear factor-1-beta in an infant with prune belly syndrome. *Am J Perinatol*. 2010 Aug;27(7):559-63. doi: 10.1055/s-0030-1248943. Epub 2010 Feb 19.
- (Hajarnis SS et al., 2015) Hajarnis SS, Patel V, Aboudehen K, Attanasio M, Cobo-Stark P, Pontoglio M, Igarashi P (2015) Transcription factor hepatocyte nuclear factor-1beta (HNF-1beta) regulates microRNA-200 expression through a long noncoding RNA. *J Biol Chem* 290:24793– 24805
- (Hajarnis S et al., 2018) Hajarnis S, Yheskel M, Williams D, Brefort T, Glaudemans B, Debaix H, Baum M, Devuyt O, Patel V. Suppression of microRNA Activity in Kidney Collecting Ducts Induces Partial Loss of Epithelial Phenotype and Renal Fibrosis. *J Am Soc Nephrol*. 2018 Feb;29(2):518-531. doi: 10.1681/ASN.2017030334. Epub 2017 Oct 11.
- (Haldorsen IS et al., 2008) Haldorsen IS, Vesterhus M, Raeder H, Jensen DK, Søvik O, Molven A, Njølstad PR. Lack of pancreatic body and tail in HNF1B mutation carriers. *Diabet Med*. 2008 Jul;25(7):782-7. doi: 10.1111/j.1464-5491.2008.02460.x.

- (Han J et al., 2012) Han J, Liu Y, Rao F, Nievergelt CM, O'Connor DT, Wang X, Liu L, Bu D, Liang Y, Wang F, Zhang L, Zhang H, Chen Y, Wang H. Common genetic variants of the human uromodulin gene regulate transcription and predict plasma uric acid levels. *Kidney Int.* 2013 Apr;83(4):733-40. doi: 10.1038/ki.2012.449. Epub 2013 Jan 23.
- (Hao J et al., 2017) Hao J, Lou Q, Wei Q, Mei S, Li L, Wu G, Mi QS, Mei C, Dong Z. MicroRNA-375 Is Induced in Cisplatin Nephrotoxicity to Repress Hepatocyte Nuclear Factor 1- β . *J Biol Chem.* 2017 Mar 17;292(11):4571-4582. doi: 10.1074/jbc.M116.754929. Epub 2017 Jan 24.
- (Hardon EM et al., 1988) Hardon EM, Frain M, Paonessa G, Cortese R. Two distinct factors interact with the promoter regions of several liver-specific genes. *EMBO J.* 1988 Jun;7(6):1711-9.
- (Harrison KA et al., 1999) Harrison KA, Thaler J, Pfaff SL, Gu H, Kehrl JH. Pancreas dorsal lobe agenesis and abnormal islets of Langerhans in Hlx9-deficient mice. *Nat Genet.* 1999 Sep;23(1):71-5.
- (Hart TC et al., 2002) Hart TC, Gorry MC, Hart PS, Woodard AS, Shihabi Z, Sandhu J, Shirts B, Xu L, Zhu H, Barmada MM, Bleyer AJ. Mutations of the UMOD gene are responsible for medullary cystic kidney disease 2 and familial juvenile hyperuricaemic nephropathy. *J Med Genet.* 2002 Dec;39(12):882-92.
- (Harvey SJ et al., 2008) Harvey SJ, Jarad G, Cunningham J, Goldberg S, Schermer B, Harfe BD, McManus MT, Benzing T, Miner JH. Podocyte-specific deletion of *dicer* alters cytoskeletal dynamics and causes glomerular disease. *J Am Soc Nephrol.* 2008 Nov;19(11):2150-8. doi: 10.1681/ASN.2008020233. Epub 2008 Sep 5.
- (Haumaitre C et al., 2003) Haumaitre C, Reber M, Cereghini S. Functions of HNF1 family members in differentiation of the visceral endoderm cell lineage. *J Biol Chem.* 2003 Oct 17;278(42):40933-42. Epub 2003 Jul 14.
- (Haumaitre C et al., 2005) Haumaitre C, Barbacci E, Jenny M, Ott MO, Gradwohl G, Cereghini S. Lack of TCF2/vHNF1 in mice leads to pancreas agenesis. *Proc Natl Acad Sci U S A.* 2005 Feb 1;102(5):1490-5. Epub 2005 Jan 24.
- (Haumaitre C et al., 2006) Haumaitre C, Fabre M, Cormier S, Baumann C, Delezoide AL, Cereghini S. Severe pancreas hypoplasia and multicystic renal dysplasia in two human fetuses carrying novel HNF1beta/MODY5 mutations. 2006 *Hum. Mol. Genet.* 15, 2363-2375.
- (Heidet L et al., 2010) Heidet L, Decramer S, Pawtowski A, Morinière V, Bandin F, Knebelmann B, Lebre AS, Faguer S, Guignon V, Antignac C, Salomon R. Spectrum of HNF1B mutations in a large cohort of patients who harbor renal diseases. *Clin J Am Soc Nephrol.* 2010 Jun;5(6):1079-90. doi: 10.2215/CJN.06810909. Epub 2010 Apr 8.
- (Heliot C et al., 2013) Heliot C, Desgrange A, Buisson I, Prunskaitė-Hyryläinen R, Shan J, Vainio S, Umbhauer M, Cereghini S. HNF1B controls proximal-intermediate nephron segment identity in vertebrates by regulating Notch signalling components and *Irx1/2*. *Development.* 2013 Feb;140(4):873-85. doi: 10.1242/dev.086538.
- (Hernandez RE et al., 2004) Hernandez RE, Rikhof HA, Bachmann R, Moens CB. *vhnf1* integrates global RA patterning and local FGF signals to direct posterior hindbrain development in zebrafish. *Development.* 2004 Sep;131(18):4511-20.
- (Hiesberger T et al., 2004) Hiesberger T, Bai Y, Shao X, McNally BT, Sinclair AM, Tian X, Somlo S, Igarashi P. Mutation of hepatocyte nuclear factor-1beta inhibits *Pkhd1* gene expression and produces renal cysts in mice. *J Clin Invest.* 2004 Mar;113(6):814-25.
- (Hiesberger T et al., 2005) Hiesberger T, Shao X, Gourley E, Reimann A, Pontoglio M, Igarashi P. Role of the hepatocyte nuclear factor-1beta (HNF-1beta) C-terminal domain in *Pkhd1* (ARPKD) gene transcription and renal cystogenesis. *J Biol Chem.* 2005 Mar 18;280(11):10578-86. Epub 2005 Jan 12.
- (Higuchi C et al., 2015) Higuchi C, Nakatsuka A, Eguchi J, Teshigawara S, Kanzaki M, Katayama A, Yamaguchi S, Takahashi N, Murakami K, Ogawa D, Sasaki S, Makino H, Wada J. Identification of circulating miR-101, miR-375 and miR-802 as biomarkers for type 2 diabetes. *Metabolism.* 2015 Apr;64(4):489-97. doi: 10.1016/j.metabol.2014.12.003. Epub 2014 Dec 18.
- (Hino K et al., 2008) Hino K, Tsuchiya K, Fukao T, Kiga K, Okamoto R, Kanai T, Watanabe M. Inducible expression of microRNA-194 is regulated by HNF-1alpha during intestinal epithelial cell differentiation. *RNA.* 2008 Jul;14(7):1433-42. doi: 10.1261/rna.810208. Epub 2008 May 20.
- (Ho JJ and Marsden PA, 2008) Ho JJ, Marsden PA. *Dicer* cuts the kidney. *J Am Soc Nephrol.* 2008 Nov;19(11):2043-6. doi: 10.1681/ASN.2008090986. Epub 2008 Oct 15.
- (Holland PW et al., 2007) Holland PW, Booth HA, Bruford EA. Classification and nomenclature of all human homeobox genes. *BMC Biol.* 2007 Oct 26;5:47.
- (Horikawa Y, 1997) Horikawa Y, Iwasaki N, Hara M, Furuta H, Hinokio Y, Cockburn BN, Lindner T, Yamagata K, Ogata M, Tomonaga O, Kuroki H, Kasahara T, Iwamoto Y, Bell GI (1997) Mutation in hepatocyte nuclear factor-1 beta gene (TCF2) associated with MODY. *Nat Genet*
- (Howes MT et al., 2010) Howes MT, Kirkham M, Riches J, Cortese K, Walser PJ, Simpson F, Hill MM, Jones A, Lundmark R, Lindsay MR, Hernandez-Deviez DJ, Hadzic G, McCluskey A, Bashir R, Liu L, Pilch P, McMahon H, Robinson PJ, Hancock JF, Mayor S, Parton RG. Clathrin-independent carriers form a high capacity endocytic sorting system at the leading edge of migrating cells. *J Cell Biol* 2010, 190:675–691
- (Hoy WE et al., 2005) Hoy WE, Hughson MD, Bertram JF, Douglas-Denton R, Amann K. Nephron number, hypertension, renal disease, and renal failure. *J Am Soc Nephrol.* 2005 Sep;16(9):2557-64. Epub 2005 Jul 27.

- (Huang W et al., 2011) Huang W, Liu H, Wang T et al. Tonicity-responsive microRNAs contribute to the maximal induction of osmoregulatory transcription factor OREBP in response to high-NaCl hypertonicity. *Nucleic Acids Res* 2011; 39:475–485.
- (Humphreys BD et al., 2010) Humphreys BD, Lin S-L, Kobayashi A, Hudson TE, Nowlin BT, Bonventre JV, Valerius MT, McMahon AP, Duffield JS: Fate tracing reveals the pericyte and not epithelial origin of myofibroblasts in kidney fibrosis. *Am J Pathol* 176: 85–97, 2010
- (Hutvagner G et al., 2001) Hutvagner G, McLachlan J, Pasquinelli AE, Bálint E, Tuschl T, Zamore PD. A cellular function for the RNA-interference enzyme Dicer in the maturation of the let-7 small temporal RNA. *Science*. 2001 Aug 3;293(5531):834-8. Epub 2001 Jul 12.
- (Ichii O et al., 2017) Ichii O, Horino T. MicroRNAs associated with the development of kidney diseases in humans and animals. *J Toxicol Pathol*. 2018 Jan;31(1):23-34. doi: 10.1293/tox.2017-0051. Epub 2017 Oct 6.
- (Ideker T et al., 2001) Ideker, T., Galitski, T., Hood, L., A new approach to decoding life: systems biology. *Annu. Rev. Genomics Hum. Genet.* 2001, 2, 343-372.
- (Igarashi P et al., 2005) Igarashi P, Shao X, McNally BT, Hiesberger T. Roles of HNF-1beta in kidney development and congenital cystic diseases. *Kidney Int.* 2005 Nov;68(5):1944-7.
- (Ito J et al., 2002 et al.,) J. Ito, Y. Nagayasu, K. Kato, R. Sato, and S. Yokoyama. Apolipoprotein A-I induces translocation of cholesterol, phospholipid, and caveolin-1 to cytosol in rat astrocytes. *J. Biol. Chem.*, vol. 277, no. 10, pp. 7929–35, Mar. 2002.
- (Jaggupilli A and Elkord E, 2012) Jaggupilli A, Elkord E. Significance of CD44 and CD24 as cancer stem cell markers: an enduring ambiguity. *Clin Dev Immunol*. 2012;2012:708036. doi: 10.1155/2012/708036. Epub 2012 May 30.
- (Janas MM and Novina CD, 2012) Janas MM, Novina CD. Not lost in translation: stepwise regulation of microRNA targets. *EMBO J*. 2012 May 30;31(11):2446-7. doi: 10.1038/emboj.2012.119. Epub 2012 Apr 20.
- (Jantos-Siwy J et al., 2009) Jantos-Siwy, J., Schiffer, E., Brand, K., Schumann, G. et al. Quantitative Urinary Proteome Analysis for Biomarker Evaluation in Chronic Kidney Disease. *J. Proteome. Res.* 2009, 8 (1), 268-281.
- (Jenkins RH et al., 2012) Jenkins RH, Martin J, Phillips AO, Bowen T, Fraser DJ. Transforming growth factor β 1 represses proximal tubular cell microRNA-192 expression through decreased hepatocyte nuclear factor DNA binding. *Biochem J*. 2012 Apr 15;443(2):407-16. doi: 10.1042/BJ20111861.
- (John B et al., 2004) John B, Enright AJ, Aravin A, Tuschl T, Sander C, Marks DS. Human MicroRNA targets. *PLoS Biol*. 2004 Nov;2(11):e363. Epub 2004 Oct 5.
- (Jiang S et al., 2003) Jiang S, Tanaka T, Iwanari H, Hotta H, Yamashita H, Kumakura J, Watanabe Y, Uchiyama Y, Aburatani H, Hamakubo T, Kodama T, Naito M. Expression and localization of P1 promoter-driven hepatocyte nuclear factor-4a (HNF4a) isoforms in human and rats. *Nucl Recept*. 2003 Aug 8;1:5. doi: 10.1186/1478-1336-1-5. eCollection 2003.
- (Jin HY and Xiao C, 2015) Xiao C2. MicroRNA Mechanisms of Action: What have We Learned from Mice? *Front Genet*. 2015 Nov 16;6:328. doi: 10.3389/fgene.2015.00328. eCollection 2015.
- (Jones TF et al., 2018) Jones TF, Bekele S, O'Dwyer MJ, Prowle JR. MicroRNAs in Acute Kidney Injury. *Nephron*. 2018 Jun 5:1-5. doi: 10.1159/000490204. [Epub ahead of print]
- (Joshi B et al., 2008) B. Joshi, S. S. Strugnell, J. G. Goetz, L. D. Kojic, M. E. Cox, O. L. Griffith, S. K. Chan, S. J. Jones, S.-P. Leung, H. Masoudi, S. Leung, S. M. Wiseman, and I. R. Nabi, Phosphorylated caveolin-1 regulates Rho/ROCK-dependent focal adhesion dynamics and tumor cell migration and invasion. *Cancer Res.*, vol. 68, no. 20, pp. 8210–20, Oct. 2008.
- (Juan D et al., 2010) Juan D, Alexe G, Antes T et al. Identification of a microRNA panel for clear-cell kidney cancer. *Urology* 2010; 75: 835–841.
- (Kato K et al., 2002) Kato K, Hida Y, Miyamoto M, et al: Overexpression of caveolin-1 in esophageal squamous cell carcinoma correlates with lymph node metastasis and pathologic stage. *Cancer* 94: 929-933, 2002.
- (Kato M et al., 2007) Kato M, Zhang J, Wang M, Lanting L, Yuan H, Rossi JJ, Natarajan R. MicroRNA-192 in diabetic kidney glomeruli and its function in TGF-beta-induced collagen expression via inhibition of E-box repressors. *Proc Natl Acad Sci U S A*. 2007 Feb 27;104(9):3432-7. Epub 2007 Feb 20.
- (Kato M et al., 2009) Kato M, Dang V, Wang M, Park JT, Deshpande S, Kadam S, Mardiros A, Zhan Y, Oettgen P, Putta S, Yuan H, Lanting L, Natarajan R. TGF- β induces acetylation of chromatin and of Ets-1 to alleviate repression of miR-192 in diabetic nephropathy. *Sci Signal*. 2013 Jun 4;6(278):ra43. doi: 10.1126/scisignal.2003389.
- (Kato M et al., 2011) Kato M, Arce L, Wang M, Putta S, Lanting L, Natarajan R. A microRNA circuit mediates transforming growth factor- β 1 autoregulation in renal glomerular mesangial cells. *Kidney Int*. 2011 Aug;80(4):358-68. doi: 10.1038/ki.2011.43. Epub 2011 Mar 9.
- (Kato N et al., 2006) Kato N, Sasou S, Motoyama T. Expression of hepatocyte nuclear factor-1beta (HNF-1beta) in clear cell tumors and endometriosis of the ovary. *Mod Pathol*. 2006 Jan;19(1):83-9.
- (Kato N et al., 2007) Kato N, Tamura G, Motoyama T. Hypomethylation of hepatocyte nuclear factor-1beta (HNF-1beta) CpG island in clear cell carcinoma of the ovary. *Virchows Arch*. 2008 Feb;452(2):175-80. Epub 2007 Dec 8.
- (Kato N 2009) Kato N, Motoyama T. Expression of hepatocyte nuclear factor-1beta in human urogenital tract during the embryonic stage. *Anal Quant Cytol Histol*. 2009 Feb;31(1):34-40.

- (Kato N et al., 2009 bis) Kato N, Motoyama T. Hepatocyte nuclear factor-1beta (HNF-1beta) in human urogenital organs: its expression and role in embryogenesis and tumorigenesis. *Histol Histopathol.* 2009 Nov;24(11):1479-86. doi: 10.14670/HH-24.1479.
- (Kaucsár T et al., 2010) Kaucsár T, Rácz Z, Hamar P. Post-transcriptional gene-expression regulation by micro RNA (miRNA) network in renal disease. *Adv Drug Deliv Rev.* 2010 Nov 30;62(14):1390-401. doi: 10.1016/j.addr.2010.10.003. Epub 2010 Oct 19.
- (Kellendonk C et al., 2000) Kellendonk C, Opherk C, Anlag K, Schütz G, Tronche F. Hepatocyte-specific expression of Cre recombinase. *Genesis.* 2000 Feb;26(2):151-3
- (Khan A et al., 2018) Khan A, Fornes O, Stigliani A, Gheorghe M, Castro-Mondragon JA, van der Lee R, Bessy A, Chèneby J, Kulkarni SR, Tan G, Baranasic D, Arenillas DJ, Sandelin A, Vandepoele K, Lenhard B, Ballester B, Wasserman WW, Parcy F, Mathelier A. JASPAR 2018: update of the open-access database of transcription factor binding profiles and its web framework. *Nucleic Acids Res.* 2018 Jan 4;46(D1):D260-D266. doi: 10.1093/nar/gkx1126.
- (Kikuchi R et al., 2007) Kikuchi R, Kusuhara H, Hattori N, Kim I, Shiota K, Gonzalez FJ, Sugiyama Y. Regulation of tissue-specific expression of the human and mouse urate transporter 1 gene by hepatocyte nuclear factor 1 alpha/beta and DNA methylation. *Mol Pharmacol.* 2007 Dec;72(6):1619-25. Epub 2007 Sep 13.
- (Kim VN et al., 2009) Kim VN, Han J, Siomi MC. Biogenesis of small RNAs in animals. *Nat Rev Mol Cell Biol.* 2009 Feb;10(2):126-39. doi: 10.1038/nrm2632.
- (Klein J et al., 2014) Klein, J., Buffin-Meyer, B., Mullen, W., Carty, D. M. et al. Clinical proteomics in obstetrics and neonatology. *Expert Rev. Proteomics.* 2014, 11 (1), 75-89.
- (Kobayashi A et al., 2008) Kobayashi A, Valerius MT, Mugford JW, Carroll TJ, Self M, Oliver G, McMahon AP: Six2 defines and regulates a multipotent self-renewing nephron progenitor population throughout mammalian kidney development. *Cell Stem Cell* 3: 169–181, 2008
- (Kolatsi-Joannou M 2001) Kolatsi-Joannou M, Bingham C, Ellard S, Bulman MP, Allen LI, Hattersley AT, Woolf AS. Hepatocyte nuclear factor-1beta: a new kindred with renal cysts and diabetes and gene expression in normal human development. *J Am Soc Nephrol.* 2001 Oct;12(10):2175-80.
- (Kompatscher A et al., 2017) Kompatscher A, de Baaij JHF, Aboudehen K, Hoefnagels APWM, Igarashi P, Bindels RJM, Veenstra GJC, Hoenderop JGJ. Loss of transcriptional activation of the potassium channel Kir5.1 by HNF1 β drives autosomal dominant tubulointerstitial kidney disease. *Kidney Int.* 2017 Nov;92(5):1145-1156. doi: 10.1016/j.kint.2017.03.034. Epub 2017 May 31.
- (Kompatscher A et al., 2018) Kompatscher A, de Baaij JHF, Aboudehen K, Farahani S, van Son LHJ, Milatz S, Himmerkus N, Veenstra GC, Bindels RJM, Hoenderop JGJ. Transcription factor HNF1 β regulates expression of the calcium-sensing receptor in the thick ascending limb of the kidney. *Am J Physiol Renal Physiol.* 2018 Jul 1;315(1):F27-F35. doi: 10.1152/ajprenal.00601.2017. Epub 2018 Mar 21.
- (Konrad M et al., 2004) Konrad M, Schlingmann KP, Gudermann T. Insights into the molecular nature of magnesium homeostasis. *Am J Physiol Renal Physiol.* 2004 Apr;286(4):F599-605.
- (Kornfeld JW et al., 2013) Kornfeld JW, Baitzel C, Könner AC, Nicholls HT, Vogt MC, Herrmanns K, Scheja L, Haumaitre C, Wolf AM, Knippschild U, Seibler J, Cereghini S, Heeren J, Stoffel M, Brüning JC. Obesity-induced overexpression of miR-802 impairs glucose metabolism through silencing of Hnf1b. *Nature.* 2013 Feb 7;494(7435):111-5. doi: 10.1038/nature11793.
- (Krupa A et al, 2010) Krupa A, Jenkins R, Luo DD, Lewis A, Phillips A, Fraser D. Loss of MicroRNA-192 promotes fibrogenesis in diabetic nephropathy. *J Am Soc Nephrol.* 2010 Mar;21(3):438-47. doi: 10.1681/ASN.2009050530. Epub 2010 Jan 7.
- (Kuchen S et al., 2010) Kuchen S, Resch W, Yamane A, Kuo N, Li Z, Chakraborty T, Wei L, Laurence A, Yasuda T, Peng S, Hu-Li J, Lu K, Dubois W, Kitamura Y, Charles N, Sun HW, Muljo S, Schwartzberg PL, Paul WE, O'Shea J, Rajewsky K, Casellas R. Regulation of microRNA expression and abundance during lymphopoiesis. *Immunity.* 2010 Jun 25;32(6):828-39. doi: 10.1016/j.immuni.2010.05.009. Epub 2010 Jun 3.
- (Lagos-Quintana M et al., 2001) Lagos-Quintana M, Rauhut R, Lendeckel W, Tuschl T. Identification of novel genes coding for small expressed RNAs. *Science.* 2001 Oct 26;294(5543):853-8.
- (Latterich M et al., 2008) Latterich, M., Abramovitz, M., Leyland-Jones, B., Proteomics: new technologies and clinical applications. *Eur. J. Cancer* 2008, 44 (18), 2737-2741.
- (Laughon A 1991) Laughon A. DNA binding specificity of homeodomains. *Biochemistry.* 1991 Dec 3;30(48):11357-67.
- (Lavie Y et al., 1998) Lavie Y, Fiucci G and Liscovitch M: Up-regulation of caveolae and caveolar constituents in multidrug-resistant cancer cells. *J Biol Chem* 273: 32380-32383, 1998
- (Lazzaro D et al., 1992) Lazzaro D, De Simone V, De Magistris L, Lehtonen E, Cortese R. LFB1 and LFB3 homeoproteins are sequentially expressed during kidney development. *Development.* 1992 Feb;114(2):469-79.
- (Lebrun G et al., 2005) Lebrun G, Vasiliu V, Bellanné-Chantelot C, Bensman A, Ulinski T, Chrétien Y, Grünfeld JP. Cystic kidney disease, chromophobe renal cell carcinoma and TCF2 (HNF1 beta) mutations. *Nat Clin Pract Nephrol.* 2005 Dec;1(2):115-9.
- (Ledig S 2010) Ledig S, Schippert C, Strick R, Beckmann MW, Oppelt PG, Wieacker P. Recurrent aberrations identified by array-CGH in patients with Mayer-Rokitansky-Küster-Hauser syndrome. *Fertil Steril.* 2011 Apr;95(5):1589-94. doi: 10.1016/j.fertnstert.2010.07.1062. Epub 2010 Aug 24.

- (Lee H 2000) H. Lee, D. Volonte, F. Galbiati, P. Iyengar, D. M. Lublin, D. B. Bregman, M. T. Wilson, R. Campos-Gonzalez, B. Bouzahzah, R. G. Pestell, P. E. Scherer, and M. P. Lisanti. Constitutive and growth factor-regulated phosphorylation of caveolin-1 occurs at the same site (Tyr-14) in vivo: identification of a c-Src/Cav-1/Grb7 signaling cassette. *Mol. Endocrinol.*, vol. 14, no. 11, pp. 1750–75, Nov. 2000.
- (Lee Y 2004) Lee Y, Kim M, Han J, Yeom KH, Lee S, Baek SH, Kim VN. MicroRNA genes are transcribed by RNA polymerase II. *EMBO J.* 2004 Oct 13;23(20):4051-60. Epub 2004 Sep 16.
- (Lee JL 2008) Lee JL, Wang MJ, Sudhir PR, Chen JY. CD44 engagement promotes matrix-derived survival through the CD44-SRC-integrin axis in lipid rafts. *Mol Cell Biol.* 2008 Sep;28(18):5710-23. doi: 10.1128/MCB.00186-08. Epub 2008 Jul 21.
- (Lee RC et al., 1993) Lee RC, Feinbaum RL, Ambros V. The *C. elegans* heterochronic gene *lin-4* encodes small RNAs with antisense complementarity to *lin-14*. *Cell.* 1993 Dec 3;75(5):843-54.
- (Leiting B 1993) Leiting B, De Francesco R, Tomei L, Cortese R, Otting G, Wüthrich K. The three-dimensional NMR-solution structure of the polypeptide fragment 195-286 of the LFB1/HNF1 transcription factor from rat liver comprises a nonclassical homeodomain. *EMBO J.* 1993 May;12(5):1797-803.
- (Lewis BP et al., 2005) Lewis BP, Burge CB, Bartel DP. Conserved seed pairing, often flanked by adenosines, indicates that thousands of human genes are microRNA targets. *Cell.* 2005 Jan 14;120(1):15-20.
- (Li H et al., 1999) Li H, Arber S, Jessell TM, Edlund H. Selective agenesis of the dorsal pancreas in mice lacking homeobox gene *Hlx9*. *Nat Genet.* 1999 Sep;23(1):67-70.
- (Li L 2003) L. Li, C. H. Ren, S. A. Tahir, C. Ren, and T. C. Thompson, "Caveolin-1 maintains activated Akt in prostate cancer cells through scaffolding domain binding site interactions with and inhibition of serine/threonine protein phosphatases PPI and PP2A." *Mol. Cell. Biol.*, vol. 23, no. 24, pp. 9389–404, 2003.
- (Li S 1996) S. Li, J. Couet, and M. P. Lisanti, "Src tyrosine kinases, Galpha subunits, and H-Ras share a common membrane-anchored scaffolding protein, caveolin. Caveolin binding negatively regulates the auto-activation of Src tyrosine kinases." *J. Biol. Chem.*, vol. 271, no. 46, pp. 29182–90, Nov. 1996.
- (Lindner TH 1999) Lindner TH, Njolstad PR, Horikawa Y, Bostad L, Bell GI, Sovik O. A novel syndrome of diabetes mellitus, renal dysfunction and genital malformation associated with a partial deletion of the pseudo-POU domain of hepatocyte nuclear factor-1beta. *Hum Mol Genet.* 1999 Oct;8(11):2001-8.
- (Lindström NO et al., 2018) Lindström NO, McMahon JA, Guo J, Tran T, Guo Q, Rutledge E, Parvez RK, Saribekyan G, Schuler RE, Liao C, Kim AD, Abdelhalim A, Ruffins SW, Thornton ME, Basking L, Grubbs B, Kesselman C, McMahon AP. Conserved and Divergent Features of Human and Mouse Kidney Organogenesis. *J Am Soc Nephrol.* 2018 Mar;29(3):785-805. doi: 10.1681/ASN.2017080887. Epub 2018 Feb 15.
- (Little MH et al., 2007) Little MH, Brennan J, Georgas K, Davies JA, Davidson DR, et al. (2007) A high-resolution anatomical ontology of the developing murine genitourinary tract. *Gene Expr Patterns* 7: 680–699
- (Little M 2010) Little M, Georgas K, Pennisi D, Wilkinson L. Kidney development: two tales of tubulogenesis. *Curr Top Dev Biol.* 2010;90:193-229. doi: 10.1016/S0070-2153(10)90005-7.
- (Little MH et al., 2014) Little MH, Brown D, Humphreys BD, McMahon AP, Miner JH, Sands JM, Weisz OA, Mullins C, Hoshizaki D; Kidney Research National Dialogue (KRND). Defining kidney biology to understand renal disease. *Clin J Am Soc Nephrol.* 2014 Apr;9(4):809-11. doi: 10.2215/CJN.10851013. Epub 2013 Dec 26.
- (Liu H 2010) Liu H, Ren H, Spear BT. The mouse alpha-albumin (afamin) promoter is differentially regulated by hepatocyte nuclear factor 1 α and hepatocyte nuclear factor 1 β . *DNA Cell Biol.* 2011 Mar;30(3):137-47. doi: 10.1089/dna.2010.1097. Epub 2010 Oct 27.
- (Loirat C 2010) Loirat C, Bellanné-Chantelot C, Husson I, Deschênes G, Guignon V, Chabane N. Autism in three patients with cystic or hyperchogenic kidneys and chromosome 17q12 deletion. *Nephrol Dial Transplant.* 2010 Oct;25(10):3430-3. doi: 10.1093/ndt/gfq380. Epub 2010 Jun 28.
- (Lokmane L 2008) Lokmane L, Haumaitre C, Garcia-Villalba P, Anselme I, Schneider-Maunoury S, Cereghini S. Crucial role of vHNF1 in vertebrate hepatic specification. *Development.* 2008 Aug;135(16):2777-86. doi: 10.1242/dev.023010. Epub 2008 Jul 17.
- (Lokmane L 2010) Lokmane L, Heliot C, Garcia-Villalba P, Fabre M, Cereghini S. vHNF1 functions in distinct regulatory circuits to control ureteric bud branching and early nephrogenesis. *Development.* 2010 Jan;137(2):347-57. doi: 10.1242/dev.042226.
- (Long J 2011) Long J, Wang Y, Wang W, Chang BH, Danesh FR. MicroRNA-29c is a signature microRNA under high glucose conditions that targets Sprouty homolog 1, and its in vivo knockdown prevents progression of diabetic nephropathy. *J Biol Chem.* 2011 Apr 1;286(13):11837-48. doi: 10.1074/jbc.M110.194969. Epub 2011 Feb 10.
- (Long M 2012) Long M, Huang SH, Wu CH, Shackelford GM, Jong A. Lipid raft/caveolae signaling is required for *Cryptococcus neoformans* invasion into human brain microvascular endothelial cells. *J Biomed Sci.* 2012 Feb 8;19:19. doi: 10.1186/1423-0127-19-19.
- (Lu P et al., 2007) Lu P, Rha GB, Chi YI. Structural basis of disease-causing mutations in hepatocyte nuclear factor 1beta. *Biochemistry.* 2007 Oct 30;46(43):12071-80. Epub 2007 Oct 9.
- (Luo Z et al., 2014) Luo Z, Wu RR, Lv L, Li P, Zhang LY, Hao QL, Li W. Prognostic value of CD44 expression in non-small cell lung cancer: a systematic review. *Int J Clin Exp Pathol.* 2014 Jun 15;7(7):3632-46. eCollection 2014.

- (Lund E and Dahlberg JE, 2006) Lund E, Dahlberg JE. Substrate selectivity of exportin 5 and Dicer in the biogenesis of microRNAs. *Cold Spring Harb Symp Quant Biol.* 2006;71:59-66.
- (Lv W et al., 2018) Lv W, Fan F, Wang Y, Gonzalez-Fernandez E, Wang C, Yang L, Booz GW, Roman RJ. Therapeutic potential of microRNAs for the treatment of renal fibrosis and CKD. *Physiol Genomics.* 2018 Jan 1;50(1):20-34. doi: 10.1152/physiolgenomics.00039.2017. Epub 2017 Nov 10.
- (Ma L and Qu L, 2013) Ma L, Qu L. The function of microRNAs in renal development and pathophysiology. *J Genet Genomics.* 2013 Apr 20;40(4):143-52. doi: 10.1016/j.jgg.2013.03.002. Epub 2013 Mar 14.
- (Ma Z et al., 2007) Ma Z, Gong Y, Patel V, Karner CM, Fischer E, Hiesberger T, Carroll TJ, Pontoglio M, Igarashi P. Mutations of HNF-1beta inhibit epithelial morphogenesis through dysregulation of SOCS-3. *Proc Natl Acad Sci U S A.* 2007 Dec 18;104(51):20386-91. Epub 2007 Dec 12.
- (Madariaga L et al., 2013) Madariaga L, Morinière V, Jeanpierre C, Bouvier R, Loget P, Martinovic J, Dechelotte P, Leporrier N, Thauvin-Robinet C, Jensen UB, Gaillard D, Mathieu M, Turlin B, Attie-Bitach T, Salomon R, Gübler MC, Antignac C, Heidet L. Severe prenatal renal anomalies associated with mutations in HNF1B or PAX2 genes. *Clin J Am Soc Nephrol.* 2013 Jul;8(7):1179-87. doi: 10.2215/CJN.10221012. Epub 2013 Mar 28.
- (Maestro MA et al., 2003) Maestro MA, Boj SF, Luco RF, Pierreux CE, Cabedo J, Servitja JM, German MS, Rousseau GG, Lemaigre FP, Ferrer J. Hnf6 and Tcf2 (MODY5) are linked in a gene network operating in a precursor cell domain of the embryonic pancreas. *Hum Mol Genet.* 2003 Dec 15;12(24):3307-14. Epub 2003 Oct 21.
- (Magalhães P et al., 2016) Magalhães, P., Schanstra, J. P., Carrick, E., Mischak, H., Zurbig, P., Urinary biomarkers for renal tract malformations. *Expert. Rev. Proteomics.* 2016, 13 (12), 1121-1129.
- (Magalhães P et al., 2017) Magalhães P, Pejchinovski M, Markoska K, Banasik M4, Klinger M, Švec-Billá D, Rychlík I, Rroji M, Restivo A, Capasso G, Bob F, Schiller A, Ortiz A, Perez-Gomez MV, Cannata P, Sanchez-Niño MD, Naumovic R, Brkovic V, Polenakovic M, Mullen W, Vlahou A, Zurbig P, Pape L, Ferrario F, Denis C, Spasovski G, Mischak H, Schanstra JP. Association of kidney fibrosis with urinary peptides: a path towards non-invasive liquid biopsies? *Sci Rep.* 2017 Dec 5;7(1):16915. doi: 10.1038/s41598-017-17083-w.
- (Mahmoudi M et al., 2003) Mahmoudi M, Willgoss D, Cuttle L, Yang T, Pat B, Winterford C, Endre Z, Johnson DW, Gobe GC. In vivo and in vitro models demonstrate a role for caveolin-1 in the pathogenesis of ischaemic acute renal failure. *J Pathol* 200; 396–405, 2003
- (Martins AS et al., 2011) A. S. Martins, J. L. Ordóñez, A. T. Amaral, F. Prins, G. Floris, M. Debiec-Rychter, P. C. W. Hogendoorn, and E. de Alava, "IGF1R signaling in Ewing sarcoma is shaped by clathrin-/caveolin-dependent endocytosis.," *PLoS One*, vol. 6, no. 5, p. e19846, 2011
- (Massa F et al., 2013) Massa F, Garbay S, Bouvier R, Sugitani Y, Noda T, Gubler MC, Heidet L, Pontoglio M, Fischer E. Hepatocyte nuclear factor 1β controls nephron tubular development. *Development.* 2013 Feb;140(4):886-96. doi: 10.1242/dev.086546.
- (Mazière P and Enright AJ, 2007) Mazière P, Enright AJ. Prediction of microRNA targets. *Drug Discov Today.* 2007 Jun;12(11-12):452-8. Epub 2007 Apr 26.
- (McMahon AP 2016) McMahon AP. Development of the Mammalian Kidney. *Curr Top Dev Biol.* 2016;117:31-64. doi: 10.1016/bs.ctdb.2015.10.010. Epub 2016 Jan 23.
- (Meij IC et al., 2000) Meij IC, Koenderink JB, van Bokhoven H, Assink KF, Groenestege WT, de Pont JJ, Bindels RJ, Monnens LA, van den Heuvel LP, Knoers NV. Dominant isolated renal magnesium loss is caused by misrouting of the Na(+),K(+)-ATPase gamma-subunit. *Nat Genet.* 2000 Nov;26(3):265-6.
- (Meister G et al., 2004) Meister G, Landthaler M, Patkaniowska A, Dorsett Y, Teng G, Tuschl T. Human Argonaute2 mediates RNA cleavage targeted by miRNAs and siRNAs. *Mol Cell.* 2004 Jul 23;15(2):185-97.
- (Mendel DB 1991) Mendel DB, Hansen LP, Graves MK, Conley PB, Crabtree GR. HNF-1 alpha and HNF-1 beta (vHNF-1) share dimerization and homeo domains, but not activation domains, and form heterodimers in vitro. *Genes Dev.* 1991 Jun;5(6):1042-56.
- (Mendel DB 1991 bis) Mendel DB, Khavari PA, Conley PB, Graves MK, Hansen LP, Admon A, Crabtree GR. Characterization of a cofactor that regulates dimerization of a mammalian homeodomain protein. *Science.* 1991 Dec 20;254(5039):1762-7.
- (Meng Z 2010) Meng Z, Fu X, Chen X, Zeng S, Tian Y, Jove R, Xu R, Huang W. miR-194 is a marker of hepatic epithelial cells and suppresses metastasis of liver cancer cells in mice. *Hepatology.* 2010 Dec;52(6):2148-57. doi: 10.1002/hep.23915. Epub 2010 Oct 26.
- (Metzinger-Le Meuth V et al., 2018) Metzinger-Le Meuth V, Fourdinier O, Charnaux N, Massy ZA, Metzinger L. The expanding roles of microRNAs in kidney pathophysiology. *Nephrol Dial Transplant.* 2018 May 25. doi: 10.1093/ndt/gfy140. [Epub ahead of print]
- (Mischak H et al., 2015) Mischak, H., Delles, C., Vlahou, A., Vanholder, R., Proteomic biomarkers in kidney disease: issues in development and implementation. *Nat. Rev. Nephrol.* 2015, 11 (4), 221-232.
- (Moreno-De-Luca 2010) Moreno-De-Luca D, Mulle JG, Kaminsky EB, Sanders SJ, Myers SM, Adam MP, Pakula AT, Eisenhauer NJ, Uhas K, Weik L, Guy L, Care ME, Morel CF, Boni C, Salbert BA, Chandraredy A, Demmer LA, Chow EW, Surti U, Aradhya S, Pickering DL, Golden DM, Sanger WG, Aston E, Brothman AR, Gliem TJ, Thorland EC, Ackley T, Iyer R, Huang S, Barber JC, Crolla JA, Warren ST, Martin CL, Ledbetter DH. Deletion 17q12 is a recurrent copy number variant that confers high risk of autism and schizophrenia. *Am J Hum Genet.* 2010 Nov 12;87(5):618-30. doi: 10.1016/j.ajhg.2010.10.004. Epub 2010 Nov 4.

- (Morita S et al., 2007) Morita S, Horii T, Kimura M, Goto Y, Ochiya T, Hatada I. *Genomics*. 2007 Jun; 89 (6): 687-96. Epub 2007 Apr 5. *Genomics*. 2007 Jun;89(6):687-96. Epub 2007 Apr 5.
- (Mouraviev V 2002) Mouraviev V, Li L, Tahir SA, et al: The role of caveolin-1 in androgen insensitive prostate cancer. *J Urol* 168: 1589-1596, 2002.
- (Mikami R 2015) S. Mikami, R. Mizuno, T. Kosaka, H. Saya, M. Oya, and Y. Okada. Expression of TNF- α and CD44 is implicated in poor prognosis, cancer cell invasion, metastasis and resistance to the sunitinib treatment in clear cell renal cell carcinomas. *Int. J. Cancer*, vol. 136, no. 7, pp. 1504–14, Apr. 2015.
- (Murchison EP and Hannon GJ 2004) Murchison EP, Hannon GJ. miRNAs on the move: miRNA biogenesis and the RNAi machinery. *Curr Opin Cell Biol*. 2004 Jun;16(3):223-9.
- (Murray PJ 2008) Murray PJ, Thomas K, Mulgrew CJ, Ellard S, Edghill EL, Bingham C. Whole gene deletion of the hepatocyte nuclear factor-1beta gene in a patient with the prune-belly syndrome. *Nephrol Dial Transplant*. 2008 Jul;23(7):2412-5. doi: 10.1093/ndt/gfn169. Epub 2008 Apr 14..
- (Musetti C 2014) Musetti C, Quaglia M, Mellone S, Pagani A, Fusco I, Monzani A, Giordano M, Stratta P. Chronic renal failure of unknown origin is caused by HNF1B mutations in 9% of adult patients: a single centre cohort analysis. *Nephrology (Carlton)*. 2014 Apr;19(4):202-9. doi: 10.1111/nep.12199.
- (Nagalakshmi VK et al., 2010) Nagalakshmi VK, Ren Q, Pugh MM, Valerius MT, McMahon AP, Yu J. Dicer regulates the development of nephrogenic and ureteric compartments in the mammalian kidney. *Kidney Int*. 2011 Feb;79(3):317-30. doi: 10.1038/ki.2010.385. Epub 2010 Oct 13.
- (Nagasawa Y 2002) Nagasawa Y, Matthiesen S, Onuchic LF, Hou X, Bergmann C, Esquivel E, Senderek J, Ren Z, Zeltner R, Furu L, Avner E, Moser M, Somlo S, Guay-Woodford L, Büttner R, Zerres K, Germino GG. Identification and characterization of Pkhd1, the mouse orthologue of the human ARPKD gene. *J Am Soc Nephrol*. 2002 Sep;13(9):2246-58.
- (Nakayama M 2010) Nakayama M, Nozu K, Goto Y, Kamei K, Ito S, Sato H, Emi M, Nakanishi K, Tsuchiya S, Iijima K. HNF1B alterations associated with congenital anomalies of the kidney and urinary tract. *Pediatr Nephrol*. 2010 Jun;25(6):1073-9. doi: 10.1007/s00467-010-1454-9. Epub 2010 Feb 13.
- (Narayana N 2001) Narayana N, Hua Q, Weiss MA. The dimerization domain of HNF-1alpha: structure and plasticity of an intertwined four-helix bundle with application to diabetes mellitus. *J Mol Biol*. 2001 Jul 13;310(3):635-58.
- (Naylor RW et al., 2012) Naylor RW, Przepiorski A, Ren Q, Yu J, Davidson AJ. HNF1 β is essential for nephron segmentation during nephrogenesis. *J Am Soc Nephrol*. 2013 Jan;24(1):77-87. doi: 10.1681/ASN.2012070756. Epub 2012 Nov 15.
- (Naylor RW et al., 2013) Naylor RW, Przepiorski A, Ren Q, Yu J, Davidson AJ. HNF1 β is essential for nephron segmentation during nephrogenesis. *J Am Soc Nephrol*. 2013 Jan;24(1):77-87. doi: 10.1681/ASN.2012070756. Epub 2012 Nov 15.
- (Nicosia A et al., 1990) Nicosia A, Monaci P, Tomei L, De Francesco R, Nuzzo M, Stunnenberg H, Cortese R. A myosin-like dimerization helix and an extra-large homeodomain are essential elements of the tripartite DNA binding structure of LFB1. *Cell*. 1990 Jun 29;61(7):1225-36.
- (Offield MF et al., 1996) Offield MF, Jetton TL, Labosky PA, Ray M, Stein RW, Magnuson MA, Hogan BL, Wright CV. PDX-1 is required for pancreatic outgrowth and differentiation of the rostral duodenum. *Development*. 1996 Mar;122(3):983-95.
- (Odom DT et al., 2004) Odom DT, Zizlsperger N, Gordon DB, Bell GW, Rinaldi NJ, Murray HL, Volkert TL, Schreiber J, Rolfe PA, Gifford DK, Fraenkel E, Bell GI, Young RA. Control of pancreas and liver gene expression by HNF transcription factors. *Science*. 2004 Feb 27;303(5662):1378-81.
- (Oliver J 1968) Oliver J: *Nephrons and Kidneys: A Quantitative Study of Development and Evolutionary Mammalian Renal Architectonics*, New York, Harper & Row, 1968
- (Oliver-Krasinski JM et al., 2009) Oliver-Krasinski JM, Kasner MT, Yang J, Crutchlow MF, Rustgi AK, Kaestner KH, Stoffers DA. The diabetes gene Pdx1 regulates the transcriptional network of pancreatic endocrine progenitor cells in mice. *J Clin Invest*. 2009 Jul;119(7):1888-98. doi: 10.1172/JCI37028.
- (Orian-Rousseau V 2010) V. Orian-Rousseau. CD44, a therapeutic target for metastasising tumours. *Eur. J. Cancer*, vol. 46, no. 7, pp. 1271–1277, 2010.
- (Orian-Rousseau V and Sleeman J, 2014) V. Orian-Rousseau and J. Sleeman. CD44 is a multidomain signaling platform that integrates extracellular matrix cues with growth factor and cytokine signals. *Adv. Cancer Res.*, vol. 123, pp. 231–254, 2014.
- (Oram RA et al., 2010) Oram RA, Edghill EL, Blackman J, Taylor MJ, Kay T, Flanagan SE, Ismail-Pratt I, Creighton SM, Ellard S, Hattersley AT, Bingham C. Mutations in the hepatocyte nuclear factor-1 β (HNF1B) gene are common with combined uterine and renal malformations but are not found with isolated uterine malformations. *Am J Obstet Gynecol*. 2010 Oct;203(4):364.e1-5. doi: 10.1016/j.ajog.2010.05.022. Epub 2010 Jul 15.
- (Ott MO 1991) Ott MO, Rey-Campos J, Cereghini S, Yaniv M. vHNF1 is expressed in epithelial cells of distinct embryonic origin during development and precedes HNF1 expression. *Mech Dev*. 1991 Dec;36(1-2):47-58.

- (Pandey P et al., 2008) Pandey P, Brors B, Srivastava PK, Bott A, Boehn SN, Groene HJ, Gretz N. Microarray-based approach identifies microRNAs and their target functional patterns in polycystic kidney disease. *BMC Genomics*. 2008 Dec 23;9:624. doi: 10.1186/1471-2164-9-624.
- (Parolini M 1999) I. Parolini, M. Sargiacomo, F. Galbiati, G. Rizzo, F. Grignani, J. A. Engelman, T. Okamoto, T. Ikezu, P. E. Scherer, R. Mora, E. Rodriguez-Boulan, C. Peschle, and M. P. Lisanti. Expression of caveolin-1 is required for the transport of caveolin-2 to the plasma membrane. Retention of caveolin-2 at the level of the golgi complex. *J. Biol. Chem.*, vol. 274, no. 36, pp. 25718–25, Sep. 1999.
- (Parton RG 2007) R. G. Parton and K. Simons. The multiple faces of caveolae. *Nat. Rev. Mol. Cell Biol.*, vol. 8, no. 3, pp. 185–94, Mar. 2007.
- (Pastore A 1992) Pastore A, De Francesco R, Castiglione Morelli MA, Nalis D, Cortese R. The dimerization domain of LFB1/HNF1 related transcription factors: a hidden four helix bundle? *Protein Eng.* 1992 Dec;5(8):749-57.
- (Pasquinelli AE et al., 2000) Pasquinelli AE, Reinhart BJ, Slack F, Martindale MQ, Kuroda MI, Maller B, Hayward DC, Ball EE, Degnan B, Müller P, Spring J, Srinivasan A, Fishman M, Finnerty J, Corbo J, Levine M, Leahy P, Davidson E, Ruvkun G. Conservation of the sequence and temporal expression of let-7 heterochronic regulatory RNA. *Nature*. 2000 Nov 2;408(6808):86-9.
- (Patel V., et al., 2012) Patel V., Hajarnis S., Williams D., Hunter R., Huynh D., Igarashi P. (2012) MicroRNAs regulate renal tubule maturation through modulation of Pkd1. *J. Am. Soc. Nephrol.* 23, 1941–1948
- (Patel V et al., 2013) Patel V, Williams D, Hajarnis S, Hunter R, Pontoglio M, Somlo S, Igarashi P (2013) miR-17~92 miRNA cluster promotes kidney cyst growth in polycystic kidney disease. *Proc Natl Acad Sci U S A* 110: 10765–10770
- (Pearson ER et al., 2004) Pearson ER, Badman MK, Lockwood CR, Clark PM, Ellard S, Bingham C, Hattersley AT. Contrasting diabetes phenotypes associated with hepatocyte nuclear factor-1alpha and -1beta mutations. *Diabetes Care*. 2004 May;27(5):1102-7.
- (Peng R et al., 2015) Peng R, Zhou L, Zhou Y, Zhao Y, Li Q, Ni D, Hu Y, Long Y, Liu J, Lyu Z, Mao Z, Yuan Y, Huang, Zhao H, Li G, Zhou Q. MiR-30a Inhibits the Epithelial--Mesenchymal Transition of Podocytes through Downregulation of NFATc3. *Int J Mol Sci*. 2015 Oct 12;16(10):24032-47. doi: 10.3390/ijms161024032.
- (Phua YL and Ho J, 2015) Phua YL, Ho J. MicroRNAs in the pathogenesis of cystic kidney disease. *Curr Opin Pediatr*. 2015 Apr;27(2):219-26. doi: 10.1097/MOP.0000000000000168.
- (Phua YL et al., 2016) Phua YL, Gilbert T, Combes A, Wilkinson L, Little MH. Neonatal vascularization and oxygen tension regulate appropriate perinatal renal medulla/papilla maturation. *J Pathol*. 2016 Apr;238(5):665-76. doi: 10.1002/path.4690.
- (Pichiorri F et al., 2010) Pichiorri F, Suh SS, Rocci A, De Luca L, Taccioli C, Santhanam R, Zhou W, Benson DM Jr, Hofmeister C, Alder H, Garofalo M, Di Leva G, Volinia S, Lin HJ, Perrotti D, Kuehl M, Aqeilan RI, Palumbo A, Croce CM. Downregulation of p53-inducible microRNAs 192, 194, and 215 impairs the p53/MDM2 autoregulatory loop in multiple myeloma development. *Cancer Cell*. 2010 Oct 19;18(4):367-81. doi: 10.1016/j.ccr.2010.09.005.
- (Pierreux CE et al., 2006) Pierreux CE, Poll AV, Kemp CR, Clotman F, Maestro MA, Cordi S, Ferrer J, Leyns L, Rousseau GG, Lemaigre FP. The transcription factor hepatocyte nuclear factor-6 controls the development of pancreatic ducts in the mouse. *Gastroenterology*. 2006 Feb;130(2):532-41.
- (Piontek K et al., 2007) Piontek K, Menezes LF, Garcia-Gonzalez MA, Huso DL, Germino GG. A critical developmental switch defines the kinetics of kidney cyst formation after loss of Pkd1. *Nat Med*. 2007 Dec;13(12):1490-5. Epub 2007 Oct 28.
- (Poll AV et al., 2006) Poll AV, Pierreux CE, Lokmane L, Haumaitre C, Achouri Y, Jacquemin P, Rousseau GG, Cereghini S, Lemaigre FP. A vHNF1/TCF2-HNF6 cascade regulates the transcription factor network that controls generation of pancreatic precursor cells. *Diabetes*. 2006 Jan;55(1):61-9.
- (Pontoglio et al., 1996) Pontoglio M, Barra J, Hadchouel M, Doyen A, Kress C, Bach JP, Babinet C, Yaniv M. Hepatocyte nuclear factor 1 inactivation results in hepatic dysfunction, phenylketonuria, and renal Fanconi syndrome. *Cell*. 1996 Feb 23;84(4):575-85.
- (Pontoglio M et al., 2000) Pontoglio M, Prié D, Cheret C, Doyen A, Leroy C, Froguel P, Velho G, Yaniv M, Friedlander G. HNF1alpha controls renal glucose reabsorption in mouse and man. *EMBO Rep*. 2000 Oct;1(4):359-65.
- (Potter EL 1972) Potter EL. *Normal and Abnormal Development of the Kidney*, Chicago, Year Book Medical Publishers, Inc., 1972
- (Pouilhe M et al., 2007) Pouilhe M, Gilardi-Hebenstreit P, Desmarquet-Trin Dinh C, Charnay P. Direct regulation of vHnf1 by retinoic acid signaling and MAF-related factors in the neural tube. *Dev Biol*. 2007 Sep 15;309(2):344-57. Epub 2007 Jul 10.
- (Power SC and Cereghini S, 1996) Power SC, Cereghini S. Positive regulation of the vHNF1 promoter by the orphan receptors COUP-TF1/Ear3 and COUP-TFII/Arp1. *Mol Cell Biol*. 1996 Mar;16(3):778-91.
- (Putta S 2012) Putta S, Lanting L, Sun G, Lawson G, Kato M, Natarajan R. Inhibiting microRNA-192 ameliorates renal fibrosis in diabetic nephropathy. *J Am Soc Nephrol*. 2012 Mar;23(3):458-69. doi: 10.1681/ASN.2011050485. Epub 2012 Jan 5.
- (Raaijmakers A 2015) Raaijmakers A, Corveleyn A, Devriendt K, van Tienoven TP, Allegaert K, Van Dyck M, van den Heuvel L, Kuypers D, Claes K, Mekahli D, Levchenko E. Criteria for HNF1B analysis in patients with congenital abnormalities of kidney and urinary tract. *Nephrol Dial Transplant*. 2015 May;30(5):835-42. doi: 10.1093/ndt/gfu370. Epub 2014 Dec 13.

- (Raciti D 2008) Raciti D, Reggiani L, Geffers L, Jiang Q, Bacchion F, Subrizi AE, Clements D, Tindal C, Davidson DR, Kaissling B, Brändli AW. Organization of the pronephric kidney revealed by large-scale gene expression mapping. *Genome Biol.* 2008;9(5):R84. doi: 10.1186/gb-2008-9-5-r84. Epub 2008 May 20.
- (Rajewsky N 2006) Rajewsky N. microRNA target predictions in animals. *Nat Genet.* 2006 Jun;38 Suppl:S8-13.
- (Rebouissou S 2005) Rebouissou S, Vasiliu V, Thomas C, Bellanné-Chantelot C, Bui H, Chrétien Y, Timsit J, Rosty C, Laurent-Puig P, Chauveau D, Zucman-Rossi J. Germline hepatocyte nuclear factor 1alpha and 1beta mutations in renal cell carcinomas. *Hum Mol Genet.* 2005 Mar 1;14(5):603-14. Epub 2005 Jan 13.
- (Reinhart BJ et al., 2000) Reinhart BJ, Slack FJ, Basson M, Pasquinelli AE, Bettinger JC, Rougvie AE, Horvitz HR, Ruvkun G. The 21-nucleotide let-7 RNA regulates developmental timing in *Caenorhabditis elegans*. *Nature.* 2000 Feb 24;403(6772):901-6.
- (Reményi A et al., 2004) Reményi A, Schöler HR, Wilmanns M. Combinatorial control of gene expression. *Nat Struct Mol Biol.* 2004 Sep;11(9):812-5. Review.
- (Resing, KA et al., 2005) Resing, K. A., Ahn, N. G., Proteomics strategies for protein identification. *FEBS Lett.* 2005, 579 (4), 885-889.
- (Rey-Campos J 1991) Rey-Campos J, Chouard T, Yaniv M, Cereghini S. vHNF1 is a homeoprotein that activates transcription and forms heterodimers with HNF1. *EMBO J.* 1991 Jun;10(6):1445-57.
- (Ringeisen F et al., 1993) Ringeisen F, Rey-Campos J, Yaniv M. The transactivation potential of variant hepatocyte nuclear factor 1 is modified by alternative splicing. *J Biol Chem.* 1993 Dec 5;268(34):25706-11.
- (Roelandt P et al., 2012) Roelandt P, Antoniou A, Libbrecht L, Van Steenberghe W, Laleman W, Verslype C, Van der Merwe S, Nevens F, De Vos R, Fischer E, Pontoglio M, Lemaigre F, Cassiman D. HNF1B deficiency causes ciliary defects in human cholangiocytes. *Hepatology.* 2012 Sep;56(3):1178-81. doi: 10.1002/hep.25876. Epub 2012 Jul 19.
- (Rose RB et al., 2000) Rose RB, Bayle JH, Endrizzi JA, Cronk JD, Crabtree GR, Alber T. Structural basis of dimerization, coactivator recognition and MODY3 mutations in HNF-1alpha. *Nat Struct Biol.* 2000 Sep;7(9):744-8.
- (Rose RB et al., 2000 bis) Rose RB, Endrizzi JA, Cronk JD, Holton J, Alber T. High-resolution structure of the HNF-1alpha dimerization domain. *Biochemistry.* 2000 Dec 12;39(49):15062-70.
- (Rumballe B et al., 2010) Rumballe B, Georgas K, Wilkinson L, Little M. Molecular anatomy of the kidney: what have we learned from gene expression and functional genomics? *Pediatr Nephrol.* 2010 Jun;25(6):1005-16. doi: 10.1007/s00467-009-1392-6. Epub 2010 Jan 5.
- (Sagen JV et al., 2003) Sagen JV, Bostad L, Njølstad PR, Søvik O. Enlarged nephrons and severe nondiabetic nephropathy in hepatocyte nuclear factor-1beta (HNF-1beta) mutation carriers. *Kidney Int.* 2003 Sep;64(3):793-800.
- (Sadler TW 1990) Sadler TW. Genitourinary system. In: Langman's medical embryology. 5th. Sadler TW (ed) Williams & Wilkins. Maltimore. pp 235-268
- (Saini HK et al., 2008) Saini HK, Enright AJ, Griffiths-Jones S. Annotation of mammalian primary microRNAs. *BMC Genomics.* 2008 Nov 27;9:564. doi: 10.1186/1471-2164-9-564.
- (Sequeira-Lopez ML et al., 2010) Sequeira-Lopez ML, Weatherford ET, Borges GR et al. The microRNAProcessing enzyme dicer maintains juxtaglomerular cells. *J Am Soc Nephrol* 2010; 21: 460-467.
- (Schott O et al., 1997) Schott O, Billeter M, Leiting B, Wider G, Wüthrich K. The NMR solution structure of the non-classical homeodomain from the rat liver LFB1/HNF1 transcription factor. *J Mol Biol.* 1997 Apr 4;267(3):673-83.
- (Short KM et al., 2014) Short KM, Combes AN, Lefèvre J, Ju AL, Georgas KM, Lambertson T, Cairncross O, Rumballe BA, McMahon AP, Hamilton NA, Smyth IM, Little MH: Global quantification of tissue dynamics in the developing mouse kidney. *Dev Cell* 29: 188-202, 2014
- (Schwarz DS et al., 2003) Schwarz DS, Hutvagner G, Du T, Xu Z, Aronin N, Zamore PD. Asymmetry in the assembly of the RNAi enzyme complex. *Cell.* 2003 Oct 17;115(2):199-208.
- (Senkel S et al., 2005) Senkel S, Lucas B, Klein-Hitpass L, Ryffel GU. Identification of target genes of the transcription factor HNF1beta and HNF1alpha in a human embryonic kidney cell line. *Biochim Biophys Acta.* 2005 Dec 20;1731(3):179-90. Epub 2005 Nov 2.
- (Septramaniam S et al., 2010) Septramaniam S, Armugam A, Lim KY et al. MicroRNA 320a functions as a novel endogenous modulator of aquaporins 1 and 4 as well as a potential therapeutic target in cerebral ischemia. *J Biol Chem* 2010; 285: 29223-29230.
- (Septramaniam S et al., 2011) Septramaniam S, Karolina DS, Armugam A et al. Micrornas: potential applications in aquaporin associated pathogenesis. In: Mulligan JA (ed.) *MicroRNA: Expression, Detection and Therapeutic Strategies.* Nova Science Publishers, Inc, 2011 pp 1-32, Chapter 1.
- (Sequeira Lopez ML et al., 2003) Sequeira Lopez ML, Chervakovskiy DR, Nomasa T, Wall L, Yanagisawa M, Gomez RA: The embryo makes red blood cell progenitors in every tissue simultaneously with blood vessel morphogenesis. *Am J Physiol Regul Integr Comp Physiol* 284: R1126-R1137, 2003
- (Schedl A 2007) Schedl A. Renal abnormalities and their developmental origin. *Nat Rev Genet.* 2007 Oct;8(10):791-802.

- (Schaub S et al., 2004) Schaub, S., Wilkins, J., Weiler, T., Sangster, K. et al. Urine protein profiling with surface-enhanced laser-desorption/ionization time-of-flight mass spectrometry. *Kidney Int.* 2004, 65 (1), 323-332.
- (Shields BM et al., 2010) Shields BM, Hicks S, Shepherd MH, Colclough K, Hattersley AT, Ellard S. Maturity-onset diabetes of the young (MODY): how many cases are we missing? *Diabetologia.* 2010 Dec;53(12):2504-8. doi: 10.1007/s00125-010-1799-4. Epub 2010 May 25.
- (Schirle NT et al., 2014) Schirle NT, Sheu-Gruttadauria JI, MacRae IJ. Structural basis for microRNA targeting. *Science.* 2014 Oct 31;346(6209):608-13. doi: 10.1126/science.1258040.
- (Schlegel A 2000) A. Schlegel and M. P. Lisanti. A molecular dissection of caveolin-1 membrane attachment and oligomerization. Two separate regions of the caveolin-1 C-terminal domain mediate membrane binding and oligomer/oligomer interactions in vivo. *J. Biol. Chem.*, vol. 275, no. 28, pp. 21605–17, Jul. 2000.
- (Schlegel A 2001) A. Schlegel, P. Arvan, and M. P. Lisanti. Caveolin-1 binding to endoplasmic reticulum membranes and entry into the regulated secretory pathway are regulated by serine phosphorylation. Protein sorting at the level of the endoplasmic reticulum. *J. Biol. Chem.*, vol. 276, no. 6, pp. 4398–408, Feb. 2001.
- (Shao X et al., 2002) Shao X, Somlo S, Igarashi P. Epithelial-specific Cre/lox recombination in the developing kidney and genitourinary tract. *J Am Soc Nephrol.* 2002 Jul;13(7):1837-46.
- (Shi S et al., 2008) Shi S, Yu L, Chiu C, Sun Y, Chen J, Khitrov G, Merckenschlager M, Holzman LB, Zhang W, Mundel P, Bottinger EP. Podocyte-selective deletion of *dicer* induces proteinuria and glomerulosclerosis. *J Am Soc Nephrol.* 2008 Nov;19(11):2159-69. doi: 10.1681/ASN.2008030312. Epub 2008 Sep 5.
- (Short KM et al., 2014) Short KM, Combes AN, Lefevre J, Ju AL, Georgas KM, Lambertson T, Cairncross O, Rumballe BA, McMahon AP, Hamilton NA, Smyth IM, Little MH. Global quantification of tissue dynamics in the developing mouse kidney. *Dev Cell.* 2014 Apr 28;29(2):188-202. doi: 10.1016/j.devcel.2014.02.017.
- (Simon DB et al., 1996) Simon DB, Karet FE, Hamdan JM, DiPietro A, Sanjad SA, Lifton RP. Bartter's syndrome, hypokalaemic alkalosis with hypercalciuria, is caused by mutations in the Na-K-2Cl cotransporter NKCC2. *Nat Genet.* 1996 Jun;13(2):183-8.
- (Sirbu IO et al., 2005) Sirbu IO, Gresh L, Barra J, Duester G. Shifting boundaries of retinoic acid activity control hindbrain segmental gene expression. *Development.* 2005 Jun;132(11):2611-22. Epub 2005 May 4.
- (Silva WI 2007) Silva WI, Maldonado HM, Velázquez G, García JO, González FA. Caveolins in glial cell model systems: from detection to significance. *J Neurochem.* 2007 Nov;103 Suppl 1:101-12.
- (Skelton TP 1998) T. P. Skelton, C. Zeng, A. Nocks, and I. Stamenkovic. Glycosylation provides both stimulatory and inhibitory effects on cell surface and soluble CD44 binding to hyaluronan. *J. Cell Biol.*, vol. 140, no. 2, pp. 431–446, 1998.
- (Sorensson J 2002) Sorensson J, Fierlbeck W, Heider T, Schwarz K, Park DS, Mundel P, Lisanti M, Ballermann BJ. Glomerular endothelial fenestrae in vivo are not formed from caveolae. *J Am Soc Nephrol* 13: 2639–2647, 2002
- (Sourdive DJ 1993) Sourdive DJ, Chouard T, Yaniv M. The HNF1 C-terminal domain contributes to transcriptional activity and modulates nuclear localisation. *C R Acad Sci III.* 1993;316(4):385-94.
- (Song J et al., 2006) Song J, Kim HJ, Gong Z, Liu NA, Lin S. *Vhnf1* acts downstream of *Bmp*, *Fgf*, and *RA* signals to regulate endocrine beta cell development in zebrafish. *Dev Biol.* 2007 Mar 15;303(2):561-75. Epub 2006 Dec 1.
- (Soutoglou E 2000) Soutoglou E, Katrakili N, Talianidis I. Acetylation regulates transcription factor activity at multiple levels. *Mol Cell.* 2000 Apr;5(4):745-51.
- (Sowa G 2012) G. Sowa. Caveolae, caveolins, cavins, and endothelial cell function: new insights. *Front. Physiol.*, vol. 2, no. January, p. 120, Jan. 2012.
- (Stenson PD et al., 2003) Stenson PD, Ball EV, Mort M, Phillips AD, Shiel JA, Thomas NS, Abeyasinghe S, Krawczak M, Cooper DN. Human Gene Mutation Database (HGMD): 2003 update. *Hum Mutat.* 2003 Jun;21(6):577-81.
- (Stenson PD 2014) Stenson PD, Mort M, Ball EV, Shaw K, Philips A, and Cooper DN (2014). The Human Gene Mutation Database: building a comprehensive mutation repository for clinical and molecular genetics, diagnostic testing and personalized genomic medicine. *Hum Genet* 133:1-9.
- (Subramaniam V 2007) V. Subramaniam, I. R. Vincent, M. Gilakjan, and S. Jothy, Suppression of human colon cancer tumors in nude mice by siRNA CD44 gene therapy. *Exp. Mol. Pathol.*, vol. 83, no. 3, pp. 332–40, Dec. 2007.
- (Sun Y et al., 2004) Sun Y, Koo S, White N, Peralta E, Esau C, Dean NM, Perera RJ. Development of a micro-array to detect human and mouse microRNAs and characterization of expression in human organs. *Nucleic Acids Res.* 2004 Dec 22;32(22):e188.
- (Sun and Hopkins 2001) Sun Z, Hopkins N. *vhnf1*, the MODY5 and familial GCKD-associated gene, regulates regional specification of the zebrafish gut, pronephros, and hindbrain. *Genes Dev.* 2001 Dec 1;15(23):3217-29.
- (Tanaka T et al., 2004) Tanaka T, Tomaru Y, Nomura Y, Miura H, Suzuki M, Hayashizaki Y. Comprehensive search for HNF-1beta-regulated genes in mouse hepatoma cells perturbed by transcription regulatory factor-targeted RNAi. *Nucleic Acids Res.* 2004 May 17;32(9):2740-50. Print 2004.

- (Tanaka K et al., 2010) Tanaka K, Terryn S, Geffers L, Garbay S, Pontoglio M, Devuyst O. The transcription factor HNF1 α regulates expression of chloride-proton exchanger CIC-5 in the renal proximal tubule. *Am J Physiol Renal Physiol*. 2010 Dec;299(6):F1339-47. doi: 10.1152/ajprenal.00077.2010. Epub 2010 Sep 1.
- (Terasawa K et al., 2006) Terasawa K, Toyota M, Sagae S, Ogi K, Suzuki H, Sonoda T, Akino K, Maruyama R, Nishikawa N, Imai K, Shinomura Y, Saito T, Tokino T. Epigenetic inactivation of TCF2 in ovarian cancer and various cancer cell lines. *Br J Cancer*. 2006 Mar 27;94(6):914-21.
- (Tian Z et al., 2008) Tian Z, Greene AS, Pietrusz JL, Matus IR, Liang M. MicroRNA-target pairs in the rat kidney identified by microRNA microarray, proteomic, and bioinformatic analysis. *Genome Res*. 2008 Mar;18(3):404-11. doi: 10.1101/gr.6587008. Epub 2008 Jan 29.
- (Thomas R et al., 2011) Thomas R, Sanna-Cherchi S, Warady BA, Furth SL, Kaskel FJ, Gharavi AG. HNF1B and PAX2 mutations are a common cause of renal hypodysplasia in the CKiD cohort. *Pediatr Nephrol*. 2011 Jun;26(6):897-903. doi: 10.1007/s00467-011-1826-9. Epub 2011 Mar 5.
- (Thongboonkerd V et al., 2005) Thongboonkerd V, Malasit P. Renal and urinary proteomics: current applications and challenges. *Proteomics*. 2005, 5 (4), 1033-1042.
- (Thorne RF et al., 2004) R. F. Thorne, J. W. Legg, and C. M. Isacke. The role of the CD44 transmembrane and cytoplasmic domains in coordinating adhesive and signalling events. *J. Cell Sci.*, vol. 117, no. Pt 3, pp. 373–380, 2004.
- (Tomei L et al., 1992) Tomei L, Cortese R, De Francesco R. A POU-A related region dictates DNA binding specificity of LFB1/HNF1 by orienting the two XL-homeodomains in the dimer. *EMBO J*. 1992 Nov;11(11):4119-29.
- (Tomura H et al., 1999) Tomura H, Nishigori H, Sho K, Yamagata K, Inoue I, Takeda J. Loss-of-function and dominant-negative mechanisms associated with hepatocyte nuclear factor-1 β mutations in familial type 2 diabetes mellitus. *J Biol Chem*. 1999 May 7;274(19):12975-8.
- (Toole BP 1997) B. P. Toole. Hyaluronan in morphogenesis. *J. Intern. Med.*, vol. 242, no. 1, pp. 35–40, 1997.
- (Tran U et al., 2010) Tran U, Zakin L, Schweickert A, Agrawal R, Döger R, Blum M, De Robertis EM, Wessely O. The RNA-binding protein bicaudal C regulates polycystin 2 in the kidney by antagonizing miR-17 activity. *Development*. 2010 Apr;137(7):1107-16. doi: 10.1242/dev.046045.
- (Tsuchiya A et al., 2003) Tsuchiya A, Sakamoto M, Yasuda J, Chuma M, Ohta T, Ohki M, Yasugi T, Taketani Y, Hirohashi S. Expression profiling in ovarian clear cell carcinoma: identification of hepatocyte nuclear factor-1 β as a molecular marker and a possible molecular target for therapy of ovarian clear cell carcinoma. *Am J Pathol*. 2003 Dec;163(6):2503-12.
- (Ulinski et al., 2006) Ulinski T, Lescure S, Beaufils S, Guignon V, Decramer S, Morin D, Clauin S, Deschênes G, Bouissou F, Bensman A, Bellanné-Chantelot C. Renal phenotypes related to hepatocyte nuclear factor-1 β (TCF2) mutations in a pediatric cohort. *J Am Soc Nephrol*. 2006 Feb;17(2):497-503. Epub 2005 Dec 21.
- (van der Made CI et al., 2015) van der Made CI, Hoorn EJ, de la Faille R, Karaaslan H, Knoers NV, Hoenderop JG, Vargas Poussou R, de Baaij JH. Hypomagnesemia as First Clinical Manifestation of ADTKD-HNF1B: A Case Series and Literature Review. *Am J Nephrol*. 2015;42(1):85-90.
- (Verbitsky M et al., 2015) Verbitsky M, Sanna-Cherchi S, Fasel DA, Levy B, Kiryluk K, Wuttke M, Abraham AG, Kaskel F, Köttgen A, Warady BA, Furth SL, Wong CS, Gharavi AG. Genomic imbalances in pediatric patients with chronic kidney disease. *J Clin Invest*. 2015 May;125(5):2171-8. doi: 10.1172/JCI80877. Epub 2015 Apr 20.
- (Verdeguer F et al., 2010) Verdeguer F, Le Corre S, Fischer E, Callens C, Garbay S, Doyen A, Igarashi P, Terzi F, Pontoglio M. A mitotic transcriptional switch in polycystic kidney disease. *Nat Med*. 2010 Jan;16(1):106-10. doi: 10.1038/nm.2068. Epub 2009 Dec 6.
- (Verhave JC et al., 2015) Verhave JC, Bech AP, Wetzels JF, Nijenhuis T. Hepatocyte Nuclear Factor 1 β -Associated Kidney Disease: More than Renal Cysts and Diabetes. *J Am Soc Nephrol*. 2016 Feb;27(2):345-53. doi: 10.1681/ASN.2015050544. Epub 2015 Aug 28.
- (Wiellette EL et al., 2003) Wiellette EL, Sive H. vhnf1 and Fgf signals synergize to specify rhombomere identity in the zebrafish hindbrain. *Development*. 2003 Aug;130(16):3821-9.
- (Wang B et al., 2010) Wang B, Herman-Edelstein M, Koh P, Burns W, Jandeleit-Dahm K, Watson A, Saleem M, Goodall GJ, Twigg SM, Cooper ME, Kantharidis P. E-cadherin expression is regulated by miR-192/215 by a mechanism that is independent of the profibrotic effects of transforming growth factor- β . *Diabetes*. 2010 Jul;59(7):1794-802. doi: 10.2337/db09-1736. Epub 2010 Apr 14.
- (Wang CC 2012) Wang CC, Mao TL, Yang WC, Jeng YM. Underexpression of hepatocyte nuclear factor-1 β in chromophobe renal cell carcinoma. *Histopathology*. 2013 Mar;62(4):589-94. doi: 10.1111/his.12026. Epub 2012 Dec 12.
- (Wang D et al., 2017) Wang D, Lu G, Shao Y, Xu D. microRNA-802 inhibits epithelial-mesenchymal transition through targeting flotillin-2 in human prostate cancer. *Biosci Rep*. 2017 Mar 15;37(2). pii: BSR20160521. doi: 10.1042/BSR20160521. Print 2017 Apr 30.
- (Wang G et al., 2010) Wang G, Kwan BC, Lai FM, Choi PC, Chow KM, Li PK, Szeto CC. Intrarenal expression of microRNAs in patients with IgA nephropathy. *Lab Invest*. 2010 Jan;90(1):98-103. doi: 10.1038/labinvest.2009.118. Epub 2009 Nov 9.
- (Wang G et al., 2010bis) Wang G, Kwan BC, Lai FM, Choi PC, Chow KM, Li PK, Szeto CC. Intrarenal expression of miRNAs in patients with hypertensive nephrosclerosis. *Am J Hypertens*. 2010 Jan;23(1):78-84. doi: 10.1038/ajh.2009.208. Epub 2009 Nov 12.

- (Wang G et al., 2011) Wang G, Tam LS, Li EK, Kwan BC, Chow KM, Luk CC, Li PK, Szeto CC. Serum and urinary free microRNA level in patients with systemic lupus erythematosus. *Lupus*. 2011 Apr;20(5):493-500. doi: 10.1177/0961203310389841. Epub 2011 Mar 3.
- (Wang L et al., 2004) Wang L, Coffinier C, Thomas MK, Gresh L, Eddu G, Manor T, Levitsky LL, Yaniv M, Rhoads DB. Selective deletion of the Hnf1beta (MODY5) gene in beta-cells leads to altered gene expression and defective insulin release. *Endocrinology*. 2004 Aug;145(8):3941-9. Epub 2004 May 13.
- (Wang XX et al., 2010) Wang XX, Jiang T, Shen Y, Caldas Y, Miyazaki-Anzai S, Santamaria H, Urbanek C, Solis N, Scherzer P, Lewis L, Gonzalez FJ, Adorini L, Pruzanski M, Kopp JB, Verlander JW, Levi M. Diabetic nephropathy is accelerated by farnesoid X receptor deficiency and inhibited by farnesoid X receptor activation in a type 1 diabetes model. *Diabetes*. 2010 Nov;59(11):2916-27. doi: 10.2337/db10-0019. Epub 2010 Aug 10.
- (Wang Y et al., 2007) Wang Y, Medvid R, Melton C, Jaenisch R, Brelloch R. *Nat Genet*. 2007 Mar; 39 (3): 380-5. Epub 2007 Jan 28. *Nat Genet*. 2007 Mar;39(3):380-5. Epub 2007 Jan 28.
- (Wang Y et al., 2012) Y. Wang, O. Roche, C. Xu, E. H. Moriyama, P. Heir, J. Chung, F. C. Roos, Y. Chen, G. Finak, M. Milosevic, B. C. Wilson, B. T. Teh, M. Park, M. S. Irwin, and M. Ohh. Hypoxia promotes ligand-independent EGF receptor signaling via hypoxia-inducible factor-mediated upregulation of caveolin-1. *Proc. Natl. Acad. Sci. U. S. A.*, vol. 109, no. 13, pp. 4892–7, Mar. 2012.
- (Wei Y et al., 1999) Y. Wei, X. Yang, Q. Liu, J. A. Wilkins, and H. A. Chapman, "A role for caveolin and the urokinase receptor in integrin-mediated adhesion and signaling.," *J. Cell Biol.*, vol. 144, no. 6, pp. 1285–94, Mar. 1999
- (Weber JA et al., 2010) Weber JA, Baxter DH, Zhang S, Huang DY, Huang KH, Lee MJ, Galas DJ, Wang K. The microRNA spectrum in 12 body fluids. *Clin Chem*. 2010 Nov;56(11):1733-41. doi: 10.1373/clinchem.2010.147405. Epub 2010 Sep 16.
- (Weber S et al., 2006) Weber S, Moriniere V, Knüppel T, Charbit M, Dusek J, Ghiggeri GM, Jankauskienė A, Mir S, Montini G, Peco-Antic A, Wühl E, Zurowska AM, Mehls O, Antignac C, Schaefer F, Salomon R. Prevalence of mutations in renal developmental genes in children with renal hypodysplasia: results of the ESCAPE study. *J Am Soc Nephrol*. 2006 Oct;17(10):2864-70. Epub 2006 Sep 13.
- (Westland R et al., 2015) Westland R, Verbitsky M, Vukojevic K, Perry BJ, Fasel DA, Zwijnenburg PJ, Bökenkamp A, Gille JJ, Saraga-Babic M, Ghiggeri GM, D'Agati VD, Schreuder MF, Gharavi AG, van Wijk JA, Sanna-Cherchi S. Copy number variation analysis identifies novel CAKUT candidate genes in children with a solitary functioning kidney. *Kidney Int*. 2015 Dec;88(6):1402-1410. doi: 10.1038/ki.2015.239. Epub 2015 Sep 9.
- (Wild W et al., 2000) Wild W, Pogge von Strandmann E, Nastos A, Senkel S, Lingott-Frieg A, Bulman M, Bingham C, Ellard S, Hattersley AT, Ryffel GU. The mutated human gene encoding hepatocyte nuclear factor 1beta inhibits kidney formation in developing *Xenopus* embryos. *Proc Natl Acad Sci U S A*. 2000 Apr 25;97(9):4695-700.
- (Williams SS et al., 2014) Williams SS, Cobo-Stark P, Hajarnis S, Aboudehen K, Shao X, Richardson JA, Patel V, Igarashi P (2014) Tissue-specific regulation of the mouse Pkhd1 (ARPKD) gene promoter. *Am J Physiol Ren Physiol* 307:F356–F368
- (Williams TM and Lisant MP, 2004) T. M. Williams and M. P. Lisanti. The Caveolin genes: from cell biology to medicine. *Ann. Med.*, vol. 36, no. 8, pp. 584–95, 2004.
- (Wright PC et al., 2012) Wright, P. C., Noirel, J., Ow, S. Y., Fazeli, A., A review of current proteomics technologies with a survey on their widespread use in reproductive biology investigations. *Theriogenology* 2012, 77 (4), 738-765.
- (Wu G et al., 2004) Wu G, Bohn S, Ryffel GU. The HNF1beta transcription factor has several domains involved in nephrogenesis and partially rescues Pax8/lim1-induced kidney malformations. *Eur J Biochem*. 2004 Sep;271(18):3715-28.
- (Wu J et al., 2014) Wu J, Zheng C, Fan Y, Zeng C, Chen Z, Qin W, Zhang C, Zhang W, Wang X, Zhu X, Zhang M, Zen K, Liu Z. Downregulation of microRNA-30 facilitates podocyte injury and is prevented by glucocorticoids. *J Am Soc Nephrol*. 2014 Jan;25(1):92-104. doi: 10.1681/ASN.2012111101. Epub 2013 Sep 12.
- (Xia H et al., 2010) H. Xia, W. Khalil, J. Kahm, J. Jessurun, J. Kleidon, and C. A. Henke, "Pathologic caveolin-1 regulation of PTEN in idiopathic pulmonary fibrosis.," *Am. J. Pathol.*, vol. 176, no. 6, pp. 2626–37, Jun. 2010.
- (Yang L et al., 2010) Yang L, Frindt G, Palmer LG. Magnesium modulates ROMK channel-mediated potassium secretion. *J Am Soc Nephrol*. 2010 Dec;21(12):2109-16. doi: 10.1681/ASN.2010060617. Epub 2010 Oct 28.
- (Yi R et al., 2003) Yi R, Qin Y, Macara IG, Cullen BR. Exportin-5 mediates the nuclear export of pre-microRNAs and short hairpin RNAs. *Genes Dev*. 2003 Dec 15;17(24):3011-6. Epub 2003 Dec 17.
- (Yorifuji T 2004) Yorifuji T, Kurokawa K, Mamada M, Imai T, Kawai M, Nishi Y, Shishido S, Hasegawa Y, Nakahata T. Neonatal diabetes mellitus and neonatal polycystic, dysplastic kidneys: Phenotypically discordant recurrence of a mutation in the hepatocyte nuclear factor-1beta gene due to germline mosaicism. *J Clin Endocrinol Metab*. 2004 Jun;89(6):2905-8.
- (Yu DD et al., 2015) Yu DD, Guo SW, Jing YY, Dong YL1, Wei LX1. A review on hepatocyte nuclear factor-1beta and tumor. *Cell Biosci*. 2015 Oct 13;5:58. doi: 10.1186/s13578-015-0049-3. eCollection 2015.
- (Zhang Y et al., 2007) Zhang Y, Wada J, Yasuhara A, Iseda I, Eguchi J, Fukui K, Yang Q, Yamagata K, Hiesberger T, Igarashi P, Zhang H, Wang H, Akagi S, Kanwar YS, Makino H. The role for HNF-1beta-targeted collectrin in maintenance of primary cilia and cell polarity in collecting duct cells. *PLoS One*. 2007 May 2;2(5):e414.
- (Zapp D et al., 1993) Zapp D, Bartkowski S, Zoidl C, Klein-Hitpass L, Ryffel GU. Genomic structure of the *Xenopus laevis* liver transcription factor LFB1. *Gene*. 1993 Dec 8;134(2):251-6.

(Zager RA 2002) Zager RA, Johnson A, Hanson S, dela Rosa V. Altered cholesterol localization and caveolin expression during the evolution of acute renal failure. *Kidney Int* 61: 1674–1683, 2002

(Zeng Y and Cullen BR 2004) Zeng Y, Cullen BR. Structural requirements for pre-microRNA binding and nuclear export by Exportin 5. *Nucleic Acids Res.* 2004 Sep 8;32(16):4776-85. Print 2004.

(Zhdanova O et al., 2011) Zhdanova O, Srivastava S, Di L, Li Z, Tchelebi L, Dworkin S, Johnstone DB, Zavadil J, Chong MM, Littman DR, Holzman LB, Barisoni L, Skolnik EY. The inducible deletion of Droscha and microRNAs in mature podocytes results in a collapsing glomerulopathy. *Kidney Int.* 2011 Oct;80(7):719-30. doi: 10.1038/ki.2011.122. Epub 2011 May 4

(Zhuang Z et al., 2011) Zhuang Z, Marshansky V, Breton S, Brown D. Is caveolin involved in normal proximal tubule function? Presence in model PT systems but absence in situ. *Am J Physiol Renal Physiol.* 2011 Jan;300(1):F199-206. doi: 10.1152/ajprenal.00513.2010. Epub 2010 Oct 27.

(Zürbig, P et al., 2008) Zürbig, P., Mischak, H., in Soloviev, M., Shaw, C., Andren, P. E. (Eds.), *Peptidomics: methods and applications*, John Wiley & Sons, Inc., Hoboken, New Jersey 2008, 155-175.